Immunochemical approaches to monitor and modulate the adaptive immune system

Luimstra, J.J.

Immunochemical approaches to monitor and modulate the adaptive immune system

Jolien Luimstra

Immunochemical approaches to monitor and modulate the adaptive immune system

Jolien Johanna Luimstra

The research described in this thesis was performed at the Department of Cell Biology at the Netherlands Cancer Institute in Amsterdam, The Netherlands, as well as at the Department of Chemical Immunology and the Department of Cell and Chemical Biology at Leiden University Medical Center in Leiden, The Netherlands. The work was financially supported by the Institute for Chemical Immunology and Oncode Institute.

ISBN: 978-94-640-2036-6

Cover: Veerle Luimstra
Layout: Valken Hout en Design
Support and catering: Robert van den Brink
Financial support: The Netherlands Cancer Institute and Leiden University
Printed by: Gildeprint

Immunochemical approaches to monitor and modulate the adaptive immune system

Proefschrift

ter verkrijging van
de graad van Doctor aan de Universiteit Leiden,
op gezag van Rector Magnificus prof. mr. C.J.J.M. Stolker,
volgens besluit van het College voor Promoties
te verdedigen op woensdag 12 februari 2020
klokke 15:00 uur

door

Jolien Johanna Luimstra

Geboren te Amsterdam
op 18 september 1987

Promotores
Prof. dr. H. Ovaa
Prof. dr. J.J.C. Neefjes

Leden promotiecommissie
Prof. dr. J.G. Borst
Prof. dr. T.J. Elliott - *University of Southampton*
Prof. dr. F.A. Ossendorp
Dr. I. Berlin
Dr. S.I. van Kasteren

"Just keep swimming, just keep swimming,
just keep swimming, swimming, swimming..."

- Dory in 'Finding Nemo' (Disney • Pixar)

Table of contents

1

General introduction and Scope of this dissertation

1

Adaptive immunity

We are in constant battle against pathogens, and throughout evolution our bodies have developed sophisticated mechanisms to protect us. Our immune system consists of two branches to prevent, cure and suppress infection[1,2]. As immediate defense, the non-specific innate immune system recognizes and responds to pathogens in a generic fashion. Recognition of danger- or pathogen-associated molecular patterns (DAMPs or PAMPs) induces inflammation, membrane attack and phagocytosis of pathogens[3]. Common PAMPs that trigger innate immunity are motifs not found in vertebrates, such as dsRNA, glycans, lipopolysaccharides or endotoxins. DAMPs can be host-derived constituents, such as DNA or RNA, that are normally contained in the nucleus or cytosol. The second branch of the immune system, adaptive immunity, is acquired throughout life[4]. This highly specialized response is the main focus of this dissertation. Its key mediators are B (bursa-derived) and T (thymus-derived) lymphocytes, which are typically activated by specific antigens[5]. In contrast to the immediate and short-lived innate immune response, the adaptive response results in long-term protection by creating immunological memory following the initial infection[6].

To evoke potent adaptive responses against pathogens without inducing auto-immunity T cells must be able to distinguish between 'self' and 'non-self' antigens. The first step in the generation of functional T cells is positive selection by matching cell surface receptors, such as CD4 and CD8[7]. Those that match undergo a second round of (negative) selection: self-reactive T cells are deleted, thus preventing autoimmunity and establishing central tolerance[8]. Stringent selection assures that only cells with functional T cell receptors (TCRs) that are not auto-reactive will leave the thymus. But before doing so, they downregulate one of the two coreceptors, maturing into either $CD4^+$ (T helper) or $CD8^+$ (cytotoxic) T cells[9]. Aberrations in T cell selection mechanisms can result in immune deficiency or autoimmunity, often causing severe disease.

Cell-mediated immunity

In adaptive immunity two pathways are distinguished: cell-mediated and humoral. The first adaptive immune pathway allows the immune system to catch a glimpse inside most cells for signs of infection or mutation and to take action if needed. The pathway is mediated by major histocompatibility complex (MHCI) class I molecules that present peptides derived from intracellular proteins on the surface of all nucleated cells (Fig. 1, left panel)[10]. $CD8^+$ T cells scan the repertoire of peptide-MHCI (pMHCI) complexes and, when they recognize peptides originating from viral or mutated (onco)proteins, set a cytotoxic response in motion[11-13]. The majority of peptides presented by MHCI are the product of proteasomal degradation of proteins that have fulfilled their function and are no longer

needed, but about 30% of newly synthesized proteins is degraded immediately after synthesis, as a result of defects in protein transcription, translation or folding[14-16]. Presentation of fragments derived from these proteins, collectively termed defective ribosomal products (DRiPs), allows processing and display of even long-lived proteins to $CD8^+$ T cells as soon as 1.5 hours post infection, thus accelerating the detection rate of infection[17]. A more recently discovered source of T cell epitopes is protein splicing: protease-mediated transpeptidation by the proteasome[18,19]. This ligation of peptide fragments broadens the repertoire of presented peptides by extending past the expressed peptidome[20,21].

Peptide fragments generated by the proteasome are transported into the endoplasmic reticulum (ER) by the transporter associated with antigen processing (TAP), where MHCI molecules await to be loaded[22]. Peptide receptive MHCI is assembled in the ER as a heterodimeric complex unstable in the absence of peptide and thus requires stabilization by chaperones[23]. Upon loading of a cognate peptide, typically comprised of 8-10 amino acids, MHCI acquires enough stability to be released from the ER and transported to the cell surface, where it can present its peptide to $CD8^+$ cells. When a naïve $CD8^+$ T cell encounters a non-self antigen, it becomes activated, resulting in proliferation of the antigen-specific T cell and lysis of the antigen-presenting cell. After an infection is cleared, most mature $CD8^+$ T cells undergo apoptosis, but a few remain in the form of memory T cells[6]. In general, the initial response is slow, while the one initiated from memory progresses much quicker. Hence, in case of challenge with a previously-encountered virus or pathogen, the infection is likely to be cleared even before symptoms occur.

Humoral immunity

The second adaptive immune pathway protects the extracellular space (body fluid – humor) and is mediated by MHC class II complexes (MHCII). These present antigens derived from extracellular proteins on the surface of professional antigen-presenting cells (APCs), such as dendritic cells (DCs), B cells and macrophages (Fig. 1, right panel)[16]. APCS can internalize proteins in various ways, including receptor-mediated endocytosis (B cells), phagocytosis (DCs) or macropinocytosis (macrophages)[24]. In lysosomes the proteins are cleaved into peptides, generally 15-24 amino acids in size, which can bind to major histocompatibility complex class II (MHCII) molecules in late endosomes[25]. Endosomes carrying peptide-loaded MHCII complexes are then transported back to the cell surface for presentation to $CD4^+$ T cells. Upon binding of non-self antigens, $CD4^+$ T cells become activated, inducing the release of cytokines that stimulate clonal expansion of B cells, thus promoting antibody production. Antibodies are subsequently released into the plasma, where they can bind cognate antigens. By doing so, antibodies are able to confer protection through three main modes of action: inhibiting infectivity

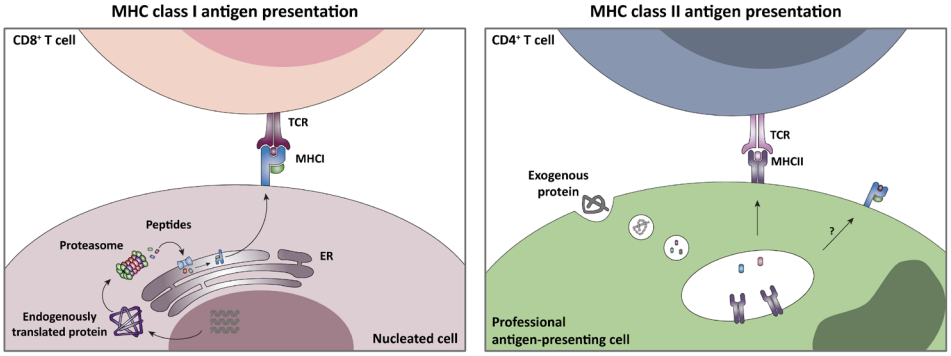

Figure 1. **Schematic representation of major histocompatibility complex (MHC) class I and class II-mediated antigen presentation.**

or toxicity by binding proteins on the pathogen's cell surface to neutralize them; marking a pathogen for phagocytosis; or activating the innate classical complement pathway.

The pathways described above are not strictly distinct: certain APCs can also process and present extracellular peptides on MHCI in a process referred to as cross-presentation. This is particularly useful for protection against pathogens that have developed strategies to evade immune detection[26]. For example, some herpes viruses produce specific proteins to interfere with host protein synthesis, mainly targeting those involved in MHCI antigen presentation and thus escaping detection by $CD8^+$ T cells[27]. Through cross-presentation of endocytosed antigen fragments on MHCI (that would normally be presented on MHCII) $CD8^+$ T cells can still get activated. It is apparent that primarily DCs are capable of cross-presenting, but the exact mechanisms by which cross-presentation occurs are still under debate[28]. Various mechanisms have proposed, yet many questions remain unanswered.

Immune response in three signals

TCR activation by recognition of an antigenic peptide on MHCs is only the first of three signals required for mounting a full-blown immune response[29]. Whether or not a peptide is presented to its matching T cell depends on a number of factors. Firstly, peptides processed by the proteasome and downstream peptidases need to be of compatible size. Peptides presented by MHCI are typically nine amino acids long, while the proteasome generates peptides of various lengths. Peptides, which are too short (less than seven amino acids), will not interact with TAP and will therefore not be translocated to the ER lumen[30]. On the other hand, long peptides (more than sixteen amino acids) will require further trimming by peptidases to enable efficient loading onto MHCI[31,32]. Secondly, the peptide sequence needs to match one of the expressed MHCI allotypes[23]. Lastly, the affinity of the peptide for its cognate MHC allele should be sufficient to sustain

presentation at the cell surface and prevent exchange for exogenous peptides[33]. The frequency of a specific T cell clone in circulation is generally low prior to encounter with its cognate peptide, so it could take a while before a presented antigen comes in contact with the right $CD8^+$ T cell. Once a peptide manages to reach the cell surface—on average a chance of 1:200—the pMHC is ready to be scrutinized by passing T cells[34]. TCRs interact not only with the exposed residues of the peptide, but also with the residues on top of the two α helices, which make up the MHC's binding groove. This interaction is highly selective: a TCR will only be potently activated by a specific combination of peptide and allele[33,35]. This feature is referred to as MHC restriction, which is essential for mounting an appropriate immune response, while maintaining self-tolerance[36].

Researchers only learned in the late 1980s of a second immune signal, provided by costimulation predominantly through the B7-1/B7-2:CD28 pathway[37]. The CD28 receptor is expressed on 95% of $CD4^+$ T cells and 50% of $CD8^+$ T cells, and constitutively on naïve T cells in humans[38]. Engagement by costimulatory ligands B7-1 (CD80) or B7-2 (CD86) on APCs provides the signals needed for T cell activation and survival, including production of the master regulator of T cell activation, IL (interleukin)-2[39-42]. A second costimulatory factor in the B7:CD28 family is CD28 homologue ICOS (inducible costimulator) and its ligand ICOS-L (B7h), a homolog of B7-1 and B7-2[43,44]. ICOS is expressed on TCR-activated $CD4^+$ and $CD8^+$ T cells and upregulates expression of helper T cell (Th)1- and Th2-polarizing cytokines, but in contrast to CD28, it does not activate IL-2 production[43,45]. ICOS and CD28 seem to work synergistically to regulate $CD4^+$ T cells[40]. In absence of costimulation, T cells activated by pMHCI will become anergic, although in some cases, when the interaction between pMHCI and TCR is very strong, T cells may remain activated, resulting in peripheral tolerance[46,47].

Although proliferation of naïve T cells can be initiated when TCR and CD28 signals are present, a productive response will only be established once specific cytokines are produced[48]. Cytokines that provide this third immune signal, required for proper development of $CD8^+$ T cell effector and memory functions, are IL-12 and type I interferons (IFNs)[29,49]. For $CD4^+$ T cells, IL-1 can be considered a general third signal, in addition to cytokines that prompt differentiation into one of the Th subsets, such as polarization towards Th1 or Th2 by IL-12 and IL-4, respectively[50-52].

MHC STRUCTURE AND FUNCTION

The functions of the two classes of MHC are similar: presentation of peptides to the immune system, but what peptides they present, in which tissues and to which cells differs between the classes. In short, MHCI presents peptide fragments

derived from intracellular proteins to $CD8^+$ T cells, resulting in a cytotoxic response against cells expressing an immunogenic antigen. MHCII, on the other hand, is only found on dedicated antigen-presenting cells and can activate $CD4^+$ T cells, leading to a B cell response. MHCI and MHCII both consist of two immunoglobulin (Ig)-like domains topped by two α helices[53-55]. MHCI consists of one long heavy chain, the α-chain, that forms an Ig-like transmembrane domain, α3, and the α1 and α2 domains that comprise the peptide-binding groove. The second Ig-like domain is provided by the light chain β2m, which associates non-covalently with the heavy chain. In MHCII, heavy chains α and β combine to form the α-helices of the peptide-binding groove. Both chains harbor Ig-like domains (α2 and β2) that anchor the complex in the membrane. The groove of MHCI is closed at both ends wherein only short peptides of 8-11 amino acids can fit, whereas MHCII has an open groove able to accommodate peptides in the range of 15-24 amino acids[56-58]. These structural features dictate binding of certain sized peptides in general, but exact sequences depends on other factors described in more detail below.

MHC polymorphisms

The three major groups of human MHC genes, referred to as HLA (human leukocyte antigens) class I, II and III, are located on chromosome 6, together with many more immunity-associated genes[59]. Unlike the HLA class I and II regions, the gene-dense HLA class III region has been poorly defined[60]. The HLA class I gene region contains three loci coding for the classical HLAI proteins involved in antigen presentation, HLA-A, HLA-B and HLA-C[61-64]. Classical HLA class II proteins HLA-DR, HLA-DP and HLA-DQ are also expressed from three loci. The loci coding for the HLAI heavy chains are among the most polymorphic in the human genome, meaning that they contain many variations in their sequence, generated by mutation, recombination and gene conversion[65,66]. Different allotypes have evolved with selection pressure, yielding a distinct distribution of allele frequencies across the globe[67-69]. Individuals can carry three to six different MHCI allotypes and three to twelve different MHCII allotypes, depending on the inheritance of their parents[33]. The majority of single nucleotide polymorphisms and deletion/insertion polymorphisms are found in the regions that code for the peptide-binding groove, resulting in differences in nature and location of binding pockets, and consequently preferred peptide motifs per allele[65,70-72]. Since only peptides with a matching motif get presented, expressing multiple allotypes allows presentation of more fragments derived from the same protein and hence provides widespread protection against numerous pathogens. There is an obvious heterozygote advantage, explaining why expression of MHC genes is even suggested to play a role in mate selection[73-75].

Over the years, vastness of information on MHC ligands and motifs has been

gathered in online databases, with SYFPEITHI and the IEDB (Immune Epitope Database) containing the largest collections[76,77]. The discovery of new alleles has greatly advanced since the development of Next-Generation Sequencing, resulting in the identification of over 15,000 subtypes registered in international databases[64,78,79]. These data are extremely valuable for immunogenicity research and the transplantation community[80,81]. For instance, using the data available, HLA types of donors and patients can be matched to increase survival rates of hematopoietic stem cell transplant recipients[82,83]. This is important because mismatch of only a single nucleotide polymorphism could affect the outcome of a transplant.

Peptide affinity and T cell activity

Which peptides can stably associate with the MHCI heavy chain depends on the interactions of the binding groove residues with the peptide backbone and occupation of defined binding pockets by the peptide side chains[84-86]. HLA-A, -B and -C heavy chains form six binding pockets, named A-F, that can accommodate a peptide's amino acid side chains[87,88]. Generally two amino acids, referred to as the anchor residues, position the peptide by docking in the pockets. Because theoretically any peptide with a matching motif will fit a certain allotype, predicting which peptides will strongly bind is extremely challenging.

The use of algorithms to predict peptide affinity in silico, such as those used by SYFPEITHI, IEDB and NetMHC, facilitates epitope prediction[76,89,90]. Although they provide an indication of binding strength, computational tools alone often fail to accurately predict immunogenicity. For a long time it was assumed that a high peptide affinity results in prolonged presentation to T cells, and hence in increased immunogenicity. Gradually, however, it became clear that binding affinity of a peptide to an MHC is not the only determinant for immunogenicity[91-93]. This is illustrated by a study by Speiser et al., who directly compared vaccination with wild-type melanoma antigen EAAGIGILTV or a higher-affinity altered peptide ligand (APL), ELAGIGILTV[94]. They found that, although more T cells were induced by vaccination with the APL, quality of the response in terms of tumor reactivity and T cell activation in vivo was higher after vaccination with the wild-type ligand. A similar observation was made by McMahan et al, who investigated T cell responses in mice with CT26 colon cancer[95]. When comparing vaccination with tumor-associated antigens or APLs, they observed proliferation of tumor antigen-specific T cells and elevated IFN-γ in response to the high-affinity APLs, but this did not correlate with anti-tumor immunity. Although a certain affinity is required for efficient loading in the ER, other factors, such as stability, conformational flexibility and formation of the immunological synapse, are also important determinants for T cell activation[92,93,96-99]. More recent epitope prediction tools therefore also include pMHC stability as an extra parameter[100,101].

1

Passing T cells may sample various antigens, but will only respond to ligands with a certain affinity[102,103]. The TCR-pMHC contact should last long enough to induce signaling, but short enough to allow serial engagement and activation of multiple T cells[104]. Because infected or mutated cells do not always express many copies of an antigen, for example due to downregulation of MHCI or other proteins involved in antigen presentation, sometimes only a few peptides survive the journey to the cell surface. Activation of multiple T cells by one pMHC-complex amplifies the immune stimulus, thus ensuring high sensitivity needed to respond to low-frequency peptides. Of course this can only be accomplished if the association and dissociation kinetics of the TCR-pMHC interaction occur at a reasonable rate. This is in line with the observation that TCR affinity for pMHC is generally low, in the micromolar range[105]. Serial engagement becomes less important when density of a certain pMHC is high, thus an optimal half-life seems to only be required for low-density pMHCs[106].

MHC and disease

Predisposition to certain infectious, inflammatory or autoimmune diseases is known to have a genetic origin, in many cases located in the MHC genes[107-112]. An estimated 5% of the population suffers from autoimmune diseases, which include the well-known type I diabetes, multiple sclerosis and rheumatoid arthritis, all diseases that have been extensively studied in relation to MHC[113-118]. In the past few decades increasing numbers of HLA subtypes have been reported in concurrence with other autoimmune diseases not initially linked to MHC, such as celiac disease, systemic lupus erythematosus, ulcerative colitis, Crohn's disease and ankylosing spondylitis[119-123]. The latter example is associated with expression of HLA-B*27:05[124,125]. It was discovered as early as 1973 that this subtype is expressed in 85-90% of ankylosing spondylitis patients, but how it relates to development of the rheumatoid disorder is still unknown[124-126]. Strikingly, individuals expressing the closely related HLA-B*27:09 do not develop the disease, although the two subtypes only differ in residue 116 found at the bottom of the F pocket (Asp in HLA-B*27:05 and His in HLA-B*27:09)[127]. Crystal structures of the two alleles complexed with the same peptide are virtually indistinguishable, however, molecular dynamics simulations show that the flexibility of peptide-bound HLA-B*27:09 is much higher than that of HLA-B*27:05[128]. This implies that peptide dynamics may play an important role in the activation of T cells, and molecular dynamics studies should therefore be included in the experimental data used to build prediction algorithms[129,130].

In some cases, combinations of MHCI and MHCII alleles convey a predisposition, such as the additional effect of HLA-A*3 on the HLA-DR15-associated susceptibility to multiple sclerosis[120]. Often, even though a genetic association is established, the mechanism by which a given HLA allotype confers protection or causes disease

is unknown. Understanding the basis of these associations can help advance personalized disease prevention and treatment[131].

A few relevant mechanisms can be envisioned, of which undesirable presentation of self-peptides or altered self-peptides is perhaps the most obvious. Alternatively, the association may have nothing to do with peptide presentation, but instead may affect the T cell repertoire, including regulatory T cells. Or there could be no effect at all, but the allotype could just be in linkage disequilibrium with another disease-causing gene and therefore act as a marker.

Altered self-peptides may arise from mutated proteins, but can also be derived from post-translationally modified proteins[132,133]. The latter appears to be the case with type 1 diabetes, where a number of modifications present on peptides have been found to trigger autoimmune responses[134-136]. In addition, citrullination, a post-translational deiminaton of arginine to form citrulline, is the hypothesized culprit in development and progression of rheumatoid arthritis[137,138]. Specifically, evidence points to dysregulation of protein citrullination in the rheumatoid joint, resulting in hypercitrullination and concurrent loss of tolerance[139]. Anti-citrullinated protein antibodies are detectable in early stages of the disease and hence provide valuable diagnostic and prognostic markers for rheumatoid arthritis[140,141].

Certain MHC alleles are not directly associated with disease, but with susceptibility to adverse drug effects, ranging from mild skin reactions, fever and nausea to even fatal reactions upon re-exposure[142,143]. Patients are often genotyped for risk alleles prior to starting treatment with a drug known to have an association[144]. One of the best known HLA-related adverse drug effects is T cell-mediated hypersensitivity to treatment with abacavir, a nucleoside analog reverse-transcriptase inhibitor used to treat HIV[145]. Treatment with abacavir induces high frequencies of reactive $CD8^+$ T cells in individuals expressing HLA-B*57:01, but not in those expressing any of the closely related allotypes HLA-B*57:02/03 or HLA-B*58:01, which only differ from HLA-B*57:01 in three or four amino acids, respectively[146]. A crystal structure of HLA-B*57:01 complexed with abacavir and an immunogenic peptide shows that abacavir binds specifically in the F pocket of HLA-B*57:01 and may alter the specificity of the MHC to allow binding and presentation of self peptides[147-149].

Cancer immunotherapy

According to its definition, i.e. 'treatment designed to produce immunity to a disease or enhance the resistance of the immune system to an active disease process', immunotherapy has been around for centuries, with first evidence of inoculation with smallpox dating from tenth century China[150]. Examples of

modern day immune-activating therapies are vaccination or immunization, whereas immune suppression is used to treat autoimmune diseases or prevent transplant rejection. A role for the immune system in the clearance of cancer has been studied for decades, and this has led to the perception that primary tumor development, especially of cancers that are virus-induced, is suppressed by the immune system[151-155]. As long as the 'cancer immunity cycle' proposed by Chen and Mellman functions properly, even distant tumor cells are eradicated[156]. Those sporadic tumors which escape, likely develop mechanisms to induce tolerance, for example by promoting expansion of anergic $CD8^+$ T cells or induction of $CD4^+$ T cells[157-161]. Immunotherapy may then restore the cycle and concurrently reestablish anti-cancer immunity.

The advance of DNA and RNA sequencing techniques has made it possible to identify tumor-associated mutations or aberrations, and to target these to cure disease. Several therapeutic strategies targeting T cell immunity are described in the next sections and in more detail in **Chapters 2, 3 and 4**.

Peptide vaccines

The majority of cancer immunotherapy efforts involve vaccination, which is not surprising in light of historical achievements of vaccination to prevent or cure disease[162]. Despite this potential, only minor successes have been accomplished using preventive or therapeutic vaccines as anti-cancer strategy[163,164]. Preventive vaccines are designed to induce humoral immunity through engendering a pool of memory B cells and antipathogenic antibodies. On the other hand, therapeutic vaccines are designed to treat an established disease by activating cellular immunity through T cells. Preventive vaccines are primarily employed against cancers caused by viruses, such as in the case of the human papilloma virus vaccine used to prevent cervical cancer[165]. The first generation of therapeutic vaccines, consisting of adjuvants or microbial or tumor preparations, was not particularly specific and chiefly aimed at establishing an inflammatory environment[166]. Current anti-cancer vaccines are more specific, comprising antigens released by tumors often complemented with adjuvants[167]. Vaccination with epitope-based peptides to specifically induce relevant T cells targeted to infected or mutated cells potentially provides effective prevention or treatment of infection or cancer. Peptide vaccines are usually aimed at activation of $CD8^+$ T cells, because of their cytolytic activity directly targeting cells that present the antigen, also at distant sites. Antigenic peptides can be self or non-self when cancer is caused by viruses[168-170]. Self-antigens can originate from highly upregulated proteins necessary for tumor growth and formation, peptide splicing by the proteasome or tumor-associated antigens such as melanoma-associated antigen (MAGE) or cancer testis antigen 1 (CTAG1, also known as NY-ESO-1)[169-174]. In many cases the TCR affinity for these self-antigens is low, which is why they could escape negative

selection[175,176]. Vaccination with such self-antigens supports T cell activation, augmenting anti-tumor responses.

Neoantigens are mutated self-antigens that arise from tumor-specific somatic DNA mutations[177]. Because neoantigens are not expressed in healthy tissue, vaccination induces only tumor-specific responses[178]. It is not difficult to imagine that for this reason neoantigens are hot targets in the development of cancer immunotherapeutics[179,180]. Spontaneous immune recognition of neoantigens is inefficient, for tumors are poor antigen-presenting cells, but anti-tumor immunity can be greatly enhanced by neoantigen-based vaccination[181]. Many pharmaceutical companies endeavor to discover neoantigens that can be exploited for treatment options[182,183]. Multiple modes of neoantigen-focused treatment have been successfully demonstrated, including vaccination with peptides or neoantigen mRNA, or adoptive transfer of neoantigen-specific T cells[184,185]. Since neoantigens are patient-specific, their identification needs to be performed on an individual basis. Somatic mutations can be discovered through sequencing and comparison of expression profiles between healthy and tumor tissues. Using binding algorithms, transcribed neoantigens may be matched to MHCI or MHCII to predict presented neoantigens[186-188]. Only a few of these predicted neoantigens will actually be expressed and presented on MHCs and even fewer will be immunogenic[189,190]. Therefore, screening of T cells using neoantigen-loaded MHC multimers, as described in **Chapter 7** of this thesis, or validation by peptide elution, is necessary to reveal true neoantigens[191,192].

Despite 20 years of peptide vaccine studies and numerous clinical trials, none have made it to the clinic yet[193,194]. Peptides alone are poorly immunogenic and consequently improving the immunogenicity of known MHCI antigens by altering amino acid sequences has been the central focus in the field[195-198]. Substitutions are primarily introduced in the anchor positions, to increase the number and quality of the interactions in the binding pockets, while the central amino acids are kept unaltered. Mutating the central amino acids can result in hyperstimulation of T cells with the risk of inducing a pool of T cells that is reactive against the altered peptide, but not the wild-type epitope[199]. This off-target activation can even be caused by modifying only the anchor residues, since they can induce conformational changes in both MHC and peptide, thus altering T cell reactivity[130]. Design of APLs that contain not only the 20 proteogenic amino acids, but also amino acids with chemically-modified side chains is elaborated upon in **Chapters 2 and 3**.

One of the reasons for low efficiency of peptide vaccines is the absence of the second signal required for immune activation; namely, costimulation. Peptides presented by MHCI are usually derived from cytosolic or nuclear proteins and undergo trimming and loading in the ER. Circulating peptides are internalized in endosomes: the archetypal MHC class II compartments. How exactly peptide

vaccines administered in the blood eventually end up in class I MHCs on the cell surface is not completely understood, but this presumably takes place through cross-presentation, exchange on the cell surface or simply by cytosolic uptake of cell-permeable peptides[200-203]. These mechanisms bypass processing by professional APCs, such as DCs, and as a result, costimulatory signals necessary for activation of T cells are insufficiently provided, which may ultimately lead to tolerance[47,204,205]. Additional immune stimulation can be provided by $CD4^+$ T cells. Accordingly, the most successful peptide vaccines to date encompass long peptides that contain both MHCI and MHCII epitopes, thus triggering both cytotoxic ($CD8^+$) and helper ($CD4^+$) T cell responses[204]. Long peptides are processed by professional APCs and have been found to induce more competent anti-viral responses in multiple studies, with anti-human papilloma virus vaccines to prevent recurrent vulvar intraepithelial dysplasia as the greatest success story[206-209]. These long peptides ideally contain multiple potential epitopes able to bind various MHC allotypes, providing intrinsically broader application. Herein lies also the risk of off-target effects, since allotypes differ per individual and therefore the epitopes within a vaccine can unfavorably activate T cells in different individuals.

Cell-based therapies

By directly administering autologous T cells, the peptide vaccination step can be skipped. Tumor-specific $CD8^+$ T cells can be isolated from peripheral blood mononuclear cells or tumor tissue, stimulated and expanded ex vivo, and then readministered to specifically attack the tumor[210,211]. Especially in the treatment of melanoma, adoptive transfer of tumor-infiltrating lymphocytes has shown remarkable reponses[212-215]. To further enhance efficacy and tumor specificity, T cells can be genetically engineered through lentiviral or retroviral transduction or transfection with DNA or RNA to express novel tumor-specific TCRs or chimeric antigen-receptors[216-218].

Another cell type that has been successfully used in cancer treatment are DCs[219-221]. They are at the center of antigen processing and presentation and activate both $CD4^+$ and $CD8^+$ T cells, providing both activation and costimulation[222,223]. DCs can be used in various ways, but the most successful strategies include vaccination with antigens coupled to DC-antibodies (e.g. DEC-205) or DCs loaded with antigens ex vivo[220,224-228]. The first therapeutic anti-cancer vaccine to get approval from the US Food and Drug Administration (FDA, in 2010) is such a DC-based vaccine: Provenge®, also called Sipuleucel-T (Dendreon, Inc.), for treatment of prostate cancer[229,230]. This vaccine contains DCs that are activated ex vivo with a prostate cancer-specific antigen, prostatic acid phosphatase, to stimulate tumor-specific $CD8^+$ T cells[231-233]. Especially in these cases it is of the utmost importance that antigens are only expressed on tumors to avoid off-tumor effects[217,234].

Checkpoint inhibition

Widespread success and fame of cancer immunotherapy came with the discovery of checkpoint inhibition. Inhibitory receptors on T cells, such as cytotoxic T-lymphocyte-associated antigen (CTLA)-4 and programmed death (PD)-1, are negative regulators of the costimulatory signal necessary for T cell activation[235-238]. The balance between inhibitory and stimulatory immune checkpoints ensures optimal immune protection, while maintaining self-tolerance and preventing autoimmunity[239]. By blocking inhibitory pathways, the brakes on immune responses are released, resulting in a boost of preexisting anti-tumor responses[240-242]. Checkpoint inhibition offers great opportunities, especially when treating cancers harboring high mutational burden and thus likely to express higher frequencies of neoantigens[243-246]. For their roles in this discovery James P. Allison and Tasuku Honjo were awarded the 2018 Nobel Prize for Physiology or Medicine[247]. The group of Allison was the first to demonstrate increased antitumor activity in vivo using antibodies blocking CTLA-4 in murine colorectal carcinoma and one year later in murine prostate cancer[240,248]. CTLA-4 is a homologue of CD28 and binds both B7-1 and B7-2, with a higher affinity than CD28[249]. This negative regulation results in inhibition of IL-2 production and blocking of cell cycle progression, thus functioning as an immune checkpoint to control lymphocyte homeostasis[250-252]. A quick search for clinical trials shows roughly 50 active and 150 recruiting/enrolling trials targeting CTLA-4 as a single or combination therapy[253]. Ipilimumab, a blocking antibody against CTLA-4, has demonstrated durable clinical responses and was approved for treatment of metastatic melanoma by the FDA and the European Medicines Agency (EMA) in 2011[254,255].

A wide range of tumors express PD-L1, the ligand for immune checkpoint receptor PD-1, thus creating an immunosuppressive environment and escaping immune surveillance[256-258]. Blocking the PD-L1/PD-1 interaction is therefore even more effective against cancer than anti-CTLA-4. Indeed, as a monotherapy, antibodies against PD-1 cause a remarkable reduction of tumor metastasis spread in mice, owing to enhanced recruitment of effector T cells[259,260]. Their efficacy is reflected in the high number of clinical trials targeting PD-1 (almost 200 active and over 800 recruiting/enrolling trials) or PD-L1 (almost 200 active and over 500 recruiting/enrolling)[253]. Two PD-1 antibodies, nivolumab and pembrolizumab, have shown durable clinical responses in various cancer types and have been approved by the FDA and EMA[261,262]. Currently, one PD-L1 antibody, atezolizumab, has been approved by the FDA and EMA for treatment of urothelial cancer and non-small cell lung carcinoma[263]. Since PD-1 and CTLA-4 function in different stages of immune activation, combination of therapies targeting both pathways leads to additive anti-tumor effects[264,265].

CTLA-4 and PD-1 were the first of many targets for immunotherapy and the

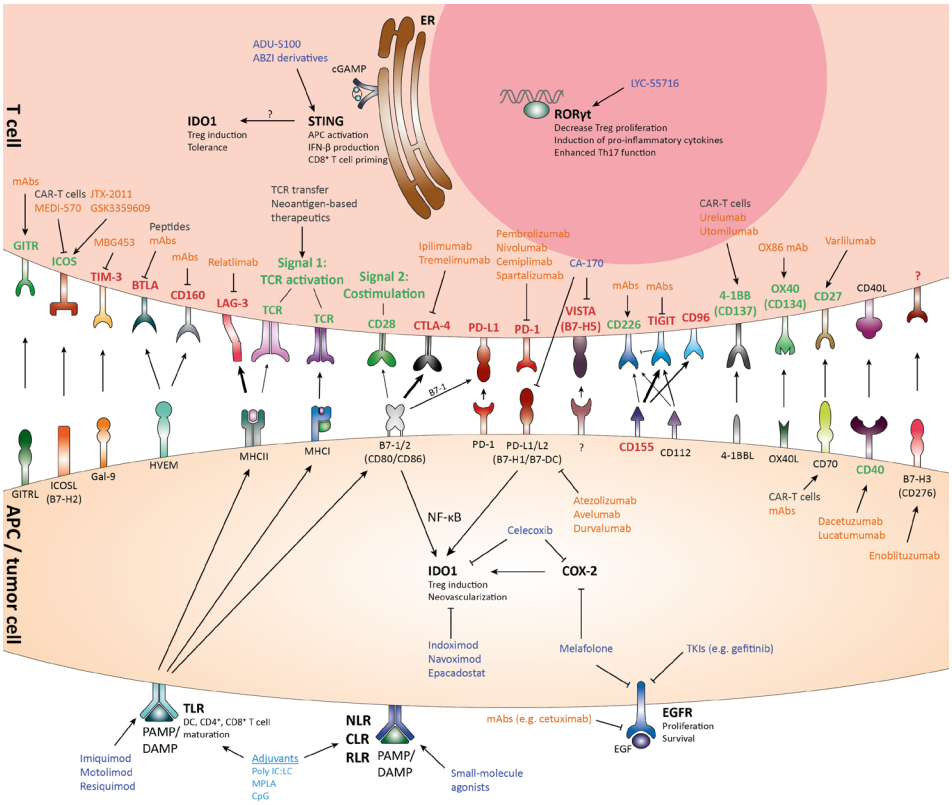

Figure 2. **Overview of checkpoint molecules and a selection of current preclinical and clinical therapeutics.** Green indicates stimulatory- and red inhibitory checkpoint molecules. Antibody therapies are depicted in orange; small molecules in dark blue; T cell therapies in grey. Arrows represent stimulation and T-bars represent inhibition. Arrow thickness corresponds to relative affinity compared to other ligands.

list is expanding immensely, as depicted in Figure 2. Both negative and positive regulators of the immune system are promising targets for cancer immunotherapy and autoimmune treatment and are actively pursued by pharmaceutical companies[266]. Combination with other treatment modalities has also led to synergistic effects, and consequently many ongoing clinical trials focus on combination therapies. Our perspective on the future of cancer immunotherapy is elaborately described in **Chapter 4**.

T CELL DETECTION THROUGH pMHCI MULTIMERS

The study of T cell interactions and specificities has immensely benefited from the development of pMHCI tetramers[267,268]. These tetramers conventionally consist of

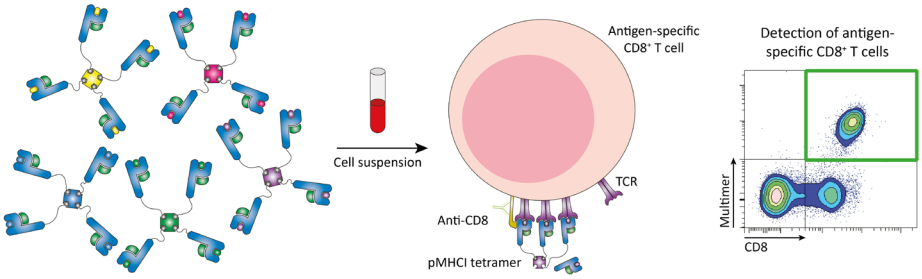

Figure 3. **Visualization and isolation of antigen-specific T cells using pMHCI tetramers.** Peptide-major histocompatibility complex class I (pMHCI) monomers are loaded with antigenic peptides and multimerized on fluorescently-labeled streptavidin. These reagents are widely used for the detection, isolation and characterization of antigen-specific $CD8^+$ T cells using flow cytometry.

MHCI monomers that are folded with a specific antigenic peptide, enzymatically biotinylated and subsequently multimerized on streptavidin. It is imperative that pMHC complexes are multimerized so that they can bind multiple TCRs on their corresponding $CD8^+$ T cell, to reduce typically high monomeric dissociation rates and remain attached to the T cell during further experimental analysis[269]. When labelled with a fluorophore these tetramers can be used to directly visualize (by flow cytometry) T cells specific for the bound antigen in a cell suspension, as depicted in Figure 3. Using this technology T cell responses can be quantified, characterized and monitored, providing invaluable information on an individual's immune status and responses to treatment[270,271]. One of the main advantages over traditional assays, such as ELISpot (enzyme-linked immune absorbent spot), cytokine staining or single-cell PCR, is that cells can even be sorted using FACS for further studies[272]. Besides diagnostics, pMHCI tetramers are widely used to study basic principles of ligand specificity, kinetics and dynamics of immune responses and employed in epitope mapping[273-276]. Although MHCII multimer technology is improving, considerable efforts are required to reach the same standards as those of MHCI multimers[277]. Progress is hampered by the difficulty to generate stable soluble forms of biotinylated MHCII, low frequency of $CD4^+$ T cells in circulation and generally low affinities of MHCII peptides[272].

Since first reports in 1996 MHCI tetramer technology has markedly improved[267]. A major step towards high-throughput analysis was made by the advance of technologies to exchange peptides on MHCI. Because MHCI molecules require a peptide (or chaperones) for stability, every specific pMHCI had to be folded with the desired peptide, and production of tetramers was therefore laborious and costly[278]. Where at first production of one or a few tetramers would take more than a week of work, the development of exchange technologies now allows generation of numerous MHCI tetramer variants in parallel. This approach involves folding of a large batch of MHCI monomers with a peptide that upon

applying a trigger exchanges for a peptide of interest. Various techniques have been investigated, utilizing dipeptides or chemicals, such as dithionite or periodate, as stoichiometric reagents[279-282]. One of the most successful exchange technologies was developed in a collaboration between the Ovaa and the Schumacher labs, and employs UV radiation as a trigger[283,284]. The peptide used for folding contains a central photocleavable amino acid, which becomes cleaved upon UV irradiation, resulting in dissociation of peptide remnants and liberation of the binding groove for association with a peptide of choice. This approach was easily extended to other alleles by incorporating the UV-cleavable amino acid in allele-specific epitopes[285]. More recently, I have developed an exchange technology based on temperature, which is described in detail in **Chapters 5 and 6**[286,287]. Unlike UV, which damages proteins and bleaches fluorophores, this exchange can be performed on already multimerized pMHCI. Exchange is induced by simply warming up the multimers, without the need for chemicals or specific lab equipment, and is therefore the easiest and most flexible exchange technology available to date.

In flow cytometry, the maximum number of detectable T cell specificities is limited by the number of available fluorochromes. Since sample volumes are often small, it is preferred to stain for as many specificities as possible in one sample. With development of combinatorial coding the number of simultaneously detectable reactivities increased from eight single stains to 28 dual combinations[288]. Adopting more complex coding strategies using six colors raises the number of detected specificities to 63, but also adds to the complexity of spectral overlap[289]. The most recently published strategy to scale up detection uses DNA labels instead of fluorophores[290], where pMHCI multimers are conjugated to a dextran backbone carrying a unique 25-oligonucleotide barcode sequence and a common fluorochrome. After assembly, different multimers are mixed and used to stain T cells in a similar fashion to conventional tetramer staining. Consequently, fluorophore-labelled T cells are isolated by FACS and their associated DNA is amplified and sequenced. This approach allows detection of over 1000 specificities in one sample in a high-throughput fashion and can be used for screening of epitopes in small sample volumes. First steps towards creating thermally-exchangeable DNA-labeled pMHCI multimers are described in **Chapter 7**.

Scope of this dissertation

The work described in this dissertation highlights how the adaptive immune system can be used to our advantage, either from a therapeutic or diagnostic perspective. In a therapeutic setting tumor- or pathogen-specific T cells can be activated to eliminate mutated or infected cells. **Chapter 2** describes the design and use of chemically enhanced altered peptide ligands as therapeutic vaccines. By modifying their anchoring residues, the affinity of wild-type epitopes to their corresponding MHC, HLA-A*02:01, could be markedly increased with the goal of improving pMHCI stability and prolonging recognition by antigen-specific T cells. The study described in **Chapter 3** then sets out to chemically enhance three HLA-A*02:01- and three HLA-A*03:01-presented influenza A epitopes, of varying affinity and immunodominance, to serve as a preventive vaccine. In vitro and in vivo assays demonstrate that affinity and immunogenicity of HLA-A*02:01 epitopes could be improved by modifying the anchoring residues, but that immunogenicity did not directly correlate with affinity. Peptide vaccines alone may not induce full anti-tumor responses, but they efficiently initiate T cell activation, thus supporting other immunotherapies. Our opinion on the potential contribution of small-molecule drugs is detailed in **Chapter 4**.

The classic reagents for studying antigen-specific T cell responses are pMHCI multimers. **Chapter 5** summarizes the development of a novel technique to exchange peptides on MHCI multimers. This method, described in a step-by-step protocol in **Chapter 6**, allows the generation of large panels of pMHCI multimers in parallel. Implementation of DNA barcoding increases the scale of detectable specificities. Such high-throughput approaches may prove particularly useful in neoantigen identification, as described in **Chapter 7**.

The findings of the research described in this dissertation are recapitulated in the final chapter, where we also provide suggestions for future directions.

1

References

1. Flajnik, M.F. & Du Pasquier, L. Evolution of innate and adaptive immunity: can we draw a line? *Trends Immunol* **25**, 640-644 (2004).
2. Vivier, E. & Malissen, B. Innate and adaptive immunity: specificities and signaling hierarchies revisited. *Nat Immunol* **6**, 17-21 (2005).
3. Medzhitov, R. & Janeway, C. Innate immune recognition: mechanisms and pathways. *Immunol Rev* **173**, 89-97 (2000).
4. Boehm, T. & Swann, J.B. Origin and Evolution of Adaptive Immunity. *Annu Rev Anim Biosci* **2**, 259-283 (2014).
5. Janeway, C.A., Jr. & Medzhitov, R. Innate immune recognition. *Annu Rev Immunol* **20**, 197-216 (2002).
6. Gourley, T.S., Wherry, E.J., Masopust, D. & Ahmed, R. Generation and maintenance of immunological memory. *Semin Immunol* **16**, 323-333 (2004).
7. Klein, L., Kyewski, B., Allen, P.M. & Hogquist, K.A. Positive and negative selection of the T cell repertoire: what thymocytes see (and don't see). *Nat Rev Immunol* **14**, 377-391 (2014).
8. Kyewski, B. & Klein, L. A central role for central tolerance. *Annu Rev Immunol* **24**, 571-606 (2006).
9. Starr, T.K., Jameson, S.C. & Hogquist, K.A. Positive and negative selection of T cells. *Annu Rev Immunol* **21**, 139-176 (2003).
10. Jensen, P.E. Recent advances in antigen processing and presentation. *Nat Immunol* **8**, 1041-1048 (2007).
11. Rock, K.L., York, I.A. & Goldberg, A.L. Post-proteasomal antigen processing for major histocompatibility complex class I presentation. *Nat Immunol* **5**, 670-677 (2004).
12. Rock, K.L., York, I.A., Saric, T. & Goldberg, A.L. Protein degradation and the generation of MHC class I-presented peptides. *Adv Immunol* **80**, 1-70 (2002).
13. Yewdell, J.W., Reits, E. & Neefjes, J. Making sense of mass destruction: quantitating MHC class I antigen presentation. *Nat Rev Immunol* **3**, 952-961 (2003).
14. Schubert, U., *et al.* Rapid degradation of a large fraction of newly synthesized proteins by proteasomes. *Nature* **404**, 770-774 (2000).
15. Reits, E.A., Vos, J.C., Gromme, M. & Neefjes, J. The major substrates for TAP in vivo are derived from newly synthesized proteins. *Nature* **404**, 774-778 (2000).
16. Neefjes, J., Jongsma, M.L., Paul, P. & Bakke, O. Towards a systems understanding of MHC class I and MHC class II antigen presentation. *Nat Rev Immunol* **11**, 823-836 (2011).
17. Khan, S., *et al.* Cutting edge: neosynthesis is required for the presentation of a T cell epitope from a long-lived viral protein. *J Immunol* **167**, 4801-4804 (2001).
18. Vigneron, N., *et al.* An antigenic peptide produced by peptide splicing in the proteasome. *Science* **304**, 587-590 (2004).
19. Liepe, J., *et al.* A large fraction of HLA class I ligands are proteasome-generated spliced peptides. *Science* **354**, 354-358 (2016).
20. Mishto, M. & Liepe, J. Post-Translational Peptide Splicing and T Cell Responses. *Trends Immunol* **38**, 904-915 (2017).
21. Mannering, S.I., So, M., Elso, C.M. & Kay, T.W.H. Shuffling peptides to create T-cell epitopes: does the immune system play cards? *Immunol Cell Biol* **96**, 34-40 (2018).
22. Blees, A., *et al.* Structure of the human MHC-I peptide-loading complex. *Nature* **551**, 525-528 (2017).
23. Ortmann, B., *et al.* A critical role for tapasin in the assembly and function of multimeric MHC class I-TAP complexes. *Science* **277**, 1306-1309 (1997).
24. Watts, C. The exogenous pathway for antigen presentation on major histocompatibility complex class II and CD1 molecules. *Nat Immunol* **5**, 685-692 (2004).
25. Bennett, K., *et al.* Antigen Processing for Presentation by Class-Ii Major Histocompatibility Complex Requires Cleavage by Cathepsin-E. *Eur J Immunol* **22**, 1519-1524 (1992).
26. Fruh, K., Gruhler, A., Krishna, R.M. & Schoenhals, G.J. A comparison of viral immune escape strategies targeting the MHC class I assembly pathway. *Immunol Rev* **168**, 157-166 (1999).
27. Horst, D., Verweij, M.C., Davison, A.J., Ressing, M.E. & Wiertz, E.J. Viral evasion of T cell immunity: ancient mechanisms offering new applications. *Curr Opin Immunol* **23**, 96-103 (2011).

28. Segura, E. & Amigorena, S. Cross-Presentation in Mouse and Human Dendritic Cells. *Adv Immunol* **127**, 1-31 (2015).
29. Mescher, M.F., *et al.* Signals required for programming effector and memory development by $CD8^+$ T cells. *Immunol Rev* **211**, 81-92 (2006).
30. Momburg, F., Roelse, J., Hammerling, G.J. & Neefjes, J.J. Peptide size selection by the major histocompatibility complex-encoded peptide transporter. *J Exp Med* **179**, 1613-1623 (1994).
31. Parcej, D. & Tampe, R. ABC proteins in antigen translocation and viral inhibition. *Nat Chem Biol* **6**, 572-580 (2010).
32. Serwold, T., Gaw, S. & Shastri, N. ER aminopeptidases generate a unique pool of peptides for MHC class I molecules. *Nat Immunol* **2**, 644-651 (2001).
33. Rock, K.L., Reits, E. & Neefjes, J. Present Yourself! By MHC Class I and MHC Class II Molecules. *Trends Immunol* **37**, 724-737 (2016).
34. Yewdell, J.W. & Bennink, J.R. Immunodominance in major histocompatibility complex class I-restricted T lymphocyte responses. *Annu Rev Immunol* **17**, 51-88 (1999).
35. Kersh, G.J., Kersh, E.N., Fremont, D.H. & Allen, P.M. High- and low-potency ligands with similar affinities for the TCR: the importance of kinetics in TCR signaling. *Immunity* **9**, 817-826 (1998).
36. Kazansky, D.B. MHC restriction and allogeneic immune responses. *J Immunotoxicol* **5**, 369-384 (2008).
37. Langenhorst, D., *et al.* CD28 Costimulation of T Helper 1 Cells Enhances Cytokine Release In Vivo. *Front Immunol* **9**, 1060 (2018).
38. Gross, J.A., Callas, E. & Allison, J.P. Identification and distribution of the costimulatory receptor CD28 in the mouse. *J Immunol* **149**, 380-388 (1992).
39. Sharpe, A.H. & Abbas, A.K. T-cell costimulation--biology, therapeutic potential, and challenges. *N Engl J Med* **355**, 973-975 (2006).
40. Greenwald, R.J., Freeman, G.J. & Sharpe, A.H. The B7 family revisited. *Annu Rev Immunol* **23**, 515-548 (2005).
41. DeSilva, D.R., Urdahl, K.B. & Jenkins, M.K. Clonal anergy is induced in vitro by T cell receptor occupancy in the absence of proliferation. *J Immunol* **147**, 3261-3267 (1991).
42. Kalia, V. & Sarkar, S. Regulation of Effector and Memory CD8 T Cell Differentiation by IL-2-A Balancing Act. *Front Immunol* **9**, 2987 (2018).
43. Hutloff, A., *et al.* ICOS is an inducible T-cell co-stimulator structurally and functionally related to CD28. *Nature* **397**, 263-266 (1999).
44. Swallow, M.M., Wallin, J.J. & Sha, W.C. B7h, a novel costimulatory homolog of B7.1 and B7.2, is induced by TNFalpha. *Immunity* **11**, 423-432 (1999).
45. Okamoto, N., Tezuka, K., Kato, M., Abe, R. & Tsuji, T. PI3-kinase and MAP-kinase signaling cascades in AILIM/ICOS- and CD28-costimulated T-cells have distinct functions between cell proliferation and IL-10 production. *Biochem Biophys Res Commun* **310**, 691-702 (2003).
46. Sharpe, A.H. & Freeman, G.J. The B7-CD28 superfamily. *Nat Rev Immunol* **2**, 116-126 (2002).
47. Bachmann, M.F., Speiser, D.E., Mak, T.W. & Ohashi, P.S. Absence of co-stimulation and not the intensity of TCR signaling is critical for the induction of T cell unresponsiveness in vivo. *Eur J Immunol* **29**, 2156-2166 (1999).
48. Curtsinger, J.M. & Mescher, M.F. Inflammatory cytokines as a third signal for T cell activation. *Curr Opin Immunol* **22**, 333-340 (2010).
49. Valenzuela, J., Schmidt, C. & Mescher, M. The roles of IL-12 in providing a third signal for clonal expansion of naive CD8 T cells. *J Immunol* **169**, 6842-6849 (2002).
50. Curtsinger, J.M., Lins, D.C. & Mescher, M.F. Signal 3 determines tolerance versus full activation of naive CD8 T cells: dissociating proliferation and development of effector function. *J Exp Med* **197**, 1141-1151 (2003).
51. Ben-Sasson, S.Z., *et al.* IL-1 acts directly on CD4 T cells to enhance their antigen-driven expansion and differentiation. *Proc Natl Acad Sci U S A* **106**, 7119-7124 (2009).
52. Scott, P. IL-12: initiation cytokine for cell-mediated immunity. *Science* **260**, 496-497 (1993).
53. Madden, D.R. The three-dimensional structure of peptide-MHC complexes. *Annu Rev Immunol* **13**, 587-622 (1995).
54. Stern, L.J. & Wiley, D.C. Antigenic peptide binding by class I and class II histocompatibility proteins. *Structure* **2**, 245-251 (1994).

55. Lafuente, E.M. & Reche, P.A. Prediction of MHC-peptide binding: a systematic and comprehensive overview. *Curr Pharm Des* **15**, 3209-3220 (2009).
56. Bouvier, M. & Wiley, D.C. Importance of peptide amino and carboxyl termini to the stability of MHC class I molecules. *Science* **265**, 398-402 (1994).
57. Chicz, R.M., *et al.* Predominant naturally processed peptides bound to HLA-DR1 are derived from MHC-related molecules and are heterogeneous in size. *Nature* **358**, 764-768 (1992).
58. Zacharias, M. & Springer, S. Conformational flexibility of the MHC class I alpha1-alpha2 domain in peptide bound and free states: a molecular dynamics simulation study. *Biophys J* **87**, 2203-2214 (2004).
59. Horton, R., *et al.* Gene map of the extended human MHC. *Nat Rev Genet* **5**, 889-899 (2004).
60. Xie, T., *et al.* Analysis of the gene-dense major histocompatibility complex class III region and its comparison to mouse. *Genome Res* **13**, 2621-2636 (2003).
61. Marsh, S.G., *et al.* Nomenclature for factors of the HLA system, 2010. *Tissue Antigens* **75**, 291-455 (2010).
62. Parham, P., Lawlor, D.A., Lomen, C.E. & Ennis, P.D. Diversity and diversification of HLA-A,B,C alleles. *J Immunol* **142**, 3937-3950 (1989).
63. The, M.H.C.s.c. Complete sequence and gene map of a human major histocompatibility complex. *Nature* **401**, 921 (1999).
64. Meyer, D., VR, C.A., Bitarello, B.D., DY, C.B. & Nunes, K. A genomic perspective on HLA evolution. *Immunogenetics* (2017).
65. Falk, K., Rotzschke, O., Stevanovic, S., Jung, G. & Rammensee, H.G. Allele-specific motifs revealed by sequencing of self-peptides eluted from MHC molecules. *Nature* **351**, 290-296 (1991).
66. de Bakker, P.I., *et al.* A high-resolution HLA and SNP haplotype map for disease association studies in the extended human MHC. *Nat Genet* **38**, 1166-1172 (2006).
67. Middleton, D., Menchaca, L., Rood, H. & Komerofsky, R. New allele frequency database: http://www.allelefrequencies.net. *Tissue Antigens* **61**, 403-407 (2003).
68. Gonzalez-Galarza, F.F., *et al.* Allele frequency net 2015 update: new features for HLA epitopes, KIR and disease and HLA adverse drug reaction associations. *Nucleic Acids Res* **43**, D784-788 (2015).
69. Meyer, D., Single, R.M., Mack, S.J., Erlich, H.A. & Thomson, G. Signatures of demographic history and natural selection in the human major histocompatibility complex Loci. *Genetics* **173**, 2121-2142 (2006).
70. Rammensee, H.G., Friede, T. & Stevanoviic, S. MHC ligands and peptide motifs: first listing. *Immunogenetics* **41**, 178-228 (1995).
71. Falk, K., Rotzschke, O., Stevanovic, S., Jung, G. & Rammensee, H.G. Pool sequencing of natural HLA-DR, DQ, and DP ligands reveals detailed peptide motifs, constraints of processing, and general rules. *Immunogenetics* **39**, 230-242 (1994).
72. Parker, K.C., *et al.* Sequence motifs important for peptide binding to the human MHC class I molecule, HLA-A2. *J Immunol* **149**, 3580-3587 (1992).
73. Chaix, R., Cao, C. & Donnelly, P. Is mate choice in humans MHC-dependent? *PLoS Genet* **4**, e1000184 (2008).
74. Ober, C., *et al.* HLA and mate choice in humans. *Am J Hum Genet* **61**, 497-504 (1997).
75. Wedekind, C. & Furi, S. Body odour preferences in men and women: do they aim for specific MHC combinations or simply heterozygosity? *Proc Biol Sci* **264**, 1471-1479 (1997).
76. Vita, R., *et al.* The immune epitope database (IEDB) 3.0. *Nucleic Acids Res* **43**, D405-412 (2015).
77. Rammensee, H., Bachmann, J., Emmerich, N.P., Bachor, O.A. & Stevanovic, S. SYFPEITHI: database for MHC ligands and peptide motifs. *Immunogenetics* **50**, 213-219 (1999).
78. Robinson, J., *et al.* The IPD and IMGT/HLA database: allele variant databases. *Nucleic Acids Res* **43**, D423-431 (2015).
79. Sette, A. & Sidney, J. HLA supertypes and supermotifs: a functional perspective on HLA polymorphism. *Curr Opin Immunol* **10**, 478-482 (1998).
80. Wiebe, C. & Nickerson, P. Human leukocyte antigen mismatch and precision medicine in transplantation. *Curr Opin Organ Transplant* (2018).
81. Bertaina, A. & Andreani, M. Major Histocompatibility Complex and Hematopoietic Stem Cell Transplantation: Beyond the Classical HLA Polymorphism. *Int J Mol Sci* **19**(2018).
82. Lee, S.J., *et al.* High-resolution donor-recipient HLA matching contributes to the success of un-

related donor marrow transplantation. *Blood* **110**, 4576-4583 (2007).
83. Flomenberg, N., *et al.* Impact of HLA class I and class II high-resolution matching on outcomes of unrelated donor bone marrow transplantation: HLA-C mismatching is associated with a strong adverse effect on transplantation outcome. *Blood* **104**, 1923-1930 (2004).
84. Garrett, T.P., Saper, M.A., Bjorkman, P.J., Strominger, J.L. & Wiley, D.C. Specificity pockets for the side chains of peptide antigens in HLA-Aw68. *Nature* **342**, 692-696 (1989).
85. Brown, J.H., *et al.* Three-dimensional structure of the human class II histocompatibility antigen HLA-DR1. *Nature* **364**, 33-39 (1993).
86. Stern, L.J., *et al.* Crystal structure of the human class II MHC protein HLA-DR1 complexed with an influenza virus peptide. *Nature* **368**, 215-221 (1994).
87. Sidney, J., Peters, B., Frahm, N., Brander, C. & Sette, A. HLA class I supertypes: a revised and updated classification. *BMC Immunol* **9**, 1 (2008).
88. van Deutekom, H.W. & Kesmir, C. Zooming into the binding groove of HLA molecules: which positions and which substitutions change peptide binding most? *Immunogenetics* **67**, 425-436 (2015).
89. Lundegaard, C., *et al.* NetMHC-3.0: accurate web accessible predictions of human, mouse and monkey MHC class I affinities for peptides of length 8-11. *Nucleic Acids Res* **36**, W509-512 (2008).
90. Lundegaard, C., Lund, O., Buus, S. & Nielsen, M. Major histocompatibility complex class I binding predictions as a tool in epitope discovery. *Immunology* **130**, 309-318 (2010).
91. Slansky, J.E. & Jordan, K.R. The Goldilocks model for TCR-too much attraction might not be best for vaccine design. *PLoS Biol* **8**(2010).
92. vanderBurg, S.H., Visseren, M.J.W., Brandt, R.M.P., Kast, W.M. & Melief, C.J.M. Immunogenicity of peptides bound to MHC class I molecules depends on the MHC-peptide complex stability. *Journal of Immunology* **156**, 3308-3314 (1996).
93. Sette, A., *et al.* The relationship between class I binding affinity and immunogenicity of potential cytotoxic T cell epitopes. *J Immunol* **153**, 5586-5592 (1994).
94. Speiser, D.E., *et al.* Unmodified self antigen triggers human CD8 T cells with stronger tumor reactivity than altered antigen. *Proc Natl Acad Sci U S A* **105**, 3849-3854 (2008).
95. McMahan, R.H., *et al.* Relating TCR-peptide-MHC affinity to immunogenicity for the design of tumor vaccines. *J Clin Invest* **116**, 2543-2551 (2006).
96. Harndahl, M., *et al.* Peptide-MHC class I stability is a better predictor than peptide affinity of CTL immunogenicity. *Eur J Immunol* **42**, 1405-1416 (2012).
97. Rosendahl Huber, S.K., *et al.* Chemical Modification of Influenza CD8$^+$ T-Cell Epitopes Enhances Their Immunogenicity Regardless of Immunodominance. *PLoS One* **11**, e0156462 (2016).
98. Corse, E., Gottschalk, R.A. & Allison, J.P. Strength of TCR-peptide/MHC interactions and in vivo T cell responses. *J Immunol* **186**, 5039-5045 (2011).
99. Cemerski, S., *et al.* The stimulatory potency of T cell antigens is influenced by the formation of the immunological synapse. *Immunity* **26**, 345-355 (2007).
100. Jorgensen, K.W., Rasmussen, M., Buus, S. & Nielsen, M. NetMHCstab - predicting stability of peptide-MHC-I complexes; impacts for cytotoxic T lymphocyte epitope discovery. *Immunology* **141**, 18-26 (2014).
101. Rasmussen, M., *et al.* Pan-Specific Prediction of Peptide-MHC Class I Complex Stability, a Correlate of T Cell Immunogenicity. *J Immunol* **197**, 1517-1524 (2016).
102. McKeithan, T.W. Kinetic proofreading in T-cell receptor signal transduction. *Proc Natl Acad Sci U S A* **92**, 5042-5046 (1995).
103. Huang, J., *et al.* The kinetics of two-dimensional TCR and pMHC interactions determine T-cell responsiveness. *Nature* **464**, 932-936 (2010).
104. Valitutti, S. The Serial Engagement Model 17 Years After: From TCR Triggering to Immunotherapy. *Front Immunol* **3**, 272 (2012).
105. Kalergis, A.M., *et al.* Efficient T cell activation requires an optimal dwell-time of interaction between the TCR and the pMHC complex. *Nat Immunol* **2**, 229-234 (2001).
106. Gonzalez, P.A., *et al.* T cell receptor binding kinetics required for T cell activation depend on the density of cognate ligand on the antigen-presenting cell. *Proc Natl Acad Sci U S A* **102**, 4824-4829 (2005).
107. Stewart, C.A., *et al.* Complete MHC haplotype sequencing for common disease gene mapping.

Genome Res **14**, 1176-1187 (2004).
108. Howell, W.M. HLA and disease: guilt by association. *Int J Immunogenet* **41**, 1-12 (2014).
109. Carrington, M. & O'Brien, S.J. The influence of HLA genotype on AIDS. *Annu Rev Med* **54**, 535-551 (2003).
110. Gao, X., *et al.* HLA-B alleles associate consistently with HIV heterosexual transmission, viral load, and progression to AIDS, but not susceptibility to infection. *AIDS* **24**, 1835-1840 (2010).
111. Garamszegi, L.Z. Global distribution of malaria-resistant MHC-HLA alleles: the number and frequencies of alleles and malaria risk. *Malar J* **13**, 349 (2014).
112. Lima-Junior Jda, C. & Pratt-Riccio, L.R. Major Histocompatibility Complex and Malaria: Focus on Plasmodium vivax Infection. *Front Immunol* **7**, 13 (2016).
113. Traherne, J.A., *et al.* Genetic analysis of completely sequenced disease-associated MHC haplotypes identifies shuffling of segments in recent human history. *PLoS Genet* **2**, e9 (2006).
114. Davies, J.L., *et al.* A genome-wide search for human type 1 diabetes susceptibility genes. *Nature* **371**, 130-136 (1994).
115. Svejgaard, A. The immunogenetics of multiple sclerosis. *Immunogenetics* **60**, 275-286 (2008).
116. Fernando, M.M., *et al.* Defining the role of the MHC in autoimmunity: a review and pooled analysis. *PLoS Genet* **4**, e1000024 (2008).
117. Black, M.H., *et al.* HLA-associated phenotypes in youth with autoimmune diabetes. *Pediatr Diabetes* **14**, 121-128 (2013).
118. Larsen, C.E. & Alper, C.A. The genetics of HLA-associated disease. *Curr Opin Immunol* **16**, 660-667 (2004).
119. Ranganathan, V., Gracey, E., Brown, M.A., Inman, R.D. & Haroon, N. Pathogenesis of ankylosing spondylitis - recent advances and future directions. *Nat Rev Rheumatol* **13**, 359-367 (2017).
120. Harbo, H.F., *et al.* Genes in the HLA class I region may contribute to the HLA class II-associated genetic susceptibility to multiple sclerosis. *Tissue Antigens* **63**, 237-247 (2004).
121. Liu, E., *et al.* Risk of pediatric celiac disease according to HLA haplotype and country. *N Engl J Med* **371**, 42-49 (2014).
122. Qiao, S.W., Iversen, R., Raki, M. & Sollid, L.M. The adaptive immune response in celiac disease. *Semin Immunopathol* **34**, 523-540 (2012).
123. Forabosco, P., *et al.* Meta-analysis of genome-wide linkage studies of systemic lupus erythematosus. *Genes Immun* **7**, 609-614 (2006).
124. Brewerton, D.A., *et al.* Ankylosing spondylitis and HL-A 27. *Lancet* **1**, 904-907 (1973).
125. Schlosstein, L., Terasaki, P.I., Bluestone, R. & Pearson, C.M. High association of an HL-A antigen, W27, with ankylosing spondylitis. *N Engl J Med* **288**, 704-706 (1973).
126. Dendrou, C.A., Petersen, J., Rossjohn, J. & Fugger, L. HLA variation and disease. *Nat Rev Immunol* **18**, 325-339 (2018).
127. Pohlmann, T., *et al.* Differential peptide dynamics is linked to major histocompatibility complex polymorphism. *J Biol Chem* **279**, 28197-28201 (2004).
128. Narzi, D., *et al.* Dynamical characterization of two differentially disease associated MHC class I proteins in complex with viral and self-peptides. *J Mol Biol* **415**, 429-442 (2012).
129. Knapp, B., *et al.* 3-Layer-based analysis of peptide-MHC interaction: in silico prediction, peptide binding affinity and T cell activation in a relevant allergen-specific model. *Mol Immunol* **46**, 1839-1844 (2009).
130. Ayres, C.M., Corcelli, S.A. & Baker, B.M. Peptide and Peptide-Dependent Motions in MHC Proteins: Immunological Implications and Biophysical Underpinnings. *Front Immunol* **8**, 935 (2017).
131. Thorsby, E. & Lie, B.A. HLA associated genetic predisposition to autoimmune diseases: Genes involved and possible mechanisms. *Transpl Immunol* **14**, 175-182 (2005).
132. Doyle, H.A. & Mamula, M.J. Post-translational protein modifications in antigen recognition and autoimmunity. *Trends Immunol* **22**, 443-449 (2001).
133. Engelhard, V.H., Altrich-Vanlith, M., Ostankovitch, M. & Zarling, A.L. Post-translational modifications of naturally processed MHC-binding epitopes. *Curr Opin Immunol* **18**, 92-97 (2006).
134. McGinty, J.W., Marre, M.L., Bajzik, V., Piganelli, J.D. & James, E.A. T cell epitopes and post-translationally modified epitopes in type 1 diabetes. *Curr Diab Rep* **15**, 90 (2015).
135. Strollo, R., *et al.* Antibodies to post-translationally modified insulin in type 1 diabetes. *Diabetologia* **58**, 2851-2860 (2015).
136. Sidney, J., *et al.* Low HLA binding of diabetes-associated $CD8^+$ T-cell epitopes is increased by

post translational modifications. *BMC Immunol* **19**, 12 (2018).
137. Schellekens, G.A., de Jong, B.A., van den Hoogen, F.H., van de Putte, L.B. & van Venrooij, W.J. Citrulline is an essential constituent of antigenic determinants recognized by rheumatoid arthritis-specific autoantibodies. *J Clin Invest* **101**, 273-281 (1998).
138. Vincent, C., Nogueira, L., Clavel, C., Sebbag, M. & Serre, G. Autoantibodies to citrullinated proteins: ACPA. *Autoimmunity* **38**, 17-24 (2005).
139. Darrah, E. & Andrade, F. Rheumatoid arthritis and citrullination. *Curr Opin Rheumatol* **30**, 72-78 (2018).
140. Fox, D.A. Citrullination: A Specific Target for the Autoimmune Response in Rheumatoid Arthritis. *J Immunol* **195**, 5-7 (2015).
141. Sebbag, M., *et al.* Clinical and pathophysiological significance of the autoimmune response to citrullinated proteins in rheumatoid arthritis. *Joint Bone Spine* **71**, 493-502 (2004).
142. Pavlos, R., *et al.* Shared peptide binding of HLA Class I and II alleles associate with cutaneous nevirapine hypersensitivity and identify novel risk alleles. *Sci Rep-Uk* **7**(2017).
143. Hetherington, S., *et al.* Hypersensitivity reactions during therapy with the nucleoside reverse transcriptase inhibitor abacavir. *Clin Ther* **23**, 1603-1614 (2001).
144. Ruiz-Iruela, C., *et al.* HLA-B*57: 01 genotyping in the prevention of hypersensitivity to abacavir: 5 years of experience. *Pharmacogenet Genomics* **26**, 390-396 (2016).
145. Siljic, M., *et al.* High Frequency of Human Leukocyte Antigen-B*57:01 Allele Carriers among HIV-Infected Patients in Serbia. *Intervirology* **60**, 43-47 (2017).
146. Chessman, D., *et al.* Human leukocyte antigen class I-restricted activation of $CD8^+$ T cells provides the immunogenetic basis of a systemic drug hypersensitivity. *Immunity* **28**, 822-832 (2008).
147. Ostrov, D.A., *et al.* Drug hypersensitivity caused by alteration of the MHC-presented self-peptide repertoire. *Proc Natl Acad Sci U S A* **109**, 9959-9964 (2012).
148. Illing, P.T., *et al.* Immune self-reactivity triggered by drug-modified HLA-peptide repertoire. *Nature* **486**, 554-558 (2012).
149. Yerly, D., *et al.* Structural Elements Recognized by Abacavir-Induced T Cells. *Int J Mol Sci* **18**(2017).
150. Gross, C.P. & Sepkowitz, K.A. The myth of the medical breakthrough: smallpox, vaccination, and Jenner reconsidered. *Int J Infect Dis* **3**, 54-60 (1998).
151. Burnet, F.M. Implications of immunological surveillance for cancer therapy. *Isr J Med Sci* **7**, 9-16 (1971).
152. Thomas, L. On immunosurveillance in human cancer. *Yale J Biol Med* **55**, 329-333 (1982).
153. Shankaran, V., *et al.* IFNgamma and lymphocytes prevent primary tumour development and shape tumour immunogenicity. *Nature* **410**, 1107-1111 (2001).
154. Klein, G. & Klein, E. Immune surveillance against virus-induced tumors and nonrejectability of spontaneous tumors: contrasting consequences of host versus tumor evolution. *Proc Natl Acad Sci U S A* **74**, 2121-2125 (1977).
155. Corthay, A. Does the immune system naturally protect against cancer? *Front Immunol* **5**, 197 (2014).
156. Chen, D.S. & Mellman, I. Oncology meets immunology: the cancer-immunity cycle. *Immunity* **39**, 1-10 (2013).
157. Pardoll, D. Does the immune system see tumors as foreign or self? *Annu Rev Immunol* **21**, 807-839 (2003).
158. Getnet, D., *et al.* Tumor recognition and self-recognition induce distinct transcriptional profiles in antigen-specific CD4 T cells. *J Immunol* **182**, 4675-4685 (2009).
159. Willimsky, G. & Blankenstein, T. Sporadic immunogenic tumours avoid destruction by inducing T-cell tolerance. *Nature* **437**, 141-146 (2005).
160. Dunn, G.P., Bruce, A.T., Ikeda, H., Old, L.J. & Schreiber, R.D. Cancer immunoediting: from immunosurveillance to tumor escape. *Nat Immunol* **3**, 991-998 (2002).
161. Schreiber, R.D., Old, L.J. & Smyth, M.J. Cancer immunoediting: integrating immunity's roles in cancer suppression and promotion. *Science* **331**, 1565-1570 (2011).
162. Mellman, I., Coukos, G. & Dranoff, G. Cancer immunotherapy comes of age. *Nature* **480**, 480-489 (2011).
163. Ochsenreither, S., *et al.* "Wilms Tumor Protein 1" (WT1) peptide vaccination-induced complete remission in a patient with acute myeloid leukemia is accompanied by the emergence of a

predominant T-cell clone both in blood and bone marrow. *J Immunother* **34**, 85-91 (2011).
164. Melief, C.J., van Hall, T., Arens, R., Ossendorp, F. & van der Burg, S.H. Therapeutic cancer vaccines. *J Clin Invest* **125**, 3401-3412 (2015).
165. Steinbrook, R. The potential of human papillomavirus vaccines. *N Engl J Med* **354**, 1109-1112 (2006).
166. Wiemann, B. & Starnes, C.O. Coley's toxins, tumor necrosis factor and cancer research: a historical perspective. *Pharmacology & therapeutics* **64**, 529-564 (1994).
167. Banchereau, J. & Palucka, K. Immunotherapy: Cancer vaccines on the move. *Nat Rev Clin Oncol* **15**, 9-10 (2018).
168. Wang, R.F. & Rosenberg, S.A. Human tumor antigens for cancer vaccine development. *Immunol Rev* **170**, 85-100 (1999).
169. Novellino, L., Castelli, C. & Parmiani, G. A listing of human tumor antigens recognized by T cells: March 2004 update. *Cancer Immunol Immunother* **54**, 187-207 (2005).
170. Parmiani, G., De Filippo, A., Novellino, L. & Castelli, C. Unique human tumor antigens: immunobiology and use in clinical trials. *J Immunol* **178**, 1975-1979 (2007).
171. Chomez, P., *et al.* An overview of the MAGE gene family with the identification of all human members of the family. *Cancer Res* **61**, 5544-5551 (2001).
172. Gnjatic, S., *et al.* NY-ESO-1: review of an immunogenic tumor antigen. *Adv Cancer Res* **95**, 1-30 (2006).
173. Hanada, K., Yewdell, J.W. & Yang, J.C. Immune recognition of a human renal cancer antigen through post-translational protein splicing. *Nature* **427**, 252-256 (2004).
174. Boon, T., Cerottini, J.C., Van den Eynde, B., van der Bruggen, P. & Van Pel, A. Tumor antigens recognized by T lymphocytes. *Annu Rev Immunol* **12**, 337-365 (1994).
175. Colella, T.A., *et al.* Self-tolerance to the murine homologue of a tyrosinase-derived melanoma antigen: implications for tumor immunotherapy. *J Exp Med* **191**, 1221-1232 (2000).
176. McWilliams, J.A., *et al.* Age-dependent tolerance to an endogenous tumor-associated antigen. *Vaccine* **26**, 1863-1873 (2008).
177. Schumacher, T.N. & Hacohen, N. Neoantigens encoded in the cancer genome. *Curr Opin Immunol* **41**, 98-103 (2016).
178. van den Bulk, J., Verdegaal, E.M. & de Miranda, N.F. Cancer immunotherapy: broadening the scope of targetable tumours. *Open Biol* **8**(2018).
179. Kreiter, S., Castle, J.C., Tureci, O. & Sahin, U. Targeting the tumor mutanome for personalized vaccination therapy. *Oncoimmunology* **1**, 768-769 (2012).
180. Wang, R.F. & Wang, H.Y. Immune targets and neoantigens for cancer immunotherapy and precision medicine. *Cell Res* **27**, 11-37 (2017).
181. Mahnke, K., *et al.* Targeting of antigens to activated dendritic cells in vivo cures metastatic melanoma in mice. *Cancer Res* **65**, 7007-7012 (2005).
182. Linnemann, C., *et al.* High-throughput epitope discovery reveals frequent recognition of neo-antigens by $CD4^+$ T cells in human melanoma. *Nat Med* **21**, 81-85 (2015).
183. Vigneron, N., Stroobant, V., Van den Eynde, B.J. & van der Bruggen, P. Database of T cell-defined human tumor antigens: the 2013 update. *Cancer Immun* **13**, 15 (2013).
184. Ott, P.A., *et al.* An immunogenic personal neoantigen vaccine for patients with melanoma. *Nature* **547**, 217-221 (2017).
185. Kreiter, S., *et al.* Mutant MHC class II epitopes drive therapeutic immune responses to cancer. *Nature* **520**, 692-696 (2015).
186. Karasaki, T., *et al.* Prediction and prioritization of neoantigens: integration of RNA sequencing data with whole-exome sequencing. *Cancer Sci* **108**, 170-177 (2017).
187. Matsushita, H., *et al.* Cancer exome analysis reveals a T-cell-dependent mechanism of cancer immunoediting. *Nature* **482**, 400-404 (2012).
188. Yadav, M., *et al.* Predicting immunogenic tumour mutations by combining mass spectrometry and exome sequencing. *Nature* **515**, 572-576 (2014).
189. Schumacher, T.N. & Schreiber, R.D. Neoantigens in cancer immunotherapy. *Science* **348**, 69-74 (2015).
190. Tran, E., *et al.* Immunogenicity of somatic mutations in human gastrointestinal cancers. *Science* **350**, 1387-1390 (2015).
191. van Rooij, N., *et al.* Tumor exome analysis reveals neoantigen-specific T-cell reactivity in an

ipilimumab-responsive melanoma. *J Clin Oncol* **31**, e439-442 (2013).
192. Rajasagi, M., *et al.* Systematic identification of personal tumor-specific neoantigens in chronic lymphocytic leukemia. *Blood* **124**, 453-462 (2014).
193. Purcell, A.W., McCluskey, J. & Rossjohn, J. More than one reason to rethink the use of peptides in vaccine design. *Nat Rev Drug Discov* **6**, 404-414 (2007).
194. Sette, A. & Fikes, J. Epitope-based vaccines: an update on epitope identification, vaccine design and delivery. *Curr Opin Immunol* **15**, 461-470 (2003).
195. Slansky, J.E., *et al.* Enhanced antigen-specific antitumor immunity with altered peptide ligands that stabilize the MHC-peptide-TCR complex. *Immunity* **13**, 529-538 (2000).
196. Cole, D.K., *et al.* Modification of MHC anchor residues generates heteroclitic peptides that alter TCR binding and T cell recognition. *J Immunol* **185**, 2600-2610 (2010).
197. Sloan-Lancaster, J. & Allen, P.M. Altered peptide ligand-induced partial T cell activation: molecular mechanisms and role in T cell biology. *Annu Rev Immunol* **14**, 1-27 (1996).
198. Hos, B.J., Tondini, E., van Kasteren, S.I. & Ossendorp, F. Approaches to Improve Chemically Defined Synthetic Peptide Vaccines. *Front Immunol* **9**, 884 (2018).
199. Rubio, V., *et al.* Ex vivo identification, isolation and analysis of tumor-cytolytic T cells. *Nat Med* **9**, 1377-1382 (2003).
200. Cruz, F.M., Colbert, J.D., Merino, E., Kriegsman, B.A. & Rock, K.L. The Biology and Underlying Mechanisms of Cross-Presentation of Exogenous Antigens on MHC-I Molecules. *Annu Rev Immunol* **35**, 149-176 (2017).
201. Ackerman, A.L., Kyritsis, C., Tampe, R. & Cresswell, P. Early phagosomes in dendritic cells form a cellular compartment sufficient for cross presentation of exogenous antigens. *Proc Natl Acad Sci U S A* **100**, 12889-12894 (2003).
202. Jensen, P.E., Weber, D.A., Thayer, W.P., Westerman, L.E. & Dao, C.T. Peptide exchange in MHC molecules. *Immunol Rev* **172**, 229-238 (1999).
203. Luft, T., *et al.* Exogenous peptides presented by transporter associated with antigen processing (TAP)-deficient and TAP-competent cells: intracellular loading and kinetics of presentation. *J Immunol* **167**, 2529-2537 (2001).
204. Bijker, M.S., *et al.* Superior induction of anti-tumor CTL immunity by extended peptide vaccines involves prolonged, DC-focused antigen presentation. *Eur J Immunol* **38**, 1033-1042 (2008).
205. Toes, R.E., *et al.* Enhancement of tumor outgrowth through CTL tolerization after peptide vaccination is avoided by peptide presentation on dendritic cells. *J Immunol* **160**, 4449-4456 (1998).
206. Kenter, G.G., *et al.* Vaccination against HPV-16 oncoproteins for vulvar intraepithelial neoplasia. *N Engl J Med* **361**, 1838-1847 (2009).
207. Ahrends, T., *et al.* CD4(+) T Cell Help Confers a Cytotoxic T Cell Effector Program Including Coinhibitory Receptor Downregulation and Increased Tissue Invasiveness. *Immunity* **47**, 848-861 e845 (2017).
208. Rosendahl Huber, S.K., *et al.* Synthetic Long Peptide Influenza Vaccine Containing Conserved T and B Cell Epitopes Reduces Viral Load in Lungs of Mice and Ferrets. *PLoS One* **10**, e0127969 (2015).
209. Bijker, M.S., *et al.* $CD8^+$ CTL priming by exact peptide epitopes in incomplete Freund's adjuvant induces a vanishing CTL response, whereas long peptides induce sustained CTL reactivity. *J Immunol* **179**, 5033-5040 (2007).
210. Oelke, M., *et al.* Generation and purification of $CD8^+$ melan-A-specific cytotoxic T lymphocytes for adoptive transfer in tumor immunotherapy. *Clin Cancer Res* **6**, 1997-2005 (2000).
211. Mackensen, A., *et al.* Phase I study of adoptive T-cell therapy using antigen-specific $CD8^+$ T cells for the treatment of patients with metastatic melanoma. *J Clin Oncol* **24**, 5060-5069 (2006).
212. Robbins, P.F., *et al.* Mining exomic sequencing data to identify mutated antigens recognized by adoptively transferred tumor-reactive T cells. *Nat Med* **19**, 747-752 (2013).
213. Kelderman, S., *et al.* Antigen-specific TIL therapy for melanoma: A flexible platform for personalized cancer immunotherapy. *Eur J Immunol* **46**, 1351-1360 (2016).
214. Kvistborg, P., *et al.* TIL therapy broadens the tumor-reactive $CD8^+$ T cell compartment in melanoma patients. *Oncoimmunology* **1**, 409-418 (2012).
215. Dudley, M.E., Wunderlich, J.R., Shelton, T.E., Even, J. & Rosenberg, S.A. Generation of tumor-infiltrating lymphocyte cultures for use in adoptive transfer therapy for melanoma patients. *J Immunother* **26**, 332-342 (2003).

216. Fesnak, A.D., June, C.H. & Levine, B.L. Engineered T cells: the promise and challenges of cancer immunotherapy. *Nat Rev Cancer* **16**, 566-581 (2016).
217. Si, W., Li, C. & Wei, P. Synthetic immunology: T-cell engineering and adoptive immunotherapy. *Synth Syst Biotechnol* **3**, 179-185 (2018).
218. Wilkins, O., Keeler, A.M. & Flotte, T.R. CAR T-Cell Therapy: Progress and Prospects. *Hum Gene Ther Methods* **28**, 61-66 (2017).
219. Dudley, M.E. & Rosenberg, S.A. Adoptive-cell-transfer therapy for the treatment of patients with cancer. *Nat Rev Cancer* **3**, 666-675 (2003).
220. Van Tendeloo, V.F., *et al.* Induction of complete and molecular remissions in acute myeloid leukemia by Wilms' tumor 1 antigen-targeted dendritic cell vaccination. *Proc Natl Acad Sci U S A* **107**, 13824-13829 (2010).
221. Palucka, K. & Banchereau, J. Dendritic-cell-based therapeutic cancer vaccines. *Immunity* **39**, 38-48 (2013).
222. Guermonprez, P., Valladeau, J., Zitvogel, L., Thery, C. & Amigorena, S. Antigen presentation and T cell stimulation by dendritic cells. *Annu Rev Immunol* **20**, 621-667 (2002).
223. Trombetta, E.S. & Mellman, I. Cell biology of antigen processing in vitro and in vivo. *Annu Rev Immunol* **23**, 975-1028 (2005).
224. Badillo-Godinez, O., *et al.* Targeting of rotavirus VP6 to DEC-205 induces protection against the infection in mice. *Vaccine* **33**, 4228-4237 (2015).
225. Bonifaz, L.C., *et al.* In vivo targeting of antigens to maturing dendritic cells via the DEC-205 receptor improves T cell vaccination. *J Exp Med* **199**, 815-824 (2004).
226. Palucka, A.K., *et al.* Dendritic cells loaded with killed allogeneic melanoma cells can induce objective clinical responses and MART-1 specific $CD8^+$ T-cell immunity. *J Immunother* **29**, 545-557 (2006).
227. O'Rourke, M.G., *et al.* Dendritic cell immunotherapy for stage IV melanoma. *Melanoma Res* **17**, 316-322 (2007).
228. Steinman, R.M. & Banchereau, J. Taking dendritic cells into medicine. *Nature* **449**, 419-426 (2007).
229. Plosker, G.L. Sipuleucel-T: in metastatic castration-resistant prostate cancer. *Drugs* **71**, 101-108 (2011).
230. Small, E.J., *et al.* Placebo-controlled phase III trial of immunologic therapy with sipuleucel-T (APC8015) in patients with metastatic, asymptomatic hormone refractory prostate cancer. *J Clin Oncol* **24**, 3089-3094 (2006).
231. Kantoff, P.W., *et al.* Sipuleucel-T immunotherapy for castration-resistant prostate cancer. *N Engl J Med* **363**, 411-422 (2010).
232. Fong, L., Ruegg, C.L., Brockstedt, D., Engleman, E.G. & Laus, R. Induction of tissue-specific autoimmune prostatitis with prostatic acid phosphatase immunization: implications for immunotherapy of prostate cancer. *J Immunol* **159**, 3113-3117 (1997).
233. Sheikh, N.A. & Jones, L.A. CD54 is a surrogate marker of antigen presenting cell activation. *Cancer Immunol Immunother* **57**, 1381-1390 (2008).
234. Hinrichs, C.S. & Restifo, N.P. Reassessing target antigens for adoptive T-cell therapy. *Nat Biotechnol* **31**, 999-1008 (2013).
235. Keir, M.E., Butte, M.J., Freeman, G.J. & Sharpe, A.H. PD-1 and its ligands in tolerance and immunity. *Annu Rev Immunol* **26**, 677-704 (2008).
236. Butte, M.J., Keir, M.E., Phamduy, T.B., Sharpe, A.H. & Freeman, G.J. Programmed death-1 ligand 1 interacts specifically with the B7-1 costimulatory molecule to inhibit T cell responses. *Immunity* **27**, 111-122 (2007).
237. Freeman, G.J., *et al.* Engagement of the PD-1 immunoinhibitory receptor by a novel B7 family member leads to negative regulation of lymphocyte activation. *J Exp Med* **192**, 1027-1034 (2000).
238. Parry, R.V., *et al.* CTLA-4 and PD-1 receptors inhibit T-cell activation by distinct mechanisms. *Mol Cell Biol* **25**, 9543-9553 (2005).
239. Abbas, A.K. The control of T cell activation vs. tolerance. *Autoimmun Rev* **2**, 115-118 (2003).
240. Leach, D.R., Krummel, M.F. & Allison, J.P. Enhancement of antitumor immunity by CTLA-4 blockade. *Science* **271**, 1734-1736 (1996).
241. Lesokhin, A.M., Callahan, M.K., Postow, M.A. & Wolchok, J.D. On being less tolerant: enhanced

cancer immunosurveillance enabled by targeting checkpoints and agonists of T cell activation. *Sci Transl Med* **7**, 280sr281 (2015).
242. Quezada, S.A., Peggs, K.S., Simpson, T.R. & Allison, J.P. Shifting the equilibrium in cancer immunoediting: from tumor tolerance to eradication. *Immunol Rev* **241**, 104-118 (2011).
243. Rizvi, N.A., *et al.* Cancer immunology. Mutational landscape determines sensitivity to PD-1 blockade in non-small cell lung cancer. *Science* **348**, 124-128 (2015).
244. Hellmann, M.D., *et al.* Tumor Mutational Burden and Efficacy of Nivolumab Monotherapy and in Combination with Ipilimumab in Small-Cell Lung Cancer. *Cancer Cell* **33**, 853-861 e854 (2018).
245. Gubin, M.M., *et al.* Checkpoint blockade cancer immunotherapy targets tumour-specific mutant antigens. *Nature* **515**, 577-581 (2014).
246. McGranahan, N., *et al.* Clonal neoantigens elicit T cell immunoreactivity and sensitivity to immune checkpoint blockade. *Science* **351**, 1463-1469 (2016).
247. NobelPrize.org. Prize announcement. Vol. Jan 2 2019 (Nobel Media AB, 2018).
248. Kwon, E.D., *et al.* Manipulation of T cell costimulatory and inhibitory signals for immunotherapy of prostate cancer. *Proc Natl Acad Sci U S A* **94**, 8099-8103 (1997).
249. Linsley, P.S., *et al.* CTLA-4 is a second receptor for the B cell activation antigen B7. *J Exp Med* **174**, 561-569 (1991).
250. Walunas, T.L., *et al.* CTLA-4 can function as a negative regulator of T cell activation. *Immunity* **1**, 405-413 (1994).
251. Waterhouse, P., *et al.* Lymphoproliferative disorders with early lethality in mice deficient in Ctla-4. *Science* **270**, 985-988 (1995).
252. Thompson, C.B. & Allison, J.P. The emerging role of CTLA-4 as an immune attenuator. *Immunity* **7**, 445-450 (1997).
253. ClinicalTrials.gov. Vol. Oct 12 2018 (2018).
254. Snyder, A., *et al.* Genetic basis for clinical response to CTLA-4 blockade in melanoma. *N Engl J Med* **371**, 2189-2199 (2014).
255. Hodi, F.S., *et al.* Improved survival with ipilimumab in patients with metastatic melanoma. *N Engl J Med* **363**, 711-723 (2010).
256. Dong, H., *et al.* Tumor-associated B7-H1 promotes T-cell apoptosis: a potential mechanism of immune evasion. *Nat Med* **8**, 793-800 (2002).
257. Iwai, Y., *et al.* Involvement of PD-L1 on tumor cells in the escape from host immune system and tumor immunotherapy by PD-L1 blockade. *Proc Natl Acad Sci U S A* **99**, 12293-12297 (2002).
258. Blank, C., Gajewski, T.F. & Mackensen, A. Interaction of PD-L1 on tumor cells with PD-1 on tumor-specific T cells as a mechanism of immune evasion: implications for tumor immunotherapy. *Cancer Immunol Immunother* **54**, 307-314 (2005).
259. Iwai, Y., Terawaki, S. & Honjo, T. PD-1 blockade inhibits hematogenous spread of poorly immunogenic tumor cells by enhanced recruitment of effector T cells. *Int Immunol* **17**, 133-144 (2005).
260. Lipson, E.J., *et al.* Antagonists of PD-1 and PD-L1 in Cancer Treatment. *Semin Oncol* **42**, 587-600 (2015).
261. Iwai, Y., Hamanishi, J., Chamoto, K. & Honjo, T. Cancer immunotherapies targeting the PD-1 signaling pathway. *J Biomed Sci* **24**, 26 (2017).
262. Hamid, O., *et al.* Safety and tumor responses with lambrolizumab (anti-PD-1) in melanoma. *N Engl J Med* **369**, 134-144 (2013).
263. Seetharamu, N., Preeshagul, I.R. & Sullivan, K.M. New PD-L1 inhibitors in non-small cell lung cancer - impact of atezolizumab. *Lung Cancer (Auckl)* **8**, 67-78 (2017).
264. Curran, M.A., Montalvo, W., Yagita, H. & Allison, J.P. PD-1 and CTLA-4 combination blockade expands infiltrating T cells and reduces regulatory T and myeloid cells within B16 melanoma tumors. *Proc Natl Acad Sci U S A* **107**, 4275-4280 (2010).
265. Wolchok, J.D., *et al.* Nivolumab plus ipilimumab in advanced melanoma. *N Engl J Med* **369**, 122-133 (2013).
266. Carreno, B.M., Carter, L.L. & Collins, M. Therapeutic opportunities in the B7/CD28 family of ligands and receptors. *Curr Opin Pharmacol* **5**, 424-430 (2005).
267. Altman, J.D., *et al.* Phenotypic analysis of antigen-specific T lymphocytes. *Science* **274**, 94-96 (1996).
268. Crawford, F., Kozono, H., White, J., Marrack, P. & Kappler, J. Detection of antigen-specific T cells

with multivalent soluble class II MHC covalent peptide complexes. *Immunity* **8**, 675-682 (1998).
269. Davis, M.M., Altman, J.D. & Newell, E.W. Interrogating the repertoire: broadening the scope of peptide-MHC multimer analysis. *Nat Rev Immunol* **11**, 551-558 (2011).
270. Nepom, G.T., *et al.* HLA class II tetramers: tools for direct analysis of antigen-specific CD4$^+$ T cells. *Arthritis Rheum* **46**, 5-12 (2002).
271. Lee, P.P., *et al.* Characterization of circulating T cells specific for tumor-associated antigens in melanoma patients. *Nat Med* **5**, 677-685 (1999).
272. Nepom, G.T. MHC class II tetramers. *J Immunol* **188**, 2477-2482 (2012).
273. Savage, P.A. & Davis, M.M. A kinetic window constricts the T cell receptor repertoire in the thymus. *Immunity* **14**, 243-252 (2001).
274. Murali-Krishna, K., *et al.* In vivo dynamics of anti-viral CD8 T cell responses to different epitopes. An evaluation of bystander activation in primary and secondary responses to viral infection. *Adv Exp Med Biol* **452**, 123-142 (1998).
275. McHeyzer-Williams, M.G., Altman, J.D. & Davis, M.M. Enumeration and characterization of memory cells in the TH compartment. *Immunol Rev* **150**, 5-21 (1996).
276. Novak, E.J., *et al.* Tetramer-guided epitope mapping: rapid identification and characterization of immunodominant CD4$^+$ T cell epitopes from complex antigens. *J Immunol* **166**, 6665-6670 (2001).
277. Jansen, D., *et al.* Flow Cytometric Clinical Immunomonitoring Using Peptide-MHC Class II Tetramers: Optimization of Methods and Protocol Development. *Front Immunol* **9**, 8 (2018).
278. Ljunggren, H.G., *et al.* Empty MHC class I molecules come out in the cold. *Nature* **346**, 476-480 (1990).
279. Saini, S.K., *et al.* Dipeptides catalyze rapid peptide exchange on MHC class I molecules. *Proc Natl Acad Sci U S A* **112**, 202-207 (2015).
280. Choo, J.A., *et al.* Bioorthogonal cleavage and exchange of major histocompatibility complex ligands by employing azobenzene-containing peptides. *Angew Chem Int Ed Engl* **53**, 13390-13394 (2014).
281. Amore, A., *et al.* Development of a hypersensitive periodate-cleavable amino acid that is methionine- and disulfide-compatible and its application in MHC exchange reagents for T cell characterisation. *Chembiochem* **14**, 123-131 (2013).
282. Rodenko, B., *et al.* Class I major histocompatibility complexes loaded by a periodate trigger. *J Am Chem Soc* **131**, 12305-12313 (2009).
283. Rodenko, B., *et al.* Generation of peptide-MHC class I complexes through UV-mediated ligand exchange. *Nat Protoc* **1**, 1120-1132 (2006).
284. Toebes, M., *et al.* Design and use of conditional MHC class I ligands. *Nat Med* **12**, 246-251 (2006).
285. Bakker, A.H., *et al.* Conditional MHC class I ligands and peptide exchange technology for the human MHC gene products HLA-A1, -A3, -A11, and -B7. *Proc Natl Acad Sci U S A* **105**, 3825-3830 (2008).
286. Luimstra, J.J., *et al.* A flexible MHC class I multimer loading system for large-scale detection of antigen-specific T cells. *J Exp Med* **215**, 1493-1504 (2018).
287. Garstka, M.A., *et al.* The first step of peptide selection in antigen presentation by MHC class I molecules. *P Natl Acad Sci USA* **112**, 1505-1510 (2015).
288. Hadrup, S.R., *et al.* Parallel detection of antigen-specific T-cell responses by multidimensional encoding of MHC multimers. *Nat Methods* **6**, 520-526 (2009).
289. Newell, E.W., Klein, L.O., Yu, W. & Davis, M.M. Simultaneous detection of many T-cell specificities using combinatorial tetramer staining. *Nat Methods* **6**, 497-499 (2009).
290. Bentzen, A.K., *et al.* Large-scale detection of antigen-specific T cells using peptide-MHC-I multimers labeled with DNA barcodes. *Nat Biotechnol* **34**, 1037-1045 (2016).

1

2

Altered peptide ligands revisited: vaccine design through chemically modified HLA-A2-restricted T cell epitopes

Rieuwert Hoppes[1*], Rimke Oostvogels[2,3*], Jolien J. Luimstra[1], Kim Wals[1], Mireille Toebes[4], Laura Bies[4], Reggy Ekkebus[1], Pramila Rijal[1], Patrick H.N. Celie[5], Julie H. Huang[2], Maarten E. Emmelot[2], Robbert M. Spaapen[1], Henk Lokhorst[3], Ton N. M. Schumacher[4], Tuna Mutis[2], Boris Rodenko[1,6], and Huib Ovaa[1]

*R. Hoppes and R. Oostvogels contributed equally to this work.

[1]Division of Cell Biology, The Netherlands Cancer Institute, Amsterdam, The Netherlands
[2]Department of Clinical Chemistry and Haematology, University Medical Center Utrecht, Utrecht, The Netherlands
[3]Department of Haematology, University Medical Center Utrecht, Utrecht, The Netherlands
[4]Division of Immunology, The Netherlands Cancer Institute, Amsterdam, The Netherlands
[5]Division of Biochemistry, The Netherlands Cancer Institute, Amsterdam, The Netherlands
[6]Institute of Infection, Immunity and Inflammation, University of Glasgow, Glasgow, United Kingdom

Journal of Immunology 193, 4803-4813 (2014)

Abstract

Virus or tumor Ag-derived peptides that are displayed by MHC class I molecules are attractive starting points for vaccine development a they induce strong protective and therapeutic cytotoxic T cell responses. In thus study, we show that the MHC binding and consequent T cell reactivity against several HLA-A*02:01-restricted epitopes can be further improved through the incorporation of non-proteogenic amino acids at primary and secondary anchor positions. We screened more than 90 non-proteogenic, synthetic amino acids through a range of epitopes and tested more than 3000 chemically enhanced altered peptide ligands (CPLs) for binding affinity to HLA-A*02:01. With this approach, we designed CPLs of viral epitopes, of melanoma-associated Ags, and of the minor histocompatibility Ag UTA2-1, which is currently being evaluated for its antileukemic activity in clinical dendritic cell vaccination trials. The crystal structure of one of the CPLs in complex with HLA-A*02:01 revealed the molecular interactions likely responsible for improved binding. The best CPLs displayed enhanced affinity for MHC, increasing MHC stability and prolonging recognition by Ag-specific T cells and, most importantly, they induced accelerated expansion of antitumor T cell frequencies in vitro and in vivo as compared with the native epitope. Eventually, we were able to construct a toolbox of preferred non-proteogenic residues with which practically any given HLA-A*02:01-restricted epitope can be readily optimized. These CPLs could improve the therapeutic outcome of vaccination strategies or can be used for ex vivo enrichment and faster expansion of Ag-specific T cells for transfer into patients.

Introduction

In the treatment of cancer and the prevention of infectious diseases, the use of therapeutic or prophylactic peptide vaccines can be a successful method to specifically direct the immune system against the right targets. The peptides administered to the patient mimic the epitopes presented on the target cells when associated with the restricting MHC and would thus be capable of inducing relevant immune responses.

For immunotherapy of cancer, various clinical applications in the past decades provided ample evidence of the feasibility, safety, and immunogenicity of this type of vaccine; however, the efficacy has mostly been limited[1,2]. Many variables in the design of peptide vaccination, such as type and length of the peptides, loading of one or multiple peptides on APCs or route of administration could potentially attribute to these disappointing observations. Selecting the right epitope is a crucial step in the design of an effective vaccine. Obviously, the

vaccine peptide needs to be presented on the targeted tumor cells at sufficient expression levels, but also peptide-MHC affinity appears to be a decisive factor for the immunogenic potential[3-7]. Recent research suggests that high-peptide MHC affinities of targeted epitopes are required for complete tumor eradication and tumor stroma destruction by specific T cells, presumably through the formation of stable synapses between the APCs and the effector T cells that are necessary for optimal stimulation of the latter[6]. In addition, the half-life of peptide-MHC (pMHC) complexes has been directly correlated to immunogenicity[8], and extension of the duration of the peptide-MHC interaction (and consequent dwell time on the cell surface) may therefore lead to more effective peptide vaccines by the induction of higher frequencies of epitope-specific T cells[9].

A frequent problem with peptide vaccinations until now is the low immunogenicity of the tumor-associated Ags used, which are usually derived from self-proteins. Because of thymic selection processes, the T cell repertoire is mainly shaped to recognize foreign Ags with high affinity in contrast to peptides derived from self-proteins[10]. To circumvent these issues, the replacement of amino acids in so-called anchor positions that contribute significantly to MHC affinity has been proposed. Epitopes modified based on amino acid substitutions are termed "altered peptide ligands" (APLs)[11]. A well-known example of such an APL is the alanine to leucine modification in the melanoma-associated Mart-1/Melan-A_{26-35} epitope EAAGIGILTV that leads to enhanced MHC-binding[12].

In general, MHC class I molecules accommodate peptides of 8-10 aas long that contain preferred MHC allele-specific residues on anchor positions (Fig. 1A)[13]. The affinity of a peptide for an MHC molecule is determined by the potential of these anchor residues to form stable molecular interactions with the MHC allele-specific pockets, depending on their shape, size, and electrostatic complementarity with proximal MHC residues[14,15]. The exact localization of the anchor residues depends on the MHC allele, but they are mainly in close proximity to the N- and C-termini of bound peptides[13,16]. In contrast, interaction with the TCRs of cytotoxic T cells heavily relies on the middle part of the peptide that extrudes out of the MHC binding groove[8,10]. Therefore, modifications aimed at increasing an epitope's affinity for MHC molecules are in principle restricted to positions near the N- and C-termini to ensure retained immunogenicity. Anchor substitutions have been introduced successfully within peptides to improve MHC class I binding and to enhance TCR activation[12,17-19]. Substitutions in the TCR interacting region, however, frequently result in heteroclitic analogs that can lead to hyperstimulation of the CTL, achieving occasionally a more potent immune response compared with the native epitope; far more often, they will cause T cell exhaustion or lead to an abrogated TCR interaction[20-22].

Synthetic engineering of peptide epitopes may confer beneficial properties to the peptide vaccine, such as improved MHC class I binding, protease resistance,

and enhanced bioavailability. Strategies that have been pursued to improve and stabilize MHC epitopes include the incorporation of residues such as nonencoded α-amino acids[23-25], photoreactive cross-linking amino acids[26], N-methylated amino acids[27] and β-amino acids[27-30], backbone reduction (reviewed in Ref. 31), (partial) retroinversion by using D-amino acids[32,33], N-terminal methylation and C-terminal amidation[27,34] and pegylation (reviewed in Ref. 35). The majority of these modifications are aimed at improving the biostability of peptide Ags, often at the cost of losing MHC affinity, immunogenicity, or both. The limited rate of success in epitope improvement might be found in the often small set of non-natural amino acids used to generate primarily monosubstituted peptide analogs. In this study, we aimed to address this issue by systematically introducing multiple substitutions in cognate Ags using a large set of synthetic amino acids. Our approach involves the replacement of primary and secondary anchor residues of known T cell epitopes with non-proteogenic amino acids (Fig. 1, A and B). The resulting non-natural peptides will be referred to as "chemically enhanced altered peptide ligands" (CPLs) as opposed to the "classical" APLs containing only proteogenic amino acid substitutions. To define the best CPLs, we modified 12 well-known T cell epitopes with more than 90 different non-proteogenic amino acids and tested 3000 peptides in total. We focused on replacing amino acids on positions close to the N- and C-termini as we aimed to improve the HLA affinity of several model epitopes without interfering with TCR recognition. For our optimization studies, we selected epitopes restricted to HLA-A*02:01, because this allele is the most abundant MHC molecule in humans of Caucasian origin.

We first used several viral epitopes and tumor-associated Ags as model peptides to test this principle. For our final experiments, we modified the recently identified minor histocompatibility Ag (mHag) UTA2-1[36]. This HLA-A*02:01-restricted Ag, because of its sole expression in hematopoietic cells, is highly relevant for the therapy of relapsed lymphoid and myeloid malignancies of the hematopoietic system after allogeneic stem-cell transplantation. UTA2-1 is currently included in clinical trials in which patients who are not responding to donor lymphocyte infusions are treated with mHag-loaded dendritic cell vaccinations.

We show that the substitution of amino acids at anchoring positions by particular non-proteogenic amino acids led to superior MHC binding in comparison with substitution with proteogenic amino acids, with concomitant improvement of the immunogenicity of these epitopes. For the immunotherapeutic mHag UTA2-1, we were able to design a CPL that in vitro and in vivo evoked significantly enhanced proliferation of UTA2-1-specific T cells. Moreover, the cytotoxic capacity of these T cells against targets expressing the natural UTA2-1 Ag was maintained, confirming the relevance of this approach for use in clinical practice.

Results

Enhancing epitope binding affinity by substitutions with non-proteogenic amino acid residues

To test our model and to attempt to enhance peptide binding to HLA-A*02:01by amino acid substitutions in the epitope, we first set out to improve the affinity of two well-known viral epitopes: Influenza Matrix 1_{58-66} epitope GILGFVFTL[37], as a stringent model epitope already having high affinity for HLA-A*02:01, and CMV $pp65_{495-503}$ peptide NLVPMVATV[38] as an intermediate model peptide having a moderate affinity for HLA-A*02:01[39]. To explore the general scope of substitutions with proteogenic amino acids, we systematically introduced all 20 proteogenic residues on all nine positions in the peptides and screened these peptides for binding capacity to HLA-A*02:01 using an MHC exchange fluorescence polarization FP assay (Table S1)[40]. Using proteogenic amino acid substitutions the HLA binding score (defined as the percent inhibition of FP tracer peptide binding) could maximally be raised from 36% for the native NLVPMVATV peptide to 70% for its related APLs and from 76% for the native GILGFVFTL peptide to 87% for the corresponding APLs. It should, however, be noted that these substitutions include those that are part of the TCR interacting region (Fig. 1A) and hence could affect TCR binding and selectivity. Having observed that specific substitutions with proteogenic amino acids can lead to enhanced binding affinity, we proceeded to further increase peptide-MHC affinity through the introduction of non-proteogenic amino acids, including the D-enantiomers of proteogenic amino acids. Making full use of the possibilities of medicinal chemistry to optimize ligand-protein interactions, we incorporated 90 non-proteogenic amino acid derivatives on the positions indicated in Figure 1A in GILGFVFTL and NLVPMVATV, leading to monosubstituted, disubstituted, and trisubstituted CPLs, and we determined the HLA binding scores of the resulting set of 500 peptides (Fig. 1C).

Several non-proteogenic residues revealed further enhancement of affinity relative to the substitutions with proteogenic amino acids. In particular, the introduction of D-α-methyl-phenylglycine (am-phg) on P_1 generally led to additional improvements in HLA binding, as seen for CPLs [am-phg][NVA]LGFV[4-FPHE]TL and [am-phg][CpALA]LGFV[4-FPHE]TL with HLA binding scores of 96% and 97%, respectively, as compared with 87% for the best APL GILGFVFPL. By introducing L-2-amino-octanoic acid (2-AOC) on P_3 of the NLVPMVATV peptide the HLA binding score was increased up to 73%. A frequent improvement was observed by the introduction of 4-fluorophenylalanine (4-FPHE) on P_{C-2}, a non-anchor position (Fig. 1, A and B). By performing similar screens through five other viral epitopes (Fig. S1), we learned which non-proteogenic amino acid substitutions frequently led to enhancement of HLA affinity, allowing us to compose a list of preferred residues (Fig. 1B). Functional assays with several donor-derived

GILGFVFTL-positive CD8+ T cell clones showed that CPLs with substitutions on P_1, P_2, and P_{C-2} and P_C were generally able to (hyper)stimulate CTLs, but CPLs with modifications on P_3 gave variable results (data not shown).

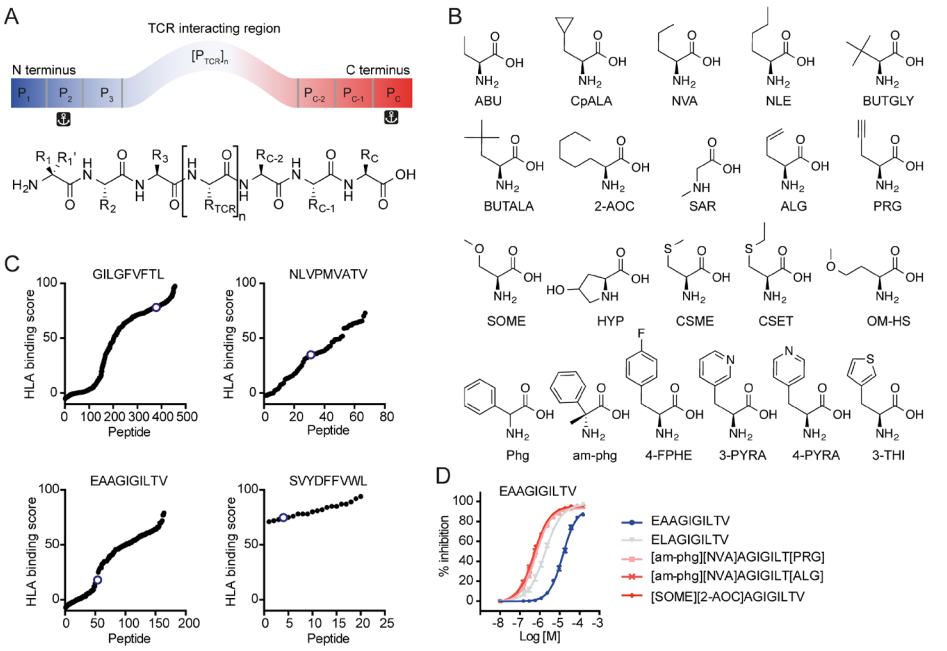

Figure 1. **Introduction of nonproteogenic amino acids leads to CPLs with higher HLA affinity than their respective index peptides.** (A) Schematic representation of amino acid positions of an HLA-A*02:01-restricted epitope. Positions P_1 to P_3 and P_{C-2} to P_C have been modified in this study, resulting in modified side chain substituents $R_{1,1}$, R_2, R_3, and R_{C-2}, R_{C-1}, and R_C. Positions P_{TCR} were left untouched to retain interaction with the TCR. P_2 and P_C anchor residues are indicated. (B) Structures of preferred non-proteogenic amino acid residues leading to enhanced HLA affinity that emerged from screening 90 different amino acid residues in 20 epitopes. L-α-Amino acids are in all upper case, and D-amino acids are in sentence case. Phg denotes a racemic mixture of DL-phenylglycine. In peptide sequences, non-proteogenic residues are enclosed in brackets. (C) Screening CPLs for HLA affinity was performed with a competitive HLA-A*02:01 ultraviolet exchange fluorescence polarization assay. HLA binding scores are the percent inhibition of FP tracer peptide binding. Each data point (•) represents a different CPL of the indicated parent epitope, accommodating one, two, or three non-proteogenic amino acid substitutions. Scores for parent epitopes are indicated by (○) and include influenza A matrix $1_{58–66}$ GILGFVFTL, CMV pp65$_{495–503}$ NLVPMVATV, melanoma Mart-$1_{26–35}$ EAAGIGILTV, and melanoma Trp-$2_{180–188}$ SVYDFFVWL. See Figure S1 for optimization of additional epitopes. (D) For the strongest binders, IC50 values were determined showing that Mart-$1_{26–35}$-based CPLs display an increase in HLA affinity by two orders of magnitude (see also Table 2).

Optimization of the HLA affinity of tumor epitopes

After showing proof of principle for improving the HLA affinity of even highly affine and immunogenic viral epitopes by incorporation of synthetic amino acids, we aimed to optimize melanoma-associated epitopes, which typically display low MHC affinity and hence low immunogenicity[8]. The HLA-A*02:01-restricted Melan-A/Mart-1 epitope EAAGIGILTV[41] has very low affinity for HLA-A*02:01, practically precluding its use in immunologic applications such as pMHC multimer staining and T cell isolation. The low MHC affinity is primarily due to the suboptimal anchor residue, alanine, on P_2, and substitution of this residue for the preferred anchor residue leucine (A2L) has been reported to enhance HLA binding[12] and has become a benchmark example of an APL facilitating the

Table 1. **Data collection and refinement statistics.**

HLA-A*02:01::[am-phg][NVA]AGIGILT[PRG][a]	
Data collection	
Space group	$P2_1$
Cell dimensions	
a, *b*, *c* (Å)	63.18, 87.14, 79.19
A, β, γ (°)	90.00, 90.15, 90.00
Resolution (Å)	40.00–1.65 (1.74–1.65)[b]
R_{sym} or R_{merge}	4.1 (48.3)
$I/\sigma I$	13.2 (1.6)
Completeness (%)	99.6 (99.8)
Redundancy	3.4 (3.5)
Refinement	
Resolution (Å)	20.00–1.65
No. of reflections	97482
R_{work}/R_{free}	15.6/17.9
Twinning	2 domains
Twin domain 1 fraction	0.748
Twin domain 1 operator	H, K, L
Twin domain 2 fraction	0.252
Twin domain 2 operator	-H, -K, -L
No. of atoms	
Protein	6851
Ligand/ion	78
Water	540
B-factors	
Protein	14.1
Ligand/ion	45.3
Water	31.8
R.m.s. deviations	
Bond lengths (Å)	0.012
Bond angles (°)	1.563

X-ray diffraction data were collected on one single crystal. [a]The crystal structure presented in this article has been submitted to the RCSB Protein Data Bank (http://www.rcsb.org/pdb/home/home.do) under identification code 4WJ5. [b]Values in parentheses are for highest-resolution shell.

Table 2. **MHC binding, TCR recognition, and T cell activating ability of chemically optimized melanoma epitopes.**

Sequence	MHC Binding (μM ± SEM)[a]	% pMHC multimer$^+$ CTLs[b]	% IFN-γ$^+$ CTLs[c] 1 h	% IFN-γ$^+$ CTLs[c] 24 h	Literature reference
EAAGIGILTV—Mart-1$_{(26–35)}$	14.56 ± 0.3	6.4 ± 0.4	43 ± 16	0 ± 0	(53)
ELAGIGILTV	1.9 ± 0.10	5.6 ± 0.4	79 ± 7	30 ± 7	(12)
[am-phg][2-AOC]AGIGILT[PRG]	0.26 ± 0.03	5.6 ± 0.5	ND	ND	
[am-phg][NLE]AGIGILT[PRG]	0.4 ± 0.01	6.0 ± 0.3	82 ± 7	49 ± 8	
[am-phg][NVA]AGIGILT[ALG]	0.41 ± 0.10	5.1 ± 0.3	86 ± 4	69 ± 6	
[am-phg][NVA]AGIGILT[PRG]	0.51 ± 0.01	6.3 ± 0.1	81 ± 7	56 ± 12	
[am-phg]LAGIGILT[PRG]	0.48 ± 0.02	5.6 ± 0.2	77 ± 7	56 ± 14	
[CSME][2-AOC]AGIGILT[PRG]	0.51 ± 0.08	5.1 ± 0.3	84 ± 6	62 ± 7	
[CSME][2-AOC]AGIGILTV	0.47 ± 0.08	6.5 ± 0.3	78 ± 7	67 ± 12	
[CSME][NLE]AGIGILTV	0.97 ± 0.06	6.1 ± 0.1	76 ± 6	60 ± 12	
[CSME][NVA]AGIGILTV	0.87 ± 0.05	6.8 ± 0.4	78 ± 5	57 ± 15	
[CSME]LAGIGILT[PRG]	1.13 ± 0.07	5.1 ± 0.1	78 ± 7	57 ± 11	
[CSME]LAGIGILTV	1.36 ± 0.03	7.3 ± 0.5	73 ± 13	52 ± 13	
[SOME][2-AOC]AGIGILTV	0.22 ± 0.03	5.1 ± 0.2	72 ± 3	66 ± 11	
[SOME]LAGIGILTV	1.13 ± 0.06	4.8 ± 0	84 ± 2	66 ± 4	
SVYDFFVWL—Trp-2$_{(180–188)}$	0.76 ± 0.15		48 ± 3	30 ± 7	(54)
[am-phg][2-AOC]YDFFVW[PRG]	0.51 ± 0.1		37 ± 5	0 ± 0	
[am-phg][2-AOC]YDFFVWL	0.71 ± 0.09		62 ± 2	56 ± 5	
[am-phg][CpALA]YDFFVW[PRG]	0.46 ± 0.08		50 ± 3	8 ± 1	
[am-phg][NVA]YDFFVW[PRG]	0.71 ± 0.09		54 ± 6	52 ± 2	
[am-phg][NVA]YDFFVWL	0.65 ± 0.08		75 ± 0	77 ± 1	
[CSME][2-AOC]YDFFVW[ALG]	0.52 ± 0.04				
[CSME][2-AOC]YDFFVWL	0.41 ± 0.1		59 ± 3	62 ± 3	
[CSME][CpALA]YDFFVW[PRG]	0.94 ± 0.11				
[CSME][NVA]YDFFVW[PRG]	0.67 ± 0.14		20 ± 6	28 ± 4	
[Phg][2-AOC]YDFFVWL	0.51 ± 0.02		54 ± 3	66 ± 3	
[Phg][CpALA]YDFFVW[PRG]	0.80 ± 0.08		34 ± 6	46 ± 2	
[PHG][CpALA]YDFFVWL	0.60 ± 0.09		56 ± 3	62 ± 3	
[Phg][NVA]YDFFVW[ALG]	0.57 ± 0.05		42 ± 11	57 ± 4	
[Phg][NVA]YDFFVW[PRG]	0.74 ± 0.07		27 ± 8	29 ± 2	
[Phg][NVA]YDFFVWL	0.57 ± 0.1		58 ± 4	64 ± 5	
RLGPTLMCL—MG-50$_{(1243–1251)}$	1.78 ± 0.65				(55)
[am-phg][2-AOC]GPTLMC[PRG]	1.69 ± 0.57				
[am-phg][2-AOC]GPTLMCL	1.05 ± 0.05				
[am-phg][CpALA]GPTLMC[PRG]	1.03 ± 0.19				
[am-phg][CpALA]GPTLMCL	1.05 ± 0.12				
[CSME][2-AOC]GPTLMC[PRG]	1.01 ± 0.3				
[CSME][2-AOC]GPTLMCL	0.46 ± 0.03				
[CSME][CpALA]GPTLMCL	0.95 ± 0.07				
[CSME][NVA]GPTLMC[PRG]	0.79 ± 0.2				
[CSME][NVA]GPTLMCL	0.86 ± 0.04				
[Phg][2-AOC]GPTLMC[PRG]	0.63 ± 0.01				
[Phg][2-AOC]GPTLMCL	0.40 ± 0.07				
[Phg][CpALA]GPTLMC[PRG]	0.62 ± 0.19				
[Phg][CpALA]GPTLMCL	0.87 ± 0.08				
[Phg][NVA]GPTLMC[PRG]	0.73 ± 0.15				
[Phg][NVA]GPTLMCL	0.93 ± 0.42				
LLFGLALIEV—Mage-C2$_{(191–200)}$	47% (50%)[d]			11.5	(56)
[Phg][2-AOC]FGLALIEV	81% (81%)[d]			13.7	

[a]IC50 values were determined by an MHC exchange FP assay with peptide concentrations ranging from 100 mM to 50 nM. Values are the average of at least three biological replicates. SEM is standard error of means. [b]TCR interaction was measured by pMHC multimer staining of EAAGIGILTV selective CTLs. [c]T cell activation is represented by the percentage of IFN-γ-producing CD8$^+$ T cells specific for EAAGIGILTV (top half) or SVYDFFVWL (bottom half) upon coincubation with T2 APCs 1 or 24 h after pulsing the APCs with wild-type or modified epitopes. Values are the average of at least three independent experiments ± SE of means. [d]Values are HLA binding scores at 24 h as described in Materials and Methods. Value in parenthesis determined at 4 h.

study of Melan-A/Mart-1 CTL responses. To enhance MHC affinity further, we scanned non-proteogenic amino acids through this benchmark epitope. After synthesizing a set of 164 variants of the EAAGIGILTV peptide, we measured their HLA binding score (Fig. 1C) and then selected the 13 highest scoring CPLs and determined their IC50 value for binding to HLA-A*02:01 (Fig. 1D and Table 2). The introduction of multiple non-proteogenic amino acid residues in EAAGIGILTV yielded CPLs with an IC50 value of up to two orders of magnitude lower than displayed by the native epitope and one order of magnitude lower than displayed by the benchmark A2L APL. Using only the limited set of preferred residues shown in Figure 1B allowed us to reduce the number of peptide variants to be synthesized and screened to arrive at CPLs with improved HLA affinity. In this way we were readily able to optimize the affinity of melanoma Trp-$2_{180\text{-}188}$ epitope SVYDFFVWL[42] (Fig. 1C) and seven other melanoma epitopes: RLGPTLMCL ($MG50_{1243\text{-}1251}$)[43], LLFGLALIEV (Mage-$C2_{191\text{-}200}$), ALKDVEERV (Mage-$C2_{336\text{-}344}$), VIWEVLNAV (Mage-C2 $HCA587_{248\text{-}256}$), GLYDGMEHL (Mage-$A10_{254\text{-}262}$), YLEPGPVTA (pmel17/$gp100_{256\text{-}264}$) and VYDFFVWLHY (Trp-$2_{181\text{-}190}$) (Fig. S1). For the variants of SVYDFFVWL and RLGPTLMCL, we further determined their IC50 value for HLA-A*02:01 binding, and significant improvements were observed as these CPLs displayed 224-fold lower IC50 values than did the native epitopes (Table 2). In general, preferred modifications on P_1 included am-phg, O-methyl-L-serine (SOME) and S-methyl-L-serine (CSME), and L/D-(racemic) phenylglycine (Phg). On anchor position P_2 residues NLE, NVA, and 2-AOC resulted in higher-affinity APLs. Unsaturated amino acids propargylglycine (PRG) and allylglycine (ALG) were the best improvements on anchor position P_C.

To understand the factors contributing to enhanced HLA affinity at the molecular level, we solved the crystal structure of HLA-A*02:01 loaded with the CPL [am-phg][NVA]AGIGILT[PRG]. The structure was solved at 1.65-Å resolution (Fig. 2A) and contains two copies of the HLA-A*02:01-peptide complex in the asymmetric unit. Comparison of this structure with the existing structure of HLA-A*02:01 bound to the ELAGIGILTV Mart-1 variant peptide (RCSB Protein Data Bank identification code 1JF1)[44] reveals that both peptides assume a similar overall structure (root mean square deviation of nine peptide Ca atoms is 0.127 Å; Fig. 2B). In addition, no striking differences are observed in the presumed TCR interacting region of the peptides (Ile4-Leu7; Fig. 2B). On P_1 the aromatic residue of am-phg, locked in the D-orientation, shows both a favorable aromatic π-π interaction with Trp167 and a cation-π interaction with the side chain of Lys66 of the HLA a2 domain, whereas the am-phg NH_2-group maintains strong H-bonding interactions with Tyr7 and Tyr171 (Fig. 2C). The contribution of aromatic-π interactions to the binding of peptide and MHC heavy chain has been described previously, in particular the effect of an APL harboring a proline substitution at P_3 in which CH-π interactions between this proline and Tyr159 are

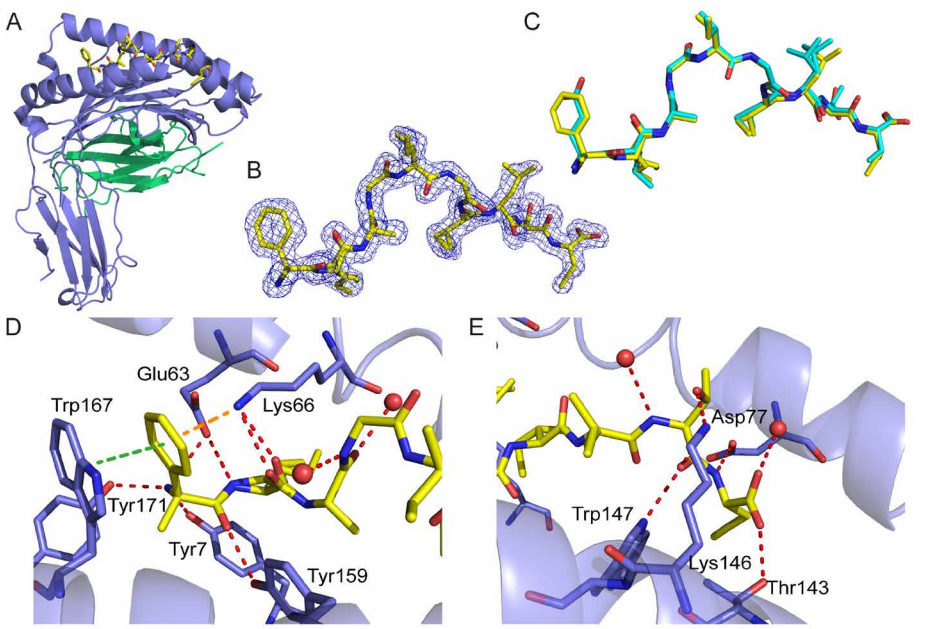

Figure 2. **The crystal structure of HLA-A*0201 loaded with a CPL reveals enhanced protein ligand interactions.** (A) The crystal structure of HLA-A*02:01::[am-phg][NVA]AGIGILT[PRG] was solved at 1.65 Å (RCSB Protein Data Bank identification code 4WJ5). The α- and β2m-chains are illustrated in blue and green, respectively. Peptide [am-phg][NVA]AGIGILT[PRG] is represented as sticks, with carbons in yellow, nitrogen in blue, and oxygen in red. (B) Peptide [am-phg][NVA]AGIGILT[PRG] represented as in (A) together with the final 2mFo-DFc electron density map (blue) displayed at a contour level of 1.0s and a radius of 1.5 Å around the peptide. (C) Overlay of the CPL shown in the same orientation as in (A) with the parent epitope ELAGIGILTV (RCSB Protein Data Bank identification code 1JF1)[35] in cyan. (D) Hydrogen bonding (red dotted lines), π-π interactions (green dotted line), and cation-π interactions (orange dotted line) explain the strong interaction of substituted residues D-am-phg on P_1 and L-NVA on P_2 with HLA-A*02:01. The NVA residue on P_2 protrudes into the hydrophobic P_2 anchor pocket. Water molecules are represented as red spheres. (E) Hydrogen bonding network of the C-terminal part of the CPL with the HLA-A*02:01 α-chain.

noteworthy to mention, as these interactions have been shown to increase the binding affinity significantly between H-2D^b and peptide[45] and to enhance the stability of the H-2D^b::peptide complex[46]. The NVA residue on P_2 protrudes into the hydrophobic anchor pocket and shows two different conformations in one of the peptides of the asymmetric unit, suggesting some degree of flexibility upon interaction with HLA-A*02:01. The NVA residue could stabilize the interaction between peptide and HLA-A*02:01 via van der Waals contact, but also via CH-π interactions with Tyr7, similar to the CH-π interactions reported between proline at P_3 and Tyr159 within the H-2Db::peptide complex[45,46]. The side chain of the PRG residue on P_C fits well into the hydrophobic F-pocket, whereas the main chain atoms form hydrogen bonds with Asp77, Thr143, and a water molecule (Fig. 2D).

Optimized melanoma epitopes are immunogenic and show prolonged activation of CTLs

To test whether CPLs maintained the ability to interact with TCRs, we used these CPLs in pMHC multimer staining experiments. We confirmed that the pMHC multimers loaded with optimized melanoma Ags (e.g., [am-phg][NVA]AGIGILT[PRG]) stained melanoma patient-derived CTLs as efficiently as pMHC multimers charged with the native epitope or with the A2L variant (Fig. 3A). To test the recognition of CPLs by CTLs, TAP-deficient T2 cells were pulsed with EAAGIGILTV-based CPLs and were incubated with HLA-A*02:01^{+} melanoma patient-derived CTLs at various time points. We monitored IFN-γ production as a marker for T cell activation; 48 h after pulsing with CPLs, the APCs were still able to elicit a strong CTL response (Fig. 3B), whereas APCs pulsed with either native EAAGIGILTV epitope or the A2L variant had lost or started losing this ability already after 24 h (Fig. 3C, Table 2). A similar trend was observed for CPLs based on the melanoma Trp-2$_{180\text{-}188}$ epitope SVYDFFVWL (Table 2). To test whether these CPLs are able to elicit an enhanced immune response in vivo, we vaccinated groups of HLA-A*02:01-transgenic mice with optimized Mart-1$_{26\text{-}35}$ and MAGE-C2$_{191\text{-}200}$[47] melanoma epitopes, and we monitored the vaccination-induced T cell frequencies by pMHC multimer staining. Vaccination with enhanced Mart-1 epitope, [am-phg][NVA]AGIGILT[PRG], induced higher frequencies of ELAGIGILTV reactive CTLs, also after a secondary vaccination at day 97 (Fig. 3D). Mice vaccinated with modified Mage-C2$_{191\text{-}200}$ epitope, [Phg][2-AOC]FGLALIEV (Table 2), produced more Mage-C2$_{191\text{-}200}$-reactive CTLs than did those vaccinated with the native epitope at all time points measured.

Selection of optimally modified mHag UTA2-1 peptides

To translate our findings to clinical applications, we proceeded with the optimization of minor histocompatibility Ag (mHag) UTA2-1, QLLNSVLTL[36]. This HLA-A*02:01-restricted epitope was modified and tested in a similar manner as the viral and melanoma peptides. Of 288 CPLs screened, 13 were selected for further analysis and showed—to various degrees—enhanced HLA binding and stability compared with the wild-type peptide (Fig. 4A). This set of CPLs was subsequently screened for recognition by the UTA2-1-specific CTL clone 503A1. Although several CPLs displayed a similar or even decreased CTL activation score compared with the wild-type peptide, CPLs 8 and 9 induced a CTL response at concentrations that were two orders of magnitude lower, indicating improved Ag presentation and recognition (Fig. 4A). These two peptides and a modified peptide that induced equal levels of CTL stimulation, CPL 5, were selected and subjected to further analysis to evaluate their immunogenic properties.

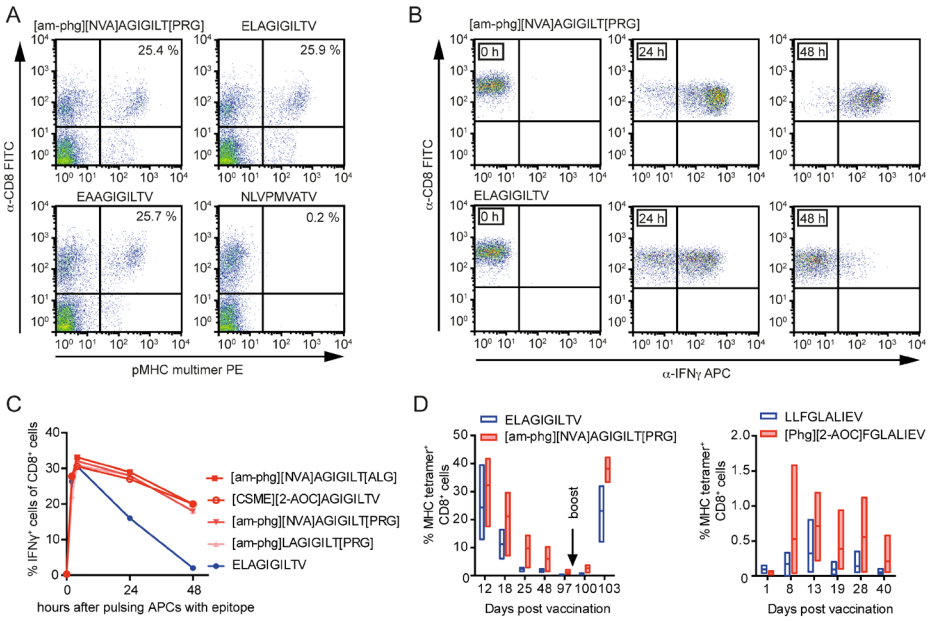

Figure 3. **CPLs are functional Ags and show prolonged activation of CTLs.** (A) Flow cytometry plots showing CTLs from HLA-A*02:01+ melanoma patients stained with pMHC exchange multimers loaded with the indicated tumor-associated Mart-$1_{26–35}$ Ag EAAGIGILTV or synthetic derivatives thereof and viral Ag NLVPMVATV as a negative control. CTLs were stained with anti-CD8-APC Ab and PE-conjugated pMHC multimers. Numbers indicate frequencies of pMHC multimer+ cells among CD8+ cells. (B) Coincubation of EAAGIGILTV specific clonal CTLs with APCs pulsed with a CPL show prolonged CTL activation (IFN-γ response) compared with the heteroclitic tumor-Ag ELAGIGILTV. (C) A time course of stimulation of EAAGIGILTV specific CTLs upon coincubation with APCs pulsed with 50 pM of the indicated peptides. (D) Enhanced T cell responses of HLA-A*02:01-transgenic mice vaccinated with CPLs. Groups of three (left panel) or four (right panel) mice were vaccinated with 100 mg of the indicated peptides, and at the indicated time points peripheral blood was drawn and analyzed by pMHC multimer staining with pMHC multimers presenting ELAGIGILTV (left panel) or LLFGLALIEV (right panel). At day 97, mice in the left panel were administered a secondary vaccination (boost).

Increased efficiency of in vitro and in vivo CTL induction with optimized UTA2-1 epitopes

To evaluate the immunogenicity of CPLs 5, 8, and 9, we first performed in vitro CTL induction experiments in which unprimed PBMCs from two healthy UTA2-1-negative donors were stimulated with these peptides. From 2 to 3 weeks after the first peptide stimulation, increased efficiency of UTA2-1-specific T cell proliferation was seen for CPLs 8 and 9, as measured with pMHC multimer staining (Fig. 4B). The responses were most pronounced for CPL 8. Most importantly, virtually all UTA2-1-specific T cells stained double-positive for the wild-type UTA2-1 tetramer and the modified peptide-specific tetramer, indicating that the induced TCRs

were cross-reactive to both the CPL and the native Ag (Fig. 4B and Fig. S2). This finding was confirmed in an in vivo immunization model in which we immunized HLA-A*02:01-transgenic mice with CPL 8, CPL 9, or the wild-type UTA2-1 peptide. Splenocytes of the immunized mice were analyzed using an IFN-γ ELISPOT assay after stimulation of these cells with naturally mHag UTA2-1-positive and -negative human EBV-LCLs, in some cases exogenously loaded with the CPLs as positive controls. This analysis revealed that CPL 8 induced significantly higher frequencies of immunized peptide-specific CTLs than the wild-type epitope did, and a similar but nonsignificant trend was seen for CPL 9 (Fig. 4C, left panel). Furthermore, both 8- and 9-reactive CTLs were also directed at the natural UTA2-1 epitope presented on the cell surface of $mHag^+$ EBV-LCLs, which was for 8-reactive CTLs a significantly higher number than for the wild-type peptide (Fig. 4C, right panel). Finally, we evaluated whether the T cell responses induced with these CPLs had also retained their cytolytic function against human malignant targets expressing the natural Ag. Therefore, a bioluminescence cytotoxicity assay was performed; it demonstrated that splenocytes from all mice immunized with the UTA2-1 peptide or one of the modified derivatives specifically lysed MM cells endogenously expressing UTA2-1 (Fig. 4D). In contrast, splenocytes from a mouse immunized with an irrelevant peptide not expressed by MM cells did not display any specific lysis of these MM cells, but even stimulated their growth, as is often the result of secreted stimulatory cytokines.

Discussion

The introduction of non-proteogenic amino acids into peptide-based vaccines in principle opens up new avenues for improvement of vaccine delivery and for rational design of epitope vaccines. In this study, we have performed a systematic survey of the structural requirements for peptide binding to the HLA-A*02:01 allele to enhance peptide-MHC affinity, while retaining the ability to activate CTLs by interaction with the TCR. Our approach consisted of the introduction of non-proteogenic, synthetic amino acids into known epitopes at positions close to the N and C termini. Although substitutions with proteogenic amino acids already led to an enhancement of MHC affinity, the introduction of non-proteogenic, synthetic amino acid residues further boosted an increase in affinity. By scanning more than 90 aa residues through a multitude of epitopes, we were able to distill a list of preferred residues that typically lead to improved HLA-A*02:01-binding peptides (Fig. 1B). Notably, substitutions on P_1 with aromatic amino acids in the D conformation (e.g., α,α di-substituted α amino acid am-phg) proved to be favorable. These substitutions induce a gain in HLA affinity that can be explained by the π-π and cation-π interactions of the aromatic ring as well

as the formation of a strong hydrogen bonding network between the NH_2 group and the HLA α-chain, as revealed by the crystal structure of Mart-1-based CPL [am-phg][NVA]AGIGILT[PRG] in complex with HLA-A*02:01 (Fig. 2C). The affinity can be improved further when these replacements at P_1 are combined with NLE, NVA, 2-AOC, and CpAla substitutions at P_2 (Table 2). These residues contain extended alkyl chains that fit into a hydrophobic pocket of the HLA peptide-binding groove. For P_2-monosubstituted variants of Mart-1 peptide EAAGIGILTV HLA binding, scores increase upon extension of the aliphatic side chain in the following order: Ala (18%), NVA (54%), Leu (58%), NLE (59%), and 2-AOC (67%). This result can be explained by more hydrophobic contact between the large alkyl side chains and HLA-A*02:01 residues forming the pocket. In addition, CH-π interactions between the alkyl chains and Tyr7 could contribute to enhanced affinity, similar to those reported for Pro at P_3 and Tyr159 within H-2D^b::peptide structures[46]. However, we cannot exclude that extension of the P_2 side chain beyond that of NVA also affects the overall conformation of the peptide or TCR interaction, as has been shown for other APLs harboring P_2 or P_3 substitutions (see Fig. S3 for a structural analysis of P_2 and P_3 mutations and their modulatory effect on peptide conformation and TCR interaction). Although substitutions on P_3 have been shown to stabilize peptide-MHC interactions and even enhance immunogenicity (this study and Refs. 20, 45, 46), modifying the P_3 position of HLA-A*02:01-restricted epitopes should be performed with caution as this can also lead to loss of immunogenicity (this study and Ref. 48). Incorporation of unsaturated amino acids (PRG and ALG) on anchor position P_C also contributes to enhanced HLA affinity to some extent. C-terminal modification may be of particular value in improving protease resistance of peptide vaccines.

In proof-of-concept studies using T cell activation assays, we showed that several chemically optimized melanoma epitopes indeed resulted in higher and more persistent T cell responses in vitro. Peptide vaccination studies in HLA-A*02:01-transgenic mice with two enhanced melanoma epitopes showed that CTL frequencies were higher and longer lasting than for vaccination with wild-type peptides. These results indicate that the affinity of the peptide for MHC may be a crucial factor in enhanced T cell activation. This greater immunogenic potential can be explained by improved stability of the pMHC complex itself (and hence prolonged lifetime) or by increased stability of the pMHC-TCR complex resulting in extended stimulation of T cells. Although consistent improvements were found in HLA binding, T cell recognition of CPLs differed to some extent from peptide to peptide for all tested modifications, indicating that for each newly selected epitope HLA binding and T cell recognition experiments must be performed before introducing the CPLs to clinical applications.

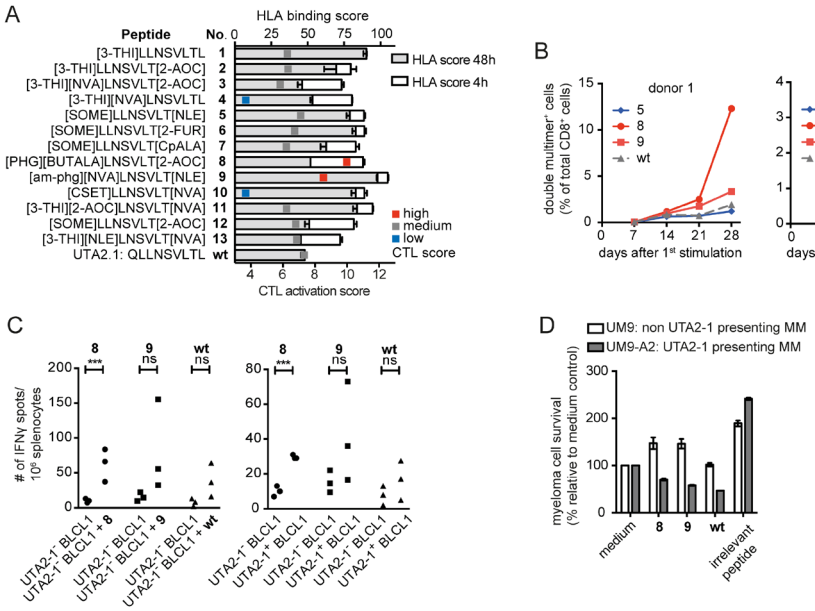

Figure 4. **CPLs of mHag UTA2-1 yield higher CTL frequencies.** (A) In all 13 modifications of the UTA2-1 epitope, an increased HLA-A*02:01 affinity was demonstrated indicated by high HLA binding scores (as in Fig. 1C), in most cases persisting up to 48 h. Coincubating the UTA2-1-specific CTL clone 503A1 together with APCs loaded with these peptides leads to CTL activation, as measured by IFN-γ release. The CTL activation score is the negative logarithm of the half-maximal effective peptide concentration (pEC50) inducing IFN-γ release; these values are representative for three experiments with comparable results. (B) In an in vitro CTL induction experiment, unprimed PBMCs from two UTA2-1$^-$ healthy donors were repeatedly stimulated with one of CPLs 5, 8, or 9 or wild-type (wt) UTA2-1. The proliferation of UTA2-1-specific T cells is strongest for CPL 8 and to a lesser extent for CPL 9, indicating increased efficiency of CTL induction compared with wt peptide, and these induced T cells largely stain double positive for the native UTA2-1 pMHC multimers and the modification-specific pMHC multimers used (Fig. S2). (C) Also in an in vivo immunization experiment with 8, 9, and the wild-type UTA2-1, the induction of Ag-specific cells, as measured by IFN-γ ELISPOT, was most efficient for 8 with significant increases in specific T cell responses against both 8 peptide-loaded and native mHag$^+$ APCs compared with mHag$^-$ APCs. With 9 and wt also specific responses were induced; however, this increase was not significant (ns) as determined with an unpaired t test. Human EBV-LCLs (BLCL1) were used as target APCs. Each replicate depicts the mean of results for every target per mouse, and each target was at least tested in duplicates. (D) The splenocytes from the mice immunized with 8, 9, or wt peptide all lysed UTA2-1 presenting MM cells in a bioluminescence cytotoxicity assay, confirming recognition of the native UTA2-1 Ag and cytotoxic potential of the induced immune response. UM9-A2 is the UTA2-1$^+$ HLA-A*02$^-$ MM cell line UM9 transduced with HLA-A*02:01.

After establishing this basic knowledge, we used the developed toolbox of preferred non-proteogenic amino acids to optimize the minor histocompatibility Ag UTA2-1, which is derived from a polymorphic region of a hematopoietic-specific protein encoded by the biallelic gene C12orf35[36]. Such polymorphic allopeptides, which are exclusively expressed on hematopoietic cells, are generally acknowledged to be ideal targets to induce graft-versus-tumor effects against hematologic tumors after allogeneic stem cell transplantation, without increasing the risk of graft-versus-host disease. For this type of non-self-antigen to which the TCR repertoire has not been negatively selected, further improvement of the immunogenicity is expected to induce antitumor responses that are even more effective. The concept of chemically altered peptides for vaccination is directly translatable to clinical applications using mHags, as the feasibility and effectiveness of dendritic cell vaccination-based immunotherapy for a number of these Ags are currently being evaluated in the clinic. In this study, we show that CPLs based on UTA2-1 can be generated that are capable of inducing an accelerated increase in frequencies of Ag-specific T cells in both in vitro and in vivo models with retained strong cytolytic potential. As such, these CPLs can be used for ex vivo enrichment and faster expansion of Ag-specific T cells for transfer into patients. Evaluation of MHC-peptide recognition by available Ag-specific T cell clones proved important for the strategy described here.

In summary, the present examples show that CPLs display enhanced MHC binding affinity and show a stronger and prolonged capacity to induce T cell activation and proliferation at concentrations lower than their respective wild-types. We have demonstrated that these results can be achieved for virtually any given epitope with a relatively small toolbox of non-proteogenic amino acids. As we increase the number of chemically immuno-optimized epitopes with this strategy, we can now explore the opportunities for clinical applications. Furthermore, a follow-up study, in which additional non-proteogenic amino acids are included that are based on our results, should lead to a more targeted approach in future efforts to improve T cell responses to CPL-based vaccines and to improve the solubility and (metabolic) stability of vaccine candidates.

Materials and Methods

Cells

EBV-transformed B cells (EBV-LCL) from individuals from a Caucasian population in the HapMap database (CEU) as well as multiple myeloma (MM) cell lines U266, UM9 and UM9-A2 (an HLA-A*02:01-transduced variant of UM9) were cultured in RPMI 1640 medium (Invitrogen, Carlsbad, CA) supplemented with 10% FBS

(Integro, Zaandam, the Netherlands) and standard antibiotics (1% penicillin/streptomycin). UTA2-1-specific T cell clone 503A1 was isolated, characterized, and cultured as described previously[36]. PBMCs for the CTL induction experiments were obtained from anonymous HLA-A*02:01^{+}UTA2-1^{-} healthy donors via Sanquin Blood Bank, the Netherlands. Other PBMC samples were obtained from healthy individuals or from patients with stage IV melanoma in accordance with local guidelines, and following informed consent. Ag-specific CD8^{+} T cell clones were generated as described elsewhere[49].

Peptide synthesis, building block synthesis, and resin loading with non-proteogenic amino acids

Peptides were synthesized in house by solid phase peptide synthesis on Multisyntech SYRO I and II peptide synthesizers. The 20 standard proteogenic amino acids (L- and D-forms) were purchased from NovaBiochem. Non-proteogenic amino acids were purchased from different suppliers, provided by Chiralix B.V., or synthesized in house.

Functionalization of solid-phase peptide synthesis resin

Where designated on the C terminus of a peptide, non-proteogenic amino acids were coupled to resin. To 1 g Tentagel S PHB resin (Rapp Polymere, substitution factor 0.27 mmol/g), 2.5 molar equivalents of amino acid were added, mixed, and taken up in 1:1 dichloromethane (Sigma-Aldrich) and N-methyl-2-pyrrolidone (Biosolve); 2.5 molar equivalents of 2,6-dicholorobenzoylchloride (Sigma-Aldrich) and 8.5 molar equivalents of pyridine (Sigma-Aldrich) were added, and the resulting solution was mixed by nitrogen flow and shaken overnight at room temperature.

Peptide binding and stability

HLA binding affinity of peptides was determined by a fluorescence polarization (FP) assay[38] based on ultraviolet-mediated MHC peptide exchange methodology[50]. Purified soluble MHC class I complexes (HLA-A*02:01) were loaded with an ultraviolet-labile peptide KILGFVFJV, in which J is photocleavable 3-amino-3-(2-nitrophenyl) propionic acid. MHC molecules were diluted in PBS supplemented with 0.5 mg/ml b-g-globulin (Sigma-Aldrich) to a final concentration of 0.75 mM and pipetted into a 96-well microplate. Tracer peptide FLPSDCFPSV (based on FLPSDFFPSV, Hepatitis B virus core protein$_{(18\text{-}27)}$) with a fluorescent TAMRA molecule covalently bound to the cysteine residue through a maleimide linkage was used as the competitor peptide[40]. This tracer peptide was diluted in PBS/b-g-globulin to a concentration of 6 nM and pipetted into a 96-well microplate. The peptides of interest were diluted in DMSO to a concentration of 125 mM and added to a 96-well microplate. The samples were prepared using a Hamilton high-throughput

liquid-handling robot at final concentrations of 0.5 mM MHC, 1 nM tracer, and 4.2 mM peptide in 30 ml together into a Corning black nonbinding surface 384-well microplate. The 384-well microplate was placed under a ultraviolet lamp (350 nm) for 30 min at 4°C to cleave the ultraviolet-labile peptide. The plate was then analyzed using a PerkinElmer Envision or BMG PHERAstar plate reader. FP values in millipolarization units were normalized to an HLA binding score that is defined as the percentage inhibition of fluorescent tracer peptide binding relative to control (100 mM of FLPSDFFPSV). Instant JChem (version 5.9, 2012) and the JChem for Excel plug-in were used for structure database management (ChemAxon, Budapest, Hungary). The percentage inhibition values of serial peptide dilutions were then used to calculate the IC50 values of peptide binding. Data were plotted in GraphPad Prism 5.01 and IC50 curves were fitted using the nonlinear regression sigmoidal dose-response formula.

Crystallization

HLA molecules were expressed and refolded as described[51] in the presence of peptide ([am-phg][NVA]AGIGILT[PRG], in which am-phg is D-alpha-methyl-phenylglycine, NVA is norvaline and PRG is propargylglycine). Subsequently, pMHC complexes were loaded on a Mono-Q anion exchange column and eluted with NaCl gradient in 20 mM Tris•Cl (pH 7.0). Complexes were further purified with gel-filtration chromatography on a Phenomex BioSep SEC-s3000 column in 20 mM Tris•Cl (pH 7.0) and 150 mM NaCl, followed by a final purification step on the Mono-Q anion exchange column and elution with NaCl gradient in 20 mM Tris•Cl (pH 7.0). Protein buffer was exchanged to 20 mM MES (pH 6.5) using a Centriprep concentrator, and final preparations were flash-frozen in liquid nitrogen and stored at 280°C. Crystals were generated essentially as described[52]. Briefly, crystals were grown from 22-24% PEG 1500, 0.1 M MES (adjusted to pH 6.5 with NaOH) using microseeding in 4-ml hanging drops (2 ml protein + 2 ml crystallization solution) at 20°C. Crystals were frozen in 30% PEG 1500, 12% glycerol, and 0.1 M MESNaOH (pH 6.5). Crystals were mounted in loops, vitrified in liquid nitrogen, and stored until data collection.

X-ray data collection and structure refinement

X-ray diffraction data for a single HLA-2.1::[am-phg][NVA]AGIGILT[PRG] crystal were collected at beamline PX3 at the Swiss Light Source (illigen, Switserland) at 100 K at a wavelength of 0.97890 Å. Data were processed using XDS[53] and integrated with SCALA[54] within the CCP4 suite[55]. A molecular replacement solution was obtained with AMORE[56] using the structure of HLA-A*02:01::ELAGIGILTV (RCSB Protein Data Bank identification code 1JF1 [http://www.rcsb.org/structure/1jf1])[44] as the search model. The structure was refined during multiple cycles of manual building and refinement using the Refinement of Macromolecular Structures

by the Maximum-Likelihood method[57]. A final refinement and evaluation was performed using the PDB_REDO webserver[58]. The final structure was resolved at 1.65 Å with R/R_{free} of 15.5/17.9%. Ninety-seven percent of the residues are within favorable regions of the Ramachandran plot, whereas 3% are within allowed regions. Rmsd values for bond lengths and angles are 0.012 Å and 1.563 Å, respectively. Data collection and refinement statistics are summarized in Table 1. The crystal structure presented in this article has been submitted to the RCSB Protein Data Bank (http://www.rcsb.org/pdb/home/home.do) under identification code 4WJ5.

T cell staining and flow cytometry

T cell staining with exchange pMHC multimers was performed essentially as described[51]. Enhanced and control peptides in DMSO were added to biotinylated MHC monomers (25 mg/ml in PBS) to a final concentration of 50 mM and ultraviolet irradiated for 30 min. Samples were left at room temperature for an additional 30 min. Subsequently, the plates were centrifuged for 5 min at 3300 × *g* to remove disintegrated MHC molecules. Streptavidin-R-PE (Life Technologies) was added to the exchanged monomers to a final concentration of 13.5 mg/ml. Resulting pMHC multimer (2 ml) was added to 100,000 T cells and incubated for 15 min at 37°C. Samples were stained with 1 ml APC Mouse Anti-Human CD8 (BD Pharmingen) and incubated for 20 min on ice. Subsequently, after two wash steps with PBS, samples were taken up in FACS buffer (0.5% BSA, 0.02% sodium azide in PBS) containing 1% propidium iodide to distinguish between live and dead T cells in the FACS analysis. Peptide-MHC binding to TCRs was analyzed by flow cytometry on either a Beckman Coulter CyAn ADP Analyzer or a BD FACSCalibur machine. Data were analyzed using FlowJo 7.6.1 (Tree Star) and Microsoft Excel 2007.

Intracellular IFN-γ staining

T cell activation assays based on IFN-γ secretion were performed using a BD Cytofix/Cytoperm fixation/permeabilization solution kit with BD GolgiPlug. To enable the immediate and sustained presentation of peptides to established T cell clones, 50,000 T2 APCs were pulsed with serial dilutions of the peptides for 1 h at 37°C in assay medium (100 ml RPMI/10% FCS) in a 96-well plate. After removing unbound peptides by centrifugation at 600 × *g* for 3 min, the peptide-pulsed T2 cells were cocultured with T cell clones (50,000 T cells per well in 100 ml assay medium supplemented with 1 ml/ml; BD GolgiPlug). Alternatively, to measure prolonged peptide presentation, peptide-pulsed T2 cells were incubated for an additional 23 or 47 h in 100 ml medium alone before incubation with T cells. After the addition of T cells, plates were centrifuged at 100 × *g* for 2 min to facilitate APC-T cell contacts. Positive controls included T cells stimulated

only with phorbol 12-myristate 13-acetate (PMA; 0.05 mg/ml) and ionomycin (1 mg/ml) in 100 ml medium. After 4 h of incubation at 37°C, plates were spun at 600 × *g* for 3 min, medium was discarded, and the cells were resuspended in 50 ml FACS buffer with FITCCD8 Ab (20 ml/ml) for 15 min in the dark at room temperature. After two spin (800 × *g* for 3 min) and wash steps with 200 ml FACS buffer cells were resuspended in 100 ml Cytofix/Cytoperm solution and incubated on ice for 20 min. The cells were then spin-washed twice with 200 ml Perm/Wash buffer and resuspended in 50 ml Perm/Wash buffer containing 20 ml/ml APC-IFN-γ Ab to incubate on ice for 30 min. After a final spin-wash with 200 ml of perm/wash buffer, cells were resuspended in FACS buffer and measured on a Beckman Coulter CyAn ADP Analyzer. Data were analyzed using FlowJo 7.6.1 (Tree Star) and Microsoft Excel 2007.

ELISA

T cell lines or clones were incubated for 20-24 h with HLA-A*02:01$^+$ UTA2-12 EBV-LCL lines pulsed with the tested peptides for 3 h at 37°C in culture medium as described elsewhere[36]. The IFN-γ content of cell-free supernatants was determined using a commercial ELISA kit (Pelipair, Sanquin) according to the manufacturer's instructions.

In vitro CTL inductions

PBMCs from HLA-A*02:01$^+$UTA2-1$^-$ healthy donors were sorted on CD8 expression by MACS following the instructions of the manufacturer (Miltenyi Biotec, Bergisch Gladbach, Germany). The CD8$^+$ fraction was used as effector cells; they were stimulated once weekly by either the CD82 fraction or bulk PBMCs pulsed for 3 hours with either one of the modified peptides or the wild-type UTA2-1 peptide and irradiated at 2500 rad. Culture medium was RPMI 1640 supplemented with 10% HS and antibiotics, rhuIL-2 was added twice a week starting from day 5. pMHC multimer staining was performed weekly, preceding each stimulation.

Bioluminescence-based cytotoxicity assays

Murine splenocytes were incubated for 20-24 h with luciferase-transduced MM cell lines in white, opaque, flat-bottom 96-well plates (Costar). After the addition of 125 mg/ml beetle luciferin, the light signal emitted from surviving multiple myeloma cells was determined using a luminometer (SpectraMax; Molecular Devices, Sunnyvale, CA). The percentage survival of MM cells was calculated using the following formula: Relative cell survival = 100% × (Experimental luciferase signal / Medium control luciferase signal).

Mouse immunizations

HLA-A*02:01 transgenic mice also containing a human CD8 binding domain (The Jackson Laboratory, Bar Harbor, ME) were injected i.v. at both sides of the tail base with 1-100 mg peptide and 50 mg CpG oligonucleotides 1826, emulsified in IFA, as adapted from Li et al.[59]. One-hundred microliters of blood was collected from the tail-tip at several time points and was analyzed for the presence of epitope-specific T cells by flow cytometry directly after collection. PE- and APC-labeled pMHC multimers containing the wild-type epitope were generated for this purpose, and 2 ml of PE-multimers and 4 ml of APC-multimers were used for dual staining of the blood samples. Prior to staining, all blood samples were erylysed.

Alternatively, for the UTA2-1 modifications and wild-type peptide, at the end of the experiment, spleens from all mice were isolated and analyzed for specific T cell responses using a commercial IFN-γ ELISPOT kit (Sanquin, Amsterdam, the Netherlands). Human EBV-LCLs either expressing or not expressing mHag UTA2-1, or exogenously loaded with one of the peptides, were used as target cells. Three mice were immunized with each peptide.

Online supplemental material

Figure S1. Affinity screening data of viral and melanoma epitope based CPLs.
Figure S2. T cells induced with CPLs are cross-reactive to pMHC multimers charged with native mHag or CPL.
Figure S3. Peptide substitutions at P_2 and P_3 modulate peptide-HLA-A*02:01 interaction and/or TCR binding.
Table S1. Peptide HLA binding scores of viral epitopes containing substitutions with proteogenic amino acids (single letter code).

Acknowledgements

We thank Henk Hilkmann and Dris El Atmioui for peptide synthesis, Dr. Carsten Linnemann for help with the modified melanoma peptide vaccination studies, beamline scientists at the Swiss Light Source (Villigen, Switzerland) for assistance during data collection experiments, and Robbie Joosten for advice with PDB_REDO and structural analysis. The authors have no financial conflicts of interest.

References

1. Hodi, F. S., S. J. O'Day, D. F. McDermott, R. W. Weber, J. A. Sosman, J. B. Haanen, R. Gonzalez, C. Robert, D. Schadendorf, J. C. Hassel, et al. 2010. Improved survival with ipilimumab in patients with metastatic melanoma. N. Engl. J. Med. 363: 711-723.
2. Rosenberg, S. A., J. C. Yang, and N. P. Restifo. 2004. Cancer immunotherapy: moving beyond current vaccines. Nat. Med. 10: 909-915.
3. Slansky, J. E., F. M. Rattis, L. F. Boyd, T. Fahmy, E. M. Jaffee, J. P. Schneck, D. H. Margulies, and D. M. Pardoll. 2000. Enhanced antigen-specific antitumor immunity with altered peptide ligands that stabilize the MHC-peptide-TCR complex. Immunity 13: 529-538.
4. Tang, Y., Z. Lin, B. Ni, J. Wei, J. Han, H. Wang, and Y. Wu. 2007. An altered peptide ligand for naı¨ve cytotoxic T lymphocyte epitope of TRP-2(180-188) enhanced immunogenicity. Cancer Immunol. Immunother. 56: 319-329.
5. Bowerman, N. A., L. A. Colf, K. C. Garcia, and D. M. Kranz. 2009. Different strategies adopted by K(b) and L(d) to generate T cell specificity directed against their respective bound peptides. J. Biol. Chem. 284: 32551-32561.
6. Engels, B., V. H. Engelhard, J. Sidney, A. Sette, D. C. Binder, R. B. Liu, D. M. Kranz, S. C. Meredith, D. A. Rowley, and H. Schreiber. 2013. Relapse or eradication of cancer is predicted by peptide-major histocompatibility complex affinity. Cancer Cell 23: 516-526.
7. Moutaftsi, M., S. Salek-Ardakani, M. Croft, B. Peters, J. Sidney, H. Grey, and A. Sette. 2009. Correlates of protection efficacy induced by vaccinia virusspecific $CD8^+$ T-cell epitopes in the murine intranasal challenge model. Eur. J. Immunol. 39: 717-722.
8. Van der Burg, S. H., M. J. Visseren, R. M. Brandt, W. M. Kast, and C. J. Melief. 1996. Immunogenicity of peptides bound to MHC class I molecules depends on the MHC-peptide complex stability. J. Immunol. 156: 3308-3314.
9. Yu, Z., M. R. Theoret, C. E. Touloukian, D. R. Surman, S. C. Garman, L. Feigenbaum, T. K. Baxter, B. M. Baker, and N. P. Restifo. 2004. Poor immunogenicity of a self/tumor antigen derives from peptide-MHC-I instability and is independent of tolerance. J. Clin. Invest. 114: 551-559.
10. Rudolph, M. G., R. L. Stanfield, and I. A. Wilson. 2006. How TCRs bind MHCs, peptides, and coreceptors. Annu. Rev. Immunol. 24: 419-466.
11. Evavold, B. D., J. Sloan-Lancaster, and P. M. Allen. 1993. Tickling the TCR: selective T-cell functions stimulated by altered peptide ligands. Immunol. Today 14: 602-609.
12. Valmori, D., J. F. Fonteneau, C. M. Lizana, N. Gervois, D. Lie´nard, D. Rimoldi, V. Jongeneel, F. Jotereau, J. C. Cerottini, and P. Romero. 1998. Enhanced generation of specific tumor-reactive CTL in vitro by selected Melan-A/MART-1 immunodominant peptide analogues. J. Immunol. 160: 1750-1758.
13. Rammensee, H. G., T. Friede, and S. Stevanoviı´c. 1995. MHC ligands and peptide motifs: first listing. Immunogenetics 41: 178-228.
14. Fremont, D. H., M. Matsumura, E. A. Stura, P. A. Peterson, and I. A. Wilson. 1992. Crystal structures of two viral peptides in complex with murine MHC class I H-2Kb. Science 257: 919-927.
15. Silver, M. L., H. C. Guo, J. L. Strominger, and D. C. Wiley. 1992. Atomic structure of a human MHC molecule presenting an influenza virus peptide. Nature 360: 367-369.
16. Falk, K., O. Ro¨tzschke, S. Stevanovic´, G. Jung, and H. G. Rammensee. 1991. Allele-specific motifs revealed by sequencing of self-peptides eluted from MHC molecules. Nature 351: 290-296.
17. Lee, J. K., G. Stewart-Jones, T. Dong, K. Harlos, K. Di Gleria, L. Dorrell, D. C. Douek, P. A. van der Merwe, E. Y. Jones, and A. J. McMichael. 2004. T cell cross-reactivity and conformational changes during TCR engagement. J. Exp. Med. 200: 1455-1466.
18. Chen, J.-L., G. Stewart-Jones, G. Bossi, N. M. Lissin, L. Wooldridge, E. M. L. Choi, G. Held, P. R. Dunbar, R. M. Esnouf, M. Sami, et al. 2005. Structural and kinetic basis for heightened immunogenicity of T cell vaccines. J. Exp. Med. 201: 1243-1255.
19. Ekeruche-Makinde, J., M. Clement, D. K. Cole, E. S. J. Edwards, K. Ladell, J. J. Miles, K. K. Matthews, A. Fuller, K. A. Lloyd, F. Madura, et al. 2012. T-cell receptor-optimized peptide skewing of the T-cell repertoire can enhance antigen targeting. J. Biol. Chem. 287: 37269-37281.
20. Tangri, S., G. Y. Ishioka, X. Huang, J. Sidney, S. Southwood, J. Fikes, and A. Sette. 2001. Structural features of peptide analogs of human histocompatibility leukocyte antigen class I epitopes that are more potent and immunogenic than wild-type peptide. J. Exp. Med. 194: 833-846.

21. Gladney, K. H., J. Pohling, N. A. Hollett, K. Zipperlen, M. E. Gallant, and M. D. Grant. 2012. Heteroclitic peptides enhance human immunodeficiency virus-specific CD8(+) T cell responses. Vaccine 30: 6997-7004.
22. Douat-Casassus, C., N. Marchand-Geneste, E. Diez, N. Gervois, F. Jotereau, and S. Quideau. 2007. Synthetic anticancer vaccine candidates: rational design of antigenic peptide mimetics that activate tumor-specific T-cells. J. Med. Chem. 50: 1598-1609.
23. Jones, M. A., J. K. Notta, M. Cobbold, M. Palendira, A. D. Hislop, J. Wilkie, and J. S. Snaith. 2008. Synthesis and ex vivo profiling of chemically modified cytomegalovirus CMVpp65 epitopes. J. Pept. Sci. 14: 313-320.
24. Weber, J. S., N. J. Vogelzang, M. S. Ernstoff, O. B. Goodman, L. D. Cranmer, J. L. Marshall, S. Miles, D. Rosario, D. C. Diamond, Z. Qiu, et al. 2011. A phase 1 study of a vaccine targeting preferentially expressed antigen in melanoma and prostate-specific membrane antigen in patients with advanced solid tumors. J. Immunother. 34: 556-567.
25. Liu, L., A. I. Bot, and D. C. Diamond, inventors; Mannkind Corporation, assignee. Peptide analogues. United States patent application 13/481,741, Publication No. US 2013/0017213 A1. 2013 Jan 17.
26. Go´mez-Nun˜ez, M., K. J. Haro, T. Dao, D. Chau, A. Won, S. Escobar-Alvarez, V. Zakhaleva, T. Korontsvit, D. Y. Gin, and D. A. Scheinberg. 2008. Non-natural and photo-reactive amino acids as biochemical probes of immune function. PLoS ONE 3: e3938.
27. Blanchet, J. S., D. Valmori, I. Dufau, M. Ayyoub, C. Nguyen, P. Guillaume, B. Monsarrat, J. C. Cerottini, P. Romero, and J. E. Gairin. 2001. A new generation of Melan-A/MART-1 peptides that fulfill both increased immunogenicity and high resistance to biodegradation: implication for molecular anti-melanoma immunotherapy. J. Immunol. 167: 5852-5861.
28. Webb, A. I., M. A. Dunstone, N. A. Williamson, J. D. Price, A. de Kauwe, W. Chen, A. Oakley, P. Perlmutter, J. McCluskey, M. I. Aguilar, et al. 2005. T cell determinants incorporating beta-amino acid residues are protease resistant and remain immunogenic in vivo. J. Immunol. 175: 3810-3818.
29. Guichard, G., A. Zerbib, F. A. Le Gal, J. Hoebeke, F. Connan, J. Choppin, J. P. Briand, and J. G. Guillet. 2000. Melanoma peptide MART-1(27-35) analogues with enhanced binding capacity to the human class I histocompatibility molecule HLA-A2 by introduction of a beta-amino acid residue: implications for recognition by tumor-infiltrating lymphocytes. J. Med. Chem. 43: 3803-3808.
30. Reinelt, S., M. Marti, S. De´dier, T. Reitinger, G. Folkers, J. A. de Castro, and D. Rognan. 2001. Beta-amino acid scan of a class I major histocompatibility complex-restricted alloreactive T-cell epitope. J. Biol. Chem. 276: 24525-24530.
31. Purcell, A. W., J. McCluskey, and J. Rossjohn. 2007. More than one reason to rethink the use of peptides in vaccine design. Nat. Rev. Drug Discov. 6: 404-414.
32. Guichard, G., F. Connan, R. Graff, M. Ostankovitch, S. Muller, J. G. Guillet, J. Choppin, and J. P. Briand. 1996. Partially modified retro-inverso pseudopeptides as non-natural ligands for the human class I histocompatibility molecule HLA-A2. J. Med. Chem. 39: 2030-2039.
33. Nair, D. T., K. J. Kaur, K. Singh, P. Mukherjee, D. Rajagopal, A. George, V. Bal, S. Rath, K. V. S. Rao, and D. M. Salunke. 2003. Mimicry of native peptide antigens by the corresponding retro-inverso analogs is dependent on their intrinsic structure and interaction propensities. J. Immunol. 170: 1362-1373.
34. Marschütz, M. K., W. Zauner, F. Mattner, A. Otava, M. Buschle, and A. Bernkop-Schnürch. 2002. Improvement of the enzymatic stability of a cytotoxic T-lymphocyte-epitope model peptide for its oral administration. Peptides 23: 1727-1733.
35. McGregor, D. P. 2008. Discovering and improving novel peptide therapeutics. Curr. Opin. Pharmacol. 8: 616-619.
36. Oostvogels, R., M. C. Minnema, M. van Elk, R. M. Spaapen, G. D. te Raa, B. Giovannone, A. Buijs, D. van Baarle, A. P. Kater, M. Griffioen, et al. 2013. Towards effective and safe immunotherapy after allogeneic stem cell transplantation: identification of hematopoietic-specific minor histocompatibility antigen UTA2-1. Leukemia 27: 642-649.
37. Morrison, J., J. Elvin, F. Latron, F. Gotch, R. Moots, J. L. Strominger, and A. McMichael. 1992. Identification of the nonamer peptide from influenza A matrix protein and the role of pockets of HLA-A2 in its recognition by cytotoxic T lymphocytes. Eur. J. Immunol. 22: 903-907.

38. Diamond, D. J., J. York, J. Y. Sun, C. L. Wright, and S. J. Forman. 1997. Development of a candidate HLA A*0201 restricted peptide-based vaccine against human cytomegalovirus infection. Blood 90: 1751-1767.
39. Buchli, R., R. S. VanGundy, H. D. Hickman-Miller, C. F. Giberson, W. Bardet, and W. H. Hildebrand. 2005. Development and validation of a fluorescence polarization-based competitive peptide-binding assay for HLA-A*02:01—a new tool for epitope discovery. Biochemistry 44: 12491-12507.
40. Rodenko, B., M. Toebes, P. H. N. Celie, A. Perrakis, T. N. M. Schumacher, and H. Ovaa. 2009. Class I major histocompatibility complexes loaded by a periodate trigger. J. Am. Chem. Soc. 131: 12305-12313.
41. Kawakami, Y., S. Eliyahu, K. Sakaguchi, P. F. Robbins, L. Rivoltini, J. R. Yannelli, E. Appella, and S. A. Rosenberg. 1994. Identification of the immunodominant peptides of the MART-1 human melanoma antigen recognized by the majority of HLA-A2-restricted tumor infiltrating lymphocytes. J. Exp. Med. 180: 347-352.
42. Parkhurst, M. R., E. B. Fitzgerald, S. Southwood, A. Sette, S. A. Rosenberg, and Y. Kawakami. 1998. Identification of a shared HLA-A*02:01-restricted T-cell epitope from the melanoma antigen tyrosinase-related protein 2 (TRP2). Cancer Res. 58: 4895-4901.
43. Mitchell, M. S., J. Kan-Mitchell, B. Minev, C. Edman, and R. J. Deans. 2000. A novel melanoma gene (MG50) encoding the interleukin 1 receptor antagonist and six epitopes recognized by human cytolytic T lymphocytes. Cancer Res. 60: 6448-6456.
44. Sliz, P., O. Michielin, J. C. Cerottini, I. Luescher, P. Romero, M. Karplus, and D. C. Wiley. 2001. Crystal structures of two closely related but antigenically distinct HLA-A2/melanocyte-melanoma tumor-antigen peptide complexes. J. Immunol. 167: 3276-3284.
45. Van Stipdonk, M. J. B., D. Badia-Martinez, M. Sluijter, R. Offringa, T. van Hall, and A. Achour. 2009. Design of agonistic altered peptides for the robust induction of CTL directed towards H-2Db in complex with the melanoma-associated epitope gp100. Cancer Res. 69: 7784-7792.
46. Uchtenhagen, H., E. T. Abualrous, E. Stahl, E. B. Allerbring, M. Sluijter, M. Zacharias, T. Sandalova, T. van Hall, S. Springer, P.-Å . Nygren, and A. Achour. 2013. Proline substitution independently enhances H-2D(b) complex stabilization and TCR recognition of melanoma-associated peptides. Eur. J. Immunol. 43: 3051-3060.
47. Ma, W., C. Germeau, N. Vigneron, A.-S. Maernoudt, S. Morel, T. Boon, P. G. Coulie, and B. J. Van den Eynde. 2004. Two new tumor-specific antigenic peptides encoded by gene MAGE-C2 and presented to cytolytic T lymphocytes by HLA-A2. Int. J. Cancer 109: 698-702.
48. Martinez-Hackert, E., N. Anikeeva, S. A. Kalams, B. D.Walker,W. A. Hendrickson, and Y. Sykulev. 2006. Structural basis for degenerate recognition of natural HIV peptide variants by cytotoxic lymphocytes. J. Biol. Chem. 281: 20205-20212.
49. Van Buuren, M. M., F. E. Dijkgraaf, C. Linnemann, M. Toebes, C. X. L. Chang, J. Y. Mok, M. Nguyen, W. J. E. van Esch, P. Kvistborg, G. M. Grotenbreg, and T. N. M. Schumacher. 2014. HLA micropolymorphisms strongly affect peptide-MHC multimer-based monitoring of antigen-specific $CD8^+$ T cell responses. J. Immunol. 192: 641-648.
50. Toebes, M., M. Coccoris, A. Bins, B. Rodenko, R. Gomez, N. J. Nieuwkoop, W. van de Kasteele, G. F. Rimmelzwaan, J. B. A. G. Haanen, H. Ovaa, and T. N. M. Schumacher. 2006. Design and use of conditional MHC class I ligands. Nat. Med. 12: 246-251.
51. Toebes, M., B. Rodenko, H. Ovaa, and T. N. M. Schumacher. 2009. Generation of peptide MHC class I monomers and multimers through ligand exchange. Curr. Protoc. Immunol. 18: 18.16.
52. Celie, P. H. N., M. Toebes, B. Rodenko, H. Ovaa, A. Perrakis, and T. N. M. Schumacher. 2009. UV-induced ligand exchange in MHC class I protein crystals. J. Am. Chem. Soc. 131: 12298-12304.
53. Kabsch, W. 2010. XDS. Acta Crystallogr. D Biol. Crystallogr. 66: 125-132.
54. Evans, P. 2006. Scaling and assessment of data quality. Acta Crystallogr. D Biol. Crystallogr. 62: 72-82.
55. Winn, M. D., C. C. Ballard, K. D. Cowtan, E. J. Dodson, P. Emsley, P. R. Evans,R. M. Keegan, E. B. Krissinel, A. G. W. Leslie, A. McCoy, et al. 2011. Overview of the CCP4 suite and current developments. Acta Crystallogr. D Biol. Crystallogr. 67: 235-242.
56. Navaza, J. 1994. AMoRe: an automated package for molecular replacement. Acta Crystollagr. A. 50: 157-163.

57. Murshudov, G. N., A. A. Vagin, and E. J. Dodson. 1997. Refinement of macromolecular structures by the maximum-likelihood method. Acta Crystallogr. D Biol. Crystallogr. 53: 240-255.
58. Joosten, R. P., K. Joosten, S. X. Cohen, G. Vriend, and A. Perrakis. 2011. Automatic rebuilding and optimization of crystallographic structures in the Protein Data Bank. Bioinformatics 27: 3392-3398.
59. Li, L.-P., J. C. Lampert, X. Chen, C. Leitao, J. Popovic, W. Müller, and T. Blankenstein. 2010. Transgenic mice with a diverse human T cell antigen receptor repertoire. Nat. Med. 16: 1029-1034.

3

Chemical modification of influenza CD8+ T-cell epitopes enhances their immunogenicity regardless of immunodominance

Sietske K. Rosendahl Huber[1]*, Jolien J. Luimstra[2,3]*, Josine van Beek[1], Rieuwert Hoppes[2], Ronald H.J. Jacobi[1], Marion Hendriks[1], Kim Kapteijn[2], Casper Ouwerkerk[2], Boris Rodenko[2], Huib Ovaa[2,3], and Jørgen de Jonge[1]

*S.K. Rosendahl Huber and J.J. Luimstra contributed equally to this work.

[1]Centre for Infectious Disease Control, National Institute for Public Health and the Environment, Bilthoven, The Netherlands
[2]Division of Cell Biology, Netherlands Cancer Institute, Amsterdam, The Netherlands
[3]Institute for Chemical Immunology, The Netherlands

PLoS One 11, e0156462 (2016)

Abstract

T cells are essential players in the defense against infection. By targeting the MHC class I antigen-presenting pathway with peptide-based vaccines, antigen-specific T cells can be induced. However, low immunogenicity of peptides poses a challenge. Here, we set out to increase immunogenicity of influenza-specific $CD8^+$ T cell epitopes. By substituting amino acids in wild type sequences with non-proteogenic amino acids, affinity for MHC can be increased, which may ultimately enhance cytotoxic $CD8^+$ T cell responses. Since preventive vaccines against viruses should induce a broad immune response, we used this method to optimize influenza-specific epitopes of varying dominance. For this purpose, HLA-A*02:01 epitopes GILGFVFTL, FMYSDFHFI and NMLSTVLGV were selected in order of decreasing MHC-affinity and dominance. For all epitopes, we designed chemically enhanced altered peptide ligands (CPLs) that exhibited greater binding affinity than their WT counterparts; even binding scores of the high affinity GILGFVFTL epitope could be improved. When HLA-A*02:01 transgenic mice were vaccinated with selected CPLs, at least 2 out of 4 CPLs of each epitope showed an increase in IFN-γ responses of splenocytes. Moreover, modification of the low affinity epitope NMLSTVLGV led to an increase in the number of mice that responded. By optimizing three additional influenza epitopes specific for HLA-A*03:01, we show that this strategy can be extended to other alleles. Thus, enhancing binding affinity of peptides provides a valuable tool to improve the immunogenicity and range of preventive T cell-targeted peptide vaccines.

Introduction

For many infectious diseases, cellular responses are required for clearance of the pathogen from the host. One such disease that causes serious health threats worldwide is influenza[1]. Preventive influenza vaccines mainly confer protection via antibodies directed against the highly variable surface proteins hemagglutinin (HA) and neuraminidase (NA). Influenza virus can escape previously induced immunity due to mutations in antigenic sites, so-called antigenic drifts. Consequently, protection is subtype or strain-specific and regular vaccine updates are required. In addition, current vaccines do not provide protection against newly emerging influenza subtypes, which has led to pandemics four times in the last century and most recently in 2009[2,3]. Cellular responses are often directed towards more conserved parts of the virus and may therefore provide cross-protection; however, eliciting these responses by vaccination remains a challenge[4,5]. Vaccination with peptides that target antigen-specific T cells is one of the approaches that could induce these cross-protective cellular responses[6].

In general, peptide vaccines may aid in treating or preventing various types of diseases[7]. Kenter et al. reported a therapeutic cancer vaccine based on long overlapping peptides that induced robust T cell responses leading to clinical effectiveness[8]. Over the past years, preclinical research and two phase I clinical trials were reported, in which preventive influenza vaccines containing a set of long overlapping peptides capable of inducing T cell responses were described[9-11]. Whether or not a peptide is capable of inducing such responses is dependent on characteristics such as length of the peptide and adjuvation. The latter is required, since peptides alone are often weak immunogens[12]. We recently described a method to increase immunogenicity of peptides in the context of therapeutic anti-tumor vaccination, by substitution with amino acids that are not naturally incorporated into proteins, so-called non-proteogenic amino acids[13]. By expanding the natural protein code, we aimed to generate peptides that increase peptide-MHC binding more than achieved by using substitution with proteogenic amino acids. The resulting chemically enhanced peptide ligands (CPLs) had increased binding affinities compared to the wild type peptides, which in turn led to enhanced T cell responses. Here, we used this approach to modify peptides encoding highly conserved influenza-specific class I epitopes of varying dominance in the immune response to influenza infection. This approach could ultimately be used for a preventive influenza vaccine.

Individuals with preexisting cytotoxic influenza-specific T cells were shown to have an immunological advantage upon encounter with influenza virus due to cross-reactivity of these T cells[14-16]. The presence of cross-reactive cytotoxic T cells has even been shown to limit disease[17]. Several preventive short (9-10 aa) peptide vaccination concepts, focusing on highly conserved CD8+ T cell-specific influenza peptides, have been described[18-21]. Immunogenicity of these peptide vaccines was enhanced by methods such as incorporation of peptides into virosomes or liposomes and ligation of the peptides to a lipid tail. These methods proved promising in mouse experiments. However, these approaches were aimed at increasing immunogenicity by adding adjuvants or by using different modes of delivery, but none increased intrinsic immunogenicity of the peptides.

Immunogenicity of a peptide is defined by three interacting partners: peptide, MHC and TCR[22]. Class I peptides are generated during degradation of a protein by the proteasome, followed by loading of the peptides on MHCI molecules[23]. Each MHC allele has a different peptide-binding groove with specific binding pockets in which amino acid side chains of a peptide's anchor residues can protrude[24,25]. Amino acid positions of peptides are referred to as P_1-P_C, P_1 being the N-terminal and P_C the C-terminal residue. By altering the anchor residues, which are usually found towards the C- and N-termini of the peptide, the number and/or quality of interactions between the peptide and MHC molecule can be altered, thereby increasing peptide affinity[26,27]. This will result in prolonged

presentation of peptides on the cell surface, which may lead to enhanced T cell immunogenicity[28,29]. Modification of the central amino acids of the peptide, on the other hand, frequently results in abrogated T cell reactivity, since this part of the epitope is directly recognized by the TCR[30-32].

In this study, we focused on improving the binding affinity of short (9-10 aa) highly conserved influenza-specific epitopes in order to enhance their immunogenicity. We selected three highly conserved influenza epitopes specific for HLA-A*02:01, the most abundant HLA allele in the Caucasian population, based on their varying binding affinities and dominance in influenza A virus infection: the highly dominant GILGFVFTL ($M1_{58-66}$), the less dominant FMYSDFHFI (PA_{46-54}) and the low affinity subdominant NMLSTVLGV ($PB1_{413-421}$) epitopes[33]. We show that substitution with non-proteogenic amino acids can lead to improved HLA binding and T cell responses as measured by IFN-γ production in both in vitro and in vivo models. Moreover, we show that this strategy can be applied to epitopes specific for other alleles by improving binding of influenza epitopes ILRGSVAHK ($NP_{265-273}$), SFSFGGFTK ($PB2_{322-330}$) and RMVLSAFDER (NP_{67-76}) (in order of decreasing dominance) to HLA-A*03:01, another frequently occurring allele in the Caucasian population[34]. Thus, by enhancing binding affinity, responses to dominant and more importantly to otherwise subdominant epitopes can be improved.

Results

Optimizing HLA-A*02:01 binding affinity of influenza epitopes

To enhance affinity for HLA-A*02:01, amino acids of the WT peptides were substituted with non-proteogenic amino acids (Fig. 1). Three influenza-specific epitopes were selected based on their varying binding affinity and dominance in the immune response. Per epitope, approximately 200 peptides were rationally designed based on available crystal structures and on side chain similarities. Binding affinity was determined by a fluorescence polarization (FP) assay (Table S1), in which CPLs compete with fluorescent tracer peptide for HLA-A*02:01 binding[35,36]. From the difference in FP of MHC with tracer alone and in combination with CPL, the binding strength of the test peptide was scored as percentage inhibition of tracer peptide binding. This method allowed for high-throughput testing of multiple peptides. Per epitope, we selected 20 CPLs for their varying binding affinities ranging from the best binding CPLs to CPLs that bound approximately equally well as the WT peptide in order to study the correlation between binding scores and in vitro and in vivo responses (Table 1). After 4 hours, many of the peptides showed increased binding, but those peptides that still showed increased binding after 24 hours are likely to have a lower

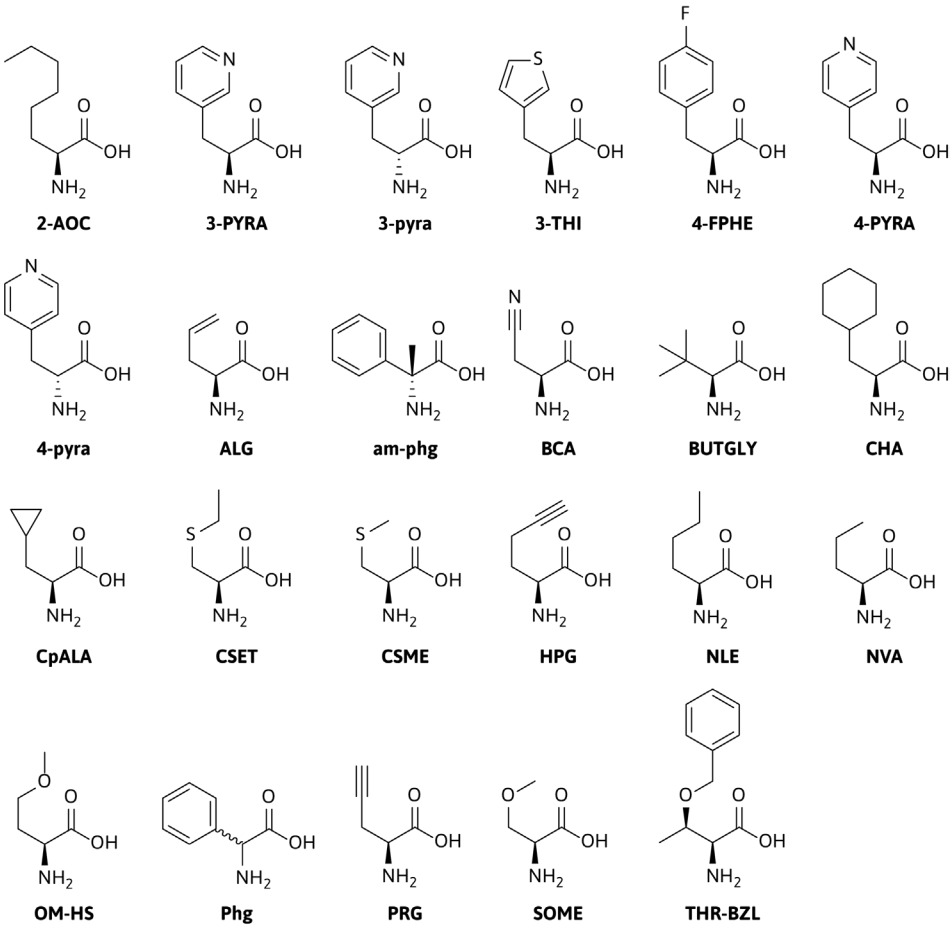

Figure 1. **Structures of non-proteogenic amino acids found in the best CPLs.** L-amino acids are denoted in uppercase characters; D-amino acids in lowercase characters. Incorporation of Phg results in a racemic mixture.

off-rate as a result of their higher affinity. As depicted in Table 1, the binding score of WT GILGFVFTL was 84% after 24 hours of incubation. Insertion of the non-proteogenic amino acid D-α-methyl-phenylglycine (am-phg) on P_1, resulted in the most successful CPL with a binding score of 98% (G1; see Table 1). Other successful substitutions on P_1 were mainly aromatic amino acids, such as DL-phenylglycine (Phg) (G7; see Table 1), or the L- (represented in uppercase) and D- (represented in lowercase) amino acids of 3'- and 4'-pyridyl-alanine (3- and 4-PYRA; 3- and 4-pyra;), which also resulted in increased binding scores (G8, G15, G4 and G10, Table 1).

Since the two less immunodominant influenza epitopes FMYSDFHFI and NMLSTVLGV naturally have lower affinities compared to GILGFVFTL, we

expected an even larger improvement for CPLs derived from these peptides. Substitution with the aromatic 4-fluorophenylalanine (4-FPHE) in combination with a substitution with L-2-amino-octanoic acid (2-AOC) resulted in CPLs with the highest binding score for both FMYSDFHFI and NMLSTVLGV epitopes. The binding score for FMYSDFHFI was raised from 75% to 94% after substitution of P_1 with 4-FPHE, in combination with 2-AOC on P_9 (F5; Table 1). 4-FPHE on P_1 in combination with 2-AOC on P_2, increased the binding score of NMLSTVLGV from 55% to 92% (N95; Table 1). Apart from these peptides, 2-AOC alone led to increased binding when substituted at or near the anchor positions P_2 and P_9 for both FMYSDFHFI and NMLSTVLGV (F143, F19, F95, N39, N41, N40; see Table 1). Thus, using non-proteogenic amino acid substitutions, we were able to increase the binding of peptides such that they nearly inhibited 100% of the tracer peptide from binding, regardless of the affinity of the WT epitope.

In vitro and ex vivo T cell activation screening assays

Since modifications could change the T cell-exposed peptide side chains in such a way that they do not resemble those of the WT peptide anymore, we investigated whether CPLs were still capable of activating WT-specific T cells. To determine this for modifications of GILGFVFTL, antigen-presenting T2 cells were pulsed with CPLs and co-cultured with a GILGFVFTL-specific T cell clone. Subsequently, IFN-γ production was determined by flow cytometry after 24 hours of culture. Approximately half of the 16 tested CPLs showed higher IFN-γ responses compared to the WT epitope (Table S3). After 24 hours, G1 and G7, the CPLs with the highest binding affinity induced high IFN-γ responses. In addition, G16 and G25 with moderately improved binding affinity also induced high IFN-γ responses; however, 4 out of 13 CPLs with similar or improved binding showed strongly reduced to no activation. Therefore, affinity is to a certain extent indicative for $CD8^+$ T cell activation, but fails as a predictor in some cases. The latter may indicate that the T cell-exposed peptide structure is altered.

Since T cell clones for FMYSDFHFI and NMLSTVLGV were not available, other assays were developed to allow pre-selection for in vivo experiments. To be able to compare the predictive value of these assays with that of the T cell clone-based assay, we also performed these assays with GILGFVFTL CPLs. The first alternative strategy included testing responses following CPL stimulation in a human HLA-$A2^+$ DC T cell co-culture model. For this purpose, HLA-$A2^+$ donors were selected based on the presence of CD8 specific IFN-γ responses after stimulation with WT peptide. Monocytes from these donors were isolated, differentiated into immature DCs and subsequently pulsed with different CPLs. After pulsing, DCs were matured and co-cultured with autologous T cells for seven days. Then, IFN-γ production of $CD8^+$ T cells was measured by flow cytometry. Several CPLs appeared to induce a higher response than their corresponding WT peptides

Table 1. **FP binding scores of selected HLA-A*02:01 peptides.**

#	GILGFVFTL	4h	SD	24h	SD
G1	[am-phg]ILGFVFTL	97	4	98	4
G7	[Phg]ILGFVFTL	96	0	94	2
G8	[3-PYRA]ILGFVFTL	94	3	93	1
G15	[4-PYRA]ILGFVFTL	93	3	93	3
G4	[3-pyra]ILGFVFTL	92	6	92	6
G12	GILGFV[4-FPHE]TL	92	3	92	5
G27	[am-phg][CpALA]LGFVFTL	92	1	91	2
G10	[4-pyra]ILGFVFTL	90	2	91	4
G9	yILGFVFTL	94	2	90	2
G16	G[NLE]LGFVFTL	91	3	90	5
G3	GILGFVFT[CpALA]	90	5	90	5
G25	[SOME]ILGFVFTL	89	12	89	13
G13	GILGFVFT[ALG]	88	8	88	7
G17	GILGFVFT[PRG]	88	3	88	5
G WT	**GILGFVFTL**	85	0	84	2
G24	fILGFVFTL	86	8	81	7
G20	GILGFV[BUTGLY]TL	82	10	79	12
G22	GILGFVFT[2-AOC]	79	14	77	15
G11	[CSME]ILGFVFTL	72	28	70	32
G26	G[2-AOC]LGFVFT[PRG]	60	4	54	2
G29	[3-PYRA]ILGFVFT[2-AOC]	44	7	38	5

#	FMYSDFHFI	4h	SD	24h	SD
F5	[4-FPHE]MYSDFHF[2-AOC]	95	2	94	2
F118	[CSET][2-AOC]YSDFHFI	95	4	93	3
F141	[THR-BZL][2-AOC]YSDFHFI	94	2	93	2
F48	F[2-AOC]YSDFHF[CHA]	93	1	92	1
F143	F[2-AOC]YSDFHFI	93	2	91	2
F102	[3-THI][2-AOC]YSDFHFI	92	0	91	0
F112	[BCA][2-AOC]YSDFHFI	92	4	91	3
F7	[am-phg]MYSDFHF[2-AOC]	91	4	90	4
F69	F[2-AOC]YSDFHF[NLE]	90	3	89	2
F49	FMYSDFHF[CHA]	88	2	86	3
F19	FMYSDFHF[2-AOC]	87	2	86	2
F193	[am-phg][NVA]YSDFHFI	85	3	81	2
F54	FMYSDFHF[CSET]	82	4	80	4
F95	[2-AOC]MYSDFHFI	82	3	80	3
F105	[4-FPHE]MYSDFHFI	86	1	78	1
F52	FMYSDFHF[CpALA]	81	3	78	4
F63	FMYSDFHF[HPG]	81	7	78	5
F142	[THR-BZL]MYSDFHFI	80	2	77	3
F WT	**FMYSDFHFI**	78	3	75	2
F100	[3-PYRA]MYSDFHFI	79	7	73	5
F111	[am-phg]MYSDFHFI	75	9	72	9

#	NMLSTVLGV	4h	SD	24h	SD
N95	[4-FPHE][2-AOC]LSTVLGV	92	1	90	1
N177	F[2-AOC]LSTVLGV	90	2	88	2
N11	[am-phg]MLSTVLG[2-AOC]	90	2	88	2
N91	[OM-HS][2-AOC]LSTVLGV	91	2	87	1
N169	[CSME][2-AOC]LSTVLGV	89	4	87	4
N172	[PHG][2-AOC]LSTVLGV	89	3	86	4
N8	[3-PYRA]MLSTVLG[2-AOC]	85	7	82	7
N92	[SOME][2-AOC]LSTVLGV	84	3	81	3
N98	[3-THI]MLSTVLG[2-AOC]	83	2	79	1
N46	[am-phg]MLSTVLGV	80	1	76	1
N41	NM[2-AOC]STVLGV	78	5	73	5
N176	[THR-BZL]MLSTVLGV	73	3	70	3
N40	N[2-AOC]LSTVLGV	71	6	67	5
N15	[NVA]MLSTVLG[2-AOC]	71	11	65	10
N39	[2-AOC]MLSTVLGV	68	8	63	7
N53	N[NLE]LSTVLGV	66	3	61	3
N122	NMLSTVLG[CpALA]	65	2	60	1
N61	[SOME]MLSTVLGV	62	1	54	7
N52	[NLE]MLSTVLGV	54	4	46	5
NWT	**NMLSTVLGV**	53	5	46	4
N43	[3-PYRA]MLSTVLGV	47	19	41	20

HLA-A*02:01 binding of CPLs of influenza epitopes; dominant GILGFVFTL (M_{158-66}), subdominant FMYSDFHFI (PA_{46-54}) and subdominant NMLSTVLGV ($PB1_{413-421}$), was determined using an FP-based competition assay. Binding was scored as percentage inhibition of tracer peptide binding after 4h and 24h in three independent experiments. Maintained binding after 24 hours indicates a lower off-rate, presumably due to increased stability. This table shows binding scores in a heat map for the WT epitopes (bold) and 20 CPLs that were selected for in vitro and ex vivo testing. Green indicates high binding scores, yellow medium and red low binding scores. Peptides highlighted in blue were used in vaccination experiments. SD: standard deviation. See Table S2 for a heat map representation.

(Table S3); however, this assay had both a high assay variation and a high variation between donors.

To limit inter-individual variation, a third strategy was developed, in which CPLs were tested ex vivo on splenocytes of HLA-A2 tg mice vaccinated with either one of the three WT epitopes. Two weeks post booster vaccination, spleen cells were isolated and restimulated for 16 hours with selected CPLs and IFN-γ levels were measured by ELISpot. In this assay, only CPLs G13 and F100 induced similar responses compared to their corresponding WT peptide (Table S3). In general, the positive results of the three assays correlate poorly, as shown in Table 2 for the upper three CPLs after ranking the results based on T cell activation for each assay. However, a correlation between the three assays was found for the lower ranked CPLs derived from GILGFVFTL and NMLSTVLGV, which allowed for negative selection. We therefore used both positive and negative results from all assays to include or exclude CPLs for further investigation.

CPLs were analyzed for their capacity to induce a response in WT-specific T cells. Therefore, three assays were developed in which IFN-γ production was used as a measure of response. The first was analysis of GILGFVFTL-CPLs on a WT-specific T cell clone (T cell clone). However, no T cell clone was available for the two other WT epitopes. Therefore, in the second assay, CPLs were loaded onto DCs of HLA-A2^{+} human donors and co-cultured for seven days with autologous CD8^{+} T cells (DC model). Due to high variation in the DC model, another assay was performed by 16 hours stimulation of splenocytes of WT-vaccinated HLA-A*02:01 mice with CPLs (mouse splenocytes). This table shows the upper three and lower three CPLs after ranking the results based on T cell activation for each assay separately. CPLs marked with the same color show similarities between CPLs in the assays and * indicates when a CPL induced a response lower than that of the WT peptide control. As visualized by the colored CPLs, a correlation between assays was found for the lower three CPLs derived from GILGFVFTL and NMLSTVLGV in all three assays. However, no correlation was found between assays for the upper CPLs.

In vivo stimulation using modified peptides

Vaccination of HLA-A2 tg mice with either of the three WT epitopes confirmed their dominance in the immune response as shown by the corresponding induction of IFN-γ as measured by ELISpot (Fig. S1A). Since the HLA-A2 tg mice had a C57BL/6 background and co-expressed H2-K^{b}, a control experiment in C57BL/6 mice was performed. In these mice, no responses to the selected WT HLA-A*02:01 epitopes were observed, which confirmed that responses in the HLA-A2 tg mice were HLA-A*02:01-specific (Fig. S1A). Subsequently, four CPLs per epitope were selected for in vivo testing. GILGFVFTL CPLs were selected based on binding scores and T cell clone data. To analyze a broad spectrum, CPLs with varying binding scores

Table 2. **Summary of pre-selection experiments**

	GILGFVFTL			FMYSDFHFI		NMLSTVLGV	
	T cell clone	DC model	Mouse splenocytes	DC model	Mouse splenocytes	DC model	Mouse splenocytes
Upper 3	G1	G26	G13	F49	F100	N172	N92*
	G16	G7*	G3*	F5	F102*	N169	N40*
	G25	G15*	G22*	F54	F143*	N41	N172*
Lower 3	G4	G24	G24	F69	F49	N11	N15
	G9	G17	G9	F19	F5	N46	N11
	G24	G20	G4	F102	F7	N8	N8

*Lower response than WT peptide

were selected (Table 1). Of these CPLs G1, G16 and G25 induced highest responses in the T cell clone, while G8 induced a response similar to that of the WT epitope (Table S3).

HLA-A2 tg mice were vaccinated with different doses of WT GILGFVFTL peptide or CPLs G1, G8, G16 or G25 on days 0 and 21. Two weeks post booster vaccination, spleen cells were isolated and stimulated for 16 hours with different peptides and analyzed using an IFN-γ ELISpot assay. First, the effect of enhanced binding affinity on a T cell response was investigated using homologous peptide as a stimulus (Fig. 2A). Overall, responses of G1-vaccinated mice were highest and those of G8-vaccinated mice lowest. Responses of G16- and G25-vaccinated mice, on the other hand, were highest at a vaccination dose of 25 nmol peptide and did not increase at higher doses. However, these CPL-specific T cells might not recognize the WT epitopes. Restimulation of splenocytes of CPL-vaccinated mice with WT peptide mimics a natural situation in which CPL-induced T cells respond to infection with a virus containing the WT epitope. As shown in Figure 2B, responses of WT-vaccinated mice were low at peptide vaccination doses of 10, 25 and 50 nmol, but increasing the dose to 100 nmol resulted in higher T cell responses. G1- and G8-vaccinated mice, on the other hand, showed a higher response compared to WT vaccinated mice at lower doses (Fig. 2B). At a dose of 100 nmol the difference between CPLs and WT-peptide vaccinated mice was reversed, which might be due to overstimulation by CPLs at these high doses. Overall, G1 and G8 were the most promising GILGFVFTL CPLs as they resulted in the largest increase in responses after restimulation with WT peptide.

Selection of CPLs for the other two epitopes was more challenging, since data obtained using the different pre-selection strategies did not correspond well (Table 2 and Table S3). We therefore selected CPLs based on data from vaccination experiments with GILGFVFTL CPLs in addition to the results of the screening assays. The final selection for FMYSDFHFI comprised F5 based on the DC co-culture model, F100 because it performed well in WT-specific mouse splenocytes and F111 and F193 based on favorable substitutions observed in pilot experiments with GILGFVFTL CPLs in mice. Mice were vaccinated with these

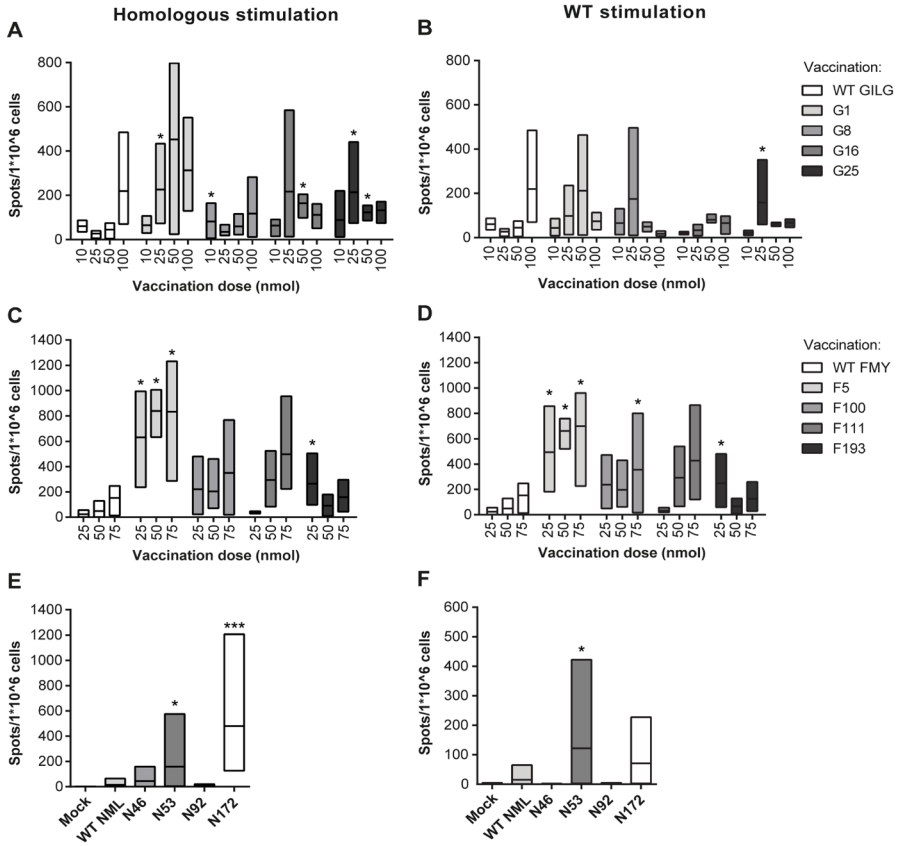

Figure 2. **Vaccination with CPLs shows enhanced IFN-γ responses in vivo compared to vaccination with WT peptide.** Mice were vaccinated with different doses of WT peptide or CPLs on day 0 and day 21 and two weeks later spleen cells were isolated and restimulated with homologous peptides or WT peptide. Responses were measured by IFN-γ ELISpot after 16 hours stimulation with 0.1 nmol peptide/well. Mice were vaccinated with mock (not shown), 10, 25, 50 or 100 nmol of WT GILGFVFTL or with the indicated CPLs. Spleen cells were restimulated with homologous (A) or WT (B) peptide. Overall, responses were highest after stimulation with CPL G1. For FMYSDFHFI mice were vaccinated with mock (not shown), 25, 50 or 75 nmol of WT peptide or the indicated CPLs. Cells were restimulated for 16 hours with homologous (C) or WT (D) peptide. Three out of four CPLs (F5, F100 and F111) induced higher responses compared to WT-peptide vaccination. For NMLSTVLGV mice were mock vaccinated or vaccinated with a dose of 75 nmol of WT peptide or respective CPLs. Spleen cells were restimulated with homologous (E) or WT (F) peptide. CPL N172 induced most T cells that responded to homologous stimulation, whereas N53 induced most T cells responding to WT peptide. Mock-vaccinated mice in experiments shown in A-D demonstrated comparable responses to mock-vaccinated mice in E and F.
Data shown in A-D represent three mice per dose. Data in E and F are derived from 7–8 mice per group, with the exception of the mock, for which three mice were included. Bars are min to max, with line at mean. Data were statistically analyzed using a Mann-Whitney test. * $p<0.05$; *** $p<0.001$ compared to the WT equivalent.

CPLs using three doses of peptide, since in the previous experiment we observed minimal responses at the lowest dose used (10 nmol). Homologous peptide restimulation showed that vaccination with all four CPLs dramatically increased T cell responses compared to WT peptide (Fig. 2C). When cells were restimulated with WT peptide three out of four CPL-vaccinated mice (F5, F100, F111) clearly showed higher IFN-γ responses than WT peptide-vaccinated mice (Fig. 2D). One CPL (F193) only showed higher responses than WT peptide at a vaccination dose of 25 nmol. Thus, modification greatly enhanced T cell responses for three out of four peptides, even at low vaccination doses.

For the epitope NMLSTVLGV, CPLs N46 and N53 were selected based on modifications that were successful in previous in vivo experiments with GILGFVFTL, N92 because it was one of the few peptides that induced a response similar to that of WT peptide in WT-specific mouse splenocytes and N172 based on the DC co-culture data. Since NMLSTVLGV is a very low affinity epitope, these CPLs had, as expected, the largest improvement in binding score (Table 1). Earlier experiments indicated that the WT peptide induced responses only in approximately one out of six mice; therefore we chose to focus on just one vaccination dose and to increase the number of mice to seven or eight per group to assure that at least 1-2 mice responded to WT peptide vaccination. Figure 2 shows that vaccination with CPLs N46, N53 and N172 increased the responses compared to vaccination with WT peptide, whereas N92-vaccinated mice did not respond to restimulation (Fig. 2, E and F). All of the N172-vaccinated mice (n=7), half of the N53-vaccinated mice (n=4) and four of the N46-vaccinated mice responded to homologous peptide restimulation. When spleen cells of N172-vaccinated mice were restimulated with WT peptide, half of these mice (n=3) responded. For CPL N53 the number of responders remained stable (n=4), while there were no responders for CPL N46. By modifying NMLSTVLGV, responses could be induced in a larger proportion of mice compared to WT peptide and these responses were higher in all cases, which is a major enhancement for this very subdominant peptide. CPL N172 was among the top binders, further showing a correlation between binding affinity and T cell reactivity.

Detailed analysis of the most immunogenic CPLs

For each of the three epitopes the most immunogenic CPL was selected for a more detailed analysis. To this extent, G1 and F5 were selected, since these CPLs induced highest and most robust responses after homologous and WT-peptide restimulation. N53 and N172 were selected since both peptides induced higher responses in a larger number of mice than WT peptide. However, first an additional control experiment was performed in C57BL/6 mice to confirm that CPL responses were HLA-A2-specific. Unexpectedly, CPL F5 induced responses in these non-transgenic mice. From this, we can conclude that part of the extent

of the responses of F5 in the HLA-A2 tg mice is due to presentation of the F5 peptide on H2-K^b. However, the response of HLA-A2 tg mice is still substantially higher; therefore the improvement observed for F5 is at least in part mediated by HLA-A*02:01 (Fig. S1B).

To provide more insight into binding affinity, serial peptide dilutions were used in the FP binding assay to determine the half-maximal inhibition of tracer binding concentration (IC50 values). Peptide binding scores as shown in Table 1 were determined at a single concentration. Analysis of the dose-response curves shows that in all cases the CPLs have a lower IC50 value than their WT counterparts (Fig. 3) do. These results are in line with findings in vaccination experiments with mice, in which the GILGFVFTL- and FMYSDFHFI-derived CPLs induced an IFN-γ response at lower doses than the WT epitope (Fig. 2). The increase in binding

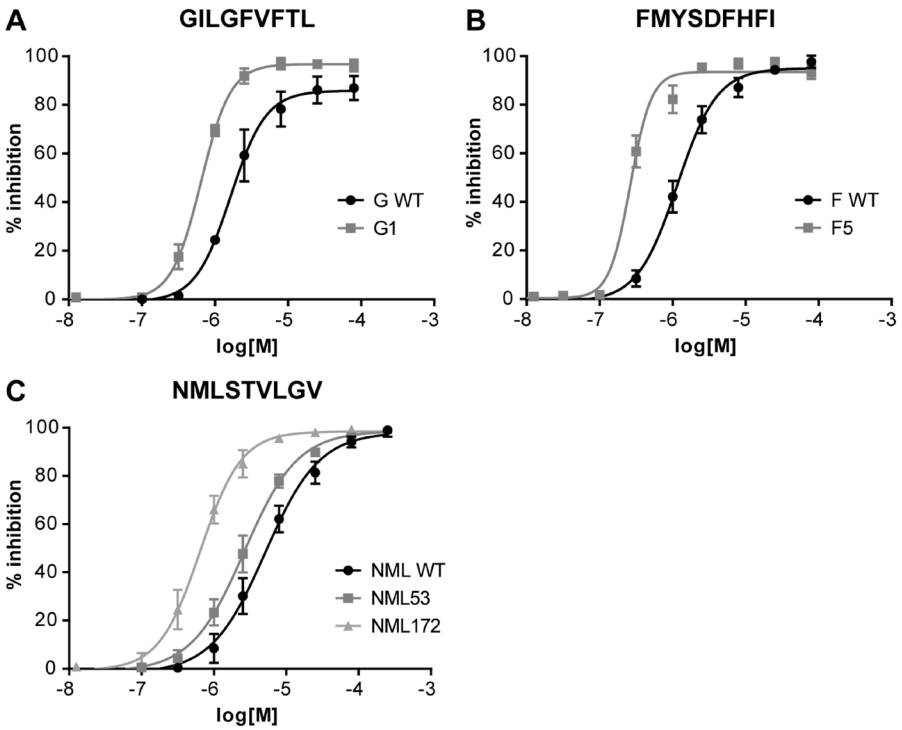

Figure 3. **Binding affinity dose-response curves of CPLs and WT peptides.** The IC50 curves of the selected CPLs show increased HLA binding affinity compared to IC50 curves of the corresponding WT-peptides. To generate IC50 curves the FP-based competition assay was performed using threefold peptide dilutions in the presence of a standard amount of tracer peptide. Shown are averages and their standard deviation of three independent experiments. Curves of CPLs are shifted to the left compared to WT peptides, indicating that a lower dose of CPLs is needed to inhibit tracer binding.

affinity probably not only results in an increased on-rate, but more importantly also a decrease in off-rate due to increased peptide-MHC (pMHC) stability[37]. This would cause a prolonged presentation to T cells and hence a higher IFN-γ response.

All responses obtained in the in vivo vaccination experiments were analyzed using an ELISpot assay with a complete pool of splenocytes. To prove that responses are indeed CD8+ T cell-specific, splenocytes were analyzed by flow cytometry. In Figure 4, flow cytometry dot plots show that the response towards CPL G1 was similar compared to WT peptide, which might be explained by the fact that a dose of 75 nmol was used. In the dose response experiments, a high dose of G1 appeared to result in suboptimal induction of IFN-γ production. Responses to CPLs F5 and N53, however, did show a major improvement as indicated by the increased production of IFN-γ by CD8+ T cells. CD4+ T cells did not produce IFN-γ in response to peptide restimulation, showing that the enhanced IFN-γ production measured in the ELISpot assay was produced by CD8+ T cells and not by CD4+ T cells (Fig. S2).

Predictive value of modifications

Next, modifications of the CPLs described above were analyzed further to determine whether an effective substitution in one epitope is a prediction for the success of that particular substitution for other epitopes. For each epitope, CPLs were synthesized with modifications that are present in G1, F5 and N53, resulting in a set of three CPLs per type of modification. Figure 5A shows IFN-γ responses of mice vaccinated with either of the selected epitopes of which P_1 was substituted for the residue am-phg, the modification that was most successful for GILGFVFTL (G1). Grey bars visualize that after stimulation with homologous peptides, enhanced responses were observed in all CPL-vaccinated mice. After WT stimulation, responses remained more or less similar, except for the response to N46, which was reduced to zero. Based on CPL F5 we introduced 4-FPHE on P_1 and 2-AOC on P_9 of GILGFVFTL and NMLSTVLGV. This combination of substitutions again led to a greatly enhanced response after restimulation with homologous peptide (Fig. 5B). However, for both epitopes, responses after WT restimulation were lower in CPL-vaccinated mice compared to responses of WT-vaccinated mice. Perhaps by changing the amino acids the structure of these CPLs differed too much from the WT, such that specificity for the WT sequence was lost. Finally, we substituted P_2 for norleucine (NLE) in GILGFVFTL and FMYSDFHFI based on CPL N53 (Fig. 5C). This substitution showed a slightly enhanced response for CPL F156 compared to its WT counterpart, but led to decreased responses for CPL G16. Although it appears difficult to predict whether a modification will work in a given epitope, an effective modification in one epitope proves in some cases also effective in other epitopes.

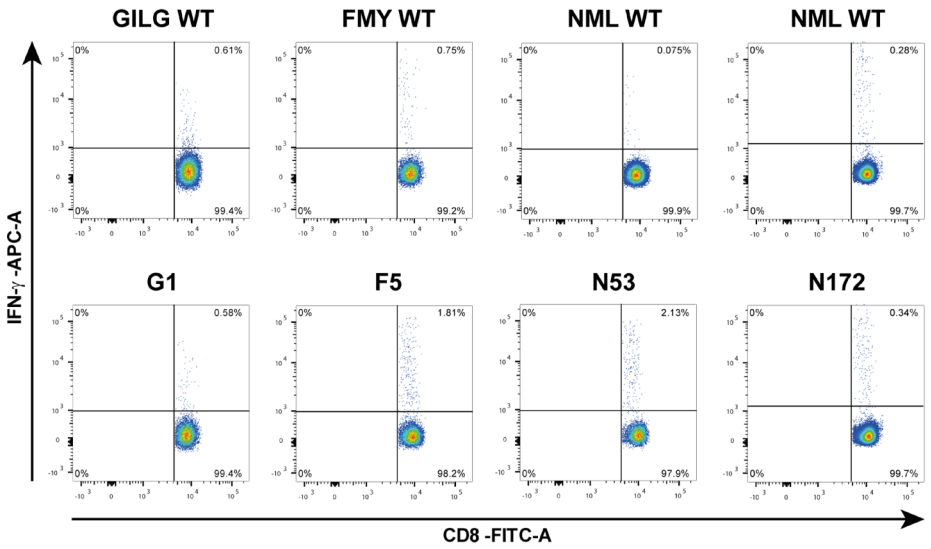

Figure 4. **Flow cytometry analysis on CD8⁺ T cell responses of CPL- and WT-vaccinated mice.** Dot plots showing IFN-γ production by CD8⁺ T cells of mice vaccinated with 75 nmol of either WT peptide or CPL (G1, F5, N53 and N172). In the upper panel, the respective WT-peptide control of that particular experiment is shown. In the lower panel, the CPL-induced IFN-γ responses are shown. Spleen cells ($2*10^6$/well) were stimulated O/N with 1 nmol/well WT peptide. Highest responders of each group are shown. Vaccination with F5 and N53 induced the largest improvement in IFN-γ production compared to WT peptide-vaccinated mice. Negative control (mock stimulated splenocytes) had an average of 0.07% with an SD of 0.1%.

Optimizing HLA-A*03:01 binding affinity of influenza epitopes

The response to vaccination can be broadened by selecting more HLA-A*02:01 peptides, but even more so by targeting multiple alleles. We therefore set out to optimize three influenza epitopes specific for HLA-A*03:01 as an example that incorporation of non-proteogenic amino acids is a strategy that can be extended to other alleles. The main difference between HLA-A*02:01 and HLA-A*03:01 is the preference of HLA-A*03:01 for long positively charged residues on P_9, demonstrated by the frequent occurrence of lysine and arginine on the C-terminal anchor position, whereas side chains of amino acids on P_2 still dock into a hydrophobic pocket[38]. Using a HLA-A*03:01-specific tracer peptide we performed the FP-based competition assay described in Materials and Methods for 96 peptides per epitope and measured binding after 4 and 24 hours[39]. Similar to HLA-A*02:01, the selected epitopes vary in affinity, with ILRGSVAHK binding to the MHC with highest affinity and being the most dominant, and 10-mer RMVLSAFDER a low affinity epitope[33,40,41]. SFSFGGFTK is an intermediate HLA-A*03:01 binder with unknown dominance. Substitution with non-proteogenic amino acids on or near anchor positions resulted in greatly enhanced binding, as shown in Table 3.

Since HLA-A*03:01 has a hydrophobic binding pocket at P_2 just like HLA-A*02:01, incorporation of norvaline (NVA) or 2-AOC on P_2 resulted in increased binding scores. Substitutions on P_9 did not enhance binding for any of the epitopes tested, probably because the lysine in the WT sequence forms strong ionic interactions that are hard to improve with the pool of amino acids tested. These data show that the technique of substituting amino acids by non-proteogenic amino acids to increase binding affinity can be applied to epitopes of other alleles, which is valuable for the development of broadly immunogenic vaccines.

Discussion

Current vaccination strategies to prevent influenza infection are mainly aimed at antibody-mediated immune responses, yet cytotoxic responses have also been proven to contribute to protection against influenza infection[14,16,17,43]. One of the approaches to induce these responses is by vaccination with peptides that encode T cell epitopes. However, immunogenicity of peptides is often inadequate; therefore, additional optimization is required. Here, we designed and synthesized CPLs with enhanced affinity for class I MHCs to improve, ultimately, T cell responses towards these peptides. Three highly conserved HLA-A*02:01-specific influenza epitopes that have varying binding affinity and dominance in the immune response were selected: GILGFVFTL, a highly immunodominant epitope; FMYSDFHFI, a less dominant epitope, and NMLSTVLGV, which is a low affinity subdominant epitope. By studying available crystal structures and by replacing amino acids at or adjacent to the anchor positions with non-proteogenic amino acids, CPLs were designed with a theoretically increased number and quality of interactions with the MHC binding groove. Using non-proteogenic amino acids, modification was no longer limited to the repertoire of naturally occurring amino acids. With this approach, we succeeded to enhance binding affinity of all three epitopes and after in vitro evaluation, the most promising CPLs were tested in mice. We showed that CPLs G1, G8, F5, F100, F111, N53 and N172 were capable of inducing improved T cell responses in HLA-A2 tg mice, as measured by IFN-γ production in splenocytes. As expected, especially the response towards the more subdominant peptides was greatly improved.

The first objective was to improve binding affinity of the peptides to MHCs by introducing non-proteogenic amino acid substitutions. Earlier, we reported improved effectivity of a melanoma-specific peptide by substitution of am-phg on P_1. This substitution led to additional interactions between the peptide and the MHC, thereby stabilizing the complex as shown in a crystal structure[13]. These findings may explain increased binding scores of CPLs G1 and N46, which contain the same substitution (Table 1). For FMYSDFHFI, introduction of am-phg

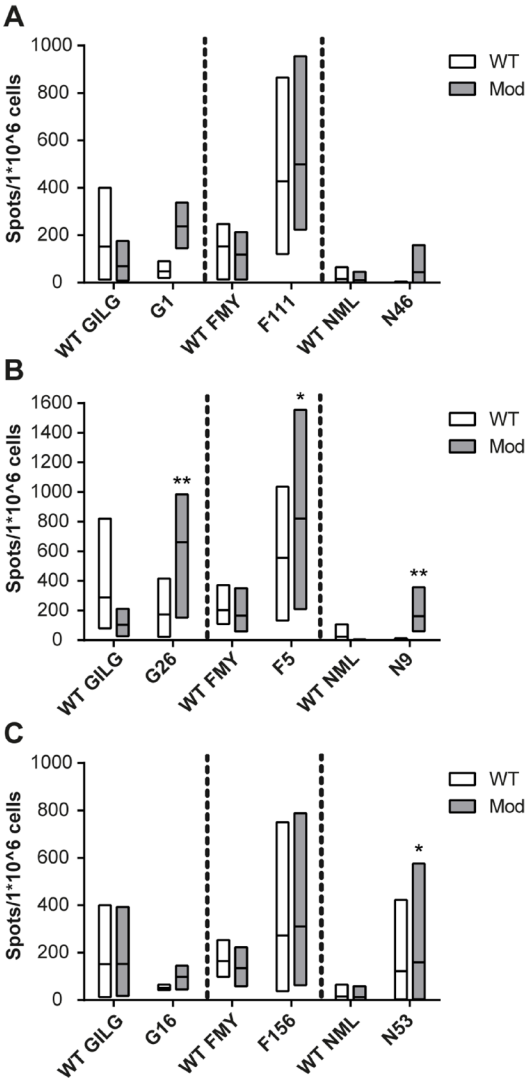

Figure 5. **Predictive value of modifications.** IFN-γ ELISpot on spleen cells of mice vaccinated with 75 nmol of either WT peptide or CPLs and stimulated for 16 hours with 0.1 nmol WT peptide or CPL per well. The three different modifications are based on final selected peptides for each epitope: (A) am-phg on P_1 based on G1, (B) 4-FPHE on P_1 and 2-AOC on P_9 based on F5 and (C) NLE on P_2 based on N53. X-axis depicts peptide used for vaccination. White boxes represents restimulation with WT peptide and grey boxes restimulation with CPL. Bars are min to max, with line at mean. Although it appears difficult to predict whether a modification will work in a certain epitope, an effective modification in one epitope is in some cases also effective in other epitopes. Bars represent a minimum of three mice (GILGFVFTL and FMYSDFHFI) and a maximum of eight (NMLSTVLGV). Data were statistically analyzed using a Mann-Whitney test. * $p<0.05$; ** $p<0.01$ compared to the WT equivalent.

Table 3. **FP binding scores of selected HLA-A*03:01 peptides**

#	ILRGSVAHK	4h	SD	24h	SD
I65	ILRGSV[2-AOC]HK	87	2	94	0
I74	I[AHA]RGSV[NLE]HK	77	2	92	1
I53	[AHA][NLE]RGSVAHK	73	0	91	2
I87	I[AHA][4-FPHE]GSVAHK	73	2	91	0
I60	[2-AOC][NLE]RGSVAHK	72	4	91	1
I89	I[AHA][CHA]GSVAHK	75	1	91	1
I59	I[AHA][2-AOC]GSVAHK	71	1	91	0
I73	I[AHA]RGSV[CSET]HK	74	3	90	1
I61	[CSME][AHA]RGSVAHK	71	2	90	1
I49	I[OrnN2]RGSVAHK	71	2	90	1
I79	I[AHA]RGSV[2-FUR]HK	77	3	90	1
I86	I[AHA][CSME]GSVAHK	71	2	89	1
I84	I[AHA][PRG]GSVAHK	71	2	89	0
I77	I[AHA]RGSV[CpALA]HK	71	2	89	1
I63	ILRGSV[NLE]HK	74	2	89	1
I17	[2-AOC][AHA]RGSVAHK	61	5	89	2
I58	I[AHA][NLE]GSVAHK	68	3	89	1
I83	I[AHA][CpALA]GSVAHK	70	3	89	0
I94	IL[4-FPHE]GSVAHK	70	4	89	1
I85	I[AHA][SOME]GSVAHK	69	2	88	1
I WT	**ILRGSVAHK**	66	3	87	1

#	SFSFGGFTK	4h	SD	24h	SD
S70	S[NVA]SFGG[2-AOC]TK	90	0	96	0
S84	SF[4-FPHE]FGGFTK	82	1	95	0
S50	S[NVA][2-AOC]FGGFTK	83	1	94	1
S74	S[NVA]SFGG[CpALA]TK	78	1	94	1
S68	S[NVA]SFGG[NLE]TK	79	2	93	0
S95	S[NVA][4-FPHE]FGGFTK	80	2	93	0
S94	S[NVA][NLE]FGGFTK	80	1	93	1
S52	S[NVA][AHA]FGGFTK	80	1	93	1
S72	S[NVA]SFGG[4-FPHE]TK	79	0	93	0
S93	S[NVA][CSME]FGGFTK	80	0	93	1
S53	S[NVA]RFGGFTK	80	1	93	1
S54	S[AHA]RFGGFTK	80	1	92	1
S92	S[NVA]SFGGF[TOME]K	80	2	92	1
S73	S[NVA]SFGG[BPG]TK	73	0	91	1
S69	S[NVA]SFGG[NVA]TK	72	2	91	0
S96	S[NVA][CpALA]FGGFTK	76	3	91	0
S56	S[NVA]SFGGFHK	78	2	91	1
S76	S[NVA]SFGG[2-FUR]TK	75	1	91	0
S71	S[NVA]SFGG[PRG]TK	70	2	90	0
S90	S[NVA]SFGGF[AHA]K	78	0	90	1
S WT	**SFSFGGFTK**	67	2	58	3

#	RMVLSAFDER	4h	SD	24h	SD
R71	R[NVA]VLSAF[2-AOC]ER	71	2	82	2
R67	R[AHA]VLSAF[2-AOC]ER	74	2	78	1
R81	RMVLSAF[AHA]ER	71	2	76	2
R38	RMVLSAF[2-AOC]ER	69	3	75	2
R70	R[NVA]VLSAF[SOME]ER	64	4	74	1
R42	RMVLSAF[CpALA]ER	65	2	73	1
R36	RMVLSAF[NLE]ER	66	4	73	1
R72	R[NVA]VLSAF[4-FPHE]ER	68	1	72	2
R83	RM[OrnN2]LSAFDER	71	3	72	2
R4	RMVLSAFDEK	61	1	69	1
R59	R[NVA]VLSAFDKR	62	4	68	0
R2	R[AHA]VLSAFDEK	58	1	67	1
R50	RM[2-AOC]LSAFDER	70	3	66	1
R55	RM[4-FPHE]LSAFDER	70	4	65	1
R68	R[AHA]VLSAF[4-FPHE]ER	67	3	64	0
R66	R[AHA]VLSAF[SOME]ER	63	3	63	1
R41	RMVLSAF[ORN]ER	65	3	63	0
R39	RMVLSAF[PRG]ER	62	4	62	1
R37	RMVLSAF[CSET]ER	60	3	60	2
R40	RMVLSAF[4-FPHE]ER	63	3	57	1
R WT	**RMVLSAFDER**	18	2	6	1

HLA-A*03:01 binding data for three influenza epitopes: ILRGSVAHK, SFSFGGFTK* and RMVLSAFDER. Affinity was determined as in Table 1 after 4h and 24h in three independent experiments. This table shows percentage inhibition in a heat map for the WT epitopes (bold) and 20 CPLs with highest binding scores. Green indicates high binding scores, yellow medium binding scores and red low binding scores. For all three epitopes binding scores could be greatly increased by substitution with non-proteogenic amino acids.
*SFSFGGFTK was incorrectly referred to in the immune epitope database; the epitope originally described as an HLA-A*03:01 binder by Assarsson et al. has amino acid sequence: SFSFGGFTFK[40,42].

on P_1 retained the binding score at a similar level as WT peptide (F111, Table 1). Surprisingly, G1 and F111, but not N46 showed improved immunogenicity in mice to the homologous and WT epitope (Fig. 5).

Since the HLA-A*02:01 allele prefers long hydrophobic residues on P_2 and the C-terminus of a peptide, other stabilizing interactions were created by introducing hydrophobic residues into the peptide. 2-AOC, NLE and NVA are examples of amino acids with hydrophobic side chains that can protrude deeply into the hydrophobic binding pockets of HLA-A*02:01[44,45]. CPLs of FMYSDFHFI and NMLSTVLGV with the largest increase in binding score indeed had a substitution of 2-AOC on P_2 or P_9, often in combination with other substitutions (Table 1). While introduction of 2-AOC did not enhance binding of GILGFVFTL-derived CPLs, introducing another hydrophobic residue, NLE, on P_2 did enhance its binding score. In addition, this NLE substitution improved homologous immunogenicity of CPLs F156 and N53 and showed improved recognition of the WT epitope (Fig. 5).

A point of interest is that from these binding results, it becomes clear that an amino acid preferred in one epitope is not necessarily preferred in another epitope, even when they are specific for the same HLA allele. Amino acid preferences are determined by the binding pockets in the binding groove of MHC and should therefore in theory be similar for every peptide specific for that allele. As discussed before, substitution of am-phg on P_1 of the GILGFVFTL epitope resulted in the highest binding score (G1, 98% compared to 84% for the WT; Table 1) and a major improvement was seen for NMLSTVLGV after the same substitution on P_1 (N46, 81% compared to 55% for the WT). The success of substitution on P_1 is not surprising, since secondary anchor residues, which for HLA-A*02:01 are found on P_1, P_3 and P_7, were previously discovered to also have significant effect on binding[46,47]. However, substitution of am-phg on P_1 in the FMYSDFHFI epitope did not increase binding scores (F111, 72% compared to 75% for the WT, Table 1). Likewise, incorporating 3-PYRA on P_1 was successful for the GILGFVFTL epitope (G8, 93%; Table 1), but did not enhance binding as much for NMLSTVLGV and FMYSDFHFI (both 73%; Table 1). This discrepancy could be due to conformational heterogeneity in the peptide backbones, since peptide binding strength is not only dependent on interactions of the side chains of anchor residues with the binding pockets, but also on those of the peptide backbone with the MHC binding groove[32,48,49]. The structure of the backbone is dependent on the size and fit of the amino acid side chains in the binding groove. Modifications may change the structure of the peptide backbone in one CPL in such a way that the interaction with the binding groove is weakened, while in another CPL there is no effect of the same substitution on this interaction. Alternatively, the change in structure of the backbone may affect the positioning of the anchor residue in such a way that it does not fit smoothly into the binding pocket.

Changes in the central region of the peptide may in turn affect recognition by the TCR[50,51]. Thus, by introducing too many modifications in one peptide, T cell responses may be perturbed significantly and therefore we substituted a maximum of two amino acids. In addition, introduction of a single non-proteogenic amino acid in one peptide at a non T cell-exposed position might influence the structure of the backbone and thus the central region, while the same amino acid in another peptide might have little or no effect[52]. This could be the reason that some modifications always seem to lead to higher responses after restimulation with a CPL, likely due to the improvement of affinity, but that these CPL-induced T cells do not always react to restimulation with WT peptide (N46, G26, N9; Fig. 5). These CPLs may induce a different subset of T cells than the WT peptide, which is not necessarily problematic in a vaccination setting as long as the CPL-induced T cells still recognize the WT peptide[53].

For the selection of CPLs for in vivo experiments, we set out to exclude CPLs that were not capable of inducing a response in WT-specific T cells as we hypothesized that these CPLs would likely not induce the correct T cells to recognize the WT epitope. Therefore, we performed three different assays in which CPLs were presented to WT-specific T cells. For the GILGFVFTL epitope a T cell clone was available, which facilitated analysis of responses of the WT-specific T cells to the CPLs. Activation of these cells by CPLs indicated that WT-specific TCRs are still capable of recognizing the CPLs (Table S3). For FMYSDFHFI and NMLSTVLGV, other methods needed to be developed and we therefore included a human DC-T cell co-culture method and analysis of WT-specific mouse splenocytes stimulated by CPLs (Table S3). The former analysis was effective in showing differences between the CPLs; however, donor variation was too large to draw definite conclusions. Analysis in splenocytes of an inbred HLA-A2 tg mouse strain allowed for little donor variation, but none of the CPLs were shown to induce better responses than the WT peptide in this model, in contrast to the other two methods. It did reveal some CPLs that induced little or no responses in the WT-specific splenocytes, allowing for negative selection. However, in these assays we were only able to mimic a reversed setting, i.e. WT-specific T cells that recognize CPLs. Such reverse immunology does not exclude the possibility that CPLs may induce T cells that are still capable of recognizing WT peptide even though this is not true for the inverted argument. For this reason, reverse immunology appears to be a suboptimal predictor for vaccine development[54]. Therefore, CPLs still needed to be tested for their ability to induce T cells that recognize the WT peptide in a vaccination setting.

Thus, we evaluated whether increased binding affinity also led to enhanced T cell responses by vaccination of HLA-A2 tg mice with a selection of CPLs (Fig. 2). Based on results from the assays described above, four CPLs per WT peptide

were selected for further in vivo testing. As our data for the GILGFVFTL-derived CPLs indicate, CPLs can facilitate a dose reduction while similar responses to WT peptide are maintained. At lower doses, vaccination with CPLs G1, G8 and G25 induced higher T cell responses after restimulation with WT peptide, compared to WT-vaccinated mice. The diminished responses at higher doses could be explained by overstimulation, as described for density of pMHC interactions on an APC[55]. In addition, modification of the FMYSDFHFI peptide led to the induction of higher T cell responses compared to the WT peptide in almost all doses tested. Surprisingly, F193 induced lowest homologous and heterologous responses, even though it did show improved binding affinity. In contrast, binding affinity of F100 and F111 were similar to that of the WT epitope, while these CPLs induced higher homologous and heterologous responses in mice. The effect of increasing binding affinity by introducing non-proteogenic amino acids on T cell responses was most remarkably shown by CPLs N53 and N172. These CPLs increased the number of responders to this subdominant epitope from approximately 1/6 to half of the mice and induced higher responses than the WT peptide, after WT restimulation. Hence, while increased binding may result in higher responses in mice, this appears not a general rule, which has some implications for vaccine development. Namely, the process to find modifications that lead to improved responses is not only affinity based, but also includes a trial and error factor. This may lengthen the development time of a peptide-based vaccine; however, with respect to the complete development process the impact is estimated to be minor.

Preventive vaccines should, most of all, induce a broad immune response, in contrast to therapeutic vaccines, where high affinity peptides are needed to overcome self-tolerance. By inducing a broad range of CTLs, the chance of generation of escape mutants decreases, rendering a vaccine more effective[56,57]. Some successful phase I clinical trials describing influenza peptide vaccines capable of inducing T cell responses have been reported[9,10]. However, these vaccines consist of long peptides and are mostly based on immunodominant epitopes, which might not be the best epitopes to induce a response to since there are indications that these epitopes overrule other T cell responses[54,58].

We have shown for six influenza epitopes, all with different characteristics, that it is possible to improve their MHC binding affinity and that the immunogenicity of the three HLA-A*02:01 epitopes could be improved considerably. Furthermore, by improving binding of HLA-A*03:01-specific peptides we have shown that it is possible to target alleles other than HLA-A*02:01, which is essential for broad population coverage. In order to enhance immunogenicity and efficacy of short peptides for T cell-targeted vaccines as used in our studies it is necessary to include adjuvants and to include a broader range of peptides. Our results illustrate the potential of inducing responses to otherwise subdominant epitopes

by modification of amino acid residues and enhancing binding affinity. Especially since there are indications that inducing a broad response is more efficacious, our approach provides a promising method to induce responses to a larger range of epitopes[58].

Materials and Methods

Ethics statement

This study was approved by the Committee on Animal Experimentation of the Netherlands Vaccine Institute (Bilthoven, the Netherlands) (permit numbers PO201200042, PO201200222) and the Committee on Animal Experimentation of the Antonie van Leeuwenhoek terrain (DEC-ALt) (permit numbers PO201300122, PO201400121, PO201400177 and PO201400188) (Bilthoven, the Netherlands). Animal handling was carried out in accordance with relevant Dutch national legislation, including the 1997 Dutch Act on Animal Experimentation. Mice were housed in filtertop macrolon III cages provided with cage enrichment (Igloo's and nestlets). Mice were provided with SRM-A food (γ-irradiated, Arie Blok BV, the Netherlands) and tap water ad libitum and checked twice daily for their health condition. When possible, mice were anesthetized during handling by isoflorane in O_2 to minimize suffering. The humane end point was defined as ruffled fur, inactive, cold and more than 20% of body weight loss. None of the animals reached the humane end point during any of the studies. When the experimental end point was reached, mice were anesthetized (isoflurane/O_2), bled by orbital puncture and terminated by cervical dislocation.

Peptide design and synthesis

Peptides were designed as described before and synthesized at the Netherlands Cancer Institute Peptide Facility by standard solid-phase peptide synthesis using Syro I and Syro II synthesizers[13]. The non-proteogenic amino acids were at first selected for their availability. Based on the results of the initial binding assays the set was narrowed down to those that increased binding. Using that knowledge the set was expanded with amino acids with similar side chain properties. Amino acids were purchased from Chiralix, NovaBiochem, Chem-Impex or Creo Salus. Resins were purchased pre-loaded with proteogenic amino acids (Nova Biochem) or loaded with non-proteogenic amino acids. Typically, 2-chlorotrityl chloride resin corresponding to a loading of 0.3 mmol (Nova Biochem) was swollen in dichloromethane (DCM, Biosolve); 0.15 mmol of amino acid and 0.51 mmol di-isopropylethylamine (DIPEA, Sigma-Aldrich) were added and the mixture was shaken for 10 minutes. Another 0.99 mmol DIPEA in DCM was added and the mixture was shaken for one hour. The reaction was quenched by addition of

methanol. For large scale testing of binding affinity, peptides were synthesized on a small scale (2 µmol). Peptides selected for the in vitro functional assays were synthesized on a large scale (25-50 µmol) and purified by reversed-phase HPLC (Waters). Masses of all peptides were analyzed by LCMS (Waters) to confirm correct synthesis.

Fluorescence polarization-based peptide binding assay

Peptide-MHC affinity was measured using a fluorescence polarization (FP) assay based on UV-mediated ligand exchange[35,36,59-61]. Since the fluorescence emission of MHC-bound tracer peptide is polarized to a greater extent than that of non-bound tracer, the total FP is a measure for the ratio of bound versus unbound tracer peptide. MHCs were refolded with conditional ligand KILGFVFJV for HLA-A*02:01 and RIYRJGATR for HLA-A*03:01, in which J is the photocleavable 3-amino-(2-nitrophenyl)propionic acid. Soluble MHC was dissolved in PBS containing 0.5 mg/ml bovine γ-globulin (BGG, Sigma-Aldrich) to a final concentration of 0.75 µM. The HLA-A*02:01 tracer peptide FLPSDCFPSV and the HLA-A*03:01 tracer peptide KVPCALINK were fluorescently labeled at the cysteine residues with 5-N-maleimide tetramethylrhodamine. Tracer peptides were diluted to a concentration of 6 nM in 1× BGG/PBS. Peptides of choice were dissolved at 125 µM in DMSO. Using a Hamilton MicroLab Liquid Handling Workstation the components were automatically transferred in triplicate into a 384-well microplate (black polystyrene, Corning). MHC, tracer and peptide were combined to reach final concentrations of 0.5 µM, 1 nM and 4.2 µM, respectively. The plate was exposed to UV light (365 nm) for 30 minutes at 4°C to exchange the UV-sensitive peptide for the desired peptides. FP values were measured using a BMG PHERAstar plate reader. To generate IC50 curves the FP-based peptide binding assay was performed using serial peptide dilutions ranging from 224 nM to 4 µM. Data were analyzed using GraphPad Prism 5 software.

IFN-γ induction in a GILGFVFTL specific T cell clone

TAP-deficient T2 cells, which are incapable of transporting peptides from the cytosol into the ER and thus only present exogenously loaded peptides, were cultured in RPMI 1640 medium (Invitrogen) supplemented with 10% FCS. The GILGFVFTL-specific T cell clone was cultured in RPMI 1640 medium containing 10% FCS supplemented with 3 U/ml IL-2. Per well of a 96-well plate, 50,000 T2 cells were pulsed with 10 pM of the desired peptides at 37°C for 1 hour. After washing away any unbound peptides, T2 cells were cultured in RPMI 1640 medium containing 10% FCS, with 50,000 specific T cells for 24 hours in presence of 1 µl/ml Golgiplug (BD Biosciences). As positive control, T cells were stimulated with 0.05 µg/ml PMA (Sigma-Aldrich) and 1 µg/ml ionomycin (Sigma-Aldrich). Unstimulated cells were included as negative control. After incubation, the plate

was centrifuged at 700 × *g* for 2 minutes. The medium was discarded and cells were resuspended and stained with 20 µl/ml CD8-FITC antibody (BD Biosciences) in PBS with 0.5% BSA and 0.02% sodium azide). Cells were fixed and permeabilized using a Cytofix/CytoPerm kit (BD Biosciences) according to manufacturer's recommendations. Then, cells were stained for intracellular IFN-γ using 20 µl/ml anti-IFN-γ-APC (BD Biosciences) and analyzed using a Beckman Coulter CyAn ADP flow cytometer. The percentage of IFN-γ+ cells was determined from the CD8+ gate. Data were analyzed using FlowJo version 7.6.1. software (Tree Star Inc).

Isolation and culture of human DCs

PBMCs of HLA-A2-typed healthy human donors were isolated from fresh blood by gradient centrifugation using Lymphoprep (Nycomed). Next, monocytes, CD8+ T cells and then CD4+ T cells were magnetically purified using CD14, CD8 or CD4 antibody-labeled magnetic beads, respectively, using LS columns according to manufacturer's recommendations (Miltenyi Biotec). Following elution from the columns, CD8+ T cells and CD4+ T cells were frozen in FCS (Hyclone) with 10% DMSO and stored at -80°C until further processing. CD14+ cells were plated in a concentration of 0.4×10^6 cells/ml in DC culture medium (IMDM (GIBCO, Invitrogen) containing 1% FCS, 100 U/ml penicillin, 100 µg/ml streptomycin, 292 µg/ml glutamine (all Sigma), supplemented with 500 U/ml human GM-CSF (PeproTech) and 800 U/ml human IL-4 (Active Bioscience) and incubated for six days at 37°C.

Maturation and co-culture of DCs

After six days of culture, half of the DC culture medium was replaced with DC culture medium containing GM-CSF only, and 1 nmol peptide per well was added. After an incubation period of one hour, 10 ng/ml E. coli LPS (Invivogen) was added to mature the DCs. After 48 hours, DCs were harvested and plated in a U-bottom 96-well plate in a concentration of 5×10^3 cells/well in co-culture medium (AIM-V (GIBCO) containing 2% human AB serum (Sigma)). Samples of the DCs were collected for analysis of maturation markers by flow cytometry. Next, autologous CD8+ and CD4+ T cells were added to the DCs in a both in a 10:1 ratio. After seven days of co-culture, cells were collected for analysis by flow cytometry.

Flow cytometry

To determine maturation status, DCs were harvested two days after addition of peptides and maturation factor LPS. Cells were stained in FACS buffer (PBS (GIBCO) containing 0.5% BSA (Sigma) and 0.5 mM EDTA (ICN Biomedicals)) for 30 minutes at 4°C with either one of two panels that contained the following maturation markers: anti-CD80-FITC, anti-CD14-PE, anti-DC-SIGN-APC, anti-HLA-DR-Pacific Blue and Live/dead-AmCyan (Invitrogen) (panel 1) or anti-

CD83-FITC, anti-CD40-PE, (BD Biosciences), anti-PD-L1-APC (eBioscience), anti-CD86-Pacific Blue (BioLegend) (panel 2). Live/dead-AmCyan (Invitrogen) was included in both panels. For analysis of the co-culture, the following markers were used: anti-CD8-FITC (Sanquin), anti-CD3-PerCP, anti-TNFα-PE-Cy7, anti-IFN-γ-APC (BD Biosciences), anti-CD4-Pacific Blue (eBioscience) and Live/dead-AmCyan (Invitrogen). Four hours prior to staining, Brefeldin A (BD Biosciences) was added to the culture; then cells were stained using the Cytofix/Cytoperm kit from BD Biosciences according to manufacturer's recommendations. Cells were measured using a FACS Canto II (BD Biosciences) and results were analyzed using FlowJo version 9.7.5 software. First, lymphocytes were gated, followed by gating of live cells, then $CD3^+$ cells and finally $CD8^+$ or $CD4^+$ cells were placed in a quadrant with TNF-α^+ or IFN-γ^+ cells.

Immunization of mice

HLA-A2 transgenic mice, B6.Cg-Tg (HLA-A/H2-D)2Enge/J (Jackson Laboratory, USA), maintained in house, or C57BL/6 mice (Charles River, Germany) were vaccinated with the indicated peptides at their respective doses in a volume of 100 µl. Peptides were adjuvanted with Incomplete Freund's Adjuvant (IFA) (1/1 (V/V)) and CpG (50 µg/mouse) by vortexing the mixture for 30 minutes. In all experiments, mice were subcutaneously vaccinated at days 0 and 21 in alternating flanks. Two weeks after booster vaccination, mice were sacrificed, spleens were excised and spleen cells were restimulated for 16 hours with WT peptide or CPL. Specific IFN-γ responses were assessed using an ELISpot assay.

ELISpot assay

IFN-γ ELISpot assays were performed according to the manufacturer's protocol (U-Cytech). Spleens were homogenized and passed through 70 µm filters (BD Biosciences), washed with RPMI 1640 containing 10% FCS, 100 U/ml penicillin, 100 µg/ml streptomycin and 292 µg/ml glutamine and counted using a Casy cell counter (Roche). Cells were plated in a concentration of 4×10^5 cells/well in an IFN-γ antibody-coated PVDF membrane plate (Millipore MSIP) and stimulated with 0.1 nmol/well of either WT peptide or corresponding CPL. After 16 hours of incubation spots were visualized according to the manufacturer's protocol (U-Cytech) and counted using an A.el.vis reader (Sanquin).

Online supplemental material

Figure S1. Epitope MHC specificity control experiment in C57BL/6 mice.
Figure S2. Flow cytometry dot plots showing IFN-γ-positive CD4+ T cells of HLA-A2+ transgenic mice.
Table S1. HLA-A*02:01 binding of CPLs of influenza epitopes; GILGFVFTL (M_{158-66}), FMYSDFHFI (PA_{46-54}) and NMLSTVLGV ($PB1_{413-421}$).
Table S2. Heat map representation of Table 1. FP binding scores of selected HLA-A*02:01 peptides.
Table S3. GILG, FMY and NML specific CD8+ T cell responses after stimulation with CPLs in in vitro and ex vivo screening models.
Table S4. Heat map representation of Table 3. FP binding scores HLA-A*03:01 peptides.

Acknowledgements

We thank Henk Hilkmann and Dris el Atmioui for peptide synthesis. Christine Soputan, Dirk Elberts and Jolanda Rigters for animal handling and Harry van Dijken, Justin Mouthaan, Sanne Spijkers and Linda van Straalen for their aid in performing the experiments.

References

1. WHO. *Fact sheet: Influenza (seasonal)*, http://www.who.int/mediacentre/factsheets/fs211/en/ (2014).
2. Iskander, J., Strikas, R. A., Gensheimer, K. F., Cox, N. J. & Redd, S. C. Pandemic influenza planning, United States, 1978-2008. *Emerg Infect Dis* **19**, 879-885, doi:10.3201/eid1906.121478 (2013).
3. Kilbourne, E. D. Influenza pandemics of the 20th century. *Emerging Infectious Diseases* **12**, 9-14 (2006).
4. Houser, K. & Subbarao, K. Influenza Vaccines: Challenges and Solutions. *Cell host & microbe* **17**, 295-300, doi:10.1016/j.chom.2015.02.012 (2015).
5. Lee, Y. T. *et al.* New vaccines against influenza virus. *Clinical and experimental vaccine research* **3**, 12-28, doi:10.7774/cevr.2014.3.1.12 (2014).
6. Pica, N. & Palese, P. Toward a universal influenza virus vaccine: prospects and challenges. *Annu Rev Med* **64**, 189-202, doi:10.1146/annurev-med-120611-145115 (2013).
7. Purcell, A. W., McCluskey, J. & Rossjohn, J. More than one reason to rethink the use of peptides in vaccine design. *Nat Rev Drug Discov* **6**, 404-414, doi:10.1038/nrd2224 (2007).
8. Kenter, G. G. *et al.* Vaccination against HPV-16 oncoproteins for vulvar intraepithelial neoplasia. *N Engl J Med* **361**, 1838-1847, doi:10.1056/NEJMoa0810097 (2009).
9. Francis, J. N. *et al.* A novel peptide-based pan-influenza A vaccine: A double blind, randomised clinical trial of immunogenicity and safety. *Vaccine*, doi:10.1016/j.vaccine.2014.06.006 (2014).
10. Pleguezuelos, O., Robinson, S., Stoloff, G. A. & Caparros-Wanderley, W. Synthetic Influenza vaccine (FLU-v) stimulates cell mediated immunity in a double-blind, randomised, placebo-controlled Phase I trial. *Vaccine* **30**, 4655-4660, doi:10.1016/j.vaccine.2012.04.089 (2012).
11. Rosendahl Huber, S. K. *et al.* Synthetic Long Peptide Influenza Vaccine Containing Conserved T and B Cell Epitopes Reduces Viral Load in Lungs of Mice and Ferrets. *PLoS One* **10**, e0127969, doi:10.1371/journal.pone.0127969 (2015).
12. Rosendahl Huber, S., van Beek, J., de Jonge, J., Luytjes, W. & van Baarle, D. T cell responses to viral infections - opportunities for Peptide vaccination. *Frontiers in immunology* **5**, 171, doi:10.3389/fimmu.2014.00171 (2014).
13. Hoppes, R. *et al.* Altered Peptide Ligands Revisited: Vaccine Design through Chemically Modified HLA-A2-Restricted T Cell Epitopes. *Journal of immunology*, doi:10.4049/jimmunol.1400800 (2014).
14. McMichael, A. J., Gotch, F. M., Noble, G. R. & Beare, P. A. Cytotoxic T-cell immunity to influenza. *N Engl J Med* **309**, 13-17, doi:10.1056/NEJM198307073090103 (1983).
15. Butchko, G. M., Armstrong, R. B. & Ennis, F. A. Specificity studies on the proliferative response of thymus-derived lymphocytes to influenza viruses. *Journal of immunology* **121**, 2381-2385 (1978).
16. Effros, R. B., Doherty, P. C., Gerhard, W. & Bennink, J. Generation of both cross-reactive and virus-specific T-cell populations after immunization with serologically distinct influenza A viruses. *The Journal of experimental medicine* **145**, 557-568 (1977).
17. Sridhar, S. *et al.* Cellular immune correlates of protection against symptomatic pandemic influenza. *Nature medicine* **19**, 1305-1312, doi:10.1038/nm.3350 (2013).
18. Matsui, M. *et al.* A CTL-based liposomal vaccine capable of inducing protection against heterosubtypic influenza viruses in HLA-A*02:01 transgenic mice. *Biochemical and biophysical research communications* **391**, 1494-1499, doi:10.1016/j.bbrc.2009.12.100 (2010).
19. Ichihashi, T., Yoshida, R., Sugimoto, C., Takada, A. & Kajino, K. Cross-protective peptide vaccine against influenza A viruses developed in HLA-A*2402 human immunity model. *PloS one* **6**, e24626, doi:10.1371/journal.pone.0024626 (2011).
20. Soema, P. C. *et al.* Influenza T-cell Epitope-Loaded Virosomes Adjuvanted with CpG as a Potential Influenza Vaccine. *Pharmaceutical research*, doi:10.1007/s11095-014-1556-3 (2014).
21. Tan, A. C. *et al.* The design and proof of concept for a CD8(+) T cell-based vaccine inducing cross-subtype protection against influenza A virus. *Immunology and cell biology* **91**, 96-104, doi:10.1038/icb.2012.54 (2013).
22. Rudolph, M. G., Stanfield, R. L. & Wilson, I. A. How TCRs bind MHCs, peptides, and coreceptors. *Annual review of immunology* **24**, 419-466, doi:10.1146/annurev.immunol.23.021704.115658 (2006).

23. Rammensee, H. G., Friede, T. & Stevanoviic, S. MHC ligands and peptide motifs: first listing. *Immunogenetics* **41**, 178-228 (1995).
24. Teng, J. M. & Hogan, K. T. Both major and minor peptide-binding pockets in HLA-A2 influence the presentation of influenza virus matrix peptide to cytotoxic T lymphocytes. *Molecular immunology* **31**, 459-470 (1994).
25. Sette, A. & Sidney, J. HLA supertypes and supermotifs: a functional perspective on HLA polymorphism. *Curr Opin Immunol* **10**, 478-482 (1998).
26. Hickman, H. D. & Yewdell, J. W. Going Pro to enhance T-cell immunogenicity: easy as pi? *European journal of immunology* **43**, 2814-2817, doi:10.1002/eji.201344095 (2013).
27. Johansen, T. E. *et al.* Peptide binding to MHC class I is determined by individual pockets in the binding groove. *Scandinavian journal of immunology* **46**, 137-146 (1997).
28. Robbins, P. F. *et al.* Single and dual amino acid substitutions in TCR CDRs can enhance antigen-specific T cell functions. *Journal of immunology* **180**, 6116-6131 (2008).
29. Trujillo, J. A. *et al.* Structural and functional correlates of enhanced antiviral immunity generated by heteroclitic CD8 T cell epitopes. *J Immunol* **192**, 5245-5256, doi:10.4049/jimmunol.1400111 (2014).
30. Cole, D. K. *et al.* Modification of MHC anchor residues generates heteroclitic peptides that alter TCR binding and T cell recognition. *J Immunol* **185**, 2600-2610, doi:10.4049/jimmunol.1000629 (2010).
31. Slansky, J. E. & Jordan, K. R. The Goldilocks model for TCR-too much attraction might not be best for vaccine design. *PLoS Biol* **8**, doi:10.1371/journal.pbio.1000482 (2010).
32. Adrian, P. E., Rajaseger, G., Mathura, V. S., Sakharkar, M. K. & Kangueane, P. Types of inter-atomic interactions at the MHC-peptide interface: identifying commonality from accumulated data. *BMC structural biology* **2**, 2 (2002).
33. Gianfrani, C., Oseroff, C., Sidney, J., Chesnut, R. W. & Sette, A. Human memory CTL response specific for influenza A virus is broad and multispecific. *Human immunology* **61**, 438-452 (2000).
34. Middleton, D., Menchaca, L., Rood, H. & Komerofsky, R. New allele frequency database: http://www.allelefrequencies.net. *Tissue antigens* **61**, 403-407 (2003).
35. Toebes, M. *et al.* Design and use of conditional MHC class I ligands. *Nat Med* **12**, 246-251, doi:10.1038/nm1360 (2006).
36. Toebes, M., Rodenko, B., Ovaa, H. & Schumacher, T. N. Generation of peptide MHC class I monomers and multimers through ligand exchange. *Curr Protoc Immunol* **Chapter 18**, Unit 18 16, doi:10.1002/0471142735.im1816s87 (2009).
37. van der Burg, S. H., Visseren, M. J., Brandt, R. M., Kast, W. M. & Melief, C. J. Immunogenicity of peptides bound to MHC class I molecules depends on the MHC-peptide complex stability. *Journal of immunology* **156**, 3308-3314 (1996).
38. McMahon, R. M. *et al.* Structure of HLA-A*03:01 in complex with a peptide of proteolipid protein: insights into the role of HLA-A alleles in susceptibility to multiple sclerosis. *Acta crystallographica. Section D, Biological crystallography* **67**, 447-454, doi:10.1107/S0907444911007888 (2011).
39. Bakker, A. H. *et al.* Conditional MHC class I ligands and peptide exchange technology for the human MHC gene products HLA-A1, -A3, -A11, and -B7. *Proc Natl Acad Sci U S A* **105**, 3825-3830, doi:10.1073/pnas.0709717105 (2008).
40. Assarsson, E. *et al.* Immunomic analysis of the repertoire of T-cell specificities for influenza A virus in humans. *Journal of virology* **82**, 12241-12251, doi:10.1128/JVI.01563-08 (2008).
41. Scheibenbogen, C. *et al.* A sensitive ELISpot assay for detection of CD8+ T lymphocytes specific for HLA class I-binding peptide epitopes derived from influenza proteins in the blood of healthy donors and melanoma patients. *Clinical cancer research : an official journal of the American Association for Cancer Research* **3**, 221-226 (1997).
42. Vita, R. *et al.* The immune epitope database (IEDB) 3.0. *Nucleic Acids Res* **43**, D405-412, doi:10.1093/nar/gku938 (2015).
43. Guo, H., Santiago, F., Lambert, K., Takimoto, T. & Topham, D. J. T cell-mediated protection against lethal 2009 pandemic H1N1 influenza virus infection in a mouse model. *Journal of virology* **85**, 448-455, doi:10.1128/JVI.01812-10 (2011).
44. Madden, D. R., Garboczi, D. N. & Wiley, D. C. The antigenic identity of peptide-MHC complexes: a comparison of the conformations of five viral peptides presented by HLA-A2. *Cell* **75**, 693-708 (1993).

45. Saper, M. A., Bjorkman, P. J. & Wiley, D. C. Refined structure of the human histocompatibility antigen HLA-A2 at 2.6 A resolution. *Journal of molecular biology* **219**, 277-319 (1991).
46. Ruppert, J. *et al.* Prominent role of secondary anchor residues in peptide binding to HLA-A2.1 molecules. *Cell* **74**, 929-937 (1993).
47. Joseph, M. A. *et al.* Secondary anchor substitutions in an HLA-A*02:01-restricted T-cell epitope derived from Her-2/neu. *Molecular immunology* **44**, 322-331, doi:10.1016/j.molimm.2006.02.027 (2007).
48. Rognan, D., Lauemoller, S. L., Holm, A., Buus, S. & Tschinke, V. Predicting binding affinities of protein ligands from three-dimensional models: application to peptide binding to class I major histocompatibility proteins. *Journal of medicinal chemistry* **42**, 4650-4658 (1999).
49. Schueler-Furman, O., Altuvia, Y., Sette, A. & Margalit, H. Structure-based prediction of binding peptides to MHC class I molecules: application to a broad range of MHC alleles. *Protein science : a publication of the Protein Society* **9**, 1838-1846, doi:10.1110/ps.9.9.1838 (2000).
50. Borbulevych, O. Y. *et al.* Structures of MART-126/27-35 Peptide/HLA-A2 complexes reveal a remarkable disconnect between antigen structural homology and T cell recognition. *Journal of molecular biology* **372**, 1123-1136, doi:10.1016/j.jmb.2007.07.025 (2007).
51. Yanover, C. & Bradley, P. Large-scale characterization of peptide-MHC binding landscapes with structural simulations. *Proceedings of the National Academy of Sciences of the United States of America* **108**, 6981-6986, doi:10.1073/pnas.1018165108 (2011).
52. Sharma, A. K. *et al.* Class I major histocompatibility complex anchor substitutions alter the conformation of T cell receptor contacts. *The Journal of biological chemistry* **276**, 21443-21449, doi:10.1074/jbc.M010791200 (2001).
53. Denkberg, G., Klechevsky, E. & Reiter, Y. Modification of a tumor-derived peptide at an HLA-A2 anchor residue can alter the conformation of the MHC-peptide complex: probing with TCR-like recombinant antibodies. *Journal of immunology* **169**, 4399-4407 (2002).
54. Keskin, D. B. *et al.* Physical detection of influenza A epitopes identifies a stealth subset on human lung epithelium evading natural CD8 immunity. *Proceedings of the National Academy of Sciences of the United States of America* **112**, 2151-2156, doi:10.1073/pnas.1423482112 (2015).
55. Gonzalez, P. A. *et al.* T cell receptor binding kinetics required for T cell activation depend on the density of cognate ligand on the antigen-presenting cell. *Proc Natl Acad Sci U S A* **102**, 4824-4829, doi:10.1073/pnas.0500922102 (2005).
56. Deng, K. *et al.* Broad CTL response is required to clear latent HIV-1 due to dominance of escape mutations. *Nature*, doi:10.1038/nature14053 (2015).
57. Hansen, S. G. *et al.* Cytomegalovirus vectors violate $CD8^+$ T cell epitope recognition paradigms. *Science* **340**, 1237874, doi:10.1126/science.1237874 (2013).
58. Tan, A. C., La Gruta, N. L., Zeng, W. & Jackson, D. C. Precursor frequency and competition dictate the HLA-A2-restricted $CD8^+$ T cell responses to influenza A infection and vaccination in HLA-A2.1 transgenic mice. *Journal of immunology* **187**, 1895-1902, doi:10.4049/jimmunol.1100664 (2011).
59. Amore, A. *et al.* Development of a hypersensitive periodate-cleavable amino acid that is methionine- and disulfide-compatible and its application in MHC exchange reagents for T cell characterisation. *Chembiochem* **14**, 123-131, doi:10.1002/cbic.201200540 (2013).
60. Rodenko, B. *et al.* Class I major histocompatibility complexes loaded by a periodate trigger. *J Am Chem Soc* **131**, 12305-12313, doi:10.1021/ja9037565 (2009).
61. Choo, J. A. *et al.* Bioorthogonal cleavage and exchange of major histocompatibility complex ligands by employing azobenzene-containing peptides. *Angew Chem Int Ed Engl* **53**, 13390-13394, doi:10.1002/anie.201406295 (2014).

4

The future of cancer immunotherapy: opportunities for small molecules

Jolien J. Luimstra[1], Jacques Neefjes[1], Jannie Borst[2], and Huib Ovaa[1]

[1]Department of Cell and Chemical Biology, Leiden University Medical Center, Leiden, The Netherlands
[2]Department of Immunohematology and Blood Transfusion, Leiden University Medical Center, Leiden, The Netherlands

Manuscript under revision

Abstract

Cancer immunotherapy has demonstrated remarkable successes, by inducing systemic anti-tumor T cell responses. However, treatment is extremely costly and effectivity is limited by several bottlenecks that require strategic interventions. Relatively new to cancer immunotherapy are small-molecule drugs that target defined pathways or cells involved in immune activation and -suppression. Chemical drugs harbor unique properties that allow systemic administration and targeting of extra- and intracellular targets. They may activate complementary pathways and help overcome tolerance and immune suppression to induce effective anti-tumor responses. Synergistic effects may be achieved by combining immunotherapy with conventional therapies and/or new small-molecule chemotherapeutics.

Engaging immune pathways to treat cancer

Immunotherapy has recently become the fourth pillar of cancer treatment, next to surgery, chemotherapy and radiotherapy. Biomedical research has previously delivered personalized cancer treatment with drugs that target critical signaling molecules in cancer cells. However, efficacy of these targeted therapies is severely hampered by acquired resistance of clonally diverse tumor cell populations. Immunotherapy presents a unique approach with the capacity to tackle the problems of genetic **heterogeneity** (see Glossary) in cancer, since the immune system has inherently evolved to deal with genetic **heterogeneity** of microorganisms. The same immunotherapy treatment can act on a great variety of different cancer types, because it relies on tumor-extrinsic mechanisms. The aim of cancer immunotherapy is to activate a systemic, tumor-specific **cytotoxic T lymphocyte (CTL)** response. Ideally, a **CTL** response is raised that can eradicate (occult) metastases, also in cases where only the primary tumor has been diagnosed[1]. Often such a response is suppressed by tumor cells through upregulation of coinhibitory receptors, or checkpoints, that dampen the T cell response (Box 1). Current clinically approved checkpoint inhibitors are antibodies targeting cytotoxic T lymphocyte-associated protein 4 (CTLA-4) or programmed death 1 (PD-1). These powerful antibodies have shown remarkable results by restoring anti-tumor immune responses, but often lead to adverse immune-related events, which are treatment-limiting and may even result in mortality. For further advance, we need new strategies based on insights into the molecular basis of immunity, as well as cancer cell biology. Such therapies should increase tumor killing efficiency without increasing damage to healthy tissue. Here, we provide our perspective on the future of immunotherapies, with an emphasis on the contribution to be expected from the field of (bio)chemistry.

Box 1. How current immunotherapy with checkpoint blockade works

Immunity to cancer may be therapeutically promoted by antibody-based inhibition of membrane receptors that dampen T cell responses ("checkpoints"), a discovery for which James Allison and Tasuku Honjo received the Nobel Prize for Physiology or Medicine in 2018. The leading immunotherapeutic monoclonal antibodies (mAbs) block the interaction between PD-1 (programmed death 1) and its ligands PD-L1/L2, or CTLA-4 (cytotoxic T lymphocyte-associated antigen 4) and its ligands CD80/CD86 (B7-1/B7-2)[89-91], and proved efficacious in the treatment of immunogenic tumors, including melanoma and lung cancer[92-94]. PD-1 is associated with the tyrosine phosphatase SHP-2 that can dephosphorylate CD3 components and CD28 and thereby block TCR-signaling and CD28 costimulation[95]. CTLA-4 binds and downregulates CD80 and CD86 and thereby blocks CD28 costimulation[6,96]. Both checkpoints can act during T cell priming as well as in the tumor microenvironment (TME) and their exact division of labor is not yet clear[97,98]. Combined PD-1 and CTLA-4 blockade proved synergistic in late stage melanoma, suggesting different mechanisms of action[99].

Three bottlenecks in the immune response against cancer

Ideally, a 'cancer immunity cycle' is operational, wherein tumor cells are recognized by T cells and eradicated before they grow out or metastasize[2]. However, whether tumor cells can be recognized as "non-self" presents the first bottleneck (Fig. 1). Clonal deletion of self-reactive T cells during their development in the thymus (**central tolerance**) serves to avoid auto-immunity, but at the same time limits the T cell repertoire able to recognize tumor cells. As a prerequisite for clearance, tumor cells must therefore be different from non-transformed cells. Virus-induced cancers carry foreign proteins and will therefore be antigenic[3]. In addition, cancer such as melanoma, lung cancers and **microsatellite-instable** colon cancer feature tumors harboring a high mutational load and therefore express so-called **neoantigens**: peptides encompassing those mutations towards which no **central tolerance** has developed. These types of tumors are particularly sensitive to checkpoint blockade[4,5]. Other cancer types may carry alternative types of antigens towards which a naïve T cell repertoire is present. Many of such tumor antigens likely remain to be discovered.

Tumor-derived proteins are taken up by professional antigen-presenting cells, in particular dendritic cells (DCs), and processed into peptides subsequently presented to T cells in secondary lymphoid organs by major histocompatibility complex class I and class II (MHCI and MHCII) molecules. In order to become activated, $CD8^+$ or $CD4^+$ T cells need to recognize peptide-MHC complexes by their T cell receptor (TCR). Additional signals required to undergo clonal expansion and effector- and memory differentiation are delivered by specific

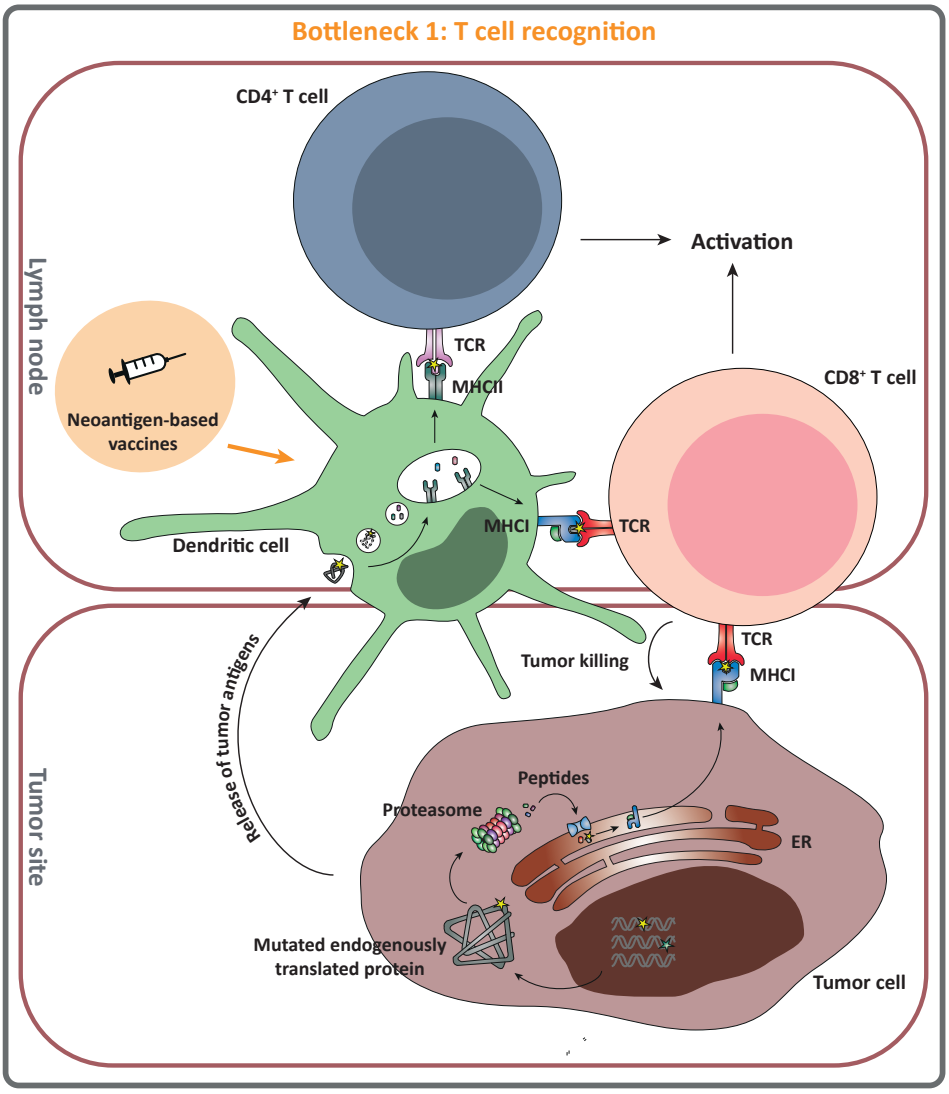

Figure 1. **The first bottleneck in the T cell response against cancer is the presence of tumor-specific T cells in the patient**. The tumor cells must generate (neo)antigens that can be presented by MHCI respectively MHCII and recognized by naïve $CD8^+$ and $CD4^+$ T cells in the patient. Neoantigen recognition leads to tumor cell lysis and release of tumor antigens. When taken up and processed by dendritic cells these contribute to the activation of T cells. Neoantigen-based vaccines boost this step in anti-tumor immunity. MHC, major histocompatibility complex; TCR, T cell receptor

costimulatory molecules and cytokines (Fig. 2). Such molecules are expressed by DCs upon pattern recognition receptor (PRR) activation by **pathogen**- or **danger-associated molecular patterns** (**PAMPs** and **DAMPs**, respectively), in concert with specific cytokines, such as type I interferons (IFNs). Tumors often do not supply these activating signals and therefore fail to activate DCs. Thymic **regulatory T cells** (t**Treg**) furthermore attenuate DC signals, in particular by downregulating costimulatory ligands CD80 and CD86 on DCs[6]. The **peripheral tolerance** that is thus imposed as a safeguard against auto-immunity constitutes the second bottleneck in the T cell response to cancer.

In case tumor-specific $CD4^+$ and/or $CD8^+$ T cells are activated by tumor-derived antigen and other signals, they differentiate into helper (Th) and cytotoxic effector cells, which exit lymphoid organs and travel via the blood to the tumor site. There, they are attracted to extravasate into the tumor tissue by chemokine signals. The tumor micro-environment (TME) and the signals it exudes in concert with the T cell response may lead to state of **immunosuppression**. The TME may present physical barriers that exclude the T cells and/or be immunosuppressive, thus erecting the third bottleneck to anti-cancer immunity (Fig. 3). It may express molecules such as IDO (indoleamine 2,3-dioxygenase) and PD-L1 (programmed death ligand 1) to directly inhibit effector T cell function, but also cytokines such as TGF-β (transforming growth factor β) and IL-10 (interleukin 10) to promote **Treg** cell expansion and function, thereby inhibiting effector T cell responses[7]. Optimal cancer treatment must ensure that all three bottlenecks, i.e. **central tolerance**, **peripheral tolerance** and tumor-associated **immune suppression** are overcome, so that tumor cells are detected and properly attacked by **CTLs**, ideally without invoking auto-immunity.

Therapeutic vaccination with (neo)antigens

The aim in therapeutic vaccination is to prime tumor-specific naïve T cells, thereby developing or augmenting T cell responses against tumors[8]. This approach can work in tumors that either do not raise a tumor-specific T cell response by themselves, or raise an ineffective one, and thus remain devoid of T cell infiltration. The advantage is that such "**cold" tumors** have likely not yet developed an immune-suppressive environment, for this generally occurs through a dialogue with activated T cells[9]. Since the advent of genome-wide DNA sequencing of cancers, the focus in therapeutic vaccination development has been on **neoantigens**: mutated self-antigens that arise from tumor-specific somatic DNA mutations[10]. While other tumor-associated antigens may lead to toxicity in healthy tissues that also express the target, **neoantigens** are exclusive to tumor cells and are hence actively pursued in cancer immunotherapy[11].

In addition to pattern recognition receptor (PRR) signals and/or inflammatory cytokines, $CD4^+$ T cells provide the help that DCs need for the initiation of effective primary and memory $CD8^+$ T cell responses[12-15]. For this reason, the most successful peptide vaccines to date are long peptides (around 40 amino acids in length) or antigen-encoding mRNA or DNA encompassing both MHCI and MHCII epitopes, thus activating both $CD8^+$ and $CD4^+$ T cells[16]. These vaccines have shown therapeutic promise in treatment of early stages of (virus-induced) cancer, but not in later stages. The inferred importance of $CD4^+$ T cells is illustrated by Sahin et al., who showed that 60% of elicited T cell responses were $CD4^+$ upon vaccination with RNAs that each encode five mutated long peptide sequences predicted for MHCI binding[17]. Likewise, Keskin et al. also observed prominent $CD4^+$ T cell responses in a phase Ib glioblastoma trial after administering a personalized **neoantigen** vaccine consisting of 20 long peptides[18]. Although vaccination successfully induced systemic and intratumoral **neoantigen**-specific immune responses, all patients eventually relapsed, indicating other challenges, including **immune suppression**, still pose significant bottlenecks. Enhancing activation of DCs by adjuvants

Therapeutic cancer vaccines as monotherapy will fail to induce potent anti-tumor responses, because they lack costimulatory signals. The use of adjuvants that activate DCs via PRRs, such as toll-like receptors (TLRs) helps overcome **peripheral tolerance**[19]. Biological adjuvants such as CpG, poly IC:LC (polyinosinic and polycytidylic acid) or (incomplete) Freund's adjuvant, are regularly included in both preventive and therapeutic vaccine, and synthetic approaches provide ample opportunities for further improvement[20-23]. An excellent example of a vaccine aimed to overcome both bottleneck 1 and 2 was recently described by Zom et al., who synthesized a dual synthetic long peptide conjugate that triggers two PRRs: NOD2 (nucleotide-binding oligomerization domain-containing protein 2) and TLR2[20,24,25].

Small molecules as DC activating, immunomodulatory drugs

Chemical drugs are potentially superior to biologicals because of their tissue-penetrating capacities and considerably lower production costs compared to mAbs[26]. They can target both intracellular proteins and cell-surface receptors, while therapeutic antibodies are restricted to membrane proteins and secreted proteins. Moreover, their half-lives are shorter, allowing more acute action, potentially reducing the chance of systemic adverse effects. We will highlight some of the most potent examples in the next paragraphs.

The first small-molecule immune-oncology drug approved by the FDA was

imiquimod, an imidazoquinoline derivative commonly used in the treatment of genital warts and approved for treatment of basal cell carcinoma[27]. Its target is TLR7, a PRR that binds conserved **PAMPs**, such as double-stranded RNA, lipopolysaccharide (LPS) or unmethylated CpG DNA[28]. Most TLRs are located on the cell surface, but TLR3, 7, 8 and 9 are located in endosomal compartments[29]. A small-molecule TLR8 agonist, motolimod (VTX-2337), has demonstrated anti-tumor activity in recurrent or metastatic squamous cell carcinomas of the head and neck (SCCHN) by stimulating natural killer (NK) cell activation, enhancing antibody-dependent cell-mediated toxicity and through the induction of Th1-polarizing cytokines[30]. A subset of treated patients demonstrated even higher responses in combination with cetuximab (anti-EGFR (endothelial growth factor)) or chemotherapy[31,32]. Imiquimod, motolimod and resiquimod, a relative of imiquimod that targets TLR7 and TLR8, were tested in a number of clinical trials for treatment of solid tumors, often as adjuvants to vaccination. The search for small molecules targeting other (and preferably multiple) TLRs continues with the help of high-throughput screening of drug libraries in cell-based assays[33].

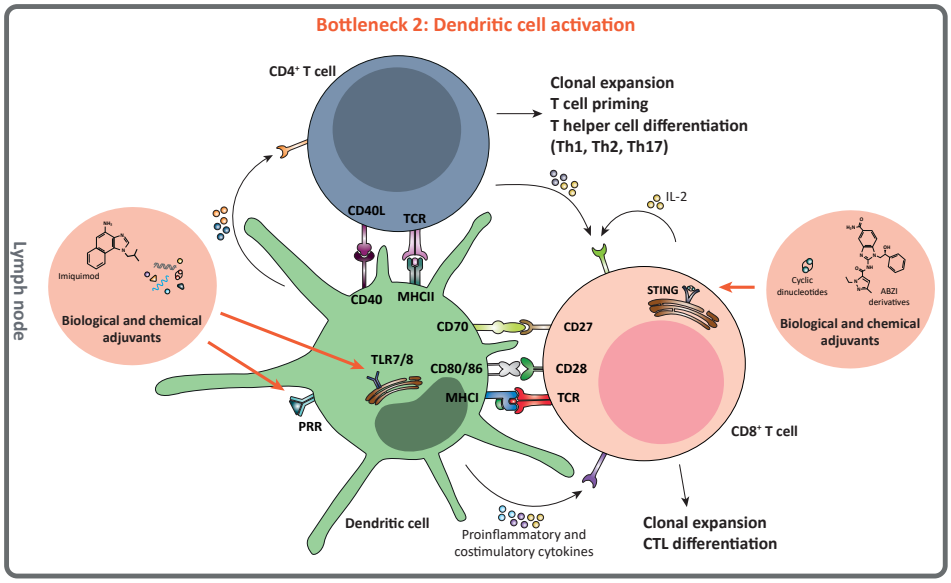

Figure 2. **The second bottleneck in anti-tumor T cell immunity is dendritic cell activation.** Dendritic cells must receive activating signals, such as DAMPs and PAMPs, in order to supply the costimulatory signals needed for priming expansion and differentiation of T cells. Tumors generally lack these activating signals and fail to prompt costimulation, even when their antigens are recognized by T cells. DC activation of can be induced by adjuvants targeted at extracellular or intracellular PRRs. CTL, cytotoxic T lymphocyte; DAMP, danger-associated molecular pattern; MHC, major histocompatibility complex; PAMP; pattern-associated molecular pattern; PRR, pattern recognition receptor; TCR, T cell receptor; Th, T helper

Other PRRs, such as NOD-like receptors (NLRs), C-type lectin receptors (CLRs) or RIG-I-like receptors (RLRs) have been less extensively studied than TLRs, but agonists targeting these families likely also enhance immune responses[34].

Another innate sensor implied in anti-tumor immunity is STING (stimulator of interferon genes), a PRR on the ER membrane that binds cyclic dinucleotides derived from cytosolic DNA converted by cGAS (cyclic-GMP-AMP synthase)[35]. The cGAS/STING pathway leads to type I IFN production, which promotes DC activation and T cell priming, as shown in response to tumors in mice[36]. This finding put STING on the map as a target for cancer immunotherapy, in addition to being a potent adjuvant. Intratumoral injection of small-molecule STING agonist DMXAA (5,6-dimethylxantheone-4-acetic acid, Vadimezan) demonstrated specificity and efficacy in controlling established and distant tumor progression in mice[37]. However, this drug was ineffective in humans because human and mouse STING are structurally different[38-40]. Considerable efforts to create derivatives of DMXAA that are active against human STING are ongoing[41]. In a high-grade serous carcinoma mouse model, a cyclic dinucleotide STING agonist combined with anti-PD-1 mAb increased systemic tumor responses to chemotherapy[42]. In a phase I clinical trial (NCT03010176) intratumoral vaccination with Merck's cyclic dinucleotide STING agonist, MK-1454, did not show remissions in monotherapy and 25% responders in combination with pembrolizumab (anti-PD-1). Aduro Biotech's STING agonist ADU-S100 is also a cyclic dinucleotide, chemically modified to enhance stability and increase efficacy[37]. ADU-S100 monotherapy led to a partial response in two out of the 40 patients enrolled and stable disease in 11 patients. The safety and efficacy as single agent and in combination with ipilimumab (anti-CTLA-4) are under investigation in an ongoing phase I study (NCT02675439) (http://investors.aduro.com/news-releases/news-release-details/aduro-announces-first-patient-dosed-phase-1-study-adu-s100?ID=2386898&c=242043&p=irol-newsArticle). The drug is currently being tested in a phase Ib clinical trial (NCT03172936) in combination with spartalizumab (former PDR001), an anti-PD-1 antibody developed by Novartis. Preliminary results presented at the 2019 American Society of Clinical Oncology (ASCO) meeting were disappointing. Five out of 83 patients achieved confirmed responses - one patient with a complete response (CR) and three with partial response (PR) among PD-1 naïve triple-negative breast cancer (TNBC) patients, and two with PR among previously immunotherapy-treated melanoma patients (http://investors.aduro.com/news-releases/news-release-details/aduro-biotech-and-novartis-present-results-ongoing-phase-1b?field_nir_news_date_value[min]=2019). A phase II trial combining ADU-S100 and anti-PD-1 for first-line treatment of PD-L1-positive recurrent or metastatic HNSCC is now recruiting (NCT03937141).

Recently, three related small-molecule STING agonists based on amidobenzimidazole (ABZI) were reported[43]. In contrast to dinucleotides, which

are rapidly degraded by phosphodiesterases in the body and therefore have to be injected intratumorally, these chemical compounds can be delivered intravenously[44,45]. Systemic administration renders them suitable for treatment of less accessible solid tumors and potentially achieves systemic efficacy. The most potent compound described in this study binds three human and one mouse STING alleles with high affinity and proved efficacious in mouse models after i.v. injection. In contrast to the reported successes, other studies showed that upregulation of cGAS/STING signaling enhanced carcinogenesis and induced immune checkpoint IDO in poorly immunogenic tumors, dampening the immune response and promoting tumor growth[46-48]. These contradicting findings highlight the complexity of the various signaling pathways, but also indicates new avenues for combination treatment.

Targeting the TME to relieve cancer-associated immune suppression

The TME can render T cells dysfunctional and attenuate the efficacy of immunotherapy[49]. Checkpoint inhibition can help to overcome $CD8^+$ T cell dysfunction, in part perhaps because responsiveness depends on specific T cell differentiation states[50,51]. Elucidating and targeting **immune suppression** and -evasion mechanisms can help to improve clinical outcomes. Small-molecule drugs may again be used to specifically target suppressive factors and to induce or restore immune reactivity in the TME. A number of small molecules that block the PD-1/PD-L1 interaction have been described, although none have been approved by the FDA. Curis' CA-170, claimed to inhibit PD-L1, PD-L2 and VISTA, is currently being tested in a phase I clinical trial to treat patients with advanced tumors and lymphomas (NCT02812875)[52].

One of the main advantages of small molecules is the fact that they can enter the cell, while mAbs cannot. A promising target in this context is RORγt (retinoic acid receptor-related orphan receptor gamma), a transcription factor involved in the pro-inflammatory IL-17 pathway. A large number of RORγt antagonists is under investigation for treatment of autoimmune and inflammatory disorders[53,54]. In contrast, RORγt agonists can induce production of cytokines and chemokines, decrease proliferation of **Tregs** and revoke **immunosuppression** by tumor cells[55,56]. Specifically, RORγt agonists have demonstrated enhanced activity, proliferation and survival of Th17 ($CD4^+$) and Tc17 ($CD8^+$) cells in vitro[57-59]. Two phase II trials have been designed to test the effects of these agonists in human. One of these trials aims to investigate the responses to RORγt agonist LYC-55716 (Lycera) in six solid tumor types (NCT02929862) and the other aims to test the safety and tolerability in combination with anti-PD-1 antibody pembrolizumab (NCT03396497). It

is unclear what the effects on tumor control will be, since the presence of Th17 cells has been associated with a poor prognosis in a number of cancer types[60-62]. In these cases, RORγt antagonists may provide therapeutic benefit, but inhibitor design proves complicated because of RORγt's large and lipophilic ligand binding domains[63]. One of the main adverse effects of stimulating this transcription factor is the occurrence of autoimmune disorders, such as inflammatory bowel disease[64]. Taking into account that the 'classical' checkpoint inhibitors anti-CTLA-4 and anti-PD-1 also induce autoimmune disorders, the combination may strongly induce side effects. The ongoing trials will tell.

Another emerging TME target in immunotherapy is IDO1, a tryptophan catabolic enzyme found to induce **immune suppression** and -evasion through

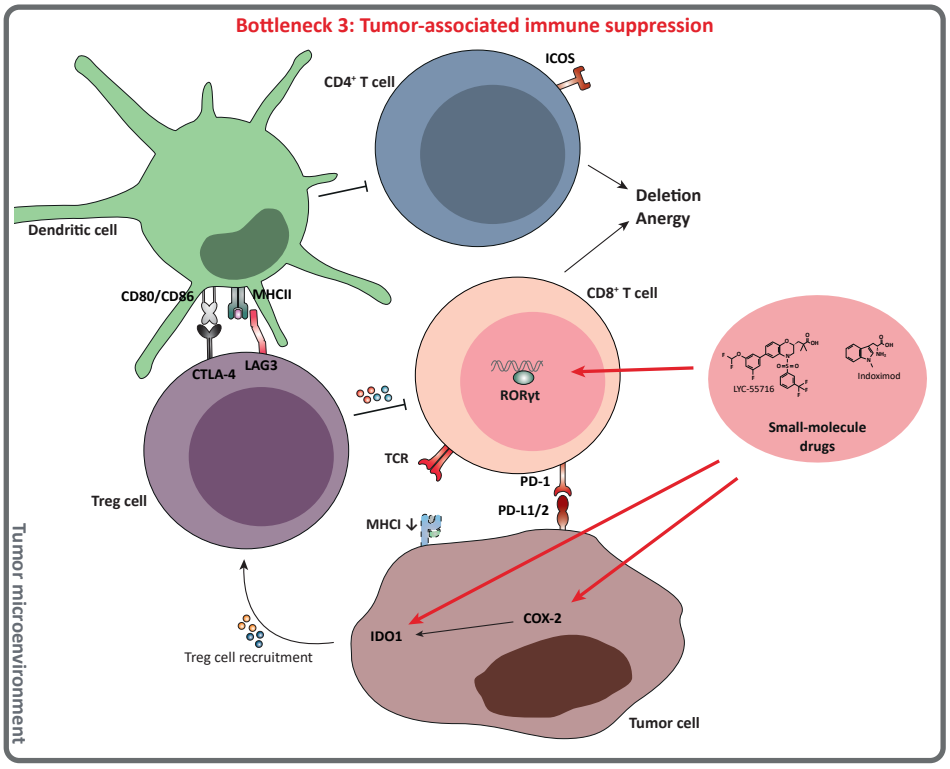

Figure 3. **Tumor-associated immune suppression presents a third bottleneck in anti-tumor T cell activity.** Tumors often establish an immunosuppressive environment through upregulation of inhibitory checkpoint molecules, such as PD-L1 (programmed death ligand 1), downregulation of MHCI or expression of regulatory T cell (Treg)-recruiting cytokines. Suppression can be relieved by small-molecule drugs targeted at relevant mechanisms. CTL, cytotoxic T lymphocyte; CTLA-4, cytotoxic T lymphocyte-associated antigen 4; LAG-3, lymphocyte-activation gene 3; MHC, major histocompatibility complex; PD-1, programmed death 1; PRR, pattern recognition receptor; TCR, T cell receptor.

the expansion of **Treg** cells[65,66]. IDO1 is the most broadly expressed of three enzymes (together with IDO2 and tryptophan 2,3-dioxyenase (TDO)) involved in the first step of the kynurenine pathway. Indoximod was the first IDO1 inhibitor to be tested in humans, but with confusing results[67]. The exact mechanism by which indoximod operates is not fully elucidated, but it has been suggested that the drug inhibits mTORC1, a downstream effector of IDO1, and not IDO1 itself. Despite promising results from multiple phase I/II trials, epacadostat, a direct IDO1 inhibitor, failed to show increased benefit in combination with anti-PD-1 in a stage III clinical trial, but the search for new inhibitors continues[68-71]. Inhibition of IDO1 alone frequently results in resistance by upregulation of IDO2 and TDO, hence broad-spectrum inhibitors targeting all three may provide most benefit[72].

One of the drivers of IDO1 expression is cyclooxygenase (COX)-2, a fairly unexplored target in immunotherapy, but a common target of non-steroidal anti-inflammatory drugs (NSAIDs)[73]. COX-2 catalyzes the synthesis of prostaglandins, lipid compounds involved in many physiological processes in response to injury and inflammation. Expression of this enzyme has been associated with several cancers and consequently celecoxib, an NSAID that inhibits COX-2 as well as IDO1, is being explored as anti-cancer therapeutic[74-76]. Buzharevski et at. developed analogues of celecoxib and showed a potent cytostatic effect on melanoma and colon cancer cell lines[77]. Concurrent inhibition of COX-2 and EGFR was previously found to have synergistic effects and recently Tang et al. reported the dual inhibition of COX-2 and EGFR, by melafolone, a naturally occurring flavonoid[78,79]. They demonstrated improved PD-1 blockade in lung cancer by downregulating PD-L1 and normalizing tumor vasculature by downregulating VEGF or TGF-β. These examples of drugs that harbor dual activity against tumor-associated molecules are very promising.

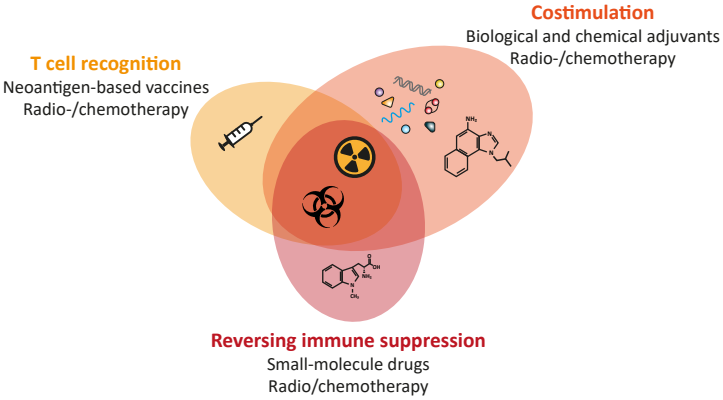

Figure 4. **Neoantigen-based vaccines, adjuvants, small-molecule drugs and conventional chemotherapeutic drugs each work at different stages of immunity.** A combination of strategies can boost T cell immunity and overcome tumor-associated immune suppression.

Concluding remarks

Immunotherapy has demonstrated potent anti-tumor T cell responses in treatment of various cancer types; however, only in a subset of patients and often accompanied by severe adverse events and systemic toxicity. Opportunities for improvement are provided by small-molecule drugs. Their pharmacokinetics allow systemic administration without the rapid degradation often hampering effectivity of biological drugs. Due to their tissue-penetrating capacities small molecules can be directed at both extra- and intracellular targets to inhibit relevant immunosuppressive pathways activated by tumor cells. Studies aimed at elucidating the molecular mechanisms responsible for tumor-associated **immune suppression** will greatly contribute to the advance of this relatively unexplored area of drug development. By combining chemical drugs with conventional strategies, cancer therapies can be improved to overcome the bottlenecks in anti-cancer T cell response, ideally achieving synergistic effects. Strategic combinations in immunotherapy will include (checkpoint) antibodies with diverse forms of therapeutic vaccination[80,81], but also combination therapies with (targeted) drugs, conventional chemotherapy or radiotherapy[82]. Both RT and CT may induce **immunogenic cell death**, resulting in release of tumor antigens and other danger signals that in turn can activate DCs via innate receptors, such as TLRs or the cGAS/STING pathway, and they modulate the TME[83-86]. These therapies operate at the level of all three bottlenecks (Fig. 4), thereby creating an immune-activating environment and as a result enhance the effect of immunotherapies, potentially rendering even **cold tumors** susceptible to immunotherapy[87,88]. In a way, the tumor then functions as its own vaccine, inducing a systemic anti-tumor response.

Acknowledgements

This work was supported by a grant from the Institute for Chemical Immunology (ICI, to H. Ovaa, J. Borst and J. Neefjes). This work is part of Oncode Institute, which is partly financed by the Dutch Cancer Society.

Glossary

Central tolerance: the absence of self-reactive T cells to avoid autoimmunity. T cells that recognize self-antigens are deleted during negative selection in the thymus.
Cold tumor: non-immunogenic tumor devoid of tumor-infiltrating lymphocytes and hence less sensitive to immunotherapy.
Cytotoxic T lymphocyte (CTL): $CD8^+$ killer T cell that recognizes intracellular alterations, in the context of major histocompatibility class I (MHCI) complexes that are expressed on all tissues and thus also on a wide variety of tumor types.
Danger-associated molecular patterns (DAMPs): danger signals released by damaged or dying cells, such as cytosolic or nuclear proteins, or DNA. Binding of DAMPs to pattern recognition receptors (PRRs) induces innate immunity and DC maturation.
Heterogeneity: phenotypical variations between tumor cells, often of genetic origin, that affect therapy response and hamper treatment design.
Immunogenic cell death: form of cell death that, in contrast to apoptosis, results in the release of immune-stimulating factors, such as danger-associated molecular patterns (DAMPs) or tumor antigens.
Immunosuppression: inhibition of immunity induced by tumor cells to escape elimination. Often mediated by induction of Treg cells, upregulation of inhibitory checkpoints or downregulation of activating signals.
Microsatellite instability: genetic predisposition to mutation caused by the loss of DNA mismatch repair activity.
Neoantigen: tumor antigen arising from somatic DNA mutations, so that no central tolerance has been raised. T cells can recognize these antigens and attack tumor cells expressing them.
Pathogen-associated molecular patterns (PAMPs): molecules not found on vertebrates that trigger innate immunity by binding pattern recognition receptors. Classic PAMPs are dsRNA, endotoxins or bacterial cell wall constituents.
Peripheral tolerance: suppression of self-reactive immune cells in the periphery that have escaped central tolerance, for example through suppression by Tregs or induction of anergy.
Regulatory T cell (Treg): subset of $CD4^+$ T cells that modulate the immune response by suppressing effector cells.

References

1. Koebel, C. M. *et al.* Adaptive immunity maintains occult cancer in an equilibrium state. *Nature* **450**, 903-907, doi:10.1038/nature06309 (2007).
2. Chen, D. S. & Mellman, I. Oncology meets immunology: the cancer-immunity cycle. *Immunity* **39**, 1-10, doi:10.1016/j.immuni.2013.07.012 (2013).
3. Corthay, A. Does the immune system naturally protect against cancer? *Front Immunol* **5**, 197, doi:10.3389/fimmu.2014.00197 (2014).
4. Hellmann, M. D. *et al.* Tumor Mutational Burden and Efficacy of Nivolumab Monotherapy and in Combination with Ipilimumab in Small-Cell Lung Cancer. *Cancer Cell* **33**, 853-861 e854, doi:10.1016/j.ccell.2018.04.001 (2018).
5. McGranahan, N. *et al.* Clonal neoantigens elicit T cell immunoreactivity and sensitivity to immune checkpoint blockade. *Science* **351**, 1463-1469, doi:10.1126/science.aaf1490 (2016).
6. Walker, L. S. & Sansom, D. M. The emerging role of CTLA4 as a cell-extrinsic regulator of T cell responses. *Nat Rev Immunol* **11**, 852-863, doi:10.1038/nri3108 (2011).
7. Schreiber, R. D., Old, L. J. & Smyth, M. J. Cancer immunoediting: integrating immunity's roles in cancer suppression and promotion. *Science* **331**, 1565-1570, doi:10.1126/science.1203486 (2011).
8. Tran, E. *et al.* Immunogenicity of somatic mutations in human gastrointestinal cancers. *Science* **350**, 1387-1390, doi:10.1126/science.aad1253 (2015).
9. Munn, D. H. & Bronte, V. Immune suppressive mechanisms in the tumor microenvironment. *Curr Opin Immunol* **39**, 1-6, doi:10.1016/j.coi.2015.10.009 (2016).
10. Schumacher, T. N. & Hacohen, N. Neoantigens encoded in the cancer genome. *Curr Opin Immunol* **41**, 98-103, doi:10.1016/j.coi.2016.07.005 (2016).
11. Wang, R. F. & Wang, H. Y. Immune targets and neoantigens for cancer immunotherapy and precision medicine. *Cell Res* **27**, 11-37, doi:10.1038/cr.2016.155 (2017).
12. Ahrends, T. *et al.* CD4(+) T Cell Help Confers a Cytotoxic T Cell Effector Program Including Coinhibitory Receptor Downregulation and Increased Tissue Invasiveness. *Immunity* **47**, 848-861 e845, doi:10.1016/j.immuni.2017.10.009 (2017).
13. Linnemann, C. *et al.* High-throughput epitope discovery reveals frequent recognition of neo-antigens by CD4+ T cells in human melanoma. *Nat Med* **21**, 81-85, doi:10.1038/nm.3773 (2015).
14. Kreiter, S. *et al.* Mutant MHC class II epitopes drive therapeutic immune responses to cancer. *Nature* **520**, 692-696, doi:10.1038/nature14426 (2015).
15. Ott, P. A. *et al.* An immunogenic personal neoantigen vaccine for patients with melanoma. *Nature* **547**, 217-221, doi:10.1038/nature22991 (2017).
16. Melief, C. J., van Hall, T., Arens, R., Ossendorp, F. & van der Burg, S. H. Therapeutic cancer vaccines. *J Clin Invest* **125**, 3401-3412, doi:10.1172/JCI80009 (2015).
17. Sahin, U. *et al.* Personalized RNA mutanome vaccines mobilize poly-specific therapeutic immunity against cancer. *Nature* **547**, 222-226, doi:10.1038/nature23003 (2017).
18. Keskin, D. B. *et al.* Neoantigen vaccine generates intratumoral T cell responses in phase Ib glioblastoma trial. *Nature* **565**, 234-239, doi:10.1038/s41586-018-0792-9 (2019).
19. Speiser, D. E. *et al.* Rapid and strong human CD8+ T cell responses to vaccination with peptide, IFA, and CpG oligodeoxynucleotide 7909. *J Clin Invest* **115**, 739-746, doi:10.1172/JCI23373 (2005).
20. Hos, B. J., Tondini, E., van Kasteren, S. I. & Ossendorp, F. Approaches to Improve Chemically Defined Synthetic Peptide Vaccines. *Front Immunol* **9**, 884, doi:10.3389/fimmu.2018.00884 (2018).
21. Kyi, C. *et al.* Therapeutic Immune Modulation against Solid Cancers with Intratumoral Poly-ICLC: A Pilot Trial. *Clin Cancer Res* **24**, 4937-4948, doi:10.1158/1078-0432.CCR-17-1866 (2018).
22. Paavonen, J. *et al.* Efficacy of human papillomavirus (HPV)-16/18 AS04-adjuvanted vaccine against cervical infection and precancer caused by oncogenic HPV types (PATRICIA): final analysis of a double-blind, randomised study in young women. *Lancet* **374**, 301-314, doi:10.1016/S0140-6736(09)61248-4 (2009).
23. Garland, S. M. *et al.* Prior human papillomavirus-16/18 AS04-adjuvanted vaccination prevents recurrent high grade cervical intraepithelial neoplasia after definitive surgical therapy: Post-hoc analysis from a randomized controlled trial. *Int J Cancer* **139**, 2812-2826, doi:10.1002/ijc.30391 (2016).

24. Zom, G. G. *et al.* Dual Synthetic Peptide Conjugate Vaccine Simultaneously Triggers TLR2 and NOD2 and Activates Human Dendritic Cells. *Bioconjug Chem* **30**, 1150-1161, doi:10.1021/acs.bioconjchem.9b00087 (2019).
25. Zom, G. G. *et al.* Efficient induction of antitumor immunity by synthetic toll-like receptor ligand-peptide conjugates. *Cancer Immunol Res* **2**, 756-764, doi:10.1158/2326-6066.CIR-13-0223 (2014).
26. Sheng, J. *et al.* Clinical Pharmacology Considerations for the Development of Immune Checkpoint Inhibitors. *J Clin Pharmacol* **57 Suppl 10**, S26-S42, doi:10.1002/jcph.990 (2017).
27. Smith, M. *et al.* Trial Watch: Toll-like receptor agonists in cancer immunotherapy. *Oncoimmunology* **7**, e1526250, doi:10.1080/2162402X.2018.1526250 (2018).
28. Kaczanowska, S., Joseph, A. M. & Davila, E. TLR agonists: our best frenemy in cancer immunotherapy. *J Leukoc Biol* **93**, 847-863, doi:10.1189/jlb.1012501 (2013).
29. Mancini, R. J., Stutts, L., Ryu, K. A., Tom, J. K. & Esser-Kahn, A. P. Directing the immune system with chemical compounds. *ACS Chem Biol* **9**, 1075-1085, doi:10.1021/cb500079s (2014).
30. Dietsch, G. N. *et al.* Coordinated Activation of Toll-Like Receptor8 (TLR8) and NLRP3 by the TLR8 Agonist, VTX-2337, Ignites Tumoricidal Natural Killer Cell Activity. *PLoS One* **11**, e0148764, doi:10.1371/journal.pone.0148764 (2016).
31. Shayan, G. *et al.* Phase Ib Study of Immune Biomarker Modulation with Neoadjuvant Cetuximab and TLR8 Stimulation in Head and Neck Cancer to Overcome Suppressive Myeloid Signals. *Clin Cancer Res* **24**, 62-72, doi:10.1158/1078-0432.CCR-17-0357 (2018).
32. Ferris, R. L. *et al.* Effect of Adding Motolimod to Standard Combination Chemotherapy and Cetuximab Treatment of Patients With Squamous Cell Carcinoma of the Head and Neck: The Active8 Randomized Clinical Trial. *JAMA Oncol* **4**, 1583-1588, doi:10.1001/jamaoncol.2018.1888 (2018).
33. Zhang, L., Dewan, V. & Yin, H. Discovery of Small Molecules as Multi-Toll-like Receptor Agonists with Proinflammatory and Anticancer Activities. *J Med Chem* **60**, 5029-5044, doi:10.1021/acs.jmedchem.7b00419 (2017).
34. Zhu, G. *et al.* Targeting pattern-recognition receptors to discover new small molecule immune modulators. *Eur J Med Chem* **144**, 82-92, doi:10.1016/j.ejmech.2017.12.026 (2018).
35. Burdette, D. L. & Vance, R. E. STING and the innate immune response to nucleic acids in the cytosol. *Nat Immunol* **14**, 19-26, doi:10.1038/ni.2491 (2013).
36. Woo, S. R. *et al.* STING-dependent cytosolic DNA sensing mediates innate immune recognition of immunogenic tumors. *Immunity* **41**, 830-842, doi:10.1016/j.immuni.2014.10.017 (2014).
37. Corrales, L. *et al.* Direct Activation of STING in the Tumor Microenvironment Leads to Potent and Systemic Tumor Regression and Immunity. *Cell Rep* **11**, 1018-1030, doi:10.1016/j.cel.rep.2015.04.031 (2015).
38. Lara, P. N., Jr. *et al.* Randomized phase III placebo-controlled trial of carboplatin and paclitaxel with or without the vascular disrupting agent vadimezan (ASA404) in advanced non-small-cell lung cancer. *J Clin Oncol* **29**, 2965-2971, doi:10.1200/JCO.2011.35.0660 (2011).
39. Shih, A. Y., Damm-Ganamet, K. L. & Mirzadegan, T. Dynamic Structural Differences between Human and Mouse STING Lead to Differing Sensitivity to DMXAA. *Biophys J* **114**, 32-39, doi:10.1016/j.bpj.2017.10.027 (2018).
40. Conlon, J. *et al.* Mouse, but not human STING, binds and signals in response to the vascular disrupting agent 5,6-dimethylxanthenone-4-acetic acid. *J Immunol* **190**, 5216-5225, doi:10.4049/jimmunol.1300097 (2013).
41. Hwang, J., Kang, T., Lee, J., Choi, B. S. & Han, S. Design, synthesis, and biological evaluation of C7-functionalized DMXAA derivatives as potential human-STING agonists. *Org Biomol Chem*, doi:10.1039/c8ob01798k (2018).
42. Ghaffari, A. *et al.* STING agonist therapy in combination with PD-1 immune checkpoint blockade enhances response to carboplatin chemotherapy in high-grade serous ovarian cancer. *Br J Cancer* **119**, 440-449, doi:10.1038/s41416-018-0188-5 (2018).
43. Ramanjulu, J. M. *et al.* Design of amidobenzimidazole STING receptor agonists with systemic activity. *Nature* **564**, 439-443, doi:10.1038/s41586-018-0705-y (2018).
44. Huck, B. R., Kotzner, L. & Urbahns, K. Small Molecules Drive Big Improvements in Immuno-Oncology Therapies. *Angew Chem Int Ed Engl* **57**, 4412-4428, doi:10.1002/anie.201707816 (2018).
45. Kato, K. *et al.* Structural insights into cGAMP degradation by Ecto-nucleotide pyrophosphatase

phosphodiesterase 1. *Nat Commun* **9**, 4424, doi:10.1038/s41467-018-06922-7 (2018).
46. Liu, H. *et al.* Nuclear cGAS suppresses DNA repair and promotes tumorigenesis. *Nature* **563**, 131-136, doi:10.1038/s41586-018-0629-6 (2018).
47. Lemos, H. *et al.* STING Promotes the Growth of Tumors Characterized by Low Antigenicity via IDO Activation. *Cancer Res* **76**, 2076-2081, doi:10.1158/0008-5472.CAN-15-1456 (2016).
48. An, X. *et al.* An Analysis of the Expression and Association with Immune Cell Infiltration of the cGAS/STING Pathway in Pan-Cancer. *Mol Ther Nucleic Acids* **14**, 80-89, doi:10.1016/j.omtn.2018.11.003 (2018).
49. Giraldo, N. A. *et al.* The clinical role of the TME in solid cancer. *Br J Cancer* **120**, 45-53, doi:10.1038/s41416-018-0327-z (2019).
50. Speiser, D. E., Ho, P. C. & Verdeil, G. Regulatory circuits of T cell function in cancer. *Nat Rev Immunol* **16**, 599-611, doi:10.1038/nri.2016.80 (2016).
51. Grywalska, E., Pasiarski, M., Gozdz, S. & Rolinski, J. Immune-checkpoint inhibitors for combating T-cell dysfunction in cancer. *Onco Targets Ther* **11**, 6505-6524, doi:10.2147/OTT.S150817 (2018).
52. Yang, J. & Hu, L. Immunomodulators targeting the PD-1/PD-L1 protein-protein interaction: From antibodies to small molecules. *Med Res Rev* **39**, 265-301, doi:10.1002/med.21530 (2019).
53. Fauber, B. P. & Magnuson, S. Modulators of the nuclear receptor retinoic acid receptor-related orphan receptor-gamma (RORgamma or RORc). *J Med Chem* **57**, 5871-5892, doi:10.1021/jm401901d (2014).
54. Gege, C. *et al.* Identification and biological evaluation of thiazole-based inverse agonists of RORgammat. *Bioorg Med Chem Lett* **28**, 1446-1455, doi:10.1016/j.bmcl.2018.03.093 (2018).
55. Sun, Z. *et al.* Requirement for RORgamma in thymocyte survival and lymphoid organ development. *Science* **288**, 2369-2373 (2000).
56. Chang, M. R. *et al.* Synthetic RORgammat Agonists Enhance Protective Immunity. *ACS Chem Biol* **11**, 1012-1018, doi:10.1021/acschembio.5b00899 (2016).
57. Zou, W. & Restifo, N. P. T(H)17 cells in tumour immunity and immunotherapy. *Nat Rev Immunol* **10**, 248-256, doi:10.1038/nri2742 (2010).
58. Ivanov, II *et al.* The orphan nuclear receptor RORgammat directs the differentiation program of proinflammatory IL-17^{+} T helper cells. *Cell* **126**, 1121-1133, doi:10.1016/j.cell.2006.07.035 (2006).
59. Hu, X. *et al.* Synthetic RORgamma agonists regulate multiple pathways to enhance antitumor immunity. *Oncoimmunology* **5**, e1254854, doi:10.1080/2162402X.2016.1254854 (2016).
60. Asadzadeh, Z. *et al.* The paradox of Th17 cell functions in tumor immunity. *Cell Immunol* **322**, 15-25, doi:10.1016/j.cellimm.2017.10.015 (2017).
61. Wang, R. *et al.* Th17 cell-derived IL-17A promoted tumor progression via STAT3/NF-kappaB/Notch1 signaling in non-small cell lung cancer. *Oncoimmunology* **7**, e1461303, doi:10.1080/2162402X.2018.1461303 (2018).
62. Lee, M. H. *et al.* Interleukin 17 and peripheral IL-17-expressing T cells are negatively correlated with the overall survival of head and neck cancer patients. *Oncotarget* **9**, 9825-9837, doi:10.18632/oncotarget.23934 (2018).
63. Kono, M. *et al.* Discovery of [cis-3-({(5 R)-5-[(7-Fluoro-1,1-dimethyl-2,3-dihydro-1 H-inden-5-yl) carbamoyl]-2-methoxy-7,8-dihydro-1,6-naphthyridin-6(5 H)-yl}carbonyl)cyclobutyl]acetic Acid (TAK-828F) as a Potent, Selective, and Orally Available Novel Retinoic Acid Receptor-Related Orphan Receptor gammat Inverse Agonist. *J Med Chem* **61**, 2973-2988, doi:10.1021/acs.jmedchem.8b00061 (2018).
64. Wang, J. *et al.* Rapid Onset of Inflammatory Bowel Disease after Receiving Secukinumab Infusion. *ACG Case Rep J* **5**, e56, doi:10.14309/crj.2018.56 (2018).
65. Prendergast, G. C., Malachowski, W. J., Mondal, A., Scherle, P. & Muller, A. J. Indoleamine 2,3-Dioxygenase and Its Therapeutic Inhibition in Cancer. *Int Rev Cell Mol Biol* **336**, 175-203, doi:10.1016/bs.ircmb.2017.07.004 (2018).
66. Curti, A., Trabanelli, S., Salvestrini, V., Baccarani, M. & Lemoli, R. M. The role of indoleamine 2,3-dioxygenase in the induction of immune tolerance: focus on hematology. *Blood* **113**, 2394-2401, doi:10.1182/blood-2008-07-144485 (2009).
67. Soliman, H. H. *et al.* A first in man phase I trial of the oral immunomodulator, indoximod, combined with docetaxel in patients with metastatic solid tumors. *Oncotarget* **5**, 8136-8146, doi:10.18632/oncotarget.2357 (2014).

68. Muller, A. J., Manfredi, M. G., Zakharia, Y. & Prendergast, G. C. Inhibiting IDO pathways to treat cancer: lessons from the ECHO-301 trial and beyond. *Semin Immunopathol* **41**, 41-48, doi:10.1007/s00281-018-0702-0 (2019).
69. Wu, J. S. *et al.* Identification of Substituted Naphthotriazolediones as Novel Tryptophan 2,3-Dioxygenase (TDO) Inhibitors through Structure-Based Virtual Screening. *J Med Chem* **58**, 7807-7819, doi:10.1021/acs.jmedchem.5b00921 (2015).
70. Mitchell, T. C. *et al.* Epacadostat Plus Pembrolizumab in Patients With Advanced Solid Tumors: Phase I Results From a Multicenter, Open-Label Phase I/II Trial (ECHO-202/KEYNOTE-037). *J Clin Oncol*, JCO2018789602, doi:10.1200/JCO.2018.78.9602 (2018).
71. Komiya, T. & Huang, C. H. Updates in the Clinical Development of Epacadostat and Other Indoleamine 2,3-Dioxygenase 1 Inhibitors (IDO1) for Human Cancers. *Front Oncol* **8**, 423, doi:10.3389/fonc.2018.00423 (2018).
72. Winters, M. *et al.* Diaryl hydroxylamines as pan or dual inhibitors of indoleamine 2,3-dioxygenase-1, indoleamine 2,3-dioxygenase-2 and tryptophan dioxygenase. *Eur J Med Chem* **162**, 455-464, doi:10.1016/j.ejmech.2018.11.010 (2019).
73. Hennequart, M. *et al.* Constitutive IDO1 Expression in Human Tumors Is Driven by Cyclooxygenase-2 and Mediates Intrinsic Immune Resistance. *Cancer Immunol Res* **5**, 695-709, doi:10.1158/2326-6066.CIR-16-0400 (2017).
74. Gong, T. *et al.* Celecoxib suppresses cutaneous squamous-cell carcinoma cell migration via inhibition of SDF1-induced endocytosis of CXCR4. *Onco Targets Ther* **11**, 8063-8071, doi:10.2147/OTT.S180472 (2018).
75. Pang, L. Y., Hurst, E. A. & Argyle, D. J. Cyclooxygenase-2: A Role in Cancer Stem Cell Survival and Repopulation of Cancer Cells during Therapy. *Stem Cells Int* **2016**, 2048731, doi:10.1155/2016/2048731 (2016).
76. Tolloczko-Iwaniuk, N., Dziemianczyk-Pakiela, D., Nowaszewska, B. K., Celinska-Janowicz, K. & Miltyk, W. Celecoxib in Cancer Therapy and Prevention - Review. *Curr Drug Targets*, doi:10.2174/1389450119666180803121737 (2018).
77. Buzharevski, A. *et al.* Carboranyl analogues of celecoxib with potent cytostatic ability against human melanoma and colon cancer cell lines. *ChemMedChem*, doi:10.1002/cmdc.201800685 (2019).
78. Tang, H. *et al.* Inhibition of COX-2 and EGFR by Melafolone Improves Anti-PD-1 Therapy through Vascular Normalization and PD-L1 Downregulation in Lung Cancer. *J Pharmacol Exp Ther*, doi:10.1124/jpet.118.254359 (2018).
79. Li, N. *et al.* Relationship between epidermal growth factor receptor (EGFR) mutation and serum cyclooxygenase-2 Level, and the synergistic effect of celecoxib and gefitinib on EGFR expression in non-small cell lung cancer cells. *Int J Clin Exp Pathol* **8**, 9010-9020 (2015).
80. Carreno, B. M. *et al.* Cancer immunotherapy. A dendritic cell vaccine increases the breadth and diversity of melanoma neoantigen-specific T cells. *Science* **348**, 803-808, doi:10.1126/science.aaa3828 (2015).
81. Goradel, N. H. *et al.* Oncolytic adenovirus: A tool for cancer therapy in combination with other therapeutic approaches. *J Cell Physiol*, doi:10.1002/jcp.27850 (2018).
82. Galon, J. & Bruni, D. Approaches to treat immune hot, altered and cold tumours with combination immunotherapies. *Nat Rev Drug Discov*, doi:10.1038/s41573-018-0007-y (2019).
83. Deng, L. *et al.* STING-Dependent Cytosolic DNA Sensing Promotes Radiation-Induced Type I Interferon-Dependent Antitumor Immunity in Immunogenic Tumors. *Immunity* **41**, 843-852, doi:10.1016/j.immuni.2014.10.019 (2014).
84. Krombach, J. *et al.* Priming anti-tumor immunity by radiotherapy: Dying tumor cell-derived DAMPs trigger endothelial cell activation and recruitment of myeloid cells. *Oncoimmunology* **8**, e1523097, doi:10.1080/2162402X.2018.1523097 (2019).
85. Diamond, J. M. *et al.* Exosomes Shuttle TREX1-Sensitive IFN-Stimulatory dsDNA from Irradiated Cancer Cells to DCs. *Cancer Immunol Res* **6**, 910-920, doi:10.1158/2326-6066.CIR-17-0581 (2018).
86. Kroon, P. *et al.* Radiotherapy and Cisplatin Increase Immunotherapy Efficacy by Enabling Local and Systemic Intratumoral T-cell Activity. *Cancer Immunol Res*, doi:10.1158/2326-6066.CIR-18-0654 (2019).
87. Beyranvand Nejad, E. *et al.* Tumor Eradication by Cisplatin Is Sustained by CD80/86-Mediated

Costimulation of CD8+ T Cells. *Cancer Res* **76**, 6017-6029, doi:10.1158/0008-5472.CAN-16-0881 (2016).
88. Heinhuis, K. M. *et al.* Enhancing anti-tumor response by combining immune checkpoint inhibitors with chemotherapy in solid tumors. *Ann Oncol*, doi:10.1093/annonc/mdy551 (2019).
89. Lesokhin, A. M., Callahan, M. K., Postow, M. A. & Wolchok, J. D. On being less tolerant: enhanced cancer immunosurveillance enabled by targeting checkpoints and agonists of T cell activation. *Sci Transl Med* **7**, 280sr281, doi:10.1126/scitranslmed.3010274 (2015).
90. Topalian, S. L. *et al.* Safety, activity, and immune correlates of anti-PD-1 antibody in cancer. *N Engl J Med* **366**, 2443-2454, doi:10.1056/NEJMoa1200690 (2012).
91. Wolchok, J. D. *et al.* Overall Survival with Combined Nivolumab and Ipilimumab in Advanced Melanoma. *N Engl J Med* **377**, 1345-1356, doi:10.1056/NEJMoa1709684 (2017).
92. Burugu, S., Dancsok, A. R. & Nielsen, T. O. Emerging targets in cancer immunotherapy. *Semin Cancer Biol* **52**, 39-52, doi:10.1016/j.semcancer.2017.10.001 (2018).
93. Ribas, A. & Wolchok, J. D. Cancer immunotherapy using checkpoint blockade. *Science* **359**, 1350-1355, doi:10.1126/science.aar4060 (2018).
94. Emens, L. A. *et al.* Cancer immunotherapy: Opportunities and challenges in the rapidly evolving clinical landscape. *Eur J Cancer* **81**, 116-129, doi:10.1016/j.ejca.2017.01.035 (2017).
95. Hui, E. *et al.* T cell costimulatory receptor CD28 is a primary target for PD-1-mediated inhibition. *Science* **355**, 1428-1433, doi:10.1126/science.aaf1292 (2017).
96. Quezada, S. A., Peggs, K. S., Simpson, T. R. & Allison, J. P. Shifting the equilibrium in cancer immunoediting: from tumor tolerance to eradication. *Immunol Rev* **241**, 104-118, doi:10.1111/j.1600-065X.2011.01007.x (2011).
97. Parry, R. V. *et al.* CTLA-4 and PD-1 receptors inhibit T-cell activation by distinct mechanisms. *Mol Cell Biol* **25**, 9543-9553, doi:10.1128/MCB.25.21.9543-9553.2005 (2005).
98. Wei, S. C. *et al.* Negative Co-stimulation Constrains T Cell Differentiation by Imposing Boundaries on Possible Cell States. *Immunity* **50**, 1084-1098 e1010, doi:10.1016/j.immuni.2019.03.004 (2019).
99. Kvistborg, P. *et al.* Anti-CTLA-4 therapy broadens the melanoma-reactive CD8+ T cell response. *Sci Transl Med* **6**, 254ra128, doi:10.1126/scitranslmed.3008918 (2014).

5

A flexible MHC class I multimer loading system for large-scale detection of antigen-specific T cells

Jolien J. Luimstra[1*], Malgorzata A. Garstka[2*], Marthe C.J. Roex[3], Anke Redeker[4], George M.C. Janssen[5], Peter A. van Veelen[5], Ramon Arens[4], J.H. Frederik Falkenburg[3], Jacques Neefjes[1], and Huib Ovaa[1]

*J.J. Luimstra and M.A. Garstka contributed equally to this work.

[1]Oncode Institute and Department of Cell and Chemical Biology, Leiden University Medical Center, Leiden, The Netherlands
[2]Core Research Lab, the Second Affiliated Hospital, School of Medicine, Xi'an Jiaotong University, Xi'an, China
[3]Department of Hematology, Leiden University Medical Center, Leiden, The Netherlands
[4]Department of Immunohematology and Blood Transfusion, Leiden University Medical Center, Leiden, The Netherlands
[5]Center for Proteomics and Metabolomics, Leiden University Medical Center, Leiden, The Netherlands

Journal of Experimental Medicine 215, 1493-1504 (2018)

Abstract

Adaptive immunity is initiated by T cell recognition of specific antigens presented by major histocompatibility complexes (MHCs). MHC multimer technology has been developed for the detection, isolation and characterization of T cells in infection, autoimmunity and cancer. Here, we present a simple, fast, flexible and efficient method to generate many different MHC class I (MHCI) multimers in parallel using temperature-mediated peptide exchange. We designed conditional peptides for HLA-A*02:01 and H-2K^{b} that form stable peptide-MHCI complexes at low temperatures, but dissociate when exposed to a defined elevated temperature. The resulting conditional MHCI complexes either alone or prepared as ready-to-use multimers can swiftly be loaded with peptides of choice without additional handling and within a short time frame. We demonstrate the ease and flexibility of this approach by monitoring the anti-viral immune constitution in an allogeneic stem cell transplant recipient and by analyzing CD8^{+} T cell responses to viral epitopes in mice infected with lymphocytic choriomeningitis virus or cytomegalovirus.

5

Introduction

Immune surveillance is mediated by major histocompatibility class I (MHCI) complexes that bind intracellular peptides for presentation to CD8^{+} T lymphocytes. This ability to distinguish between self and foreign is fundamental to adaptive immunity and failure can result in the development of autoimmune disease. During life humans are under continuous attack by pathogens, such as viruses. Some of them establish lifelong infections, where the virus persists in a latent state without causing symptoms, but occasionally reactivates. One class of such viruses causing recurring infections are the herpesviruses[1]. Normally reactivation does not lead to disease, because the infection is rapidly cleared by T cells upon recognition of viral antigens. However, in the context of transplantation, when patients are immunocompromised, reactivation of herpesviruses such as cytomegalovirus (CMV) or Epstein-Barr virus (EBV) can result in serious health threats[2,3]. It is therefore important to monitor virus-specific T cell numbers in transplant recipients to follow the fate of the recurring infections and to decide if intervention is needed.

Since their first use in 1996 by Altman et al., MHC multimers – oligomers of MHC monomers loaded with antigenic peptides and tagged with fluorochrome(s) – have been the most extensively used reagents for the analysis and monitoring of antigen-specific T cells by flow cytometry[4]. However, multimer generation involves many time-consuming steps, including expression of MHCI heavy

chain and β2-microglubulin in bacteria, refolding with a desired peptide, purification, biotinylation and multimerization[4]. Initially, all these steps had to be undertaken for every individual peptide-MHCI complex, since empty MHCI molecules are unstable[5]. This prompted the search for ways to generate peptide-receptive MHCI molecules at will for the parallel production of multiple MHCI multimers from a single input MHCI-peptide complex. Several techniques aimed at peptide exchange on MHCI have been developed by us and by others, including dipeptides as catalysts or periodate or dithionite as chemical triggers to cleave conditional ligands in situ, after which peptide remnants can dissociate to be replaced by a peptide of choice[6-9]. Alternatively, MHCI monomers are prepared with a photocleavable peptide that gets cleaved upon UV exposure, after which MHCI molecules can be loaded with peptides of choice and subsequently multimerized[10-12]. This approach has facilitated the discovery of a myriad of epitopes and the monitoring of corresponding T cells[11,13-15]. However, UV exchange technology requires the use of a photocleavable peptide and a UV source. UV exposure and ligand exchange are not compatible with fluorescently-labeled multimers and the biotinylated peptide-loaded MHCI molecules need to be multimerized on streptavidin post peptide exchange. Other disadvantages include the generation of reactive nitroso species upon UV-mediated cleavage and photodamage of MHCI and/or exchanged peptides, while the generated heat causes sample evaporation[16].

To develop a faster, more convenient technology for peptide exchange on multimers we explored our original observation that early in MHCI assembly, low-affinity peptides continuously bind and dissociate from MHC molecules until a high affinity/low off-rate peptide is bound for presentation[17]. This process was strongly dependent on temperature: low-affinity peptides that stably associated at low temperature were released at slightly elevated temperatures and replaced with higher-affinity peptides[17,18]. Here, we describe a direct application of this observation: the design of peptides with a low off-rate at 4°C that in a temperature-dependent manner can be exchanged for exogenous peptides of interest. We provide proof-of-concept for H-2K^b and HLA-A*02:01 multimers, representatives of dominant mouse and human MHC alleles, respectively. From a single standard batch of these MHCI multimers we generated within hours multiple correctly loaded MHCI multimers, just by incubation with selected peptides at a defined temperature. We made many different MHC multimers to detect specific T cell responses in virus-infected mice and to measure T cell kinetics against various viral reactivations in a human transplant recipient. Temperature-exchangeable MHCI multimers will provide simple, fast and convenient tools for epitope discovery and immune monitoring of large sets of potential antigenic peptides.

Results

Identification of MHCI-peptide combinations suitable for temperature exchange
When designing peptides suitable for MHCI temperature exchange the most important criterion is that the MHCI complex loaded with a conditional ligand should be stable at low temperatures, but unstable at higher temperatures for replacement by exogenous peptides (Fig. 1A). The main determinant for MHCI-peptide stability is peptide off-rate[17]. We have selected peptides known to bind to the respective MHCI molecules with low off-rates and substituted their anchor residues to increase their off-rates.

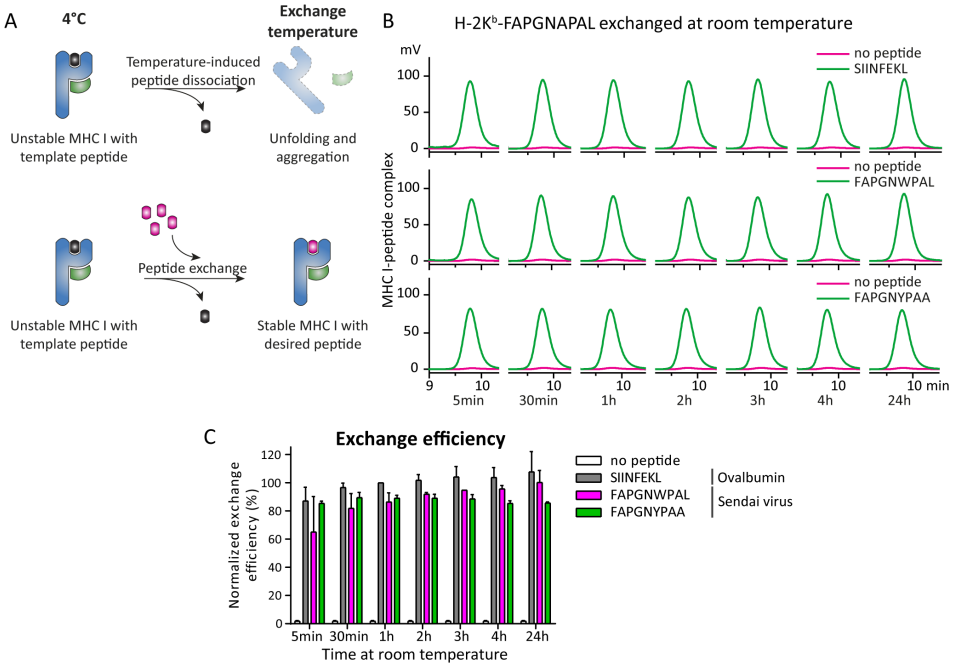

Figure 1. **Temperature-induced peptide exchange allows for the generation of MHCI complexes with high- and low-affinity peptides.** (A) Schematic representation of temperature-induced peptide exchange on MHCI molecules. The thermolabile MHCI-peptide complex is stable at 4°C, but undergoes unfolding and degradation under thermal challenge (upper panel). Addition of a higher affinity peptide stabilizes the MHCI, preventing its degradation (lower panel). (B) Primary data of temperature-induced peptide exchange analyzed by gel filtration chromatography at room temperature. Peptide-MHCI (H-2K^b-FAPGNAPAL) monomers were incubated with indicated peptides at room temperature over a range of time points. The following exchange peptides were used: optimal binder: SIINFEKL (OVA); suboptimal binders: FAPGNWPAL or FAPGNYPAA. One of three representative experiments is shown. (C) The exchange efficiency was calculated from the area under the curve measured by HPLC and normalized to binding of the optimal peptide SIINFEKL for 1 h. Average values ±SD from three independent experiments are shown.

We have previously produced murine H-2K^b complexes with low-affinity peptides derived from Sendai virus epitope FAPGNYPAL ($NP_{324-332}$) and analyzed their stability and kinetics of peptide binding[17]. From the seven peptides tested, only FAPGN**A**PAL (boldface indicates amino acid changes compared to wild-type sequence) fulfilled the criteria required for peptide exchange. The melting temperature of the H-2K^b complex with FAPGN**A**PAL, defined as midpoint of thermal denaturation, is ~33°C (Fig. S1). In line with this, FAPGN**A**PAL swiftly dissociated from and did not rebind to H-2K^b at either of the two elevated temperatures tested (26°C and 32°C)[17]. This indicates that the H-2K^b-FAPGN**A**PAL complex is sufficiently stable to refold at 4°C, but unstable at elevated temperatures and could therefore be a suitable complex for temperature-induced peptide exchange.

In order to translate the exchange technology to human applications, we set out to identify a suitable peptide for HLA-A*02:01, the most frequently occurring human MHCI allele in the Caucasian population. We designed peptides based on the HIV-1 epitope ILKEPVHGV ($RT_{476-484}$) with one (I**A**KEPVHGV or ILKEPVHG**A**) or both anchors (I**A**KEPVHG**A**) modified. HLA-A*02:01 complexes with modified peptides were produced and thermal stability experiments carried out, where tryptophan fluorescence was monitored over a wide temperature range to assess HLA-A*02:01-peptide complex unfolding. Out of four complexes tested,

Table 1. **Relative quantification of exchange efficiency by MS.**

MHCI allele	MHCI monomer folded with	Template peptide exchanged for	Efficiency of exchange (%)
H-2K^b	FAPGNAPAL	SIINFEKL	105.5 ± 4.7
		FAPGNWPAL	94.2 ± 10.8
		FAPGNYPAA	84.4 ± 6.2
		FAPGNAPAL	4.2 ± 0.1
		-	0.1 ± 0.1
	SIINFEKL	-	107.4 ± 12.6
HLA-A*02:01	IAKEPVHGV	NLVPMVATV	101.3 ± 13.2
		LLDQLIEEV	86.0 ± 14.6
		GLCTLVAML	70.7 ± 16.3
		IAKEPVHGV	27.4 ± 2.7
		-	7.2 ± 2.2
	NLVPMVATV	-	80.5 ± 15.3

Peptide exchange on MHCI was performed with 0.5 µM monomers (H-2K^b or HLA-A*02:01), incubated with 50 µM peptide as described in Materials and Methods. Monomers were also incubated in the absence of peptide to determine the stability of the complexes under these conditions. To quantify the amount of eluted peptide, standard curves were created with the respective synthetic peptides. H-2K^b-SIINFEKL and HLA-A*02:01-NLVPMVATV were measured as positive controls.

HLA-A*02:01-I**A**KEPVHGV showed the lowest melting temperature (~38°C) (Fig. S1). This melting temperature is lower than that of the HLA-A*02:01-antigen complexes (which is around 57°C, Fig. S1), providing a temperature window for exchange from the HLA-A*02:01-I**A**KEPVHGV template.

Temperature-labile MHCI-peptide monomers efficiently exchange for a range of peptides

We next evaluated the peptide exchange efficiency of H-2K^b in complex with FAPGN**A**PAL over a temperature range using analytical size exclusion HPLC. We found that the complex itself is unstable at room temperature (20°C), resulting in denaturation and aggregation. This is illustrated by the absence of an MHCI peak when analyzed by size exclusion HPLC (Fig. 1B, in magenta). When incubated in the presence of a high affinity peptide (SIINFEKL, $OVA_{257-264}$) a clear peak was observed, demonstrating that H-2K^b could be ''rescued'' from unfolding (Fig. 1B, upper panel, compare green to magenta). Exchange of FAPGN**A**PAL (K_D>4 μM[17]) for SIINFEKL (K_D=1.4 nM[19]) was almost complete within 30 min. The efficiency increased only by 15% after 24 h (Fig. 1B, upper panel; and quantification in 1C, grey bar).

Similarly, HLA-A*02:01 in complex with either of four peptides based on ILKEPVHGV were tested for exchange with a high affinity binding peptide (vaccinia virus (VACV) $B19R_{297-305}$, K_D=0.06 nM[20]) at different temperatures and time points. HLA-A*02:01 in complex with ILKEPVHGV or ILKEPVHG**A** remained stable at room temperature. Even at elevated temperatures intact HLA-A*02:01 could be detected (in magenta, 37 or 42°C, Fig. S2, A and B). Considering their high melting temperatures (~57 and 47°C, respectively, Fig. S1) and dissociation constants (ILKEPVHGV - K_D=2.5 nM[21]; ILKEPVHG**A** - K_D=1.1 μM, predicted with NetMHC[22,23]), ILKEPVHGV and ILKEPVHG**A** fail as input peptides in the exchange reaction.

We continued the search for optimal peptides binding to HLA-A*02:01 allowing efficient temperature-induced exchange. Complexes of HLA-A*02:01 with I**A**KEPVHGV (K_D=7.3 μM predicted with NetMHC[22,23]) or I**A**KEPVHG**A** (K_D=19.1 μM predicted with NetMHC[22,23]) were considerably less stable, even at room temperature (Fig. S2, C and D). As a result of higher stability, the refolding efficiency of HLA-A*02:01-I**A**KEPVHGV (at 4°C) was substantially higher than that of HLA-A*02:01-I**A**KEPVHG**A** (Fig. S2), as was maximum rescue with exogenous peptide WLIGFDFDV (Fig. S2, C and D, compare green to magenta). HLA-A*02:01-I**A**KEPVHGV was efficiently exchanged at two temperatures: at 37°C for 1 h or at 32°C for 3 h (Fig. S2C, compare green to magenta). We selected HLA-A*02:01-I**A**KEPVHGV as the best candidate complex for peptide exchange applications, despite its higher temperature required for optimal exchange. In conclusion, we have identified two MHCI-peptide pairs allowing efficient temperature-induced exchange reactions.

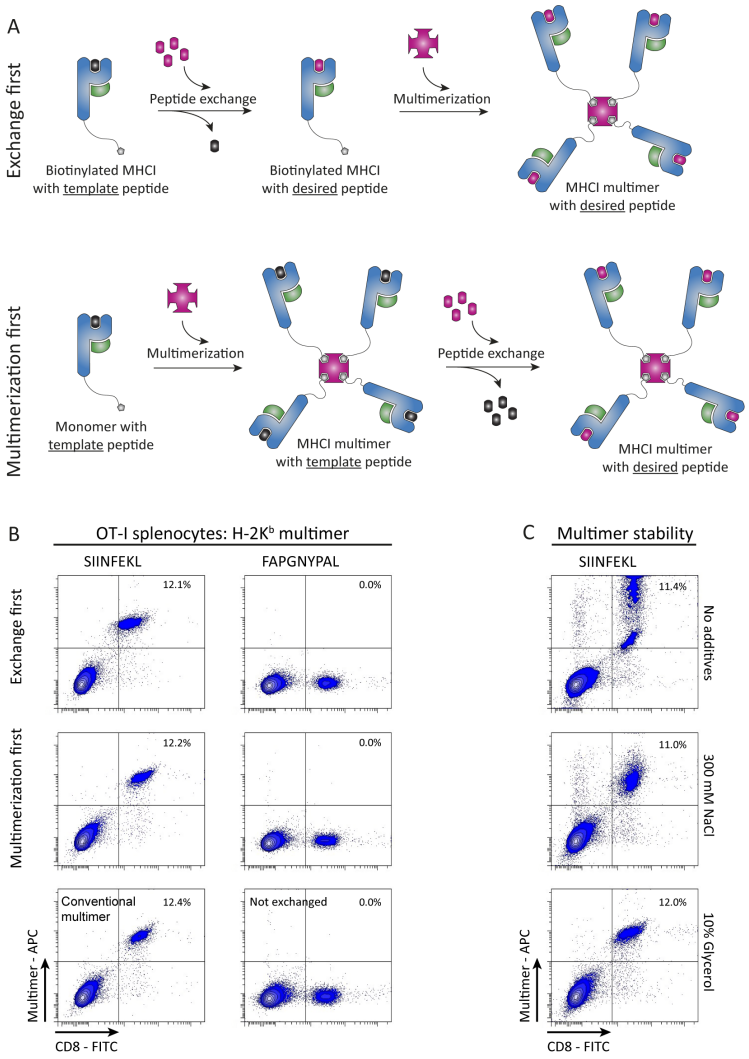

Figure 2. **Temperature-exchanged H-2K^b multimers efficiently stain antigen-specific CD8$^+$ T cells.** (A) Schematic representation of MHCI peptide exchange on monomers (Exchange first, upper panel) or on multimers (Multimerization first, lower panel). (B) Dot plots of pMHCI multimer staining of splenocytes from OT-I mice analyzed by flow cytometry. Multimers were prepared after or before exchanging the template peptide for either a relevant peptide (SIINFEKL, OVA, left column) or an irrelevant peptide (FAPGNYPAL, Sendai virus, right column) for 30 min at room temperature. Control multimers were prepared using conventional refolding followed by multimerization. One of three representative experiments is shown. (C) Thermolabile multimers of H-2K^b-FAPGNAPAL are stable over time when stored at -80°C in the presence of 300 mM NaCl or 10% glycerol. H-2K^b-FAPGNAPAL multimers were thawed and FAPGNAPAL was exchanged for SIINFEKL prior to staining OT-I splenocytes (performed once). Multimer$^+$ CD8$^+$ T cells are depicted as percentage of total live single cells. The gating strategy is described in detail in Figure S4A.

When used for broad applications in immunology, MHCI multimers should exchange their peptides for numerous different peptides, including those with a relatively low affinity, including many tumor neoantigens[24]. To test this, we exchanged H-2K^b-FAPGN**A**PAL for either FAPGN**W**PAL (K_D=33 nM at 26°C and K_D=33 nM at 32°C[17]) or FAPGNYPA**A** (K_D=18 nM at 26°C and K_D=144 nM at 32°C[17]). For both suboptimal peptides, the exchange efficiency reached 80-90% of the level observed for SIINFEKL (Fig. 1B, quantified in C), as further confirmed by mass spectrometry analysis (Table 1). After exchange the conditional peptide FAPGNAPAL could not be detected, which demonstrates that all MHCI-peptide complexes contained the exogenous peptide.

Detection of antigen-specific CD8$^+$ T cells using ready-to-use temperature-exchanged MHCI multimers

The technology of peptide exchange would be more attractive if it could be applied directly on ready-made MHCI multimers, a severe limitation of current parallel exchange technologies. In current exchange technologies monomers are first exchanged and then multimerized (Fig. 2A, upper panel), but the method described here can be applied directly to multimers (Fig. 2A, lower panel). To test this, we incubated H-2K^b-FAPGNAPAL multimers, stored batch-wise at -80°C, at room temperature either with or without 50 µM SIINFEKL peptide. After 5 min following incubation the multimers were used to stain SIINFEKL-specific OT-I T cells. Multimers prepared by temperature exchange performed indistinguishably from conventional multimers. No positive staining was observed when multimers were not exchanged or exchanged for an irrelevant peptide (FAPGNYPAL, Fig. 2B). When assessing multimer stability upon freezing, we found that multimers alone suffered from freeze-thaw cycles, but addition of 300 mM NaCl or 10% glycerol before freezing, as published before[25], ensured stability during freeze-thaw cycles (Fig. 2C). We conclude that temperature-mediated peptide exchange can be used to produce MHC multimers with antigenic peptides from temperature-exchangeable multimer stocks within minutes. This represents a significant advantage by taking away any time-consuming preparation preceding multimer staining experiments.

The immune responses to lymphocytic choriomeningitis virus (LCMV) and murine cytomegalovirus (MCMV) infections in C57BL/6 mice have been extensively characterized and we used these infections as a model to illustrate the quality of our temperature-exchanged multimers in the detection of antigen-specific CD8$^+$ T cells[26-29]. We measured the CD8$^+$ T cell responses to the following immunodominant epitopes: LCMV epitope NP238-K^b/SGYNFSLGAAV and MCMV epitopes M38-K^b/SSPPMFRV and IE3-K^b/RALEYKNL (Table S1). We first validated exchange on H-2K^b monomers by HPLC. As for SIINFEKL, all three peptides could be loaded with high efficiency within 5 min at room temperature and produced

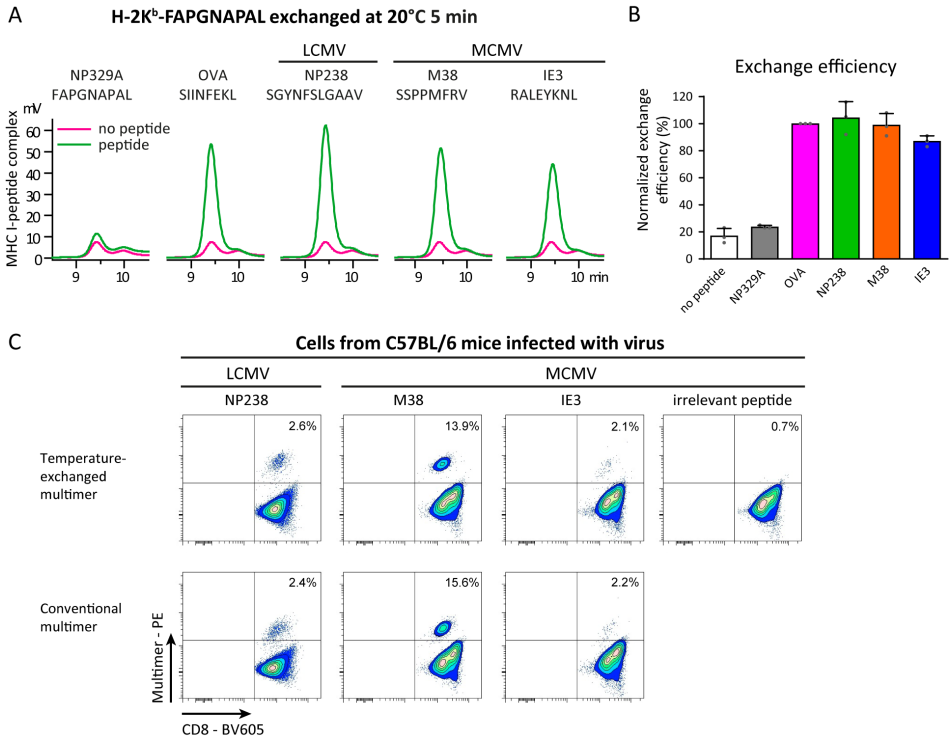

Figure 3. **Temperature-exchanged H-2K^b multimers are suitable for staining antigen-specific T cells from virus-infected mice.** H-2K^b-FAPGNAPAL monomers (A-B) or multimers (C) were exchanged for FAPGNAPAL (Sendai virus), SIINFEKL (OVA), SGYNFSLGAAV (LCMV NP238), SSPPMFRV (MCMV M38) or RALEYKNL (MCMV IE3) for 5 min at 20°C. (A) Primary data of temperature-induced peptide exchange on H-2K^b monomers analyzed by analytical gel filtration chromatography at room temperature. One of three representative experiments is shown. (B) Exchange efficiency calculated from the area under the curve from HPLC chromatograms normalized to the binding of optimal peptide (SIINFEKL). Average values ±SD from three independent experiments (single data points depicted as grey dots) are shown. (C) H-2K^b-FAPGNAPAL multimers were exchanged for the indicated peptides and subsequently used to stain corresponding CD8$^+$ T cells in PBMCs of an LCMV-infected mouse or splenocytes from an MCMV-infected mouse. Percentages of CD8$^+$ T cells detected by flow cytometry were comparable between temperature-exchanged multimers and conventional multimers. Irrelevant peptide: FAPGNYPAL (Sendai virus). One of two representative experiments is shown. Multimer$^+$ CD8$^+$ T cells are indicated as percentage of total CD8$^+$ cells. Cells were gated as described in Figure S4B.

stable H-2K^b complexes, which was not observed for exchange reactions without peptide or with an excess of high off-rate template peptide FAPGNAPAL (Fig. 3A, quantified in B). Subsequently, we again replaced the poorly H-2K^b-binding peptide FAPGNAPAL for these three viral epitopes on H-2K^b multimers and used these multimers, all generated from stocks stored at -80°C as described above,

to stain blood samples from LCMV-infected mice or splenocytes from MCMV-infected mice. Within 5 min after taking the multimers with temperature-sensitive peptides from the freezer, the antigenic peptide-loaded multimers were ready and stained antigen-specific $CD8^+$ T cells as efficiently as conventional multimers (Fig. 3C), demonstrating the easy and broad use of temperature exchange technology.

Likewise, HLA-A*02:01-IAKEPVHGV monomers could be readily exchanged for selected viral epitopes (HCMV pp65-A2/NLVPMVATV, HCMV IE-1-A2/VLEETSVML, EBV LMP2-A2/CLGGLLTMV, EBV BMLF-1-A2/GLCTLVAML, EBV BRLF1-A2/YVLDHLIVV and human adenovirus (HAdV) E1A-A2/LLDQLIEEV, details in Table S1), when incubated at 32°C for 3 h or 37°C for 45 min (Fig. 4 and Fig. S3). HPLC analysis revealed no MHCI peak following incubation at 32°C without peptide, indicating unfolding and precipitation of MHCI monomers (Fig. 4A, magenta). However, incubation with peptide at 32°C for 3 h revealed a peak of MHCI monomers as high as the original input complexes for all peptides (Fig. 4A, quantified in B). Incubation at 37°C for 45 min likewise resulted in efficient rescue, with the exception of EBV BMLF-1-A2/GLC (Fig. S3). Considering the relatively low predicted affinity of this epitope (K_D=138.63 nM predicted with NetMHC[22,23]), EBV BMLF-1-A2/GLC may not stabilize HLA-A2*02:01 sufficiently at elevated temperatures during a prolonged period of time. We selected 3 h incubation with exogenous peptides at 32°C as optimal exchange condition for HLA-A*02:01. Mass spectrometry analysis showed that HLA-A*02:01-IAKEPVHGV monomers exchanged for NLVPMVATV, LLDQLIEEV, GLCTLVAML or template peptide IAKEPVHGV contained only the desired peptides. The rescue of the MHCI monomers was proportional to the predicted affinity of the peptides, as observed in the HPLC quantifications (Table 1 and Fig. 4B).

Within 3 h after addition of peptide to the preformed conditional HLA-A*02:01 multimers they were ready for staining of $CD8^+$ T cell clones with corresponding specificities. Detected percentages of multimer-positive $CD8^+$ T cells corresponded to those detected using either conventional or UV-exchanged multimers, confirming their proper function. No staining was observed with multimers exchanged for irrelevant peptides (Fig. 4C).

Exchanged MHCI-peptide multimers are effective reagents for immune monitoring

To demonstrate a direct application of our reagents in clinical practice, we compared our temperature-exchanged multimers with conventional multimers in an immune monitoring setting. Because patients are heavily immunocompromised after T cell-depleted allogeneic stem cell transplantation (allo-SCT), T cell reconstitution is critical to prevent morbidity and mortality caused by post-transplant infections with herpesviruses like HCMV and EBV[2,3]. Therefore, patients are intensively monitored until the donor-derived immune system has developed.

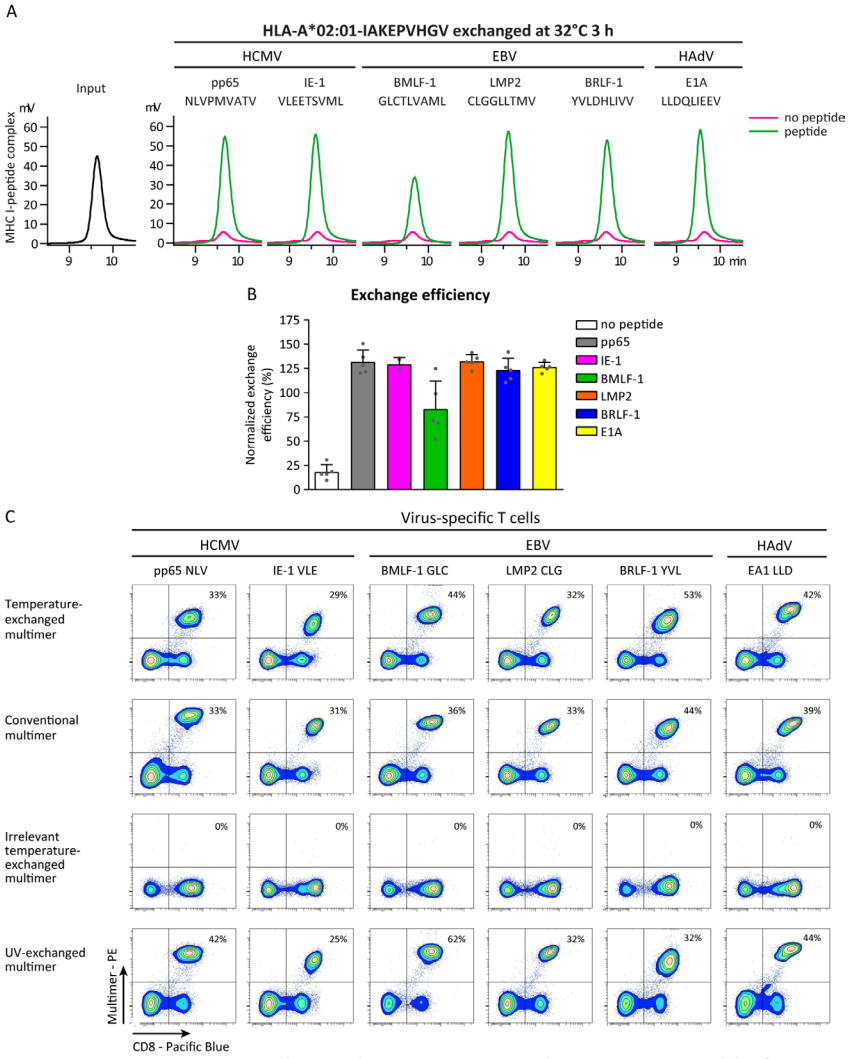

Figure 4. **Temperature-exchanged HLA-A*02:01 multimers are suitable for staining virus-specific T cells. (A-C)** HLA-A*02:01-IAKEPVHGV monomers (A-B) or multimers (C) were exchanged for HCMV pp65-A2/NLVPMVATV, HCMV IE-1-A2/VLEETSVML, EBV BMLF-1-A2/GLCTLVAML, EBV LMP2-A2/CLGGLLTMV, EBV BRLF-1-A2/YVLDHLIVV or HAdV E1A-A2/LLDQLIEEV) for 3 h at 32°C. (A) Representative chromatograms of exchange on monomers analyzed by gel filtration chromatography at room temperature. (B) Efficiency of exchange calculated from the area under the curve from HPLC chromatograms normalized to input peptide-MHCI. Average values ±SD from five independent experiments are shown. Single data points are depicted as grey dots. (C) HLA-A*02:01-IAKEPVHGV multimers were exchanged for the indicated peptides and subsequently used for staining of specific $CD8^+$ T cell clones or cell lines. Detected percentages of multimer-positive $CD8^+$ T cells were comparable between temperature-exchanged multimers and conventional multimers. One of two representative flow cytometry experiments is shown. $Multimer^+$ $CD8^+$ T cells are indicated as percentage of total $CD8^+$ cells. Cells were gated as described in Figure S4C.

Ready-to-use multimers are valuable immune monitoring reagents that allow prompt action as needed in these cases.

We exchanged PE-labeled HLA-A*02:01-IAKEPVHGV multimers (stored at -80°C and exchanged following the conditions as described above) for a selection of HCMV- and EBV-derived epitopes in parallel and used these to monitor T cell frequencies in peripheral blood mononuclear cells (PBMCs) obtained at weekly intervals after allo-SCT. The kinetics of $CD8^+$ T cells specific for HCMV pp65-A2/NLV are in concordance with the HCMV reactivation illustrated by the expansion of HCMV viral DNA detected in blood (Fig. 5, upper panel). Although a positive EBV DNA load was measured only once, $CD8^+$ T cells specific for EBV LMP2-A2/CLG and to a lesser extent those specific for EBV BMLF-1-A2/GLC expanded over time (Fig. 5, lower panel). No significant responses were detected against HCMV IE-1-A2/VLE (Fig. 5, upper panel) or EBV BRLF1-A2/YVL (Fig. 5, lower panel). Frequencies of specific T cells were comparable between conventional and temperature-exchanged multimers. This illustrates the efficiency and flexibility of our technology to rapidly produce many different MHCI multimers ad hoc from a stored and ready-to-use stock for the detection of antigen-specific T cells, even at the low frequencies typically found in primary immune monitoring samples.

5

Discussion

We describe a reliable approach that allows the parallel generation of large sets of different MHCI multimers. Our approach can be applied in all laboratories, since it requires only a freezer for storage of exchangeable multimer stocks and a thermoblock, water bath or PCR machine for incubation at the optimal temperature for exchange. This system is faster and less laborious than the generation of multimers from single MHCI-peptide combinations, either made by producing individual complexes by refolding and purification or by cleaving an MHC-embedded peptide for chemically-triggered or UV-mediated peptide exchange[7-10]. Our approach allows fast and near quantitative peptide exchange on multimers, whereas parallel multimer generation using UV-mediated exchange is variable due to uneven evaporation across and between sample plates and cannot be performed on preformed MHCI multimers due to fluorophore bleaching. We have established a method where ready-made temperature-sensitive MHCI multimers can be stored at -80°C and while thawing can ad hoc be incubated with peptides of choice to allow peptide exchange within 5-180 minutes, depending on the MHCI allele. This is the most robust technique for multimer production developed to date, that will facilitate immune monitoring and discovery of new (neo)antigens. We anticipate that rapid, robust, and inexpensive detection of MHC-antigen-specific T cells will have a strong impact

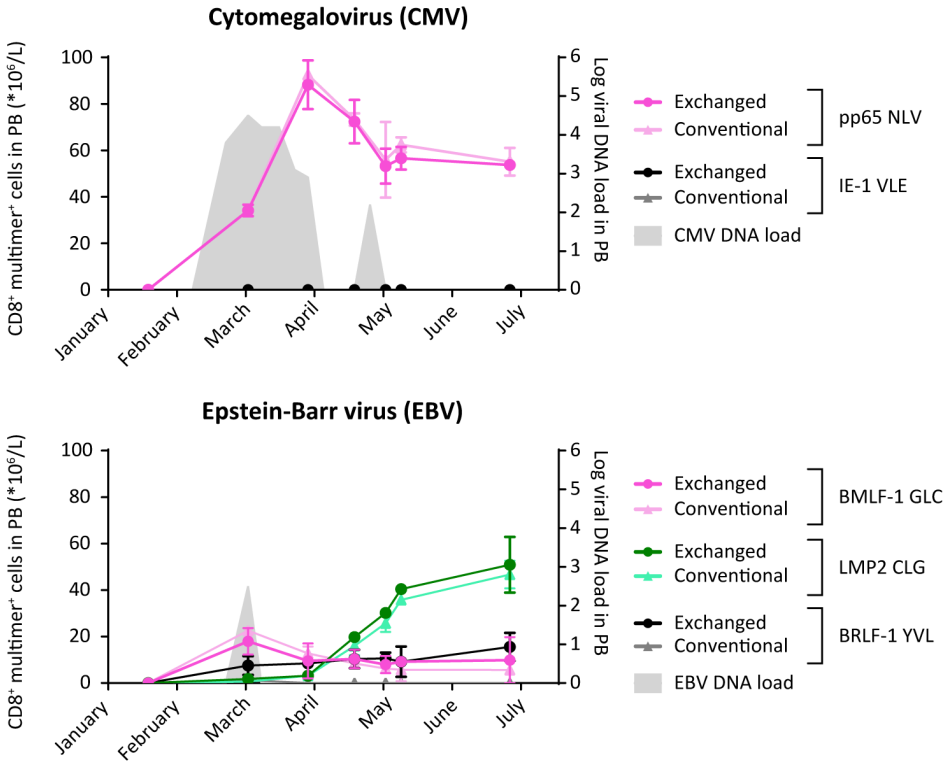

Figure 5. **Temperature-exchanged HLA-A*02:01 multimers can be used for monitoring of HCMV- and EBV-specific CD8+ T cells in peripheral blood of an allogeneic stem cell transplant recipient.** Peripheral blood (PB) samples taken after allogeneic stem cell transplantation were analyzed for virus-specific CD8+ T cells in relation to viral DNA loads (grey). The frequency of HCMV- and EBV-specific T cells within the CD8+ T cell populations was determined using temperature-exchanged (dark colors) and conventional (light colors) MHCI multimer staining analyzed by flow cytometry. Average values ±SD from two experiments performed on the same day are shown.

on the immune monitoring of responses to infection, cancer immunotherapies as well as vaccines[15,30-32]. Immunotherapy, aimed at either suppressing or enhancing cellular immune responses, has advanced greatly over the last decade. Several immune checkpoint inhibitors, including antibodies against CTLA-4 and PD-1/PD-L1, have been approved for use in the clinic and have shown remarkable responses in the treatment of various cancers, including melanoma, non-small-cell lung cancer and renal-cell cancer[33-37]. As a consequence of checkpoint blockade, T cell responses elicited against neoantigens are markedly increased, leading to improved killing of cancer cells[38,39]. A combination of therapies directed at immune checkpoints and the information in the cancer mutanome holds great promise in personalized cancer treatment. Identifying T cell responses against neoantigens and other cancer-specific epitopes will contribute to the success of

immunotherapy, especially when combined with vaccination.

We have shown for two MHCI alleles, one murine and one human, that temperature-exchanged multimers can be as efficient as conventional- or UV-exchanged multimers to stain specific $CD8^+$ T cells, including those present at low frequencies. We have demonstrated for both the H-$2K^b$-FAPGNAPAL and HLA-A*02:01-IAKEPVHGV combinations that the temperature-labile input peptide may be exchanged for both high- and low-affinity peptides, illustrating the application for a broad array of T cell specificities (Fig. 1, B and C; Fig. 3; Fig. 4; and Table S1). These MHCI multimers loaded with desired peptides are highly specific, as no difference in background stain as compared to conventional or UV-exchanged multimers was observed (Fig. 2, Fig. 3 and Fig. 4). Their use in monitoring viral reactivation in an allo-SCT recipient illustrates the flexibility of temperature-exchangeable MHCI multimers that can be produced within hours, as required for clinical use (Fig. 5).

We previously showed that MHCI-peptide complexes at a given temperature undergo a conformational change, which results in full peptide dissociation[17]. Below this temperature, the complexes are fairly stable and due to a high off-rate allow exchange for a more stable low off-rate peptide. We designed peptides to form stable complexes with MHCI at low temperatures that can be released at elevated temperatures. The selection of optimal peptides allowing low temperature exchange and full replacement by exogenous peptides, is not obvious. A number of options include peptides with suboptimal length, smaller anchor residues and altered N- or C- termini[17]. Even then, many peptide sequences have to be tested to identify the optimal MHCI-peptide combination, as we describe here for the most frequently used mouse and human MHCI alleles. The design of peptides suitable for temperature exchange on HLA-A*02:01 proved more challenging than H-$2K^b$, possibly because of the intrinsically higher stability of human MHCI complexes compared to murine MHCI. Yet, expanding this principle to the many other MHCI alleles could provide a standard procedure where viral or tumor antigens are sequenced, the fragments that may bind are predicted and synthesized within a day, and loaded on the ready-to-use MHCI multimers (as stored in the -80°C freezer). Within two days a patient's T cell responses could then be monitored, as the production of the MHCI multimers loaded with the correct peptides is no longer the time limiting factor.

In conclusion, we present a fast, easy and reproducible method for the generation of ready-to-use MHCI multimers loaded with epitopes at wish. This approach will render MHC multimer technology accessible to any research or clinical chemistry laboratory.

Materials and methods

Peptide synthesis and purification

Peptides were synthesized in our lab by standard solid-phase peptide synthesis in *N*-methyl-2-pyrrolidone using Syro I and Syro II synthesizers. Amino acids and resins were used as purchased from Nova Biochem. Peptides were purified by reversed-phase HPLC using a Waters HPLC system equipped with a preparative Waters X-bridge C18 column. The mobile phase consisted of water/acetonitrile mixtures containing 0.1% TFA. Peptide purity and composition were confirmed by LC-MS using a Waters Micromass LCT Premier mass spectrometer equipped with a 2795 separation module (Alliance HT) and 2996 photodiode array detector (Waters Chromatography B.V.). LC-MS samples were run over a Kinetex C18 column (Phenomenex, United States, CA) in a water/acetonitrile gradient. Analysis was performed using MassLynx 4.1 software (Waters Chromatography). Peptides were purified twice if necessary.

Protein expression and purification

MHC class I (MHCI) complexes were expressed and refolded according to previously published protocols[40]. Refolded complexes of H-2K^b were purified twice using anion exchange (0 to 1 M NaCl in 20 mM Tris•Cl pH 8; Resource Q column) and size exclusion chromatography (150 mM NaCl, 20 mM Tris•Cl pH 8; Superdex 75 16/600 column) on an ÄKTA (GE Healthcare Life Sciences) or NGC system (Bio-Rad). We discovered that recovery was considerably lower when purifying using anion exchange and size exclusion chromatography, as compared to using size exclusion only, possibly caused by strong interaction between peptide and ion-exchange resin. Therefore, to maximize purification yields, refolded complexes of HLA-A*02:01 were purified using only size exclusion chromatography (300 mM NaCl, 20 mM Tris•Cl pH 8). Purified properly folded complexes were concentrated using Amicon Ultra-15 30 kDa MWCO centrifugal filter units (Merck Millipore), directly biotinylated using BirA ligase where needed, purified again using size exclusion chromatography and stored in 300 mM NaCl, 20 mM Tris•Cl pH 8 with 15% glycerol at -80°C until further use.

Protein unfolding

Thermal unfolding of different H-2K^b- and HLA-A*02:01-peptide complexes was determined using an Optim 1000 (Avacta Analytical Ltd) machine. MHCI-peptide complexes were measured in 150 mM NaCl, 20 mM Tris•Cl pH 7.5 or phosphate-buffered saline (PBS) at a protein concentration of 0.2 mg/ml. Samples were heated using a 1°C step gradient with 30 s temperature stabilization for each step. Unfolding was followed by measuring tryptophan fluorescence emission at a range from 300 to 400 nm following excitation at 266 nm. Barycentric

fluorescence was determined according to the equation:

$$BCM\lambda = (\sum I[\lambda] \times \lambda) / (\sum I[\lambda])$$

where BCMλ is the Barycentric mean fluorescence in nm, I[λ] is the fluorescence intensity at a given wavelength, and λ is the wavelength in nm.

The melting temperature (T_m) was calculated using Barycentric fluorescence as a function of temperature according to the equation:

$$T_m = max \frac{dBCM}{dt}(T)$$

where max is the local maximum and $\frac{dBCM}{dt}(T)$ is the first derivative of Barycentric fluorescence as a function of temperature in $[\frac{nm}{°C}]$.

Analysis was performed with Optim Analysis Software v 2.0 (Avacta Analytical Ltd).

Multimerization of MHCI monomers

MHCI monomers were complexed with allophycocyanin (APC)- or phycoerythrin (PE)-labeled streptavidin to form multimers for T cell analysis. Typically, temperature-labile peptide-MHCI complexes were multimerized on ice by stepwise addition of fluorochrome-labeled streptavidin with one minute intervals. Full biotinylation was verified by HPLC. Aliquots of multimers were snap frozen in 150 mM NaCl, 20 mM Tris•Cl pH 7.5 containing 15% glycerol.

HPLC analysis of temperature-mediated peptide exchange

To initiate peptide exchange 0.5 µM MHCI-peptide complex was incubated with 50 µM exchange peptide in 110 µl PBS under defined exchange conditions. After incubation exchange solutions were centrifuged at 14,000 × *g* for 1 min at RT and subsequently the supernatant was analyzed by gel filtration on a Shimadzu Prominence HPLC system equipped with a 300 × 7.8 mm BioSep SEC-s3000 column (Phenomenex) using PBS as mobile phase. Data were processed and analyzed using Shimadzu LabSolutions software (version 5.85).

Relative exchange efficiency determined by mass spectrometry

In order to quantify peptide exchange on H-2K^b, 0.5 µM H-2K^b monomers (H-2K^b–FAPGNAPAL) were incubated with 50 µM peptide (SIINFEKL, FAPGNWPAL, FAPGNYPAA or FAPGNAPAL) in PBS for 45 min at room temperature. For quantification of peptide exchange on HLA-A*02:01, 0.5 µM HLA-A*02:01 monomers were incubated with 50 µM of peptide in PBS for 3 hours at 32°C.

Before analysis, exchanged monomers were spun at 14,000 × *g* for 1 min at room temperature to remove aggregates and subsequently purified using a Microcon-30 kDa Centrifugal Filter Unit with Ultracel-30 membrane (Merck Millipore, pre-incubated with tryptic BSA digest to prevent stickiness of the peptides to the membrane) to remove unbound excess peptide. After washing twice with PBS and twice with ammonium bicarbonate at room temperature, MHC-bound peptides were eluted by the addition of 200 µl 10% acetic acid followed by mixing at 600 rpm for 1 min at room temperature. Eluted peptides were separated using a Microcon-30 kDa Centrifugal Filter Unit with Ultracel-30 membranes. Eluates were lyophilized and subjected to mass spectrometry (MS) analysis.

For MS analysis, peptides were dissolved in 95/3/0.1 v/v/v water/acetonitrile/formic acid and subsequently analyzed by on-line nanoHPLC MS/MS using an 1100 HPLC system (Agilent Technologies), as described previously[41]. Peptides were trapped at 10 µl/min on a 15-mm column (100-µm ID; ReproSil-Pur C18-AQ, 3 µm, Dr. Maisch GmbH) and eluted to a 200 mm column (50-µm ID; ReproSil-Pur C18-AQ, 3 µm) at 150 nl/min. All columns were packed in house. The column was developed with a 30-min gradient from 0 to 50% acetonitrile in 0.1% formic acid. The end of the nanoLC column was drawn to a tip (5-µm ID), from which the eluent was sprayed into a 7-tesla LTQ-FT Ultra mass spectrometer (Thermo Electron). The mass spectrometer was operated in data-dependent mode, automatically switching between MS and MS/MS acquisition. Full scan MS spectra were acquired in the Fourier-transform ion cyclotron resonance (FT-ICR) with a resolution of 25,000 at a target value of 3,000,000. The two most intense ions were then isolated for accurate mass measurements by a selected ion-monitoring scan in FT-ICR with a resolution of 50,000 at a target accumulation value of 50,000. Selected ions were fragmented in the linear ion trap using collision-induced dissociation at a target value of 10,000. To quantify the amount of eluted peptide standard curves were created with the respective synthetic peptides.

Mice

Wild-type C57BL/6 mice (Charles River) were maintained at the Central Animal Facility of the Leiden University Medical Center (LUMC) under specific pathogen-free conditions. Mice were infected intraperitoneally with 5×10^4 PFU murine cytomegalovirus (MCMV)-Smith (American Type Culture Collection VR-194; Manassas, VA), derived from salivary gland stocks from MCMV-infected BALB/c mice, or with 2×10^5 PFU lymphocytic choriomeningitis virus (LCMV) Armstrong propagated on baby hamster kidney cells. Virus titers were determined by plaque assays as published[42]. All animal experiments were performed with approval of the Animal Experiments Committee of the LUMC and according to the Dutch

Experiments on Animals Act that serves the implementation of 'Guidelines on the protection of experimental animals' by the Council of Europe and the guide to animal experimentation set by the LUMC.

Collection of primary human material

Peripheral blood samples were obtained from a HLA-A*02:01-positive multiple myeloma patient after T cell-depleted allogeneic stem cell transplantation (allo-SCT), after approval by the LUMC and written informed consent according to the Declaration of Helsinki. To monitor viral reactivation Epstein-Barr virus (EBV) and human cytomegalovirus (HCMV) DNA loads on fresh whole blood were assessed by quantitative polymerase chain reaction (qPCR). Peripheral blood mononuclear cells (PBMCs) were collected using Ficoll Isopaque separation (LUMC Pharmacy, Leiden, The Netherlands) and cryopreserved in the vapor phase of liquid nitrogen. Virus-specific $CD8^+$ T cell reconstitution was determined on thawed PBMCs by flow cytometry.

Antibodies and reagents

Ficoll Isopaque was obtained from the LUMC Pharmacy (Leiden, The Netherlands). Fluorochrome-conjugated antibodies were purchased from several suppliers. V500 anti-mouse CD3, FITC anti-mouse CD8, FITC anti-human CD4, Pacific Blue anti-human CD8, APC anti-human CD14 were purchased from Becton Dickinson (BD) Biosciences. BV605 anti-mouse CD8 was purchased from BioLegend. Fluorochrome-conjugated streptavidin and 7-AAD were purchased from Invitrogen. DAPI was purchased from Sigma. Conventional HLA-A*02:01 PE-labeled tetramers were produced as described previously for all indicated T cell specificities[4]. Human interleukin-2 (IL-2) was purchased from Chiron (Amsterdam, The Netherlands). Human serum albumin was purchased from Sanquin Reagents (Amsterdam, The Netherlands).

Flow cytometry analysis of murine $CD8^+$ T cells

H-$2K^b$-FAPGNAPAL multimers were exchanged for selected peptides for 5 min at RT and subsequently used for staining of the H-$2K^b$-restricted $OVA_{257-264}$-specific TCR transgenic line (OT-I), described previously[43]. Generally, 200,000 cells were stained first with APC- or PE-labeled temperature-exchanged or conventional multimers for 10 min at RT and then with surface marker antibodies (anti-CD8-FITC) at 4°C for 20 min. Cells were washed twice with and then resuspended in FACS buffer (0.5% BSA and 0.02% sodium azide in PBS). DAPI was added at a final concentration of 0.1 µg/ml. Samples were measured using a BD FACSAria Fusion flow cytometer and data were analyzed with BD FACSDiva software (version 8.0.2, gating strategy in Fig. S4).

Virus-specific T cells were analyzed in blood samples of LCMV-infected mice

after erythrocyte lysis or splenocytes obtained from MCMV-infected, 8-10 weeks old mice (infected at 6-8 weeks). Erythrocytes were lysed using a hypotonic ammonium chloride buffer (150 mM NH_4Cl, 10 mM $KHCO_3$; pH 7.2 ± 0.2). Cells were simultaneously stained with appropriate temperature-exchanged multimers and surface markers (7-AAD, anti-CD3-V500, anti-CD8-BV605) for 30 min at 4°C. Multimers were titrated to establish optimal T cell staining. Generally, a dilution of 1:20-1:40 was sufficient to stain 10,000-100,000 T cells in 50 µl FACS buffer. Cells were washed twice with and resuspended in FACS buffer. Sample data were acquired using a BD Fortessa flow cytometer and analyzed using BD FACSDiva software (version 8.0.2, gating strategy in Fig. S4).

Flow cytometry analysis of human CD8⁺ T cells

Multimers of HLA-A*02:01-IAKEPVHGV were exchanged for selected peptides at 32°C for 3 h and used to stain corresponding $CD8^+$ T cells. UV-exchanged multimers were produced and exchanged following published protocols[10,11]. Clones or cell lines of the indicated viral T cell specificities (cultured in Iscove's Modified Dulbecco's Medium (IMDM) supplemented with 10% human serum and 100 IU/ml IL-2) were mixed with PBMCs of a HLA-A*02:01-negative donor to be able to discriminate multimer-positive from multimer-negative cells. Following incubation with PE-labeled temperature-exchanged, conventional or UV-exchanged multimers for 10 min at 4°C, cells were stained with surface marker antibodies (anti-CD8-Pacific Blue and anti-CD14-APC) for 20 min at 4°C. Multimers were titrated to establish optimal T cell staining without background. Cells were washed twice with and resuspended in FACS buffer (0.5% human serum albumin in PBS). Samples were acquired using a BD FACSCanto II flow cytometer and analysis was performed with BD FACSDiva software (version 8.0.2, gating strategy in Fig. S4). Absolute numbers of multimer positive $CD8^+$ T cells were calculated based on the percentage of multimer positive cells within the $CD8^+$ T cell population and the concentration of $CD8^+$ T cells in whole blood.

Online supplemental material

Figure S1. Thermal denaturation of selected MHCI-peptide complexes analyzed to determine melting temperatures.
Figure S2. Temperature stability of HLA-A*02:01 in complex with peptides of the ILKEKVHGV series, investigated using analytical gel filtration chromatography.
Figure S3. Exchange of HLA-A*02:01-IAKEPVHGV at 37°C for 45 minutes is efficient for high-affinity peptides, but not for low-affinity peptides.
Figure S4. Gating strategies used in flow cytometry experiments.
Table S1. List of all peptides and K_Ds mentioned in this article.

Acknowledgements

We thank Dris el Atmioui and Cami Talavera Ormeño (Department of Chemical Immunology, Leiden University Medical Center (LUMC), Leiden, The Netherlands) for synthesis of peptides. We are grateful to Mireille Toebes (Department of Immunology, Netherlands Cancer Institute (NKI), Amsterdam, The Netherlands) and Inge Jedema (Department of Hematology, LUMC, Leiden, The Netherlands) for discussions and support, Alexander Fish (Department of Biochemistry, NKI, Amsterdam, The Netherlands) for assistance with protein unfolding measurements and Martijn van Baalen (Flow Cytometry Facility, NKI, Amsterdam, The Netherlands) for assistance with initial flow cytometry measurements. We would also like to thank Kees L.M.C. Franken (Department of Infectious Diseases, LUMC, Leiden, The Netherlands), Michel GD Kester and Lois Hageman (Department of Hematology, LUMC, Leiden, The Netherlands) for supplying conventional multimers. We thank Sebastian Springer (Jacobs University Bremen, Germany), Pengbo Zhang and Ke Li (Second Affiliated Hospital of Xi'an Jiaotong University, Xi'an, China) for reading the manuscript.

This work was supported by a grant from the Institute for Chemical Immunology (ICI, to H. Ovaa) and grants from the Second Affiliated Hospital of Xi'an Jiaotong University and Xi'an Jiaotong University (number 1191329726 to M.A. Garstka). This work is part of Oncode Institute, which is partly financed by the Dutch Cancer Society.

J.J. Luimstra, M.A. Garstka, J. Neefjes and H. Ovaa have filed a patent application for the temperature-mediated peptide exchange technology. The remaining authors declare no competing financial interests.

Author contributions: J.J.L., M.A.G., J.N. and H.O., conceived and designed the study. J.J.L. and M.A.G. designed peptides, produced peptide-MHCI complexes and performed HPLC analyses. M.A.G. performed protein unfolding measurements. G.M.C.J. and P.A.V performed peptide elutions and subsequent mass spectrometric analyses. J.J.L. and A.R. conducted murine T cell staining experiments with guidance from R.A. J.J.L. and M.C.J.R. performed T cell staining experiments on human T cell lines and clones and patient samples with guidance from J.H.F.F. J.J.L. and M.A.G. wrote the manuscript with input from all authors.

References

1. Grinde, B. Herpesviruses: latency and reactivation - viral strategies and host response. *J Oral Microbiol* **5**(2013).
2. Broers, A.E., *et al.* Increased transplant-related morbidity and mortality in CMV-seropositive patients despite highly effective prevention of CMV disease after allogeneic T-cell-depleted stem cell transplantation. *Blood* **95**, 2240-2245 (2000).
3. Green, M.L., *et al.* Cytomegalovirus viral load and mortality after haemopoietic stem cell transplantation in the era of pre-emptive therapy: a retrospective cohort study. *Lancet Haematol* **3**, e119-127 (2016).
4. Altman, J.D., *et al.* Phenotypic analysis of antigen-specific T lymphocytes. *Science* **274**, 94-96 (1996).
5. Ljunggren, H.G., *et al.* Empty MHC class I molecules come out in the cold. *Nature* **346**, 476-480 (1990).
6. Saini, S.K., *et al.* Dipeptides catalyze rapid peptide exchange on MHC class I molecules. *Proc Natl Acad Sci U S A* **112**, 202-207 (2015).
7. Amore, A., *et al.* Development of a hypersensitive periodate-cleavable amino acid that is methionine- and disulfide-compatible and its application in MHC exchange reagents for T cell characterisation. *Chembiochem* **14**, 123-131 (2013).
8. Rodenko, B., *et al.* Class I major histocompatibility complexes loaded by a periodate trigger. *J Am Chem Soc* **131**, 12305-12313 (2009).
9. Choo, J.A., *et al.* Bioorthogonal cleavage and exchange of major histocompatibility complex ligands by employing azobenzene-containing peptides. *Angew Chem Int Ed Engl* **53**, 13390-13394 (2014).
10. Rodenko, B., *et al.* Generation of peptide-MHC class I complexes through UV-mediated ligand exchange. *Nat Protoc* **1**, 1120-1132 (2006).
11. Toebes, M., *et al.* Design and use of conditional MHC class I ligands. *Nat Med* **12**, 246-251 (2006).
12. Bakker, A.H., *et al.* Conditional MHC class I ligands and peptide exchange technology for the human MHC gene products HLA-A1, -A3, -A11, and -B7. *Proc Natl Acad Sci U S A* **105**, 3825-3830 (2008).
13. Hadrup, S.R., *et al.* Parallel detection of antigen-specific T-cell responses by multidimensional encoding of MHC multimers. *Nat Methods* **6**, 520-526 (2009).
14. Andersen, R.S., *et al.* Dissection of T-cell antigen specificity in human melanoma. *Cancer Res* **72**, 1642-1650 (2012).
15. Bentzen, A.K., *et al.* Large-scale detection of antigen-specific T cells using peptide-MHC-I multimers labeled with DNA barcodes. *Nat Biotechnol* **34**, 1037-1045 (2016).
16. Pattison, D.I., Rahmanto, A.S. & Davies, M.J. Photo-oxidation of proteins. *Photoch Photobio Sci* **11**, 38-53 (2012).
17. Garstka, M.A., *et al.* The first step of peptide selection in antigen presentation by MHC class I molecules. *Proc Natl Acad Sci U S A* **112**, 1505-1510 (2015).
18. De Silva, A.D., *et al.* Thermolabile H-2Kb molecules expressed by transporter associated with antigen processing-deficient RMA-S cells are occupied by low-affinity peptides. *J Immunol* **163**, 4413-4420 (1999).
19. Vitiello, A., *et al.* Immunodominance analysis of CTL responses to influenza PR8 virus reveals two new dominant and subdominant Kb-restricted epitopes. *J Immunol* **157**, 5555-5562 (1996).
20. Ishizuka, J., *et al.* Quantitating T cell cross-reactivity for unrelated peptide antigens. *J Immunol* **183**, 4337-4345 (2009).
21. Madden, D.R., Garboczi, D.N. & Wiley, D.C. The antigenic identity of peptide-MHC complexes: a comparison of the conformations of five viral peptides presented by HLA-A2. *Cell* **75**, 693-708 (1993).
22. Andreatta, M. & Nielsen, M. Gapped sequence alignment using artificial neural networks: application to the MHC class I system. *Bioinformatics* **32**, 511-517 (2016).
23. Nielsen, M., *et al.* Reliable prediction of T-cell epitopes using neural networks with novel sequence representations. *Protein Sci* **12**, 1007-1017 (2003).
24. Duan, F., *et al.* Genomic and bioinformatic profiling of mutational neoepitopes reveals new rules to predict anticancer immunogenicity. *J Exp Med* **211**, 2231-2248 (2014).

25. Hadrup, S.R., *et al.* Cryopreservation of MHC multimers: Recommendations for quality assurance in detection of antigen specific T cells. *Cytometry A* **87**, 37-48 (2015).
26. Rodriguez, F., Slifka, M.K., Harkins, S. & Whitton, J.L. Two overlapping subdominant epitopes identified by DNA immunization induce protective CD8(+) T-cell populations with differing cytolytic activities. *J Virol* **75**, 7399-7409 (2001).
27. Matloubian, M., Concepcion, R.J. & Ahmed, R. $CD4^+$ T cells are required to sustain $CD8^+$ cytotoxic T-cell responses during chronic viral infection. *J Virol* **68**, 8056-8063 (1994).
28. Wherry, E.J., Blattman, J.N., Murali-Krishna, K., van der Most, R. & Ahmed, R. Viral persistence alters CD8 T-cell immunodominance and tissue distribution and results in distinct stages of functional impairment. *J Virol* **77**, 4911-4927 (2003).
29. van der Most, R.G., *et al.* Identification of Db- and Kb-restricted subdominant cytotoxic T-cell responses in lymphocytic choriomeningitis virus-infected mice. *Virology* **240**, 158-167 (1998).
30. La Rosa, C., *et al.* MVA vaccine encoding CMV antigens safely induces durable expansion of CMV-specific T cells in healthy adults. *Blood* **129**, 114-125 (2017).
31. Grassmann, A.A., *et al.* Discovery of Novel Leptospirosis Vaccine Candidates Using Reverse and Structural Vaccinology. *Front Immunol* **8**, 463 (2017).
32. El Bissati, K., *et al.* Adjuvanted multi-epitope vaccines protect HLA-A*11:01 transgenic mice against Toxoplasma gondii. *JCI Insight* **1**, e85955 (2016).
33. Hodi, F.S., *et al.* Improved survival with ipilimumab in patients with metastatic melanoma. *N Engl J Med* **363**, 711-723 (2010).
34. Page, D.B., Yuan, J. & Wolchok, J.D. Targeting cytotoxic T-lymphocyte antigen 4 in immunotherapies for melanoma and other cancers. *Immunotherapy* **2**, 367-379 (2010).
35. Tumeh, P.C., *et al.* PD-1 blockade induces responses by inhibiting adaptive immune resistance. *Nature* **515**, 568-571 (2014).
36. Topalian, S.L., *et al.* Safety, activity, and immune correlates of anti-PD-1 antibody in cancer. *N Engl J Med* **366**, 2443-2454 (2012).
37. Robert, L., *et al.* Distinct immunological mechanisms of CTLA-4 and PD-1 blockade revealed by analyzing TCR usage in blood lymphocytes. *Oncoimmunology* **3**, e29244 (2014).
38. van Rooij, N., *et al.* Tumor exome analysis reveals neoantigen-specific T-cell reactivity in an ipilimumab-responsive melanoma. *J Clin Oncol* **31**, e439-442 (2013).
39. Fourcade, J., *et al.* PD-1 is a regulator of NY-ESO-1-specific $CD8^+$ T cell expansion in melanoma patients. *J Immunol* **182**, 5240-5249 (2009).
40. Toebes, M., Rodenko, B., Ovaa, H. & Schumacher, T.N. Generation of peptide MHC class I monomers and multimers through ligand exchange. *Curr Protoc Immunol* **Chapter 18**, Unit 18 16 (2009).
41. Meiring, H.D., van der Heeft, E., ten Hove, G.J. & de Jong, A.P.J.M. Nanoscale LC-MS(n): technical design and applications to peptide and protein analysis. *J Sep Sci* **25**, 557-568 (2002).
42. Welten, S.P.M., *et al.* The viral context instructs the redundancy of costimulatory pathways in driving CD8(+) T cell expansion. *Elife* **4**(2015).
43. Hogquist, K.A., *et al.* T cell receptor antagonist peptides induce positive selection. *Cell* **76**, 17-27 (1994).
44. Kotturi, M.F., *et al.* The CD8(+) T-cell response to lymphocytic choriomeningitis virus involves the L antigen: Uncovering new tricks for an old virus. *Journal of Virology* **81**, 4928-4940 (2007)

6

Production and thermal exchange of conditional peptide-MHCI multimers

Jolien J. Luimstra[1], Kees L.M.C. Franken[2], Malgorzata A. Garstka[3], Jan W. Drijfhout[2], Jacques Neefjes[1], and Huib Ovaa[1]

[1]Oncode Institute and Department of Cell and Chemical Biology, Leiden University Medical Center, Leiden, The Netherlands;
[2]Department of Immunohematology and Blood Transfusion, Leiden University Medical Center, Leiden, The Netherlands;
[3]Core Research Laboratory, National & Local Joint Engineering Research Center of Biodiagnosis and Biotherapy, Liver and Spleen Diseases Research Center, The Second Affiliated Hospital, School of Medicine, Xi'an Jiaotong University, Xi'an, China.

Current Protocols in Immunology 126, e85 (2019)

Abstract

Cytotoxic CD8+ T cells mediate cellular immunity through recognition of specific antigens presented by MHC class I on all nucleated cells. Studying T cell interactions and responses provides invaluable information on infection, autoimmunity and cancer. Fluorescently-labeled multimers of MHCI can be used to quantify, characterize and isolate specific CD8+ T cells using flow cytometry. In this unit we describe the production and use of conditional MHCI multimers that can be loaded with peptides of choice just by incubating them with the desired peptide at a defined temperature. These multimers are folded with a template peptide that forms a stable complex at low temperature, but dissociates at a defined elevated temperature. Using this technology multiple MHCI multimers can be generated in parallel, to allow staining and isolation of large sets of antigen-specific CD8+ T cells, especially when combined with barcoding technologies.

Introduction

Major histocompatibility class I (MHCI) molecules complexed with antigenic peptides and multimerized on a streptavidin backbone are the classical reagents to visualize, characterize and isolate antigen-specific CD8+ T cells[1]. By labeling peptide-MHCI (pMHCI) multimers with a fluorophore they can be used for analysis and isolation of CD8+ T cells specific for a given antigen using flow cytometry. Many

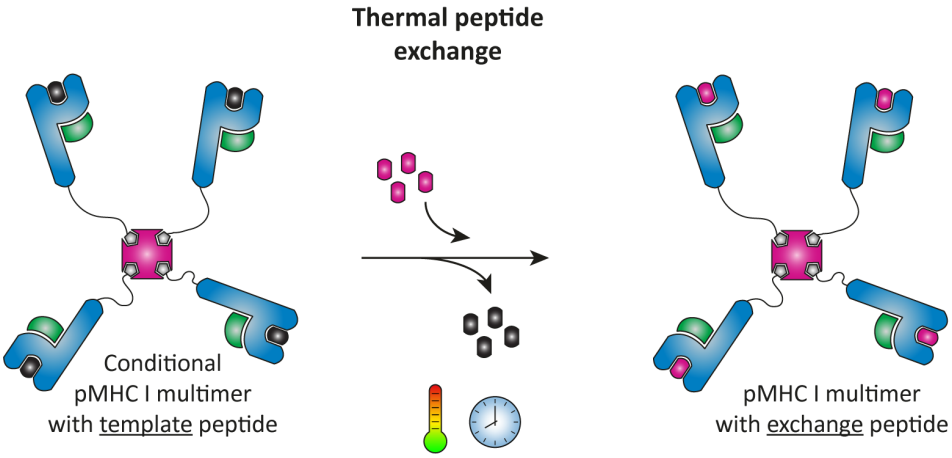

Figure 1. **Schematic representation of thermal peptide exchange on MHCI multimers.** Conditional MHCI monomers are folded with a low-affinity peptide, multimerized using streptavidin and stored at -80°C. To induce exchange conditional pMHCI multimers are warmed up in the presence of a peptide of interest.

different specificities can be identified in parallel using combinatorial coding, mass cytometry or DNA barcoding technologies[2-4]. Conventional production of pMHCI complexes is a laborious process: for every T cell specificity a new pMHCI complex with a different peptide has to be produced, as MHCs are unstable without peptide and can therefore not be folded empty[5]. We have recently reported a peptide exchange technology that allows generation of a large batch of pMHCI multimers and exchange of the peptide using thermal dissociation (Fig. 1)[6]. We have established exchange conditions for the most common human MHCI allele in the Caucasian population, HLA-A*02:01, and the murine allele H-2K^b. The design of template peptides suitable for thermal exchange on other MHCI alleles requires careful selection of proper peptides that dissociate under low-temperature conditions and the generation of conditional multimers for those alleles is anticipated in the near future.

In Basic Protocol 1 of this unit we describe the production of conditional pMHCI monomers and in Basic Protocol 2 we describe the validation of thermal dissociation and peptide-mediated stabilization. The procedures for multimerization and exchange are described in Basic Protocols 3 and 4. In the support protocols we describe the expression and purification of MHCI heavy chain and β2m inclusion bodies, folding of β2m and determination of the biotinylation efficiency.

BASIC PROTOCOL 1: FOLDING, BIOTINYLATION AND PURIFICATION OF CONDITIONAL pMHCI MONOMERS

The procedure for folding and biotinylation of MHCI complexes is based on previously described protocols, with some adaptations[7-9]. Conditional complexes are produced from MHCI heavy chain inclusion bodies, prefolded β2m (described in Support Protocol 2) and a template peptide (IAKEPVHGV for HLA-A*02:01 or FAPGNAPAL for H-2K^b). The MHCI heavy chain contains a 15-amino acid C-terminal recognition sequence for the BirA biotin ligase, which enzymatically conjugates a biotin molecule to the lysine in that sequence. The degree of biotinylation of pMHCI monomers following Basic Protocol 1 should be (near) complete, but it is recommended to determine the degree of biotinylation for each batch of pMHCI as described in Support Protocol 3. The present protocol describes a 50-ml folding reaction, but can be scaled up as desired. Alternative steps for large-scale folding reactions are mentioned when applicable.

Materials

Denaturing buffer (8 M urea/100 mM Tris•Cl, pH 8)
MHCI heavy chain inclusion bodies (Support Protocol 1)

Folding buffer (see recipe)
Template peptide: IAKEPVHGV for HLA-A*02:01; or FAPGNAPAL for H-2K^b (commercial sources or prepared through standard solid-phase peptide synthesis)
Dimethyl sulfoxide (DMSO)
Prefolded β2m (Support Protocol 2)
Milli-Q water
MHC buffer (300 mM NaCl/20 mM Tris•Cl, pH 8)
Biotinylation solution (see recipe)
Glycerol
Liquid nitrogen (for freezing)

1.5-ml reaction tubes
Rotator
50-ml conical tubes
Ice bucket with ice
Sonicator
Microcentrifuge
Syringe and 0.22- and 0.45-µm syringe filters
Water bath at 10°C
30-kDa MWCO centrifugal concentrators, 0.5- and 15-ml (e.g., Amicon Ultra centrifugal filters; Merck Millipore)
Illustra NAP-10 column (GE Healthcare)
Spin-X centrifuge tube filters 0.22 µm (Corning)
FPLC system with gel-filtration column (e.g., Superdex 75 10/300 (GE Healthcare))
PCR tubes or 1.5-ml polypropylene screw cap microcentrifuge tubes (Sarstedt)
Additional reagents and equipment for SDS gel electrophoresis and staining of proteins[10,11] and gel-filtration chromatography[12]

Folding of pMHCI complexes

1. Prepare 500 µl fresh denaturing buffer.
2. In a 1.5-ml reaction tube dissolve ~2.5 mg of MHCI heavy chain inclusion bodies (Support Protocol 1) in 500 µl denaturing buffer. Rotate at room temperature for at least 2 hr and preferably overnight to ensure complete dissolution.
3. Set up 50 ml folding buffer in a 50-ml conical tube, rotate ~15 min at RT, and then cool on ice for 1-1.5 hours.
4. In the meantime, dissolve 3 mg of template peptide in ~500 µl DMSO and sonicate 10-15 min.

Peptides that contain hydrophobic amino acids dissolve poorly in polar solvents, such as PBS or water. Therefore, it is recommended to dissolve peptides in DMSO and store them as 10-mM stocks at -20°C. Sonication of freshly prepared solutions, preferably in a warm water bath, improves solubility.

5. Add template peptide solution to 50 mL of folding buffer (60 µM final concentration).
6. Thaw a 1.2-mg aliquot of prefolded β2m (Support Protocol 2).
7. Microcentrifuge β2m and MHCI heavy chain for 2 min at 16,000 × *g* , save 1 µl of each supernatant at -20°C as a reference for SDS-PAGE analysis (step 18), and add the remainder of each supernatant to the folding buffer containing template peptide (final concentrations: 6 µM β2m and 3 µM MHCI heavy chain).
8. Filter the folding solution through a 0.22-µm filter using a syringe and leave in a 10°C water bath for 4-5 days.

Large-scale reactions can be filtered using a bottle-top filter.

Biotinylation of pMHCI complexes

NOTE: Folded complexes will dissociate at elevated temperatures, so from this point, keep all solutions and reagents on ice and centrifuges at 4°C!

9. Sediment aggregates in the folding solution by centrifugation for 10 min at 4,000 × *g*, 4°C, and filter supernatant through a 0.45-µm filter using a syringe.

Depending on the purity of the inclusion bodies some protein aggregates may form during folding. Removing precipitates by centrifugation and filtering prevents obstruction of the filters used for concentration.

10. Wash a 15-ml 30-kDa MWCO centrifugal concentrator first with Milli-Q water and then with MHC buffer by centrifugation for 10 min each at 4,000 × *g*, 4°C. Add the fitlered folding reaction (from step 9) and concentrate to ≤1 ml by centrifugation for 10 min at 4,000 × *g*, 4°C.

For concentration of large-scale reactions use a 30 kDa MWCO PES Vivaflow 200 protein concentrator system (Sartorius), driven by a peristaltic pump.

11. In a cold room, recover concentrated sample and exchange folding buffer for MHC buffer using a NAP-10 column: wash the column 3 times with 1 ml MHC buffer, apply sample, and elute with an additional 1 ml MHC buffer.
12. Filter concentrated folding reaction through a SpinX centrifuge tube filter by centrifugation for 2 min (or longer if necessary) at 16,000 × *g*, 4°C.
13. Prepare biotinylation solution (see recipe) on ice, and add 1 ml biotinylation

solution to the 1 ml pMHCI solution. Incubate overnight at 4°C, preferably on a rotator.

The enzymatic activity of BirA biotin ligase is low at 4°C and therefore the biotinylation reaction requires overnight incubation (~16 h).

Purification of biotinylated pMHCI

14. Sediment aggregates in the folding solution by centrifugation for 10 min at 4,000 × *g*, 4°C.

    Some precipitation may form overnight. Sedimentation prevents obstruction of the filters used for concentration.

15. Wash a 0.5-ml 30-kDa MWCO centrifugal concentrator with Milli-Q water and then with MHC buffer. Concentrate biotinylation reaction to ~500 µl by centrifugation for 10 min at 16,000 × *g*, 4°C.
16. Filter concentrated folding reaction through a SpinX centrifuge tube filter by centrifugation for 2 min (or longer if necessary) at 16,000 × *g*, 4°C.
17. Purify biotinylated pMHCI complexes by gel-filtration chromatography at 4°C, for example, using an FPLC system equipped with a Superdex 75 10/300 column (GE Healthcare).

    One 50-ml folding reaction typically yields between 0.1 and 2 mg of folded complex depending on the peptide and MHCI allele. The total volume can be concentrated to ~500 µl for one injection on an S75 10/300 column. Larger-scale reactions yield higher protein quantities and should be purified in multiple 500-µl runs or using a larger column, such as an S75 16/600.

18. Analyze fractions using SDS-PAGE. For reference include a protein standard, such as SeeBlue™ Pre-stained Protein Standard, and the reference MHCI heavy chain and β2m samples (set aside in step 7). Figure 2 shows a typical FPLC chromatogram and corresponding gel.

    We typically run our complexes on a 10% Bis-Tris gel for 30 min at 200V in MES buffer. On a denaturing gel, the complex dissociates and two bands will be visible: one at ~36 kDa corresponding to the heavy chain, and one at ~10 kDa, corresponding to β2m. The peptide is too small to visualize on gel.

19. Pool fractions that contain pMHCI, and concentrate to 2-5 mg/ml using a 15-ml 30-kDa MWCO centrifugal concentrator (prewashed with Milli-Q water and MHC buffer).

    pMHCI complexes are more stable at higher concentrations.

The concentration can be measured using a Nanodrop spectrophotometer and the Lambert-Beer Law: $c = A/\varepsilon \times L$. The extinction coefficient (ε) at OD_{280} can be estimated from the number of tryptophans (W) and tyrosines (Y) in the protein sequence according to the following formula: $\varepsilon = (nW \times 5{,}500) + (nY \times 1{,}490)$.

20. Determine the volume of the sample and add glycerol to a final concentration of 15%.

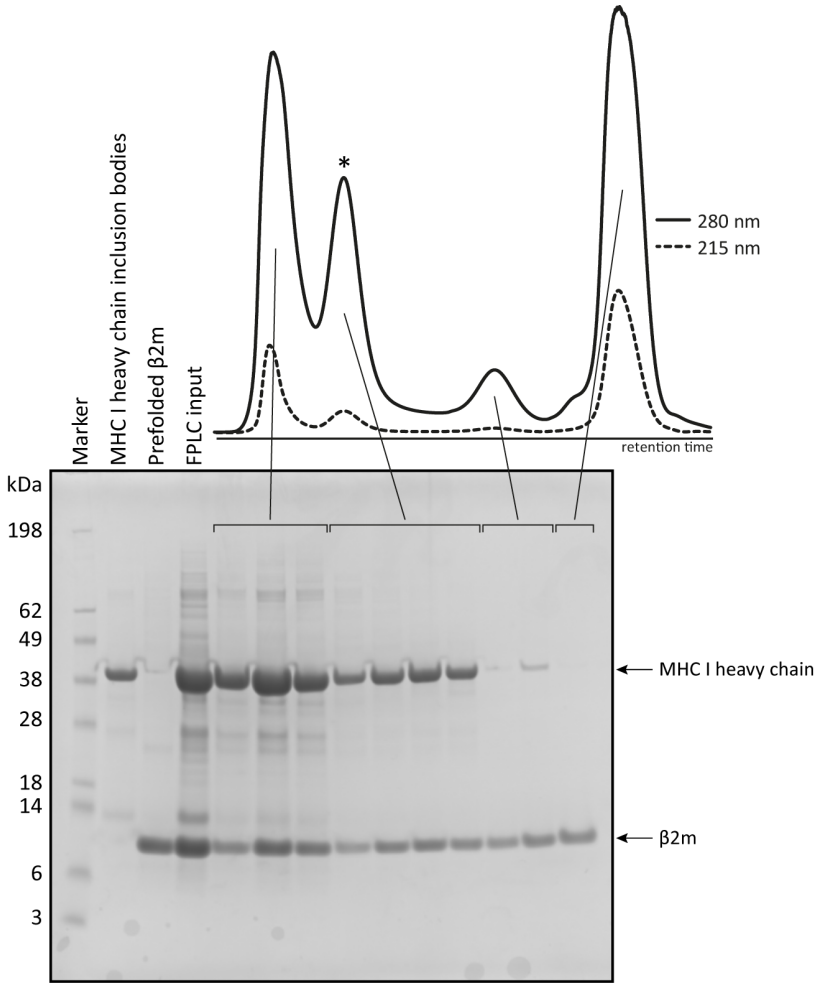

Figure 2. **SDS-PAGE analysis (10% Bis-Tris gel in MES running buffer) of a typical pMHCI purification using FPLC.** The first peak in the chromatogram contains mostly aggregates, whereas the second peak (marked with an asterisk) contains properly folded, pure pMHCI complexes, visible on this denaturing gel as two separate bands for the heavy chain (~36 kDa) and β2m (~10 kDa). Later peaks contain free heavy chain and free β2m. A protein marker, MHCI heavy chain inclusion bodies and prefolded β2m are included for reference.

Glycerol is added as a cryoprotectant. It forms strong hydrogen bonds with water molecules, thus preventing the formation of ice crystals that can damage proteins.

21. Aliquot the sample into PCR tubes or 1.5-ml polypropylene screw cap tubes, depending on the desired volume. Snap-freeze aliquots in liquid nitrogen and store at -80°C.

    We typically store aliquots of 5, 10 and 25 µl. Frozen conditional pMHCI monomers can be stored at -80°C for at least a year. We recommend validation of the exchange performance (Basic Protocol 2) before moving on to multimerization.

BASIC PROTOCOL 2: CONFIRMING THERMAL EXCHANGE PERFORMANCE OF CONDITIONAL pMHCI MONOMERS BY GEL FILTRATION HPLC

For each batch of conditional pMHCI monomers, the thermal exchange performance should be validated. This protocol describes the use of gel filtration HPLC to confirm exchange at pre-established conditions, but can also be used to test additional exchange times and temperatures. When incubated at a higher temperature without peptide, the pMHCI monomer peak should disappear (Fig. 3, magenta line compared to black line), but in the presence of an exchange peptide the complex is stabilized and the peak should remain visible (Fig. 3, green line). For efficient stabilization the exchange peptide should have a higher affinity for its corresponding MHCI than the template peptide (<4,000 nM for H-2K^b-FAPGNAPAL and <7,288 nM for HLA-A*02:01). A link to an affinity prediction tool is provided in Internet Resources.

Materials (also see Basic Protocol 1)

Conditional pMHCI monomers (Basic Protocol 1)

Cold phosphate-buffered saline (PBS, pH 7.4, tablets reconstituted in 500 ml demineralized water; Gibco)

10 mM exchange peptide in DMSO stock, higher affinity than the template peptide (e.g., cytomegalovirus peptide NLVPMVATV for HLA-A*02:01 or ovalbumin peptide SIINFEKL for H-2K^b)

HPLC system with gel filtration column (e.g., 300 × 7.8 mm BioSep SEC-s3000, Phenomenex, cat. no. 00H-2146-K0)

PCR machine, Thermoblock or incubator

Testing the stability of pMHCI monomers at room temperature

1. Thaw conditional pMHCI monomers on ice. Typically, a 5 µl aliquot of 2-5 mg/ml pMHCI is enough for four to ten 100-µl injections of 0.5 µM pMHCI monomers.
2. In a 1.5-ml screw-cap microcentrifuge tube, dilute conditional pMHCI monomers to a 0.5 µM in PBS.

   We typically prepare 10% extra to allow for variance when drawing up the sample for injection.

3. Sediment aggregates by centrifugation for 1 min at 16,000 × *g*, room temperature.
4. Analyze the sample by HPLC using a gel filtration column, such as a 300 × 7.8 mm BioSep SEC-s3000 column (Phenomenex) with PBS as running buffer.

   *Analysis of this sample provides information on the stability of the conditional complex at room temperature. Expect to see a sharp peak when injecting HLA-A*02:01-IAKEPVHGV, but no peak when injecting H-2K^b-FAPGNAPAL, which is unstable at room temperature (see Fig. 3, pMHCI input; black lines).*

Analysis of peptide-mediated stabilization of pMHCI monomers post thermal exchange

5. Prepare 0.5 µM pMHCI in PBS containing 50 µM exchange peptide to confirm stabilization of the exchanged complex.
6. Incubate at established exchange conditions in a PCR machine, Thermoblock or incubator (3 hr at 32°C for HLA-A*02:01; 5 min at room temperature for H-2K^b).
7. Sediment aggregates by centrifugation for 1 min at 16,000 × *g*, room temperature.
8. Analyze by gel-filtration HPLC.

   When incubated with an exchange peptide, the MHC monomer peak should be at least as high as the input peak.

Thermal dissociation of conditional pMHCI monomers

9. Prepare a 0.5 µM pMHCI solution in PBS.
10. Incubate at established exchange conditions in a PCR machine, Thermoblock or incubator (3 hours at 32°C for HLA-A*02:01 or 5 min at room temperature for H-2K^b).
11. Sediment aggregates by centrifugation for 1 min at 16,000 × *g*, room temperature.
12. Analyze by gel-filtration HPLC.

*At the optimal exchange conditions (3 hr at 32°C for HLA-A*02:01, and 5 min at room temperature for H-2K^b) the monomer peak should virtually disappear when incubated without peptide (Fig. 3).*

BASIC PROTOCOL 3: MULTIMERIZATION OF CONDITIONAL pMHCI MONOMERS

The low affinity of a T cell receptor (TCR) for pMHCI monomers enables sequential activation of multiple T cells by one pMHC in vivo. Through multimeric binding, the avidity of pMHC binding to TCRs becomes sufficiently high to stably label specific CD8$^+$ T cells for visualization and isolation[13]. Therefore, pMHCI monomers are biotinylated for multimerization on streptavidin in order to create tetrameric complexes. In addition, labeled streptavidin can be used to incorporate desired

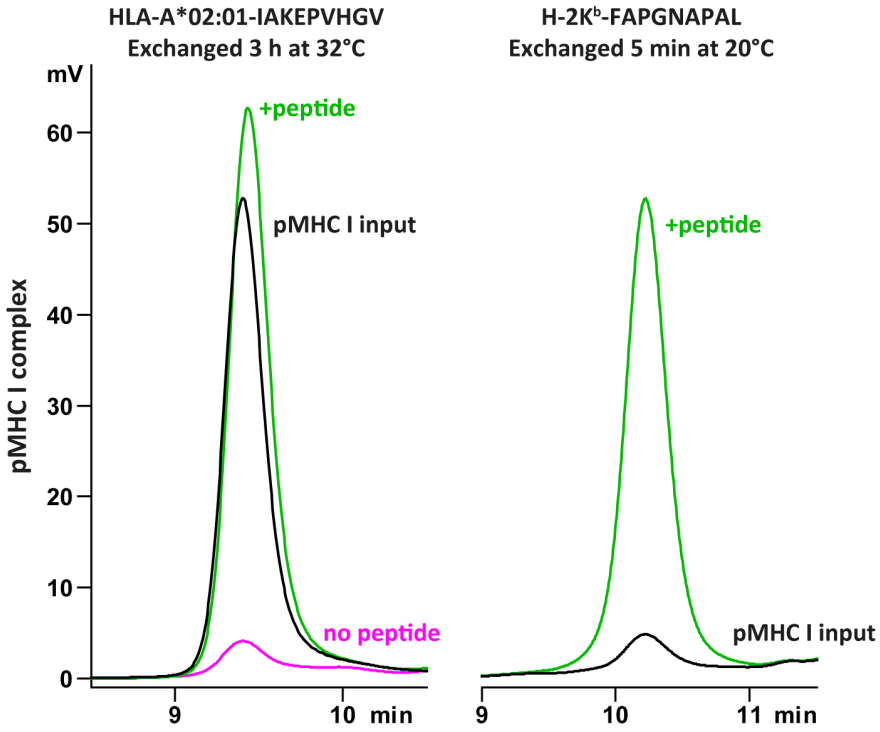

Figure 3. **Overlay of typical gel filtration HPLC chromatograms that confirm thermal exchange of conditional HLA-A*02:01 monomers (left) and H-2K^b monomers (right).** When incubated without peptide the HLA-A*02:01 monomer peak (0.5 µM) disappears (no peptide, magenta line), indicating dissociation, whereas in presence of a high-affinity peptide (50 µM) the complex remains stable (+peptide, green line) compared to nonincubated monomers (pMHCI input, black line). H-2K^b-FAPGNAPAL dissociates at room temperature (pMHCI input black line), which can be 'rescued' by addition of a high-affinity peptide (+peptide, green line).

fluorophores. Allophycocyanin (APC) and phycoerythrin (PE) are typically used, but other fluorophores have also been successfully used in combination with pMHCI multimers. This protocol describes the preparation of 80 µl pMHCI multimer solution (0.625 µM final), but the reaction can be scaled depending on concentration and volume of pMHCI aliquots.

Materials (also see Basic Protocols 1 and 2)

Biotinylated conditional pMHCI monomers (Basic Protocol 1)

1 mg/ml APC-conjugated streptavidin (SA-APC; Thermo Fisher Scientific, Invitrogen, cat. no. S868) or 1 mg/ml PE-conjugated streptavidin (SA-PE; Thermo Fisher Scientific, Invitrogen, cat. no. S866)

Cold glycerol

NOTE: Folded complexes will dissociate at elevated temperatures, so keep all solutions and reagents on ice and (micro)centrifuges at 4°C!

1. On ice, dilute biotinylated conditional pMHCI monomers in cold PBS to a concentration of 5 µM.

2a. If making APC-labeled multimers: Add 53.6 µl cold PBS to 10 µl of pMHCI monomers.

2b. If making PE-labeled multimers: Add 52.4 µl cold PBS to 10 µl of pMHCI monomers.

3. Add either 1.4 µl SA-APC or 2.6 µl SA-PE. To ensure saturation of all four biotin-binding sites, add streptavidin conjugates stepwise. For example, three 0.47-µl additions of SA-APC or three 0.87-µl additions of SA-PE at 5-min intervals.

   To saturate all four of streptavidin's binding sites, 0.125 µM streptavidin should be added to 0.5 µM pMHCI monomer, corresponding to 2 µg of SA-APC (molecular weight ~160 kDa) or 3.75 µg of SA-PE (molecular weight ~300 kDa) per 100 µl pMHCI solution. To ensure binding sites are fully saturated, we add 70% of these amounts for a ratio of ~6 pMHCI monomers to 1 streptavidin. With an excess of streptavidin not all binding sites would be saturated, resulting in the formation of lower order MHCI multimers that poorly bind T cells due to lower avidity. Ideally a little residual MHCI monomer remains present, ensuring full saturation of streptavidin.

4. Add 15 µl cold glycerol and mix well.

5. Aliquot into PCR tubes or 1.5-ml polypropylene screw cap tubes, depending on the desired volume. Snap-freeze aliquots in liquid nitrogen and store at –80°C.

   We typically prepare 8-µl aliquots. Frozen pMHCI multimers can be stored at –80°C for at least a year.

BASIC PROTOCOL 4: THERMAL PEPTIDE EXCHANGE ON CONDITIONAL pMHCI MULTIMERS

This protocol describes the thermal exchange of conditional pMHCI multimers for any number of desired peptides in parallel. Conditional multimers are temperature-labile and should be kept on ice until a peptide is added. For efficient stabilization the exchange peptide should have a higher affinity for its corresponding MHCI than the template peptide (<4,000 nM for H-2K^{b}-FAPGNAPAL and <7,288 nM for HLA-A*02:01). One 10 µl aliquot of exchanged multimer is typically enough to stain ten to twenty samples, each containing 1,000,000 peripheral blood mononuclear cells (PBMCs).

Materials (also see Basic Protocols 1 to 3)
10 mM exchange peptide(s) stock solution
Conditional pMHCI multimers (Basic Protocol 3)

1. Dilute 10 mM exchange peptide stock(s) to 250 µM in PBS.

   Hydrophobic peptides do not readily dissolve in PBS. Therefore it is recommended to dissolve peptides in DMSO and store them as 10-mM stocks at -20°C.

2. Take an 8-µl aliquot of MHCI multimer from freezer and immediately place on ice.

   Conditional MHCI multimers may dissociate at room temperature and should be kept cold prior to exchange, so make sure to keep them on ice when moving them from freezer to bench. Especially H-2K^{b}-FAPGNAPAL is prone to rapid dissociation and should remain frozen until an exchange peptide is added.

3. Add 2 µl 250 µM exchange peptide solution to frozen 8 µl MHCI multimer. As the mixture thaws, briefly pipette up and down to mix.
4. Briefly spin and incubate exchange reactions in a PCR machine, Thermoblock or incubator at defined temperature and time to induce exchange.

   *H-2K^{b}-FAPGNAPAL readily exchanges within 5 min at room temperature. Exchange of HLA-A*02:01-IAKEPVHGV multimers is complete after a 3-hr incubation at 32°C.*

5. Briefly spin the tubes. The exchanged multimers are now ready for staining of T cells.

   Exchanged multimers can be stored at 4°C and used for at least a week

without loss of function. They can typically be diluted 1:40 dilution to stain 1,000,000 PBMCs in 40 µl of FACS buffer.

SUPPORT PROTOCOL 1: BACTERIAL EXPRESSION AND PURIFICATION OF MHCI HEAVY CHAIN AND β2M INCLUSION BODIES

The procedure for bacterial expression and purification of MHCI heavy chain and β2m inclusion bodies is based on protocols described previously[7-9]. Both proteins can be expressed in parallel following the same steps. This protocol describes expression in 2 L and can be scaled up or down accordingly.

Materials

Competent *E. coli* strain BL21 (DE3) (Novagen, cat. no. 69450)
MHCI heavy chain and human β2m expression constructs (see recipe)
Liquid LB medium (sterilized, e.g., BD Difco™ LB Broth, cat. no. 244620)
Ampicillin (Roche Diagnostics)
1 M isopropyl β-D-1-thiogalactopyranoside (IPTG) in de-ionized water
Lysis buffer (see recipe)
10 mg/ml lysozyme (Roche Diagnostics) in lysis buffer
1 M $MgCl_2$ in de-ionized water
1 M $MnCl_2$ in de-ionized water
10 mg/ml DNase I stock (see recipe)
Detergent buffer (see recipe)
Wash buffer (see recipe)

Incubator (shaking and stationary)
LB agar plate containing 50 µg/ml ampicillin
Sterile pipette tip
Inoculation tube (with foil or cap)
Spectrophotometer and cuvettes
2-L Erlenmeyer flasks
High-speed centrifuge and 250-ml to 1-liter buckets
Sonicator

Protein expression in E. coli

1. Express MHCI heavy chains and β2m separately. Transform 100-200 ng plasmid DNA (MHCI heavy chain or β2m) into 50-100 µl competent *E. coli* cells in a reaction tube for 30 min on ice, 2 min at 42°C, 5 min on ice, respectively.
2. Add 500 µl LB medium and incubate 30-60 min at 37°C with shaking.
3. Plate 200 µl of inoculate on an LB agar plate containing 50 µg/ml ampicillin,

and incubate overnight at 37°C.

The LB plate can be stored at 4°C for up to 4 days.

4. Use sterile pipette tips to select two single colonies from the LB plate, and drop each tip into an inoculation tube containing 10 ml liquid LB medium with 50 µg/ml ampicillin. Cover the tube loosely with foil or a cap that is not air tight and incubate ~6 hr with shaking to an OD_{600} of 0.8, and then store at 4°C overnight.
5. Add the 10-ml inoculates to 2L of liquid LB medium containing 50 µg/ml ampicillin. Divide between four 2-L Erlenmeyer flasks and incubate the cultures at 37°C with shaking to an OD_{600} of 0.6.

   The cultures should reach an OD_{600} of 0.6 in 3 to 4 hr. Bacteria grow exponentially, so check regularly.

6. Take a 1-ml sample of the culture for SDS-PAGE analysis. Pellet bacteria by centrifugation for 10 min at 12,000 × *g*, 4°C. Discard supernatant ans store pellet at -20°C.
7. Induce protein expression by adding 200 µl of 1 M IPTG to each Erlenmeyer flask containing 500 ml *E. coli* cell culture (fincal concentration, 0.4 mM IPTG).
8. Incubate ~4 hr at 37°C with shaking.
9. Take a 0.5-ml sample for SDS-PAGE analysis. Pellet bacteria by centrifugation for 10 min at 12,000 × *g*, 4°C. Discard supernatant ans store pellet at -20°C.
10. Harvest the remainder of the induced bacteria by centrifugation for 15 min at 4,000, 4°C. Suspend the cell pellet(s) 25 ml lysis buffer per 2-L culture, transfer the suspension to a 50-ml conical tube. Store suspended cells at -80°C for at least a year or -20°C for a few days.

Isolation and purification of inclusion bodies

11. Thaw the bacteria from 2 L culture.
12. Once the suspension is thawed, add 2.5 ml lysozyme (10 mg/ml in lysis buffer), and incubate 20 min on ice or on a rotator in a cold room.

    The solution must become viscous before proceeding.

13. Add the following:
    275 µl 1 M $MgCl_2$ stock (10 mM final)
    27.5 µl 1 M $MnCl_2$ stock (1 mM final)
    27.5 µl 10 mg/ml DNase I (10 µg/ml final)

14. Incubate 30 min at room temperature.

    The solution must become fluid.

15. Sonicate at 50% for 2 min with 20 s on, 20 s off intervals.
16. Centrifuge lysates for 10 min at 12,000 × *g*, 4°C, and discard the supernatant.
17. Add 25 ml detergent buffer, and sonicate at 30% for 30 2 with 10 s on, 10 s off intervals.
18. Centrifuge lysate 10 min at 12,000 × *g*, 4°C, and discard the supernatant.
19. Add 20 ml wash buffer, and sonicate at 30% for 30 s with 10 s on, 10 s off intervals.
20. Centrifuge lysate 10 min at 12,000 × *g*, 4°C, and discard the supernatant.
21. Repeat steps 19 and 20 twice.
22. Add 20 ml wash buffer without Triton, and sonicate at 30% for 30 s with 10 s on, 10 s off intervals.
23. Centrifuge lysate 10 min at 12,000 × *g*, 4°C, and discard the supernatant.
24. Repeat steps 22 and 23.
25. Suspend inclusion bodies in 10 ml wash buffer without Triton, and measure the protein concentration, e.g., using the Bradford assay.

    Depending on the construct, expression yields are between 50 and 250 mg/l with a protein purity of 90-98%.

26. Prepare desired aliquots, and pellet inclusion bodies by centrifugation for 5 min at 16,000 × *g*, room temperature, and discard the supernatant.

    We recommend freezing aliquots of 2.5 mg (or multiples thereof), since we typically use 2.5 mg inclusion bodies per 50-ml folding reaction. Inclusion bodies can be stored at -80°C for at least a year.

SUPPORT PROTOCOL 2: FOLDING OF HUMAN β2M

Human β2m is used for the production of both human and murine MHCI complexes, because of its higher stability compared to its murine counterpart. Using prefolded β2m for folding of pMHCI ensures stabilization of MHCI and increases folding yields compared to using β2m inclusion bodies.

Materials

Denaturing buffer (8 M urea/100 mM Tris•Cl, pH 8)
Purified human β2m inclusion bodies (Support Protocol 1)
Phosphate-buffered saline (PBS, pH 7.4, tablets (Gibco) reconstituted in 500 ml demineralized water)
10 mM Tris•Cl (pH 7) in PBS
Dialysis tubing (10 kDa MWCO) and large beaker or bucket

1. Suspend pelleted β2m inclusion bodies to 3 mg/ml in freshly-prepared denaturing buffer.
2. Transfer the solution to a dialysis tube, and dialyze overnight against 2 L 10 mM Tris•Cl (pH 7) in PBS at 4°C.
3. The next day, dialyze against two changes of fresh buffer, 4 hr each.

   During dialysis, some β2m will precipitate, that can be collected, dissolved in fresh denaturing buffer and dialyzed in a new dialysis tube for increased protein yield.

4. Transfer dialyzed, folded β2m to a 1.5-ml reaction tube and sediment insoluble material by centrifugation for 20 min at 12,000 × *g*, 4°C.
5. Analyze 10 µl of supernatant and samples from steps 6 and 9 of Support Protocol 1, bySDS-PAGE.

   Suspend pellets from step 6 and 9 of Support Protocol 1 in 100 µl sample buffer, and analyze 10 µl each.

6. Determine the concentration of the folded β2m protein, e.g., using a Bradford assay.
7. Prepare desired aliquots of folded β2m, snap freeze, and store at -80°C.

   A typical 50-ml pMHCI folding reaction requires one aliquot of 1.2 mg β2m.

SUPPORT PROTOCOL 3: DETERMINATION OF THE BIOTINYLATION EFFICIENCY

This protocol describes how to use HPLC to determine the degree of biotinylation of MHCI monomers. Each batch of pMHCI monomers and preferably also each batch of streptavidin should be tested. MHCI multimers will form by addition of streptavidin, and the height of the monomer peak in the chromatogram will decrease with increasing ratios of streptavidin (Fig. 4). Generally, 90-95% of pMHCI monomers will be biotinylated. When testing highly unstable complexes, such as H-2K^b-FAPGNAPAL, exchange peptide should be added for stabilization. If samples can be measured on a cooled (4°C) HPLC system, the peptide can be omitted.

Materials

Conditional pMHCI monomers (Basic Protocol 1)

Exchange peptide (of higher affinity than the template peptide; e.g., cytomegalovirus peptide NLVPMVATV for HLA-A*02:01 or ovalbumin peptide SIINFEKL for H-2K^b)

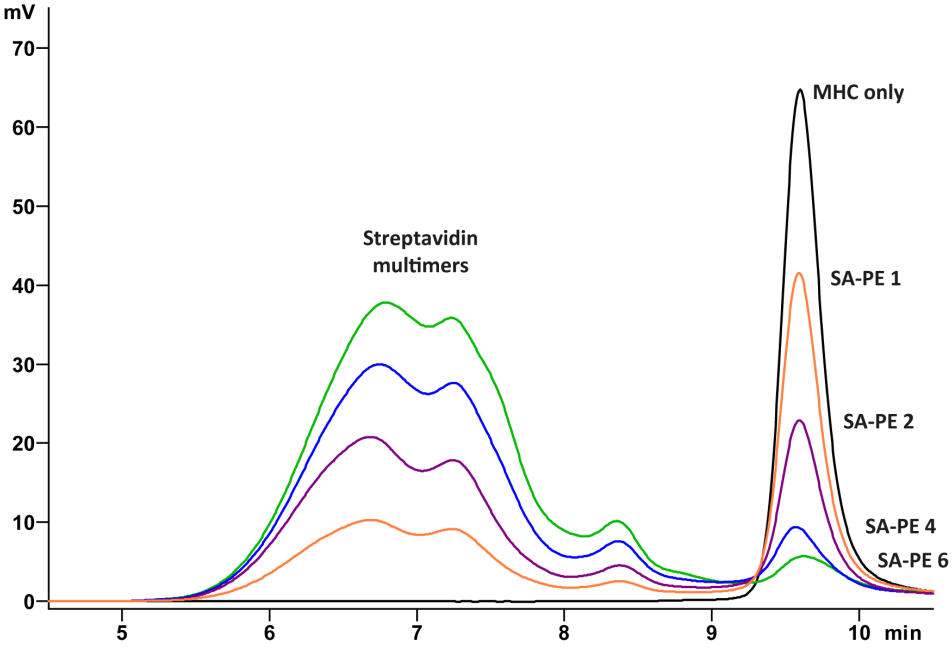

Figure 4. **Overlay of HPLC chromatograms that confirm biotinylation of pMHCI monomers.** When incubated with increasing ratios of PE-conjugated streptavidin (SA-PE) the monomer peak decreases, whereas the streptavidin multimer peak increases, indicating the formation of pMHCI multimers.

1. Prepare five samples in 1.5-ml Sarstedt tubes to determine the biotinylation efficiency in 100 µl pMHCI monomer solution (0.5 µM). Prepare each sample fresh before analysis.

   Add the components in the order listed. Keeping to this order will ensure the peptide is in solution and available for exchange and stabilization of MHCI. We typically prepare 10% extra to allow for variance when drawing up the sample for injection into the HPLC.

   PE can be bleached by UV light. Keep the SA-PE on ice and away from light as much as possible.

	pMHCI only	SA-PE 1	SA-PE 2	SA-PE 4	SA-PE 6
PBS	Fill to 100 µl final volume				
Exchange peptide	Optional, 50 µM final				
pMHCI monomers	0.5 µM final				
SA-PE (µl)	-	1	2	4	6

2. Incubate the sample on ice in the dark for 5 min to allow all biotinylated monomers to bind.
3. Sediment aggregates by centrifugation for 1 min at 16,000 × *g*, room

temperature.

4. Analyze each sample by HPLC using a gel filtration column (e.g., 300 × 7.8 mm BioSep SEC-s3000 column (Phenomenex) with PBS as running buffer.

   By adding sequential ratios of SA-PE the degree of biotinylation of pMHCI monomers can be determined.

Reagents and solutions

Biotinylation solution (1 ml)
40 µl 5 mM D-biotin in 100 mM NaP, pH 7.5 (0.2 mM final concentration)
40 µl 0.5 M ATP in 1 M Tris•Cl, pH 9.5 (20 µM final concentration)
1.5 µg BirA biotin ligase (commercial sources, such as Avidity)
200 µl 10× ligase buffer (50 mM $MgCl_2$ in 0.2 M Tris•Cl, pH 7.5; 10 mM final $MgCl_2$ concentration)
80 µl cOmplete EDTA-free Protease Inhibitor Cocktail (1 tablet in 2 ml Milli-Q water)
640 µl Milli-Q water
Prepare fresh

Detergent buffer
0.2 M NaCl
1% (w/v) sodium deoxycholate monohydrate
1% (v/v) Nonidet P-40 substitute
20 mM Tris•Cl (pH 7.5)
2 mM EDTA
Store up to one year at room temperature

DNase I stock solution, 10 mg/ml
10 mg/ml DNase I (Roche Diagnostics)
50% (v/v) glycerol
150 mM NaCl
Store up to 1 year at -20°C

Folding buffer (50 ml)
4.2 g L-arginine-HCl (400 mM final concentration)
5 ml 1 M Tris•Cl, pH 8 (100 mM final concentration)
0.2 ml 0.5 M EDTA (2 mM final concentration)
5% (v/v) glycerol
Adjust to 47 ml with Milli-Q water
Filter sterilize through a 0.22-µm filter, and store at 4°C for at least a few weeks

Immediately before folding reaction, add:
76.8 mg or 2.5 ml 100 mM reduced glutathione (5 mM final concentration)
16.4 mg or 0.5 ml 50 mM oxidized glutathione (0.5 mM final concentration)
0.5 tablet cOmplete EDTA-free Protease Inhibitor Cocktail (Roche Diagnostics)
Adjust to 50 ml total with Milli-Q water if necessary

Lysis buffer
50 mM Tris•Cl (pH 8)
25% (w/v) sucrose
1 mM EDTA
Filter sterilize and store at 4°C for up to 1 year

Triton wash buffer
50 mM Tris•Cl (pH 8)
100 mM NaCl
1 mM EDTA (pH 8)
0.5% (v/v) Triton X-100
Filter sterilize and store at 4°C for up to 1 year

COMMENTARY

Background Information
The ability to distinguish between healthy and infected or mutated cells is crucial for maintaining the balance between immunity and tolerance. This immune recognition is mediated by T cells, the key players of the highly specific adaptive arm of immunity. By displaying peptides derived from intracellular proteins on their surface, all nucleated cells can provide cytotoxic $CD8^+$ T cells with a glimpse of the ongoing processes inside the cell. Upon recognition of a non-self (i.e. viral or mutated) peptide $CD8^+$ T cells become activated, resulting in proliferation and killing of the target cell. After clearance of the infection or cancer most $CD8^+$ T cells disappear, but some remain to become memory T cells. The memory response is much faster than the first response and ensures that the infection will be rapidly cleared in case of re-infection with the same pathogen.

The molecules responsible for presentation of intracellular peptides are major histocompatibility complex class I (MHCI) molecules, heterotrimeric complexes that consist of an immunoglobulin (Ig)-like heavy chain, beta-2 microglobulin (β2m) and the peptide that resides in a binding groove formed by two α helices in the heavy chain. MHCI typically binds peptides of 8-10 amino acids that have been generated by proteasomal processing. These peptides fit in a peptide-binding groove that is closed at two ends, thus fixing the length of peptides.

Longer peptides can bind with the two ends of the peptide fixed and the center of the peptide bulging out of the binding groove. Which peptides bind is determined by the interactions between the amino acid side chains of the peptide and the binding pockets present in the MHC's specific peptide-binding groove. The MHC heavy chain is highly polymorphic, which means that many variants exist due to mutation, recombination and gene conversion. For this reason, MHCI (and MHCII, the other predominant polymorphic protein class) are the major transplantation antigens. Most of the polymorphisms are found in the DNA regions that code for the binding groove and therefore the location and nature of the binding pockets differs between MHCI subtypes. As a consequence each subtype (allele) has its preferred peptide motifs. Every individual has three MHC class I heavy chain genes that in human are named HLA-A, HLA-B and HLA-C. Since these can differ between parents, each human individual expresses three to six different allotypes. This collection of HLAs provides broad protection against intracellular pathogens, since different peptide fragments of their proteins can be presented by different MHCI alleles.

Cytotoxic T cells distinguish between self and non-self peptides through their T cell receptors (TCRs). These TCRs are highly diverse and recognize only specific peptide-MHCI (pMHCI) combinations. The frequency of a specific T cell in circulation is typically low if it has never encountered its cognate antigen and therefore analyzing T cell frequencies in blood or tissue samples provides valuable information on an individual's immune status. In addition, $CD8^+$ T cells are potent targets for immune therapy due to their cytotoxic activity directed only at infected or mutated cells. Characterizing and visualizing $CD8^+$ T cell responses using MHCI multimers enables the study of antigen-specific T cell populations and the efficacy of immune intervention strategies.

To facilitate parallel production of multimers with different specificities a number of peptide exchange technologies have been developed. These methods allow the folding of one large batch of pMHCI monomers and the exchange of the template peptide using chemicals or dipeptides as catalysts, or by cleaving a UV-labile peptide[14-18]. We have recently developed an exchange technology that does not rely on chemicals or UV that can damage the protein, but instead uses temperature to induce exchange (Fig. 1)[6]. Our method was based on the finding that MHCI on-rates of peptides with various affinities are comparable at a range of temperatures, but off-rates increase with temperature[19]. For both HLA-A*02:01 and $H\text{-}2K^b$ we have designed template peptides with an affinity that is high enough for efficient folding at 4°C, but low enough for dissociation at elevated temperatures. This novel exchange technology is superior to preceding techniques in its potential for peptide exchange on MHC multimers, reducing pre-staining handling time even further.

Critical Parameters and Troubleshooting

The folding buffer is an aqueous solution and therefore template peptides with poor water solubility may precipitate, as may the peptides used for exchange, which is performed in PBS. We therefore recommend to use only peptides from stocks in DMSO, preferably sonicated before use, both for folding and exchange. Filtering the folding buffer removes precipitates, thus increasing folding yields.

The conditional monomers and multimers produced through this protocol are sensitive to elevated temperatures. Therefore as soon as they are folded, pMHCI monomers and other reagents used should be kept on ice and (micro)centrifuges should be kept at 4°C. Peptides used for folding should be very pure (>99%). Since the peptides used for thermal exchange have a low affinity for MHCI any impurity in the form of a peptide may result in folding of anincorrect complex. Presence of a truncated higher-affinity peptide may result in a stable complex not suitable for thermal exchange. By checking the exchange performance of every batch of pMHCI monomers this undesirable stabilization can be discovered timely. Likewise, we recommend to determine the degree of biotinylation for every batch of biotinylated pMHCI. Failure to saturate all streptavidin binding sites results in lower order multimers (trimers or even dimers) that may poorly bind TCRs due to lower avidity. This would result in decreased staining efficiency and a higher background signal.

The efficiency of exchange is related to the affinity of the exchange peptide. Lower-affinity peptides are less potent in stabilizing MHCI at elevated temperatures and therefore exchange for low-affinity peptides may be less efficient at the exchange conditions.

Understanding Results

The efficiency of the MHCI folding reaction is dependent on the peptide used for folding; in general folding with higher affinity peptides results in a higher yield. Since the template peptide should have a low affinity to allow temperature-mediated exchange, folding yields are expected to be low. We have previously observed yields of ~25-30% for HLA-A*02:01-IAKEPVHGV (~800-1000 µg from a 50-ml folding reaction) and ~2-5% for H-2K^{b}-FAPGNAPAL (~70-170 µg from a 50-ml folding reaction).

Time Considerations

Folding, biotinylation and purification of pMHCI monomers (Basic Protocol 1) takes 5-6 days, of which 3-4 days are merely incubation time and can be spent otherwise. Monomers can be stored in a -80°C freezer until tested (Basic Protocol 2) or multimerized (Basic Protocol 3), which only takes little time. This is not different from conventional MHCI multimer production. Peptide exchange (Basic Protocol 4) takes only minutes for multimers of H-2K^{b}-FAPGNAPAL and 3 hours

for multimers of HLA-A*02:01-IAKEPVHGV. Bacterial expression of MHCI heavy chains and β2m (Support Protocol 1) takes about a week, including folding of β2m (Support Protocol 2). These procedures need to be executed only occasionally, since large batches can be produced and stored for later use. Determining the biotinylation efficiency (Support Protocol 3) takes a few hours, depending on the HPLC system and column used.

Acknowledgements

The authors would like to thank Veerle M. Luimstra for critical reading of the manuscript.

This work was supported by a grant from the Institute for Chemical Immunology (ICI, to H. Ovaa and J. Neefjes) and grants from the Second Affiliated Hospital of Xi'an Jiaotong University and National Natural Science Foundation of China (grant numbers 81700691 and 81870536 to M.A. Garstka). This work is part of Oncode Institute, which is partly financed by the Dutch Cancer Society.

J.J. Luimstra, M.A. Garstka, J. Neefjes and H. Ovaa are listed as inventors on an international patent application (WO/2019/083370 A1) owned by Stichting Het Nederlands Kanker Instituut-Antoni van Leeuwenhoek Ziekenhuis, Leids Universitair Medisch Centrum.

References

1. Altman, J.D., *et al.* Phenotypic analysis of antigen-specific T lymphocytes. *Science* **274**, 94-96 (1996).
2. Bentzen, A.K., *et al.* Large-scale detection of antigen-specific T cells using peptide-MHC-I multimers labeled with DNA barcodes. *Nat Biotechnol* **34**, 1037-1045 (2016).
3. Hadrup, S.R., *et al.* Parallel detection of antigen-specific T-cell responses by multidimensional encoding of MHC multimers. *Nat Methods* **6**, 520-526 (2009).
4. Newell, E.W., *et al.* Combinatorial tetramer staining and mass cytometry analysis facilitate T-cell epitope mapping and characterization. *Nat Biotechnol* **31**, 623-629 (2013).
5. Ljunggren, H.G., *et al.* Empty MHC class I molecules come out in the cold. *Nature* **346**, 476-480 (1990).
6. Luimstra, J.J., *et al.* A flexible MHC class I multimer loading system for large-scale detection of antigen-specific T cells. *J Exp Med* **215**, 1493-1504 (2018).
7. Rodenko, B., *et al.* Generation of peptide-MHC class I complexes through UV-mediated ligand exchange. *Nat Protoc* **1**, 1120-1132 (2006).
8. Toebes, M., Rodenko, B., Ovaa, H. & Schumacher, T.N. Generation of peptide MHC class I monomers and multimers through ligand exchange. *Curr Protoc Immunol* **Chapter 18**, Unit 18 16 (2009).
9. Garboczi, D.N., Hung, D.T. & Wiley, D.C. HLA-A2-peptide complexes: refolding and crystallization of molecules expressed in Escherichia coli and complexed with single antigenic peptides. *Proc Natl Acad Sci U S A* **89**, 3429-3433 (1992).
10. Ghallager, S.R. One-dimensional SDS gel electrophoresis of proteins. *Curr Protoc Immunol* **75**, 8.4.1-8.4.37 (2006).
11. Sasse, J., & Gallagher, S.R. Staining Proteins in Gels. *Curr Protoc Immunol* **58**, 8.9.1–8.9.25 (2003).
12. Hagel, L. Gel-filtration chromatography. *Curr Protoc Mol Biol* **44**, 10.9.1–10.9.2 (1998).
13. Davis, M.M., Altman, J.D. & Newell, E.W. Interrogating the repertoire: broadening the scope of peptide-MHC multimer analysis. *Nat Rev Immunol* **11**, 551-558 (2011).
14. Toebes, M., *et al.* Design and use of conditional MHC class I ligands. *Nat Med* **12**, 246-251 (2006).
15. Amore, A., *et al.* Development of a hypersensitive periodate-cleavable amino acid that is methionine- and disulfide-compatible and its application in MHC exchange reagents for T cell characterisation. *Chembiochem* **14**, 123-131 (2013).
16. Choo, J.A., *et al.* Bioorthogonal cleavage and exchange of major histocompatibility complex ligands by employing azobenzene-containing peptides. *Angew Chem Int Ed Engl* **53**, 13390-13394 (2014).
17. Saini, S.K., *et al.* Dipeptides catalyze rapid peptide exchange on MHC class I molecules. *Proc Natl Acad Sci U S A* **112**, 202-207 (2015).
18. Rodenko, B., *et al.* Class I major histocompatibility complexes loaded by a periodate trigger. *J Am Chem Soc* **131**, 12305-12313 (2009).
19. Garstka, M.A., *et al.* The first step of peptide selection in antigen presentation by MHC class I molecules. *P Natl Acad Sci USA* **112**, 1505-1510 (2015).

Internet Resources

http://www.cbs.dtu.dk/services/NetMHC/
Web site used to predict peptide-MHCI binding affinities.

7

Screening for neoantigen-specific CD8+ T cells using thermally-exchanged pMHCI multimers

Jolien J. Luimstra[1], Christina Heeke[2], Jitske van den Bulk[3], Brett Hos[4], Ferry Ossendorp[4], Noel F.C.C. de Miranda[3], Sine R. Hadrup[2], Jacques Neefjes[1], and Huib Ovaa[1]

[1]Department of Cell and Chemical Biology, Leiden University Medical Center, Leiden, The Netherlands
[2]Section for Immunology and Vaccinology, National Veterinary Institute, Technical University of Denmark, Copenhagen, Denmark
[3]Department of Pathology, Leiden University Medical Center, Leiden, The Netherlands
[4]Department of Immunohematology and Blood Transfusion, Leiden University Medical Center, Leiden, The Netherlands

Abstract

A role for T cell immunity in the clearance of tumor cells has well been established and is effectively put to use in therapies that selectively boost anti-tumor responses. It is proposed that the efficacy of checkpoint blockade immunotherapy largely relies on T cell reactivity to neoantigens: peptides derived from mutated (onco)proteins that are presented on major histocompatibility complex class I. Rapid detection of neoantigen-reactive T cells can support the development of specific immunotherapies as well as monitor response to therapy. In this study we aim to identify responses directed at HLA-A*02:01- or H-2K^{b}-binding neoantigens predicted from human colorectal cancer patients and from the murine colorectal cancer model MC38, respectively. We generated panels of DNA-barcoded major histocompatibility class I complexes loaded with predicted neoantigens using thermal MHC exchange technology and used them to identify T cell specificities from human and murine cell samples. We provide first evidence of the feasibility of the technique by confirming previously detected viral responses from healthy donors in two separate experiments. However, identification of true mouse or human neoantigens has proven challenging. Low cell counts and presumably the low neoantigen frequencies were bottlenecks in these first tests. Future work will focus on resolving the technical difficulties and on increasing the sensitivity of the technology.

Introduction

Oncogenesis is accompanied by the occurrence of somatic mutations in cancer cells. DNA nucleotide substitutions as well as insertions or deletions at protein-coding regions can result in the expression of mutated antigens[2]. Presentation of these so-called neoantigens on major histocompatibility complexes (MHCs) on the cell surface flags tumor cells for detection by neoantigen-specific T cells, potentially resulting in tumor clearance[3]. Due to their somatic origin, later in life, no central tolerance has been raised specifically against neoantigens supporting their potential as immunotherapeutic targets[4]. Unlike traditional tumor-associated antigens (TAAs) originating from overexpressed self-proteins, neoantigens are solely expressed on tumors and therefore neoantigen-based vaccines are expected to less frequently induce autoimmunity[5]. For this reason neoantigens are hot targets in the development of cancer therapeutics[6,7]. Vaccination with neoantigens through various delivery modes has resulted in therapeutic benefit in a number of preclinical and clinical studies[8-11].

Discovery of neoantigen-directed T cell reactivity in cancer patients is of high interest as it can support immunotherapeutic approaches. Unfortunately,

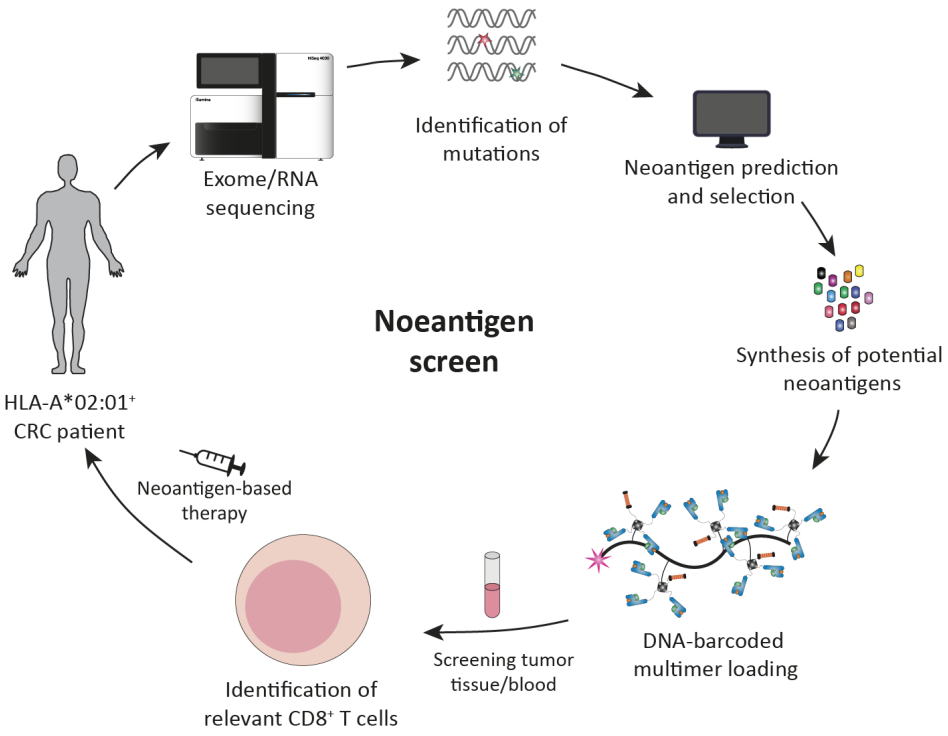

Figure 1. **Workflow of the anticipated neoantigen screen.** RNA and exomes from HLA-A*02:01+ colorectal cancer (CRC) patients are sequenced to identify mutations in expressed proteins. Potential neoantigens are predicted based on their HLA-A*02:01 binding motif. These peptides are then synthesized and loaded on conditional pMHCI multimers through thermal exchange. Consequently, these multimers can be used for screening of neoantigen-specific CD8+ T cells from patient material.

the detection of neoantigen-reactive T cells can prove challenging at several levels. Since neoantigens arise from patient-specific mutations they have to be identified on an individual basis[12-14]. Furthermore, most cancer mutations occur outside mutation "hotspots" and affect so-called "passenger" genes that are generally not analyzed in targeted, diagnostic procedures. By performing DNA sequencing of healthy and tumor tissues, somatic mutations can be identified and, in combination with RNA sequencing, transcribed putative neoantigens can be selected for a given cancer. The functional detection of neoantigen-reactive T cells often relies on the selection of mutated peptides predicted to bind a patient's MHC class I alleles[15,16]. Major efforts contribute to the development of advanced bioinformatic tools and algorithms, but these often fail to achieve accurate prediction[17-19].

Physical measurements, such as mass-spectrometric analyses of peptides eluted from tumor cells or tumor-infiltrating T cells (TILs) or functional assays to

measure cytokine secretion, are used to validate predicted neoantigens, but they require large numbers of cells and often lack sensitivity[20]. Another strategy is to characterize neoantigen-specific CD8+ T cells using pMHCI multimers. By using one fluorescent label per peptide, several multimers can be used simultaneously to identify specific T cells from a larger population using flow cytometry[21]. Conventional preparation of multimers required separate folding with each peptide for every specificity, but the development of several exchange techniques allows for the generation of multiple specificities in parallel[22-25]. We have recently described a novel exchange technology based on an increase in temperature, which is superior to preceding techniques in its potential for exchange on MHC

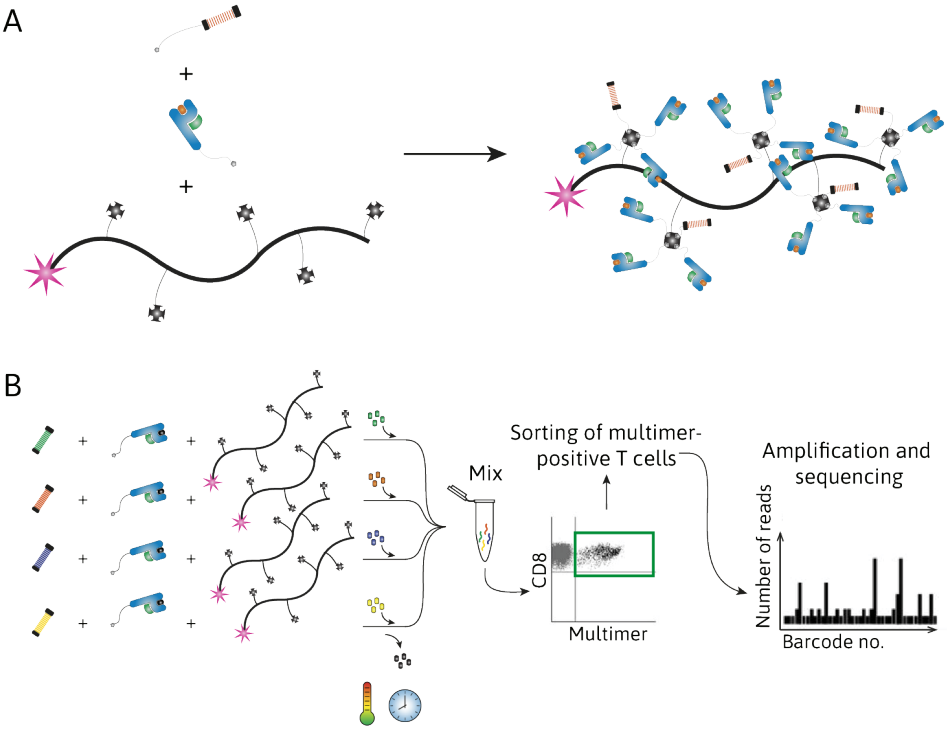

Figure 2. **Overview of generation and use of temperature-exchangeable DNA-barcoded MHCI multimers.** (A) DNA barcodes and MHCI monomers, both biotinylated, are added to fluorescently-labelled streptavidin-conjugated dextran backbones to form temperature-exchangeable DNA-barcoded MHCI multimers. (B) Dextran backbones and MHCI monomers with exchangeable peptide are combined with a specific DNA barcode per well. Each multimers is then loaded with a desired peptide and incubated at set exchange conditions. After exchange is complete, multimers are pooled, concentrated and added to a cellular suspension, from which multimer-positive CD8+ T cells are sorted on their fluorescent label. The DNA barcodes are then amplified using PCR and sequenced to identify the specific antigen-responsive T cells in the sample. (Picture adapted from Bentzen et al.[1]).

multimers, reducing pre-staining handling time even further[26].

In flow cytometry the number of parameters that can be measured simultaneously is limited by the number of fluorophores that can be detected simultaneously. Combinatorial coding has greatly increased the number of combinatorial parameters up to 63, but for large screens this number is insufficient[27,28]. Bentzen et al. devised a strategy to overcome this restriction by labelling with DNA barcodes[1]. Each multimer consists of a PE-labelled dextran backbone that accommodates multiple streptavidin moieties for conjugation of biotinylated MHC monomers and 25-oligonucleotide barcodes. Using this technology over 1000 T cell specificities can be detected from one sample. Labelled T cells are sorted using FACS based on their PE label, followed by amplification of the DNA barcodes using PCR and subsequent analysis with next-generation sequencing (NGS).

In this study, we combined our thermal exchange technology with DNA barcoding to screen for neoantigens in a colorectal cancer (CRC) mouse model (MC38) and in human HLA-A*02:01+ patients (Fig. 1). A group of CRC patients exhibit high microsatellite instability, giving rise to a high frequency of mutations and consequently this may result in a high number of neoantigens and increased responsiveness to immunotherapy[29]. We aim to identify bona fide neoantigens displayed by these patients in order to unravel therapeutic targets for immunotherapy.

Results

HLA-A*02:01 proof-of-principle

As a proof-of-principle we used thermally-exchanged multimers to detect virus-specific CD8+ T cells in buffy coats from three healthy HLA-A*02:01+ donors. We selected eight common virus epitopes (see Table 1) originating from influenza A virus (IAV), Epstein-Barr virus (EBV), cytomegalovirus (CMV) or HIV, for which specific T cells were previously detected in one or more of the three buffy coats used in this experiment. Because the signal-to-noise ratio would be low when staining with only eight different DNA-barcoded pMHCI multimers, the selection of peptides was included in a larger panel consisting of 48 melanoma antigens (data not shown). This total of 56 peptides were loaded on DNA-barcoded HLA-A*02:01 multimers using thermal peptide exchange as depicted in Figure 2, A and B, and described in the Materials and Methods section. Next, these were used for staining of the buffy coats obtained from the HLA-A*02:01+ volunteers. CD8+multimer+ T cells were isolated using FACS and DNA barcodes in this population were identified by next-generation sequencing (NGS). In all three buffy coats, viral responses were detected in earlier studies. Using DNA-barcoded

Table 1. **Viral epitopes used for thermal exchange and MHCI multimer staining of CD8+ T cells in buffy coats from healthy volunteers.**

#	Sequence	Origin	BC83	BC104	BC112
V1	GILGFVFTL	IAV MP1	0.00%	**0.06%**	0.01%
V2	CLGGLLTMV	EBV LMP2	0.00%	**0.04%**	0.01%
V3	GLCTLVAML	EBV BMLF1	**0.81%**	**0.17%**	**1.64%**
V4	FLYALALLL	EBV LMP2	**0.09%**	**0.04%**	**0.02%**
V5	NLVPMVATV	CMV pp65	0.01%	0.00%	**7.48%**
V6	YVLDHLIVV	EBV BRLF1	**0.88%**	**0.11%**	**0.21%**
V7	VLEETSVML	CMV IE1	0.00%	0.00%	0.01%
V8	ILKEPVHGV	HIV Pol	0.00%	0.00%	0.01%

Frequencies indicate estimated percentages of antigen-specific T cells from total CD8+ T cells determined by sequencing of DNA barcodes. Values highlighted in bold face and green indicate specificities previously detected in that patient. BC, buffy coat; CMV, cytomegalovirus; EBV, Epstein-Barr virus; HIV, human immunodeficiency virus; IAV, influenza A virus.

thermally-exchanged HLA-A*02:01 multimers we detected all of them in similar frequencies (Table 1, highlighted in bold and marked in green), demonstrating the experimental feasibility of our approach.

Screening for neoantigens predicted from HLA-A*02:01+ CRC patients

After establishing proof-of-principle we set out to validate neoantigens predicted for five HLA-A*02:01-expressing CRC patients. Cancer exomes and transcriptomes were sequenced and compared to healthy tissue to reveal somatic mutations potentially giving rise to neoantigens. From these potential neoantigens, HLA-A*02:01-binding peptides of high and intermediate affinity were predicted using NetMHC, yielding 6, 13, 17, 136 and 336 sequences for patients P1 to P5, respectively (see Table S3 for sequences). The eight common viral epitopes used in the proof-of-principle (Table 1), were included as an experimental control, as well as a non-exchanged negative control. Multimers loaded with the predicted neoantigens or viral antigens were pooled and used to screen for reactive CD8+ T cells from a number of samples obtained from the tumor, peripheral blood or lymph node, as well as buffy coats from two healthy volunteers. Additional TIL subsets were included for patients P2, P3 and P4, based on a study by Duhen et al.[30] They described a unique subset of CD8+ TILs present in the tumor microenvironment, but not peripheral blood, that express both CD39 (a T cell exhaustion marker often co-expressed with PD-1) and CD103 (a cadherin involved in cytotoxic lysis)[31,32]. They found that this subset of T cells is enriched for tumor-reactive T cells. Therefore we included TILs selected for expression of both (double positive, DP), either (single positive, SP) or none (double negative, DN) of these two markers in an attempt to detect higher neoantigen-specific T cell frequencies in the DP subset.

As expected, barcodes corresponding to viral peptides were retrieved in one of the healthy controls and in some of the patient samples (Fig. 3). The peptides corresponding to the top 10 barcode reads increased compared to baseline are listed in Table S4. Consistent with the proof-of-principle experiment, CD8+ T cells specific for viral peptides V3, V4 and V6 were detected in buffy coat (BC) 83. Viral antigens were also detected in a number of the patient samples, but not in all of the sample types from the same patient. In patient P3, viral responses were

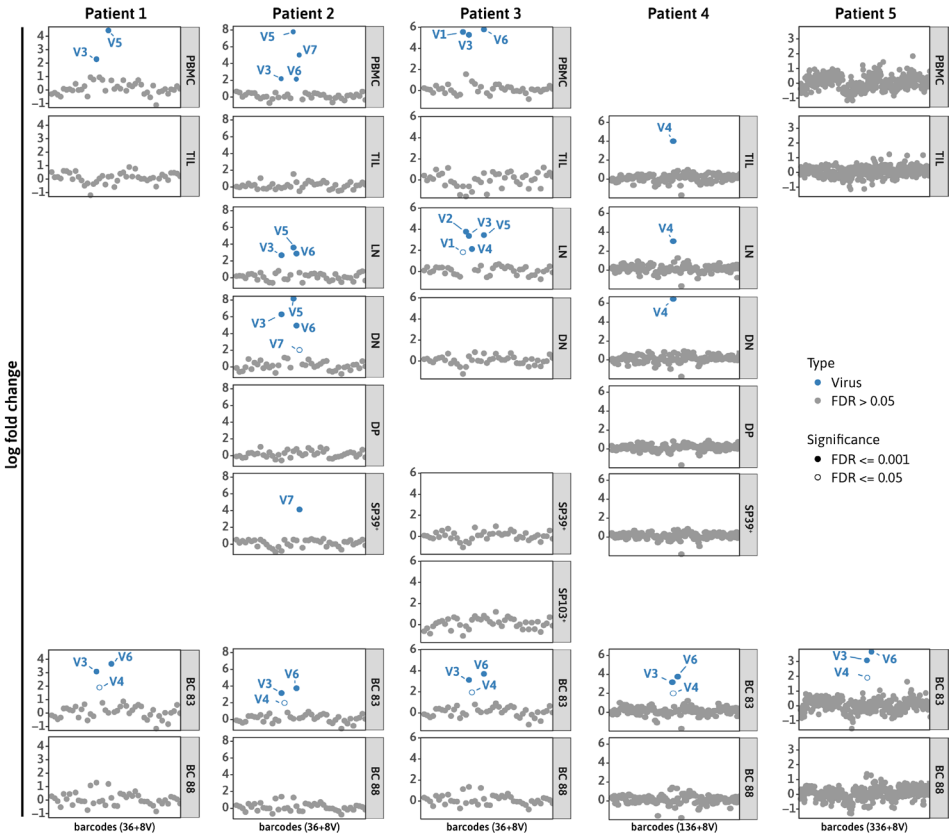

Figure 3. **Barcodes retrieved from the five human colorectal cancer (CRC) patients included in this study.** Patient samples were stained with a pool of HLA-A*02:01 multimers thermally exchanged for a selection of predicted neoantigens and eight common viral antigens (denoted with V, sequences listed in Table 1). Peptides predicted for patients P1, P2 and P3 were combined for a total of 36, while for patients P4 and P5, respectively, 136 and 336 neoantigens were predicted. Barcodes corresponding to viral antigens were detected in volunteer buffycoat 83 and in a number of patient samples. No significant neoantigen -specific responses were detected. FDR, false discovery rate; PBMCs, peripheral blood mononuclear cells; TIL, tumor-infiltrating lymphocyte; LN, lymph node; DN, double negative TIL subset expressing both CD39 and CD103; DP, double positive TIL subset; SP39+, single positive TIL subset expressing CD39; SP103+, single positive TIL subset expressing CD103.

detected in the lymph node and PBMC (peripheral blood mononuclear cell) samples, but not the TILs. TILs are likely more reactive against tumor antigens than against viral antigens, so this is not remarkable. In patient P2, virus-specific T cells were also detected in the double-negative (supposedly less tumor-reactive) TIL subset. Unfortunately, in none of the samples increased numbers of barcodes corresponding to predicted neoantigens were detected. This is not surprising, since neoantigen frequencies are generally low and hence do not give rise to high T cell numbers as viral antigens do. However, one of the peptides included in this set, TLVIYVARL (#268), was previously picked up in an activation assay using PBMCs from patient P4, but not in this screen. This hit will be validated in co-culture assays to determine if the result emanating from the first assay was a true or false positive.

Screening for MC38 neoantigen-specific CD8$^+$ T cells

To screen for neoantigens in the MC38 mouse model, a total of 1020 mutated H-2K^b binders were predicted based on expression profiles in tumor and healthy tissue. Neoantigen-specific responses were analyzed in naïve C57BL/6 mice that were untreated, vaccinated with irradiated MC38 tumor cells, or vaccinated with irradiated MC38 cells in combination with DMXAA (5,6-dimethylxanthenone-4-acetic acid). DMXAA is a murine STING (Stimulator of Interferon Genes) agonist that has demonstrated durable preclinical benefit by activating dendritic cells, anti-tumor CD8$^+$ T cells and inducing interferon (IFN-)β production[33,34]. Vaccination with irradiated tumor cells provides TAAs and danger signals (caused by radiation-induced immunogenic cell death) and consequently should result in priming and expansion of tumor-specific T cells. Mice were sacrificed one week after finishing a scheme of three vaccinations with two-week intervals.

In a first test of the experimental set-up, a small selection of 102 potential neoantigens were screened (see Table S5). These predicted neoantigens and OVA peptide SIINFEKL were loaded on DNA-barcoded H-2K^b multimers through thermal exchange and used to stain splenocytes isolated from vaccinated or untreated C57BL/6 mice. A no-peptide control was included as negative control and as experimental control OT-I T cells were spiked into the non-vaccinated sample (1% of total cells) for detection by SIINFEKL-loaded multimers.

After staining of the murine splenocytes, antigen-specific T cells were isolated using FACS. A clear population of multimer$^+$ CD8$^+$ T cells was visible in the non-vaccinated sample spiked with OT-I cells (Fig. 4, left), which was expected to consist of the SIINFEKL-specific OT-I T cells spiked in to the cell sample. However, even though the barcode corresponding to SIINFEKL (#104) was among the top 10 for the OT-I-spiked sample, only slightly more reads were detected in the sample compared to the baseline. This was the case for most barcodes: in all samples combined only two barcodes were detected above the significance threshold

Table 2. **Top 10 peptide specificities retrieved from the murine cell samples included in this study.**

		Used directly post exchange		
Sort count		204	221	573
	Sample	Non-vaccinated (+OT-I)	Vaccinated (MC38)	Vaccinated (MC38+DMXAA
Top 10 specificities	1	#24	#74	#17
	2	#89	#16	#16
	3	#63	#64	#64
	4	#60	#68	#63
	5	#87	#17	#28
	6	#70	#20	**#21**
	7	**#104**	#65	#24
	8	#12	#26	#78
	9	#72	#66	#20
	10	#74	#70	#15

Conditional H-2K^b multimers were exchanged for 102 predicted neoantigens and OVA peptide SIINFEKL. These were used to stain splenocytes isolated from non-vaccinated mice spiked with OT-I cells, mice vaccinated with irradiated MC38 tumor cells or from mice vaccinated with MC38 cells and DMXAA (5,6-dimethylxanthenone-4-acetic acid). Barcodes corresponding to peptides highlighted in red were detected at significantly increased levels (log fold change ≥2) compared to baseline reads. OVA peptide SIINFEKL is marked green in bold face; previously detected peptides are marked blue in bold face.

(log fold change ≥2). This can be explained by the low cell numbers used for staining, and consequently the low number of sorted cells (Table 2). After thawing splenocyte counts were relatively low, so that only 100,000-500,000 cells per condition could be included, when in fact 1,000,000-2,000,000 are preferred. The lower limit of detection is about 20 copies of a specific CD8+ T cell and this number is challenging to reach with low numbers of PBMCs. Repeating this screen with more cells will likely yield more relevant and more reproducible data.

Discussion

The discovery of immune checkpoints as anti-cancer targets has sparked the field of cancer immunotherapy. Blocking of inhibitory molecules, such as CTLA-4 or the PD-1/PD-L1 interaction, results in reestablishment of pre-existing immune responses[35,36]. Accordingly, responses to checkpoint inhibition are highest in cancers with a high mutational burden where more neoantigens can be generated[37,38]. Vice versa, the efficacy of checkpoint inhibition can be further increased by priming of anti-tumor T cells through neoantigen-based

therapies[39]. The success of these therapies relies on neoantigens and hence it is important to know their identity. Identification of mutations has become relatively straightforward with the development of NGS, but predicting the immunogenicity of predicted neoantigens is less trivial. In this study we set out to validate predicted neoantigens by characterizing neoantigen-specific immune responses using conditional pMHCI multimers. Thermal exchange technology provides an easy method to generate large numbers of specific MHCI multimers in parallel. Using DNA barcode labeling up to 1000 peptides can be tested from a single sample, thus greatly reducing the sample volume required for analysis. Especially in the tumor field this provides huge benefit compared to conventional multimer staining. It has long been established that peptides with a high affinity for their cognate MHCI are not necessarily more immunogenic and hence potent immunogenic peptides may be missed by applying strict selection parameters[40,41]. Combining MHCI exchange technology with DNA barcoding allows broadening of the selection criteria to also include less obvious potential neoantigens that would otherwise not be included in screens. The experiments described here are

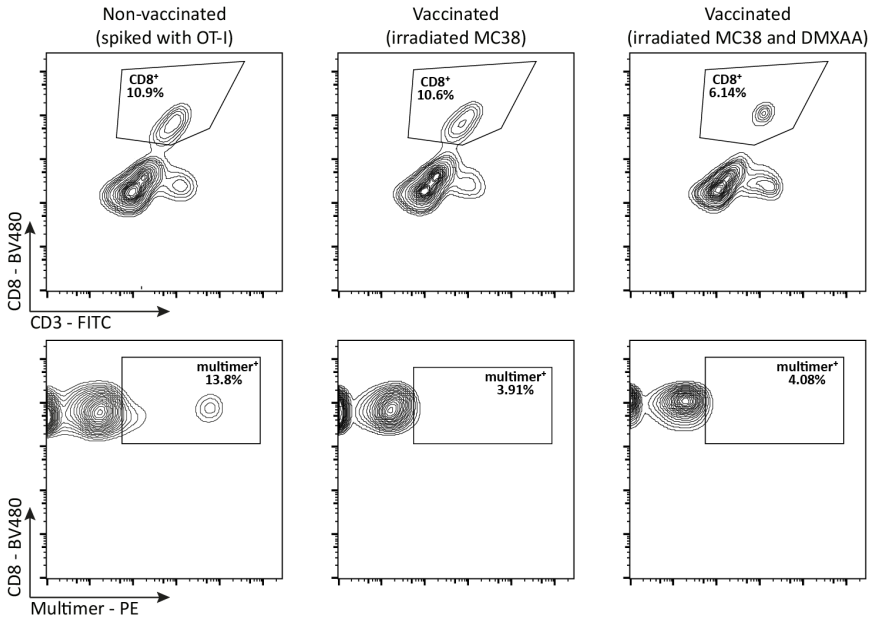

Figure 4. **FACS plots of MC38 splenocytes stained with a pool of 102 thermally-exchanged H-2K^b multimers (used immediately post exchange).** CD3$^+$CD8$^+$multimer$^+$ T cells were sorted based on fluorescence of the PE label conjugated to the multimerization backbone. Left: splenocytes isolated from non-vaccinated mice spiked with OT-I cells (1%). The population on the right likely shows OT-I cells stained with H-2K^b multimer exchanged for OVA peptide SIINFEKL. Center: splenocytes from mice vaccinated with irradiated MC38 tumor cells. Right: cells isolated from mice vaccinated with irradiated tumor cells and DMXAA (5,6-dimethylxanthenone-4-acetic acid).

a first step towards implementing DNA barcoding technology in combination with temperature-based MHC exchange technology to increase the throughput of the technology.

The screen performed with HLA-A*02:01 multimers exchanged for viral and melanoma epitopes served as a proof-of-principle, demonstrating that previously detected T cell responses against viral epitopes could be picked up using DNA-barcoded thermally-exchanged multimers. The fact that those same viral responses were detected in our human CRC patient screen was very promising, but in contrast no neoantigen barcodes were retrieved. Peptide #268 (TLVIYVARL) was shown to activate CD8+ T cells in PBMCs from patient P4, but in the pMHCI multimer screen we did not detect its corresponding barcode. This peptide is predicted to weakly bind HLA-A*02:01 and this may affect pMHCI multimer loading, although the predicted affinity of 235 nM is well beyond that of the template peptide IAKEPVHGV, which is 7,288 nM. Determining the exchange efficiency using HPLC can resolve whether impaired loading accounts for not detecting this peptide.

It is known that only few predicted peptides are bona fide neoantigens and that frequencies of neoantigen-specific T cells are low, hampering detection. Furthermore, in our study only a single MHCI allele was included, whereas each individual expresses up to six distinct HLA alleles. Inclusion of pMHCI multimers with additional patient-matched HLAs will undoubtedly increase the neoantigen discovery rate. Advancing thermal exchange technology will allow screening across the full range of HLA haplotypes expressed by each individual patient.

In an attempt to increase neoantigen-specific T cell frequencies, the mice used in our MC38 screen were vaccinated with irradiated MC38 tumor cells, with and without DMXAA. Despite FACS analysis clearly demonstrating a population in the OT-I spiked sample and the barcode corresponding to SIINFEKL turning up in the top 10 of elevated reads, no significant increase in reads compared to baseline was found. Due to the low cell count no T cell specificities were detected above the threshold and repetition of this screen with more cells will be necessary to demonstrate the potential of DNA-barcoded pMHCI screens for neoantigen discovery.

Materials and methods

Ethical approval

All animal experiments were approved by the animal ethics committee of the LUMC, which has been licensed by the Dutch Central Animal Experiments Committee. Experiments were performed by Federation of European Laboratory Animal Science Associations (FELASA)-accredited animal-handlers and monitored

by the animal welfare body according to the Dutch Act on animal experimentation (ex art. 14a, b, and c) and EU Directive 2010/63/EU ('On the protection of animals used for scientific purposes').

All patient material was collected under approval by the Medical Ethical Committee of the Leiden University Medical Centre (LUMC, protocol P15.282). Patient samples were anonymized and handled according to the medical ethical guidelines described in the Code of Conduct for Proper Secondary Use of Human Tissue of the Dutch Federation of Biomedical Scientific Societies. This research was conducted according to the recommendations outlined in the Helsinki declaration.

Human cell samples

PBMCs from patients were isolated from heparinized venous blood by use of Ficoll-Amidotrizoate (LUMC Pharmacy, Leiden, NL) density centrifugation. Tumor material and respective healthy colorectal and lymph node samples were obtained during surgery, cut into small fragments and digested using gentleMACS C tubes (Miltenyi Biotec), collagenase D (Roche) and DNAse I (Roche). The digested cells were incubated for 30 min at 37°C interrupted by three runs on the gentleMACS Dissociator (Miltenyi Biotec) and subsequently filtered by use of a 0.7 µm mesh filter. The tumor fragments and single cell digests were cryopreserved for analysis and culturing at later stages.

TIL collection was performed by culturing of tumor fragments in a 24-well plate with T cell medium (IMDM (Lonza BioWhittaker or Thermo Fisher), supplemented with 8% heat-inactivated pooled human serum, penicillin (100 IU/ml), streptomycin (100 µg/ml) and L-glutamine (4 mM)) and rIL-2 (1000 IU/ml). After 14-21 days of culturing, TILs were harvested and cryopreserved for later use. To increase the number of T cells available for screening, rapid expansion of TILs was performed by culturing with rIL-2 (3000 IU/ml), OKT3 (Miltenyi Biotec, 60 µg/ml) and irradiated (40 Gy) feeder cells (100-200×) for 4-5 days. Subsequently, culturing was continued up to two weeks in T cell medium supplemented with rIL-2 (3000 IU/ml).

A mixed lymphocyte tumor culture (MLTC) was performed by co-culturing PBMCs with lethally irradiated (100 Gy) tumor fragments in T cell medium. Recombinant human IL-4 was added at day 0 to prevent NK cell outgrowth. $PD1^+$ cell selection was performed after day 1 of co-culture. Cells were harvested and stained with PE-conjugated anti-PD1 antibodies (BD Biosciences). Subsequently, MACS was performed by use of magnetic anti-PE beads (Miltenyi Biotec) and magnetic separation (MS) columns (Miltenyi Biotec). $PD1^+$ cells and flow through were each cultured with irradiated (40 Gy) feeder cells (100-200×) and high-dose rIL-2 (3000 IU/ml). Culture medium containing rIL-2 was refreshed on alternate days. Cells were cryopreserved after a culturing period of two weeks.

CD39/CD103 double negative (DN), single positive (SN) and double positive (DP) TILs were isolated as described by Duhen et al.[30]. Briefly, cryopreserved PBMCs and TILs were thawed and enriched for T cells using a T cell enrichment kit (STEMCELL Technologies) and for TILs using EpCAM beads (STEMCELL Technologies). The enriched fractions were then labeled and sorted on a FACSAria II cell sorter (BD Biosciences). From the TILs memory T cell ($CD3^+CD4^-CD8^+CD45RA^-CR7^{+/-}$) subsets were sorted as $CD39^-CD103^-$ (DN), $CD39^-CD103^+$ (SP), and $CD39^+CD103^+$ (DP). For expansion sorted T cell subsets were cultured in complete RPMI 1640 medium supplemented with 2 mM glutamine, 1% (v/v) nonessential amino acids, 1% (v/v) sodium pyruvate, penicillin (50 U/ml), streptomycin (50 µg/ml), and 10% fetal bovine serum (Hyclone).

Sorted T cells were stimulated polyclonally with 1 µg/ml Phytohemagglutinin A (PHA, Sigma) in the presence of irradiated (40 Gy) allogeneic feeder cells (PBMC; 2×10^5 cells/well) and 10 ng/ml of IL-15 (BioLegend) in a 96-well round-bottom plate (Corning/Costar). T cell lines were maintained in complete medium with IL-15 for 2-3 weeks and then cryopreserved until analysis.

Murine cell samples

Female C57BL/6 mice of 8-10 weeks were purchased form Envigo, Harlan Laboratories and acclimatized for 1 week to the animal facility of the LUMC. The mice were housed in individually-ventilated-cage (IVC) systems in specific pathogen-free conditions and kept at room temperature. MC38 (murine colon carcinoma) cells were cultured in IMDM medium (Lonza) supplemented with 8% Fetal Calf Serum (FCS, Greiner), 100 IU/ml penicillin/streptomycin (Gibco), 2 mM glutamine (Gibco) and 25 mM 2-mercaptoethanol (culture medium). Cell lines were mycoplasma- and MAP-tested before injection. Mice were subcutaneously injected thrice in the right-flank with 5×10^6 irradiated (15,000 rads) MC38 cells in 200 µL of PBS with a two week interval, whereby one group of MC38 injections was adjuvanted with 100 µg of DMXAA (5,6-dimethylxanthenone-4-acetic acid, InvivoGen).

Spleens from the mice were obtained one week after the final injection and mashed on single cell strainers with the blunt end of a 5 ml syringe and washed with culture medium. Cellular precipitates after centrifugation were treated with 5 ml of lysis buffer for 3 minutes at room temperature and subsequently washed with culture medium. Splenocytes were frozen in 10% DMSO in FCS at a concentration of 10×10^6 cells/ml and stored in liquid nitrogen. Similarly, OT-I/Thy1.1/CD45.2 cells were obtained from the spleens of in-house bred transgenic mice, although samples were enriched for $CD8^+$ lymphocytes (Mouse CD8 T Lymphocyte Enrichment Set, BD IMag) and frozen at a concentration of 4×10^6 cells/mL.

Peptide prediction and synthesis

For exome sequencing, reads were mapped against the human reference genome (hg38) using the Burrows-Wheeler Aligner (BWA-mem version 0.7.15) algorithm with default parameters[42]. Duplicate reads were removed using Picard Tools (http://picard.sourceforge.net). Genome Analysis Toolkit (GATK version 3.8; Broad Institute) was used for base quality recalibration[43]. Subsequently, single-nucleotide variants and indels were called using a combination of three popular software tools: muTect 2, varScan 2 and Strelka[44-46]. The resulting vcf files were combined into a single file using GATK CombineVariants. Variants were then functionally annotated using the ensembl Variant Effect Predictor (VEP)[47]. Variants annotated as protein disrupting or altering were further investigated if at least one read with the alternative allele was present in the RNAseq data. Reads generated by RNAseq were mapped against the same hg38 genome build using gsnap[48]. Integrative Genomics Viewer (IGV) was used for visually inspecting variants[49,50]. Manual review of aligned reads was used to reduce the risk of false positives and incorrect calls[51]. Prediction of binding to HLA-A*02:01 was performed for 8-12 amino acid peptide sequences using NetMHC and NetMHCpan. All strong and weak binders were selected for multimer screening. Murine MC38 neoantigen prediction was performed as described by Hos et al.[52]

Peptides were synthesized in our lab using standard solid-phase peptide synthesis or ordered from Pepscan. Synthesis was performed using Syro I and Syro II synthesizers using *N*-methyl-2-pyrrolidone as solvent. Resins and amino acids were purchased from Nova Biochem. Peptides were purified by reversed-phase HPLC over a preparative Waters X-bridge C18 column in a Waters HPLC system using water/acetonitrile mixtures containing 0.1% TFA. Peptide purity and composition were analyzed sample-wise by LC-MS using a Micromass LCT Premier mass spectrometer (Waters) equipped with a 2795 separation module (Alliance HT) and 2996 photodiode array detector (Waters). The samples were separated using a water/acetonitrile gradient over a Kinetix C18 column (Phenomenex). Analysis was performed using MassLynx 4.1 software (Waters Chromatography).

Multimer preparation

Temperature-exchangeable HLA-A*02:01-IAKEPVHGV and H-2K^{b}-FAPGNAPAL complexes were expressed and folded essentially as described previously[24,26,53], with minor alterations. Folded complexes were concentrated using a 30 kDa MWCO PES Vivaflow 200 protein concentrator system (Sartorius), driven by a Masterflex L/S peristaltic pump. Consequently the buffer was exchanged for 300 mM NaCl and 20 mM Tris•Cl, pH 8 using a NAP-10 column. Samples were filtered using a Spin-X column and biotinylated overnight using BirA ligase, supplemented with ATP, biotin and protease inhibitors. The following day samples were concentrated using Amicon Ultra-15 30 kDa MWCO centrifugal filter units (Merck Millipore)

and purified by gel filtration size exclusion chromatography (300 mM NaCl and 20 mM Tris•Cl, pH 8; Superdex 75 16/600 column, GE Healthcare) on an NGC system (Bio-Rad). After another round of concentration to 2-4 mg/ml using Amicon Ultra-15 30 kDa filters, they were snap-frozen and stored at -80°C in the same buffer supplemented with 15% glycerol. Biotinylation was verified by incubation of biotinylated MHCI monomers with streptavidin, followed by gel filtration chromatography on a Shimadzu Prominence system equipped with a 300 × 7.8 mm BioSep SEC-s3000 column (Phenomenex) using PBS as mobile phase. Data were analyzed using Shimadzu LabSolutions software (version 5.85).

Multimers were assembled as described by Bentzen et al.[1]. Briefly, PE- and streptavidin-conjugated dextran backbones (Fina Biosolutions, final concentration 6.92×10^{-8} M) were added to 5'-biotinylated AxBy DNA barcodes (DNA Technology, sequences in Table S1 and Table S2), which were titrated per batch of dextran. After incubating for 30 min at 4°C MHCI monomers were added at a final concentration of 30 µg/ml, followed by another 30-min incubation at 4°C. To each well a different peptide was added at a final concentration of 60 µM, and plates were incubated at previously described exchange temperatures (5 minutes at room temperature for H-2K^{b} and 3 hours at 32°C for HLA-A*02:01). For stability and to saturate unoccupied streptavidin binding sites a solution containing 500 µM D-biotin, 100 µg/ml herring DNA, 0.5% BSA, 2 mM EDTA and 5% glycerol (in PBS) was added and incubated for 20 min on ice.

Barcode-labelled exchangeable multimers were centrifuged at 3300 × *g* for 5 min at 4°C to sediment aggregates and then pooled at 0.043 µg pMHC per sample. Pools were collected in reservoirs that were pre-saturated for at least 2 hours with 2% BSA to prevent sticking. Using (also pre-saturated) Vivaspin6 or Vivaspin20 centrifugal concentrators (100 kDa MWCO, Sartorius) to a volume of ~80 µl per sample. Concentrated pools were centrifuged for 5 min at 3300 × *g* before adding to cell suspension. A 5 µl aliquot was stored at -20°C for later use as baseline sample.

pMHCI multimer staining and sorting

Cryopreserved cell suspensions were thawed in and washed with RPMI supplemented with 10% FCS, and subsequently washed with barcode cytometry buffer (BCB; PBS with 0.5% BSA, 100 µg/ml herring DNA, 2 mM EDTA) and incubated with 50 nM dasatinib for 30 min at 37°C. For human samples 2×10^{6} cells and for murine samples ~4×10^{5} cells were stained with pooled DNA-barcoded multimers in 100 µl BCB total volume for 15 min at 37°C. Human samples were stained with antibody mix composed of anti-CD8-V510, dump channel FITC-conjugated antibodies against CD4, CD14, CD16, CD19 and CD40 (all BD Biosciences), and near-IR viability dye (Invitrogen), for 30 min at 4°C. Murine samples were stained with antibody mix composed of anti-CD3-FITC (BioLegend), anti-CD8-BV480

(BD Horizon) and near-IR viability dye (Invitrogen), for 30 min at 4°C. Cells were washed three times with BCB, filtered and fixed in 1% PFA for overnight storage.

Stained cells were washed three times in BCB prior to sorting on a FACSAria or FACSMelody (BD Biosciences) into pre-saturated tubes containing 200 µl BCB. From human samples the population of single, live $CD8^+$, $dump^-$, PE $(multimer)^+$ lymphocytes was sorted using FACSDiva (BD Biosciences) software. From murine samples single, live $CD8^+$, $CD3^+$, PE $(multimer)^+$ lymphocytes were sorted. Further analysis was performed using FACSDiva or FlowJo (FlowJo, LLC) software.

DNA barcode amplification and analysis

DNA barcodes were amplified using a Taq PCR Master Mix Kit with 0.3 µM appropriate forward- (with a distinct sample ID embedded) and reverse primers comprising Ion Torrent PGM 5' and 3' adaptors. Sorted cells (in less than 20 µl buffer) and the stored baseline aliquot (diluted 10,000× in H_2O) were amplified using a PCR program with the following conditions: 95°C 10 min; 36 cycles: 95°C 30 s, 60°C 45 s, 72°C 30 s and 72°C 4 min. PCR products were analyzed using gel electrophoresis (E-Gel, Invitrogen), pooled at similar concentrations according to visual inspection and then purified using the QIAquick PCR Purification kit (Qiagen) according to standard procedure. The amplified barcodes were sequenced at Sequetech (USA) or the LUMC Sequence Analysis Support Core (SASC, NL). Sequencing data were analyzed and visualized using the online tool 'Barracoda' (http://www.cbs.dtu.dk/services/barracoda) developed at DTU.

Acknowledgements

The authors thank Cami Talavera Ormeño and Paul Hekking (Department of Cell and Chemical Biology, LUMC, Leiden, Netherlands) for synthesis of peptides. We also thank Dina Ruano (Department of Pathology, LUMC, Leiden, Netherlands), for sequencing of the human CRC screen and assistance with analysis.

This work was supported by a grant from the Institute for Chemical Immunology (ICI, to H. Ovaa) and is part of Oncode Institute, which is partly financed by the Dutch Cancer Society.

Author contributions: J.J. Luimstra, J. Neefjes, and H. Ovaa conceived and designed the study with input from N. de Miranda and F. Ossendorp. J. van den Bulk prepared human cell samples and B. Hos prepared murine cell samples. N.F. de Miranda predicted peptides. J.J. Luimstra and C. Heeke generated DNA-barcoded multimers and performed T cell staining experiments. J.J. Luimstra wrote the manuscript with input from all authors.

References

1. Bentzen, A. K. *et al.* Large-scale detection of antigen-specific T cells using peptide-MHC-I multimers labeled with DNA barcodes. *Nat Biotechnol* **34**, 1037-1045, doi:10.1038/nbt.3662 (2016).
2. Schumacher, T. N. & Hacohen, N. Neoantigens encoded in the cancer genome. *Curr Opin Immunol* **41**, 98-103, doi:10.1016/j.coi.2016.07.005 (2016).
3. Tran, E. *et al.* Immunogenicity of somatic mutations in human gastrointestinal cancers. *Science* **350**, 1387-1390, doi:10.1126/science.aad1253 (2015).
4. Corthay, A. Does the immune system naturally protect against cancer? *Front Immunol* **5**, 197, doi:10.3389/fimmu.2014.00197 (2014).
5. Kreiter, S., Castle, J. C., Tureci, O. & Sahin, U. Targeting the tumor mutanome for personalized vaccination therapy. *Oncoimmunology* **1**, 768-769, doi:10.4161/onci.19727 (2012).
6. Schumacher, T. N. & Schreiber, R. D. Neoantigens in cancer immunotherapy. *Science* **348**, 69-74, doi:10.1126/science.aaa4971 (2015).
7. Aldous, A. R. & Dong, J. Z. Personalized neoantigen vaccines: A new approach to cancer immunotherapy. *Bioorg Med Chem* **26**, 2842-2849, doi:10.1016/j.bmc.2017.10.021 (2018).
8. Sahin, U. *et al.* Personalized RNA mutanome vaccines mobilize poly-specific therapeutic immunity against cancer. *Nature* **547**, 222-226, doi:10.1038/nature23003 (2017).
9. Bezu, L. *et al.* Trial watch: Peptide-based vaccines in anticancer therapy. *Oncoimmunology* **7**, e1511506, doi:10.1080/2162402X.2018.1511506 (2018).
10. Keskin, D. B. *et al.* Neoantigen vaccine generates intratumoral T cell responses in phase Ib glioblastoma trial. *Nature* **565**, 234-239, doi:10.1038/s41586-018-0792-9 (2019).
11. Ott, P. A. *et al.* An immunogenic personal neoantigen vaccine for patients with melanoma. *Nature* **547**, 217-221, doi:10.1038/nature22991 (2017).
12. Vita, R. *et al.* The immune epitope database (IEDB) 3.0. *Nucleic Acids Res* **43**, D405-412, doi:10.1093/nar/gku938 (2015).
13. Lundegaard, C. *et al.* NetMHC-3.0: accurate web accessible predictions of human, mouse and monkey MHC class I affinities for peptides of length 8-11. *Nucleic Acids Res* **36**, W509-512, doi:10.1093/nar/gkn202 (2008).
14. Capietto, A. H., Jhunjhunwala, S. & Delamarre, L. Characterizing neoantigens for personalized cancer immunotherapy. *Curr Opin Immunol* **46**, 58-65, doi:10.1016/j.coi.2017.04.007 (2017).
15. Karasaki, T. *et al.* Prediction and prioritization of neoantigens: integration of RNA sequencing data with whole-exome sequencing. *Cancer Sci* **108**, 170-177, doi:10.1111/cas.13131 (2017).
16. Wilson, E. A. & Anderson, K. S. Lost in the crowd: identifying targetable MHC class I neoepitopes for cancer immunotherapy. *Expert Rev Proteomics* **15**, 1065-1077, doi:10.1080/14789450.2018.1545578 (2018).
17. Altmann, D. M. New tools for MHC research from machine learning and predictive algorithms to the tumour immunopeptidome. *Immunology* **154**, 329-330, doi:10.1111/imm.12956 (2018).
18. Blaha, D. T. *et al.* High-Throughput Stability Screening of Neoantigen/HLA Complexes Improves Immunogenicity Predictions. *Cancer Immunol Res* **7**, 50-61, doi:10.1158/2326-6066.CIR-18-0395 (2019).
19. Bjerregaard, A. M. *et al.* An Analysis of Natural T Cell Responses to Predicted Tumor Neoepitopes. *Front Immunol* **8**, 1566, doi:10.3389/fimmu.2017.01566 (2017).
20. Bassani-Sternberg, M. *et al.* Direct identification of clinically relevant neoepitopes presented on native human melanoma tissue by mass spectrometry. *Nat Commun* **7**, 13404, doi:10.1038/ncomms13404 (2016).
21. Altman, J. D. *et al.* Phenotypic analysis of antigen-specific T lymphocytes. *Science* **274**, 94-96 (1996).
22. Saini, S. K. *et al.* Dipeptides catalyze rapid peptide exchange on MHC class I molecules. *Proc Natl Acad Sci U S A* **112**, 202-207, doi:10.1073/pnas.1418690112 (2015).
23. Amore, A. *et al.* Development of a hypersensitive periodate-cleavable amino acid that is methionine- and disulfide-compatible and its application in MHC exchange reagents for T cell characterisation. *Chembiochem* **14**, 123-131, doi:10.1002/cbic.201200540 (2013).
24. Rodenko, B. *et al.* Generation of peptide-MHC class I complexes through UV-mediated ligand exchange. *Nat Protoc* **1**, 1120-1132, doi:10.1038/nprot.2006.121 (2006).
25. Toebes, M., Rodenko, B., Ovaa, H. & Schumacher, T. N. Generation of peptide MHC class I mo-

nomers and multimers through ligand exchange. *Curr Protoc Immunol* **Chapter 18**, Unit 18 16, doi:10.1002/0471142735.im1816s87 (2009).
26. Luimstra, J. J. *et al.* A flexible MHC class I multimer loading system for large-scale detection of antigen-specific T cells. *J Exp Med* **215**, 1493-1504, doi:10.1084/jem.20180156 (2018).
27. Newell, E. W., Klein, L. O., Yu, W. & Davis, M. M. Simultaneous detection of many T-cell specificities using combinatorial tetramer staining. *Nat Methods* **6**, 497-499, doi:10.1038/nmeth.1344 (2009).
28. Hadrup, S. R. *et al.* Parallel detection of antigen-specific T-cell responses by multidimensional encoding of MHC multimers. *Nat Methods* **6**, 520-526, doi:10.1038/nmeth.1345 (2009).
29. Dudley, J. C., Lin, M. T., Le, D. T. & Eshleman, J. R. Microsatellite Instability as a Biomarker for PD-1 Blockade. *Clin Cancer Res* **22**, 813-820, doi:10.1158/1078-0432.CCR-15-1678 (2016).
30. Duhen, T. *et al.* Co-expression of CD39 and CD103 identifies tumor-reactive CD8 T cells in human solid tumors. *Nat Commun* **9**, 2724, doi:10.1038/s41467-018-05072-0 (2018).
31. Gupta, P. K. *et al.* CD39 Expression Identifies Terminally Exhausted CD8+ T Cells. *PLoS Pathog* **11**, e1005177, doi:10.1371/journal.ppat.1005177 (2015).
32. Djenidi, F. *et al.* CD8+CD103+ tumor-infiltrating lymphocytes are tumor-specific tissue-resident memory T cells and a prognostic factor for survival in lung cancer patients. *J Immunol* **194**, 3475-3486, doi:10.4049/jimmunol.1402711 (2015).
33. Corrales, L. *et al.* Direct Activation of STING in the Tumor Microenvironment Leads to Potent and Systemic Tumor Regression and Immunity. *Cell Rep* **11**, 1018-1030, doi:10.1016/j.celrep.2015.04.031 (2015).
34. Woo, S. R. *et al.* STING-dependent cytosolic DNA sensing mediates innate immune recognition of immunogenic tumors. *Immunity* **41**, 830-842, doi:10.1016/j.immuni.2014.10.017 (2014).
35. Blank, C., Gajewski, T. F. & Mackensen, A. Interaction of PD-L1 on tumor cells with PD-1 on tumor-specific T cells as a mechanism of immune evasion: implications for tumor immunotherapy. *Cancer Immunol Immunother* **54**, 307-314, doi:10.1007/s00262-004-0593-x (2005).
36. Iwai, Y. *et al.* Involvement of PD-L1 on tumor cells in the escape from host immune system and tumor immunotherapy by PD-L1 blockade. *Proc Natl Acad Sci U S A* **99**, 12293-12297, doi:10.1073/pnas.192461099 (2002).
37. Hellmann, M. D. *et al.* Tumor Mutational Burden and Efficacy of Nivolumab Monotherapy and in Combination with Ipilimumab in Small-Cell Lung Cancer. *Cancer Cell* **33**, 853-861 e854, doi:10.1016/j.ccell.2018.04.001 (2018).
38. McGranahan, N. *et al.* Clonal neoantigens elicit T cell immunoreactivity and sensitivity to immune checkpoint blockade. *Science* **351**, 1463-1469, doi:10.1126/science.aaf1490 (2016).
39. van den Bulk, J., Verdegaal, E. M. & de Miranda, N. F. Cancer immunotherapy: broadening the scope of targetable tumours. *Open Biol* **8**, doi:10.1098/rsob.180037 (2018).
40. vanderBurg, S. H., Visseren, M. J. W., Brandt, R. M. P., Kast, W. M. & Melief, C. J. M. Immunogenicity of peptides bound to MHC class I molecules depends on the MHC-peptide complex stability. *Journal of Immunology* **156**, 3308-3314 (1996).
41. Rosendahl Huber, S. K. *et al.* Chemical Modification of Influenza CD8+ T-Cell Epitopes Enhances Their Immunogenicity Regardless of Immunodominance. *PLoS One* **11**, e0156462, doi:10.1371/journal.pone.0156462 (2016).
42. Li, H. & Durbin, R. Fast and accurate long-read alignment with Burrows-Wheeler transform. *Bioinformatics* **26**, 589-595, doi:10.1093/bioinformatics/btp698 (2010).
43. McKenna, A. *et al.* The Genome Analysis Toolkit: a MapReduce framework for analyzing next-generation DNA sequencing data. *Genome Res* **20**, 1297-1303, doi:10.1101/gr.107524.110 (2010).
44. Cibulskis, K. *et al.* Sensitive detection of somatic point mutations in impure and heterogeneous cancer samples. *Nat Biotechnol* **31**, 213-219, doi:10.1038/nbt.2514 (2013).
45. Koboldt, D. C. *et al.* VarScan 2: somatic mutation and copy number alteration discovery in cancer by exome sequencing. *Genome Res* **22**, 568-576, doi:10.1101/gr.129684.111 (2012).
46. Saunders, C. T. *et al.* Strelka: accurate somatic small-variant calling from sequenced tumor-normal sample pairs. *Bioinformatics* **28**, 1811-1817, doi:10.1093/bioinformatics/bts271 (2012).
47. McLaren, W. *et al.* The Ensembl Variant Effect Predictor. *Genome Biol* **17**, 122, doi:10.1186/s13059-016-0974-4 (2016).
48. Wu, T. D. & Watanabe, C. K. GMAP: a genomic mapping and alignment program for mRNA and EST sequences. *Bioinformatics* **21**, 1859-1875, doi:10.1093/bioinformatics/bti310 (2005).

49. Robinson, J. T. *et al.* Integrative genomics viewer. *Nat Biotechnol* **29**, 24-26, doi:10.1038/nbt.1754 (2011).
50. Thorvaldsdottir, H., Robinson, J. T. & Mesirov, J. P. Integrative Genomics Viewer (IGV): high-performance genomics data visualization and exploration. *Brief Bioinform* **14**, 178-192, doi:10.1093/bib/bbs017 (2013).
51. Robinson, J. T., Thorvaldsdottir, H., Wenger, A. M., Zehir, A. & Mesirov, J. P. Variant Review with the Integrative Genomics Viewer. *Cancer Res* **77**, e31-e34, doi:10.1158/0008-5472.CAN-17-0337 (2017).
52. Hos, B.J. *et al.* Identification of a neo-epitope dominating endogenous CD8 T cell responses to MC-38 colorectal cancer. *OncoImmunology* doi:10.1080/2162402X.2019.1673125 (2019).
53. Toebes, M. *et al.* Design and use of conditional MHC class I ligands. *Nat Med* **12**, 246-251, doi:10.1038/nm1360 (2006).

Supplementary Data

Supplementary Table 1. **Oligo A sequences used in this study**

Oligo A #	Barcode Sequence
A1	CGAGGGCAATGGTTAACTGACACGT
A2	CAGAAAGCAGTCTCGTCGGTTCGAA
A3	TAAGTAGCGGGCATAATGTACGCTC
A5	GGGCTGCGGAGCGTTTACTCTGTAT
A6	AAACGTATGTGCTTTGTCGGATGCC
A7	ATATCATCATAGGCTTAGCGACGTA
A8	AGGAAAATCTGCTACCGCCAATGAT
A9	CTGATTGACTGCATGGAGGCTATAC
A10	GTGGCGACTTCACGATTATCTGAAC
A11	CCTGTATTGAAGGTTCAGTCCTGTT
A12	GGCTCTATAAGGTTTCCTCAAAGGT
A14	AGAGAATATGTCGCTCCCGTTATGT
A15	GCAGTTAGATATGCAGTTACCTGAC
A16	CTTCACCCGAACATGCAGTGTTATT
A17	AAAGCCGTTGCAGTATCGTCTGAGC
A18	GCTGGATGTTAATAACTGCGGTCCG
A19	ACGAGTTGACATGGACGGATCCCTC
A20	TTCATCACTCATTGTTCTGAGTAGG
A21	ATGTTTAATCTAACTTGATGCCTCC
A22	TAATACGCCTGAGGTGTTGGGTTGC
A23	AGTCGGCATTGCTACCATAACTGTT
A24	CCGGACCGCTATTAACCTTGTACTG
A25	CTAGATGCTGCGAACGGAAGCTGTC
A26	TGTTCCAAGCGGTTGAACGATTAGC

Supplementary Table 2. **Oligo B sequences used in this study**

Oligo B #	Barcode Sequence
B61	GTTAGGTCGGCAGGTCAGTATGACC
B62	CGGGAGTTGGATCTGCGTAGAGTCC
B63	CCGGTTTTATACCCTCGTTCCCCGA
B64	CAGAACTACAGGCTGGCATGGATGC
B65	ATTCTGATGGGTAGAAACCGTTCCC
B66	GAGCGTGAGTTCCATGGAAAATTAC
B67	AGTAAAGGCTCACTGCTATCGCACT
B68	ATTTATTCGCACAATCGCCGAGTGC
B69	TACTCAACGACGTGGGGTAGGATCC
B70	GATATTCGGATCTTGGCTCGGACTG
B71	TTTCCTTGTTCGGATCGGTCGAGAA
B72	TGGAAACGACTGGTGTATGCATTCC
B73	GCTGTCAGTAGCGCCAGTACAATTT
B74	CTTTATGGGATAGCAAGACCTCTCC
B75	CATATGGATTTGTTGCATCCTGATG
B76	TGCAATATGGGTCGCGTTCAGTCGT

Supplementary Table 2 (continued). **Oligo B sequences used in this study**

Oligo B #	Barcode Sequence
B77	TAATTGCCTTGCGGTGCGTGTTGAT
B78	GGCAGGCTAGCTTAGTTGTAGCGGT
B79	CACATACTCAGACTCCCTGTCATAG
B80	TTGATCACAGCACGAATACGTTTCC
B81	TTTGAATAACCTTTCGCCTCTCGTG
B82	TGATTGCTTTGCCCTATAGCTACGT
B83	AGTGAAGTTACCTGGTGTTCCCTTC
B84	GCGGGATGTGCATTGCCAAGTTACC
B85	TTAAGTTGCCCAATTATTGTCCGCC
B86	GACAATGTAGGGGCCGTCTCAAGTA
B87	GCCATAGAGTCTACCGTCACCTCCG
B88	GTGCTACCATCGAGCGGAGGTATTT
B89	GAGTCCGATTGCTTTATCTGCTACC
B90	AATGGGCCTGCTACTCGCCATTATT
B111	CGTTGAAATAGTCGCATCTCTCACG
B113	TAAATGGCCTACATTCGAACGGTTG
B115	GTTATCCGTAGAGCGGTGCAAGTCC
B116	TCTTCGACATCTGGCATCACGACCT
B117	TTGGTTTATGATCACTGAAATGCCC
B118	ATGGGGATAGCCATCAGTTGGGCTA
B120	AATCGTAGTCGTCAGCCGCTAATAA
B121	GTCTTGTCGTGGGACGCATGTATCC
B122	GAAGTGAGGCGCTAACGCTCTAGGG
B124	GGTCATTCTAGTGAACTAATCCCCT
B200	GCTGAGGCGTTCCACTTGGATCGTT
B201	ATTGGGGACTTCCCTTTGCATTCTT
B202	AAATGGGACCGACACACTCTTAGCA
B203	GGCTTTACGGAACCCCGTGACTAGA
B204	AAGGTACTGGGCCGGTCCAATACAG
B205	TAGTAATACATACGCCCAGGCGGTA
B206	TACATGTTCGTTCTGCGTTACTCAC
B207	CTAATCAATGGTCCACGTTCTAGGG
B208	GCTACTACACCCGAGGTCGAGAGGA
B209	GTTCTGCAATTTCAATTCCCGGTCC
B210	AAGGCTTTCTAGCCACGTATGCGAA
B211	TGTACTGAGGGAGTAACTGCCCGTT
B212	ATTGTCAGATGTCGTAGGTCGCCGC
B213	AAATCCATTTATCGGTCTGTCGTGA
B214	AGTCATATAGTTGTATTCTCCCTGC
B215	ATTTGGACAGCATATTGACGTCGGA
B216	CGCATTCCGACAATATCGTGTTGTA
B217	CCCAGAACGTGAGTCAGTGTTCGCA
B218	TCCTTAGTTTTCCGGCTAAATGAGA
B219	GATGTTATTGCTTGCACAACGGCTG

Supplementary Table 3. **HLA-A*02:01 neoantigen sequences predicted from five colorectal cancer (CRC) patients, with DNA barcode annotations**

#	Sequence	Patient	Barcode
1	ALAAAQCSA	P5	A1B61
2	ALALVVAMA	P5	A1B62
3	ALGSTAPPA	P4	A1B63
4	ALQDMSSTA	P5	A1B64
5	CLAAWVPAPA	P5	A1B65
6	FHIFYQLLGA	P5	A1B66
7	FLELSLRA	P5	A1B67
8	FLPSSCSLA	P4	A1B68
9	FLPSSCSLAPA	P4	A1B69
10	FLRTKLCFA	P5	A1B70
11	FQECHIPFPA	P5	A1B71
12	GLACLGLSWYA	P5	A1B72
13	GLDDRSPQA	P5	A2B61
14	GLGGTHHMA	P4	A2B62
15	GLNHGNFFA	P2	A2B63
16	HIWPKGFEA	P4	A2B64
17	HLYDTLHWA	P3	A2B65
18	ILGSGTSFA	P5	A2B66
19	KLAYFSLSA	P4	A2B67
20	KLDLKVPKA	P5	A2B68
21	KLVFLGLDNA	P4	A2B69
22	KMPEMSIKA	P4	A2B70
23	KVMLTAPPA	P5	A2B71
24	LIISEYFTA	P4	A2B72
25	LLFLGPLAPA	P5	A3B61
26	LLISQGLKA	P4	A3B62
27	LLSPPEPQA	P5	A3B63
28	LMAPLSPGA	P5	A3B64
29	MLGQLSAEA	P5	A3B65
30	MLILGKDTA	P5	A3B66
31	MLLPPRPAA	P4	A3B67
32	MLSASIMYA	P5	A3B68
33	MMMGQFERDA	P4	A3B69
34	QLLLLLPRA	P5	A3B70
35	RLDLSAGPTA	P5	A3B71
36	RLYHPDTHHA	P5	A3B72
37	RMFIPAAAA	P5	A5B61
38	RMWVSMCPA	P5	A5B62
39	SLAEPSPPA	P2	A5B63
40	SLAQAPIPA	P5	A5B64
41	SLFDSVYGA	P5	A5B65
42	SLLGGVLRRA	P5	A5B66
43	SLQPPTLGA	P4	A5B67
44	TLAIRFISA	P5	A5B68
45	VIAASVPRA	P5	A5B69
46	WLCGWTSSA	P5	A5B70
47	WLLGLLMPFRA	P2	A5B71
48	WVLPSLPMA	P4	A5B72
49	YISRCAPPA	P4	A6B61
50	YLNLTVLA	P5	A6B62
51	YMDLILASA	P4	A6B63
52	YMQWVWGA	P4	A6B64
53	YTDRALAFYA	P4	A6B65
54	LLLPEGIRC	P4	A6B66
55	LLDDNQAPF	P5	A6B67
56	SLDDIIRHDF	P5	A6B68
57	YLQKLSVEF	P4	A6B69
58	ALAPRSATI	P5	A6B70
59	CLFEFLTGI	P5	A6B71
60	CMGGMNWRPI	P2	A6B72
61	FAHNRNWYI	P4	A7B61
62	FLEENCADI	P5	A7B62
63	FLNGATPYEKGI	P3	A7B63
64	FLPPRLKKI	P5	A7B64
65	FMMPPEETI	P4	A7B65
66	FTEKNLWLI	P5	A7B66
67	FVAPLVPLPI	P5	A7B67
68	GLHRQLLYI	P4	A7B68
69	GLHSVGAYI	P5	A7B69
70	GMEEATVAI	P5	A7B70
71	GMIHMLDGI	P5	A7B71
72	GMWAQLPCI	P4	A7B72
73	GVYPVEGFEI	P5	A8B61
74	HLPAGWGEALQI	P5	A8B62
75	ILDPSYHI	P4	A8B63
76	ILIYSWCRI	P5	A8B64
77	ILLGTFLAI	P5	A8B65
78	ILLKMEIQI	P5	A8B66
79	ILSDPENNI	P5	A8B67
80	IRPPLLPYIVNI	P4	A8B68
81	IVLGSCVYI	P5	A8B69
82	KIAFHIKSI	P5	A8B70
83	KLCQGMHQI	P3	A8B71
84	KLINPDKKI	P4	A8B72
85	KLLHTQKVVYI	P5	A9B61
86	KLNGQTMEI	P5	A9B62
87	KMEIQIFKI	P5	A9B63
88	KQLAVSICI	P5	A9B64
89	KTGMEILLWI	P5	A9B65
90	LIMVYLFSI	P4	A9B66
91	LLAVVIQFQI	P5	A9B67
92	LLIDLMEQEI	P5	A9B68
93	LLILCVHAKI	P5	A9B69
94	LLPPPTEWLI	P5	A9B70
95	LLPPPTEWLIPI	P5	A9B71
96	LLWILLKMEI	P5	A9B72
97	MLHRGLLLI	P5	A1B73
98	MMLATKLTI	P4	A1B74
99	RLFGTWINKI	P4	A1B75
100	SLKDSQFSI	P5	A1B76
101	SLLLLPEGI	P4	A1B77
102	SLPTTPLYFI	P5	A1B78
103	SLSHILTCGI	P4	A1B79
104	SLYYDYEPPI	P5	A1B80
105	SMSSTPLTI	P5	A1B81
106	STAAEVVAI	P5	A1B82
107	TLLSRLPAI	P4	A1B83
108	TLSPAITSI	P5	A1B84
109	TMQPWPCSI	P5	A2B73
110	VIAGGIWHI	P2	A2B74
111	VLNPYVKHSI	P5	A2B75
112	VLVEEVAEKCI	P5	A2B76
113	WLGPGLRMGI	P5	A2B77
114	WLSRSAFYCI	P5	A2B78
115	YITAFFCWI	P4	A2B79
116	YLDLYLIHWPI	P5	A2B80

Supplementary Table 3 (continued). **HLA-A*02:01 neoantigen sequences predicted from five colorectal cancer (CRC) patients, with DNA barcode annotations**

#	Sequence	Patient	Barcode
117	YLLKVCERI	P1	A2B81
118	YLQKLSVEFQI	P4	A2B82
119	YLVASDQRPI	P1	A2B83
120	YPQLKALPPI	P5	A2B84
121	ALGPAASAL	P5	A3B73
122	ALLPPPTEWL	P5	A3B74
123	ALNPSAPSL	P5	A3B75
124	ALPRLPVPL	P5	A3B76
125	ALSLDTQNL	P5	A3B77
126	ALVKSSEEL	P4	A3B78
127	ALWSAVTLL	P5	A3B79
128	AMAAALGVL	P5	A3B80
129	AMAQVTHPL	P4	A3B81
130	AMVAVPMVL	P5	A3B82
131	ASLQNLLFKL	P4	A3B83
132	AVFGHHFSL	P5	A3B84
133	CLAAEITRL	P4	A5B73
134	CMADGSTAL	P5	A5B74
135	FGMSVCSWPL	P5	A5B75
136	FIQQMVHAL	P5	A5B76
137	FLARPLPWPL	P4	A5B77
138	FLFSDKLGEL	P3	A5B78
139	FLLAGAHL	P5	A5B79
140	FLLKNIIFL	P4	A5B80
141	FLLPGKKIL	P5	A5B81
142	FLMHLYLEL	P5	A5B82
143	FLMVLVWLPL	P5	A5B83
144	FLNKPSIIL	P2	A5B84
145	FLPGSTPSL	P5	A6B73
146	FLPPLLLLLL	P4	A6B74
147	FLSHYLQKL	P4	A6B75
148	FLSLPETAL	P5	A6B76
149	FLSTLPHL	P2	A6B77
150	FLTTSSLML	P4	A6B78
151	FLVQNIHTLAGL	P4	A6B79
152	FLYNNLVESL	P5	A6B80
153	FMFRTWGRML	P5	A6B81
154	FMRWIIGL	P4	A6B82
155	FPMPNYQAAL	P4	A6B83
156	FSWSNTTLL	P1	A6B84
157	GLEVSGAFPQL	P5	A7B73
158	GLFSEDGATL	P4	A7B74
159	GLHLHPSPAL	P5	A7B75
160	GLIDGMHMHL	P5	A7B76
161	GLLPQTKTL	P5	A7B77
162	GLNLGPQVAL	P5	A7B78
163	GLPPEPEVPPAL	P5	A7B79
164	GLQDQEPSL	P5	A7B80
165	GLQKEIAEL	P4	A7B81
166	GLRMGIGLNL	P5	A7B82
167	GLRTEAPPTL	P4	A7B83
168	GLSAQHVPSL	P5	A7B84
169	GLSSFGQSL	P5	A8B73
170	GLTEPVLIWL	P4	A8B74
171	GMGGSTITL	P5	A8B75
172	GMHSRLSSL	P4	A8B76
173	GMLTVIGQGL	P5	A8B77
174	GVHPSLAPL	P5	A8B78
175	HLDTFHLSL	P5	A8B79
176	HLHESCMLSL	P4	A8B80
177	HLISQCEQL	P5	A8B81
178	HLQIRWPNLPRL	P5	A8B82
179	HLTHLEAAL	P4	A8B83
180	IIATVLYGPL	P5	A8B84
181	ILANTVKPFL	P4	A9B73
182	ILDPSYHIPPL	P4	A9B74
183	ILKLWLGPGL	P5	A9B75
184	ILPMKIPRQL	P5	A9B76
185	ILTHIIECL	P5	A9B77
186	IMPMNILYL	P2	A9B78
187	IMYACVFCL	P5	A9B79
188	ITLGFGWML	P5	A9B80
189	KISFENLHL	P5	A9B81
190	KISHCPHLL	P4	A26B115
191	KLFEMAYKRWHL	P4	A9B83
192	KLIYQGHLL	P2	A9B84
193	KLMKNIQFPL	P5	A10B61
194	KLMPWNCCL	P5	A10B62
195	KLQAETEEL	P4	A10B63
196	KLTTEYLSL	P4	A10B64
197	KPLLSYPLVL	P5	A10B65
198	LLAACPLHL	P5	A10B66
199	LLAEVDVPKL	P3	A10B67
200	LLAPSGHLL	P5	A10B68
201	LLFGLKGEL	P5	A10B69
202	LLIQQINFHL	P4	A10B70
203	LLKKIASTFYL	P4	A10B71
204	LLKYVRTPTL	P5	A10B72
205	LLLALPHEL	P5	A11B61
206	LLLCVQALL	P4	A11B62
207	LLLPGWCRL	P5	A11B63
208	LLLQQPPPL	P5	A11B64
209	LLSQICSHL	P3	A11B65
210	LLVDKHKYFL	P5	A11B66
211	LLVGSNQWEL	P5	A11B67
212	LMLSAQLCL	P4	A11B68
213	LMPGGSCWRL	P5	A11B69
214	LMPIFSPEL	P4	A11B70
215	LQAECDQYL	P4	A11B71
216	MEKLADIVTEL	P5	A11B72
217	MLAPPFPPPL	P4	A12B61
218	MLLNTPFTL	P5	A12B62
219	MLNTQDSSILPL	P4	A12B63
220	MLTAPPASL	P5	A12B64
221	MLVPGGTRVCQL	P5	A12B65
222	MMEAGLSEL	P5	A12B66
223	NLELDPIFL	P5	A12B67
224	NLGPSLVGL	P2	A12B68
225	NMLCFNFKL	P5	A12B69
226	NMSKVETGL	P5	A12B70
227	NVLSSLWYL	P5	A12B71
228	PLSFVLHFL	P5	A12B72
229	QLGKEDLGL	P4	A14B61
230	QLQIIFLEL	P5	A14B62
231	RLHTWSQGL	P4	A14B63
232	RLLDSEEPL	P5	A14B64

Supplementary Table 3 (continued). **HLA-A*02:01 neoantigen sequences predicted from five colorectal cancer (CRC) patients, with DNA barcode annotations**

#	Sequence	Patient	Barcode
233	RLMTHYCAML	P5	A14B65
234	RLPRPAHAL	P5	A14B66
235	RLSSSELSPL	P5	A14B67
236	RLWPVLDPCCPL	P5	A14B68
237	RMAATRTSL	P5	A14B69
238	RMQGLGFLL	P5	A14B70
239	RPLLALVNSL	P5	A14B71
240	RVYPRPRVAL	P5	A14B72
241	SELSPLTPRL	P5	A15B61
242	SIYPPPRAL	P4	A15B62
243	SLHFLCWSL	P5	A15B63
244	SLIFGLILKL	P5	A15B64
245	SLLEKVSKKRL	P5	A15B65
246	SLLPSCCAL	P5	A15B66
247	SLLRQPVQL	P5	A15B67
248	SLLSCPPFL	P4	A15B68
249	SLNWPEALPHL	P5	A15B69
250	SLPAGPSAL	P5	A15B70
251	SLPCTPLWL	P5	A15B71
252	SLPSTQLPL	P5	A15B72
253	SLQNLLFKL	P4	A16B61
254	SLVGTQTLL	P5	A16B62
255	SLVPRGTPL	P5	A16B63
256	SLVSFLMHL	P5	A16B64
257	SLYPQNMTL	P4	A16B65
258	SMAPTQTCL	P4	A16B66
259	SMCPAGTWCL	P5	A16B67
260	SQSEQGLLL	P5	A16B68
261	SQTPVPPGL	P5	A16B69
262	STFGMSVCSWPL	P5	A16B70
263	TLAGLHVHL	P5	A16B71
264	TLAQPELFL	P2	A16B72
265	TLGFGWMLIL	P5	A17B61
266	TLLLKAPTL	P5	A17B62
267	TLMDCHWQPL	P4	A17B63
268	TLVIYVARL	P4	A17B64
269	TLWPSLPSSTL	P5	A17B65
270	TMGGYCGYL	P4	A17B66
271	TMNDSKHKL	P5	A17B67
272	TMVDFIKSTL	P4	A17B68
273	TMVQGPAGL	P4	A17B69
274	TVLSQGWEL	P5	A17B70
275	VELMKHFAWL	P4	A17B71
276	VIFSGALLGL	P4	A17B72
277	VLDPEGIRGL	P5	A18B61
278	VLILGTKRL	P5	A18B62
279	VLQKKRILL	P5	A18B63
280	VLREKVPCL	P5	A18B64
281	VLSMTTRIFL	P5	A18B65
282	VLSSLWYLNL	P5	A18B66
283	VLTQLVLNL	P5	A18B67
284	VLVESKLRGL	P5	A18B68
285	WLCSPAPWL	P5	A18B69
286	WLGMALIPL	P4	A18B70
287	WLGTLWPSL	P5	A18B71
288	WLLQKSPQL	P4	A18B72
289	WLNTKMKFFL	P5	A10B73
290	YCLFAASLLL	P4	A10B74
291	YIFTILSSL	P4	A10B75
292	YLDSIGNLPFEL	P5	A10B76
293	YLIFKPDVML	P4	A10B77
294	YLKIKHLLL	P3	A10B78
295	YLNTNPVCGL	P4	A10B79
296	YQAQLRISL	P5	A10B80
297	YTLVPSTVAL	P3	A10B81
298	YTYLTIFDL	P5	A10B82
299	YVLPRALSL	P2	A10B83
300	YYLMTVMERL	P5	A10B84
301	ALIPLPGM	P4	A11B73
302	FCLLVVVVLM	P5	A11B74
303	FLAKDPHPM	P5	A11B75
304	FLFTVPIEDM	P5	A11B76
305	FLTGIPLSM	P5	A11B77
306	FLVLSMPAM	P4	A11B78
307	ILLWILLKM	P5	A11B79
308	ILNSLPSSM	P4	A11B80
309	ILSMEKIPPM	P4	A11B81
310	KMICRGMTM	P4	A11B82
311	RLHRLILPM	P5	A11B83
312	RLQPMISVRM	P4	A11B84
313	RLYQSVLSM	P5	A12B73
314	RMLETVLRM	P4	A12B74
315	RMVWVELEM	P5	A12B75
316	SLDDWSLIYM	P3	A12B76
317	SLRMLVQPEM	P5	A12B77
318	TQMSNLVNM	P4	A12B78
319	YVQAFQVGM	P5	A12B79
320	TLIDFFCEDKKP	P5	A12B80
321	FLMRKRWPS	P5	A12B81
322	FLQSHVPKS	P5	A12B82
323	RPLWCLLPPS	P4	A12B83
324	AIIDFSVWT	P5	A12B84
325	ALLWDTETT	P5	A14B73
326	ALWPYGPLT	P5	A14B74
327	FLFKEEEFTT	P5	A14B75
328	FLPNADMET	P4	A14B76
329	FPLVALLWDT	P5	A14B77
330	HLHHHLPTT	P5	A14B78
331	ILAPKLLST	P5	A14B79
332	KMPPFVSTT	P5	A14B80
333	VLLKKIAST	P4	A14B81
334	VVMGVCPFT	P5	A14B82
335	WLIPIAMAT	P5	A14B83
336	YLAFFPPT	P5	A14B84
337	YLLARYYYT	P5	A15B73
338	YLTIFDLLET	P5	A15B74
339	YPLPPWPWST	P5	A15B75
340	AINDVLWACV	P5	A15B76
341	ALDLYHVLV	P5	A15B77
342	ALGLDVIDQV	P1	A15B78
343	ALKIPQGQRV	P4	A15B79
344	ALKQYACTV	P5	A15B80
345	ALMPPSPLPSRV	P5	A15B81
346	ALPHLLLLV	P5	A15B82
347	ALPQLEHQV	P5	A15B83
348	ALRPHPAAV	P5	A15B84

Supplementary Table 3 (continued). **HLA-A*02:01 neoantigen sequences predicted from five colorectal cancer (CRC) patients, with DNA barcode annotations**

#	Sequence	Patient	Barcode
349	ALSEALWVV	P4	A16B73
350	ALSKHLTNPFLV	P5	A16B74
351	ALSWRNVPV	P5	A16B75
352	ALTEELHQKV	P5	A16B76
353	ALVWLKDPV	P4	A16B77
354	AMIVEQPEV	P5	A16B78
355	APLDLRLAWV	P5	A16B79
356	AQHCLLLLV	P5	A16B80
357	AQIQRPIQV	P5	A16B81
358	AQSGPLSFV	P5	A16B82
359	CLSPMGLGV	P5	A16B83
360	CMNEHWMPV	P5	A16B84
361	ELWAVDHLQV	P5	A17B73
362	FHLCSVATRV	P4	A17B74
363	FLCEKEQIV	P4	A17B75
364	FLGNMFHV	P5	A17B76
365	FLINTFEGV	P5	A17B77
366	FLKFLQGV	P5	A17B78
367	FLLGMATV	P4	A17B79
368	FLQGVALAV	P5	A17B80
369	FLRGCAPSWV	P5	A17B81
370	FLRLQVEGV	P4	A17B82
371	FLSHYLQKLSV	P4	A17B83
372	FQNRGEAAV	P5	A17B84
373	FQVLVRILPV	P5	A18B73
374	FSAPPNSLV	P5	A18B74
375	GLAVTYGV	P5	A18B75
376	GLDFFWKQEV	P5	A18B76
377	GLGEPKQPV	P4	A18B77
378	GLGSFVVGV	P5	A18B78
379	GLLPLASTV	P5	A18B79
380	GLPLAMAQV	P4	A18B80
381	GLPPRHHGV	P5	A18B81
382	GLVEEPMEDV	P5	A18B82
383	GMATVNNCV	P4	A18B83
384	GMEHFSTPV	P5	A18B84
385	GMKLLGITLV	P5	A1B111
386	GVVTSGPGV	P5	A1B113
387	HLAPPRYSPQV	P4	A1B115
388	HLIKERPLV	P5	A1B116
389	HLLWRLPAPV	P4	A1B117
390	HLSEKALEV	P4	A1B118
391	HTYSSIPVV	P1	A1B120
392	IIAGGASLV	P5	A1B121
393	ILASGFIDV	P5	A1B122
394	ILGEGRAEAV	P5	A1B124
395	ILLVNSLKV	P5	A26B116
396	ILSAITQPV	P5	A19B113
397	ILSALRVSPV	P5	A2B111
398	ILYPDEVACMV	P5	A2B113
399	IMGKMEADPEV	P3	A2B115
400	ITITFVTAV	P3	A2B116
401	ITSAAIYHV	P5	A2B117
402	IVAAGVASGV	P5	A2B118
403	KAFFGPVYYV	P5	A2B120
404	KIVAYMYLV	P1	A2B121
405	KLAIHVGLAV	P5	A2B122
406	KLESPALKQV	P5	A2B124
407	KLQGAVCVV	P5	A20B111
408	KLSLFIVCTV	P5	A20B113
409	KLSVEFQIV	P4	A3B111
410	KMDLDGMLTV	P5	A3B113
411	KQVMLQLYV	P5	A3B115
412	KVGDILQAV	P5	A3B116
413	KVSGTLLTV	P4	A3B117
414	LFSYMQWV	P4	A3B118
415	LLAAWAAPSGV	P5	A3B120
416	LLGSPDPEGV	P5	A3B121
417	LLHILSFVV	P5	A3B122
418	LLLAVRSFV	P5	A3B124
419	LLLKFTASV	P5	A21B111
420	LLSEHAVIV	P5	A21B113
421	LLSRVEILPV	P4	A5B111
422	LLTDLTSWGV	P5	A5B113
423	LLVIEKNLMV	P5	A5B115
424	LMTAKIVGNV	P5	A5B116
425	LMVDPSHEV	P5	A5B117
426	LMVSAGRGLWAV	P3	A5B118
427	LTNAGMLEV	P5	A5B120
428	LVMKGQIPV	P5	A5B121
429	MIISRHLASV	P4	A5B122
430	MLDVDLDEV	P4	A5B124
431	MLHKSIPV	P5	A22B111
432	MLNVNLDPPV	P5	A22B113
433	MLVPGGTRV	P5	A6B111
434	MMMRNQENV	P5	A6B113
435	NLEEPPSSV	P5	A6B115
436	NLQAMSLYV	P5	A6B116
437	NLYGMSKVAV	P4	A6B117
438	PLVHITEEV	P4	A6B118
439	QIFPITPPV	P5	A6B120
440	QLAGKRIGV	P5	A6B121
441	QLAIQVLLV	P5	A6B122
442	QLHPQLLLPV	P3	A6B124
443	QLILLILCV	P5	A23B111
444	QLPGSATYPV	P4	A23B113
445	RLEFIAHV	P5	A7B111
446	RLFICISGV	P5	A7B113
447	RLLGQTDMAV	P4	A7B115
448	RLMAGQQQV	P4	A7B116
449	RLQPMISV	P4	A7B117
450	RLTQMSNLV	P4	A7B118
451	RMKRLPVAV	P5	A7B120
452	RMQCVAVFAV	P5	A7B121
453	RQLPQMSKV	P5	A7B122
454	RSFDEVEGV	P5	A7B124
455	RTGPHILIV	P5	A24B111
456	SLAECGARGV	P4	A24B113
457	SLASWDVPV	P5	A8B111
458	SLCRLWPV	P5	A8B113
459	SLHGHVAAV	P4	A8B115
460	SLIEFDTLV	P5	A8B116
461	SLILSFQRV	P4	A8B117
462	SLLHTTFPHRQV	P5	A8B118
463	SLPMIATV	P5	A8B120
464	SLPSSMEIAV	P4	A8B121

Supplementary Table 3 (continued). **HLA-A*02:01 neoantigen sequences predicted from five colorectal cancer (CRC) patients, with DNA barcode annotations.** V, viral epitope

#	Sequence	Patient	Barcode
465	SLPVTSLSSV	P5	A8B122
466	SLQWPLKSRV	P4	A8B124
467	SLRTDCLLAV	P5	A25B111
468	SLVPEREKMLV	P5	A25B113
469	SLWYLNLTV	P5	A9B111
470	SMFVGSDTV	P5	A9B113
471	SMRECALHTV	P5	A9B115
472	SMTCKVMTSWAV	P5	A9B116
473	SQMDGLEV	P5	A9B117
474	SQVQLAIQV	P5	A9B118
475	SVFPNILNV	P4	A9B120
476	TALDVLANV	P5	A9B121
477	TETFALILYV	P5	A9B122
478	TLEERTSSV	P5	A9B124
479	TLGAALPPWPV	P4	A26B111
480	TLGAMDLGV	P5	A26B113
481	TLRQTTSVPV	P5	A19B115
482	TLSVIRDYLV	P5	A19B116
483	TLVEELITV	P5	A19B117
484	VIGAVVATV	P4	A19B118
485	VISAISEAV	P5	A19B120
486	VLAENVNMCV	P5	A19B121
487	VLKPCLIPV	P5	A19B122
488	VLKPFLFTV	P5	A19B124
489	VLLQSESGTAPV	P5	A22B115
490	VLLVLVLAV	P4	A22B116
491	VLMGCWLEV	P5	A22B117
492	VLSKGEIVV	P5	A22B118
493	WLASGRPCV	P5	A20B115
494	WLIVLTQLV	P5	A20B116
495	WLPKMPPFV	P5	A20B117
496	WLRELTSIV	P3	A20B118
497	WMTMDHLLV	P5	A20B120
498	WVLAALLAV	P5	A20B121
499	YLAHTVNAYKLV	P5	A20B122
500	YLEQLKMTV	P3	A20B124
501	YLGDILLAV	P5	A23B115
502	YLPPGFMFKV	P3	A23B116
503	YLPRTMDFGINV	P5	A23B117
504	YLSGRQKFWV	P2	A23B118
505	YMACKDEGCKLV	P3	A21B115
506	YQSAGITGV	P5	A21B116
507	YTWLGAMPV	P4	A21B117
508	SLWGNPTQY	P5	A21B118

#	Sequence	Origin	Barcode
V1	GILGFVFTL	FLU MP1	A21B120
V2	CLGGLLTMV	EBV LMP2	A21B121
V3	GLCTLVAML	EBV BMLF1	A21B122
V4	FLYALALLL	EBV LMP2	A21B124
V5	NLVPMVATV	CMV pp65	A24B115
V6	YVLDHLIVV	EBV BRLF1	A24B116
V7	VLEETSVML	CMV IE1	A24B117
V8	ILKEPVHGV	HIV Pol	A24B118
X	No peptide control		A25B115

Supplementary Table 4. **Top 10 peptide specificities retrieved from the five human colorectal cancer (CRC) patients included in this study.**

	Patient 1		Patient 2						Patient 3						Patient 4					Patient 5		BC 83	BC 88
						TIL subsets						TIL subsets					TIL subsets						
Sample ->	TILs	PBMCs	TILs	PBMCs	LN	DP	DN	SP39	TILs	PBMCs	LN	DN	SP39	SP103	TILs	LN	DP	DN	SP39	TILs	PBMCs		
Top 10 specificities 1	#15	V5	V5	V5	V5	**#264**	V5	V7	**#63**	V6	V2	**#502**	**#400**	**#400**	V4	V4	**#52**	V4	**#115**	**#128**	**#457**	V6	V3
2	#110	V3	**#264**	V7	V6	**#110**	V3	#117	#264	V1	V6	#117	**#502**	V6	**#115**	V6	V4	**#19**	V6	**#474**	**#418**	V3	V5
3	#209	V1	#400	V3	V3	#400	V6	#404	**#209**	V3	V3	V6	#264	**#502**	V6	**#115**	**#90**	**#276**	**#490**	**#64**	**#114**	V4	V1
4	#264	V4	#117	V6	V2	#119	V7	V5	#117	V2	V4	#264	#117	#110	**#31**	**#343**	**#19**	**#115**	**#328**	**#480**	**#494**		
5	#224	V2	#404	#199	**#186**	V6	V4	**#186**	**#399**	V4	V1	**#400**	#186	#186	**#19**	**#490**	**#343**	**#9**	**#24**	**#410**	**#398**		
6	#199	#502	**#149**	**#186**	#83	#502	#502	**#264**	#110	**#502**	#404	#186	**#316**	**#496**	**#490**	**#363**	**#353**	**#31**	**#19**	**#446**	**#64**		
7	#400	**#117**	V6	#294	**#264**	**#186**	#209	#199	#149	#404	**#400**	V3	#119	V7	**#52**	**#449**	**#115**	**#490**	**#367**	**#398**	**#109**		
8	#83	#400	**#186**	#209	V7	#404	#400	#209	#186	#264	V5	**#316**	V6	#117	**#448**	**#306**	**#438**	**#118**	**#118**	**#5**	**#256**		
9	#63	V6	#119	V1	V1	V5	**#264**	V4	V6	**#400**	#110	#119	**#209**	**#500**	**#53**	**#19**	**#367**	**#52**	**#414**	**#79**	**#319**		
10	#316	#110	#209	#399	**#15**	#117	#119	**#149**	**#316**	**#209**	#186	#404	**#138**	#504	**#191**	**#215**	**#51**	**#448**	**#438**	**#354**	**#436**		

Various samples from five patients were stained with a pool of HLA-A*02:01 multimers thermally exchanged for a selection of predicted neoantigens and common viral antigens (denoted with V, sequences listed in Table 1 and Table S3). Barcodes corresponding to peptides highlighted in red were detected at significantly increased levels (log fold change ≥2) compared to baseline reads; peptides in yellow at slightly increased levels (1≤ log fold change ≤2). Underlined peptides in bold are peptides predicted specifically for that patient. TIL, tumor-infiltrating lymphocyte; PBMC, peripheral blood mononuclear cell; LN, lymph node; DP, double positive TIL subset expressing both CD39 and CD103; DN, double negative; $SP39^{+}$, single positive expressing CD39; $SP103^{+}$, single positive expressing CD103.

Supplementary Table 5. **H2-K^b neoantigen sequences predicted from MC38 mice, with DNA barcode annotations**

#	Sequence	Barcode
1	SIIVFNLL	A1B212
2	IVFNLLEL	A1B213
3	FVIDFKPL	A1B200
4	KFNFKTAL	A1B201
5	ALPVRFSL	A1B202
6	MARPWGLL	A1B203
7	RHCWYLAL	A1B205
8	FSLQFALL	A1B204
9	SSMVPSAL	A1B206
10	FALLMGTL	A1B207
11	RNRRIFAL	A1B208
12	SPFLLITL	A1B209
13	LAPIKFAL	A1B210
14	VNSIHALL	A1B211
15	ASASLSRL	A2B200
16	VSLWPDLL	A2B201
17	TAIELGTL	A2B202
18	STPQLLPL	A2B203
19	VLESYLNL	A2B205
20	VGPRYDFL	A2B204
21	KILTFDRL	A2B206
22	LTFDRLAL	A2B207
23	EAERFANL	A2B208
24	VTVFVNNL	A2B209
25	PMFLFKTL	A2B210
26	SASRYALL	A2B211
27	SSIKVVGL	A3B200
28	VNMDGASL	A3B201
29	TVVGLSNL	A3B202
30	TGSVFGEL	A3B203
31	ANVLFFGL	A3B205
32	QILVFLIL	A3B204
33	LGVLFSQL	A3B206
34	YMYVPTAL	A3B207
35	LGSIFSTL	A3B208
36	RSVLHGCL	A3B209
37	FINLYGLL	A3B210
38	IHPVMSTL	A3B211
39	AALSPASL	A5B200
40	VQFMSCNL	A5B201
41	GAFVLQLL	A5B202
42	SSFVPVGL	A5B203
43	TSIGMLYL	A5B205
44	RLYETFNL	A5B204
45	FTPSHPPL	A5B206
46	RTLCVGNL	A5B207
47	LAIMTQHL	A5B208
48	AWVPFGGL	A5B209
49	FSYIVELL	A5B210
50	LTFFHSGL	A5B211
51	FTFLFFAL	A6B200
52	VVWFFTFL	A6B201
53	TFLFFALL	A6B202
54	RGLIRYRL	A6B203
55	AVIGYSLL	A6B205
56	VTLKPPFL	A6B204
57	SSSTAAAL	A6B206
58	SNHVLGHL	A6B207
59	LSVEPFRL	A6B208
60	LGYSSVGL	A6B209
61	VGLPWVTL	A6B210
62	VSRHHRAL	A6B211
63	RTVLRLLSL	A7B200
64	VVIAIFIIL	A7B201
65	YSMGKDAGL	A7B202
66	VAVLPVLSL	A7B203
67	IGACKAMNL	A7B205
68	VGQSVWLGL	A7B204
69	VMIAGKVAL	A7B206
70	CVVPFTDLL	A7B207
71	IVGHFYGGL	A7B208
72	VAQTPHGFL	A7B209
73	LDFGFWHEL	A7B210
74	IANFQLCPL	A7B211
75	ISRDLASML	A8B200
76	VKRTRFLRL	A8B201
77	SHPRRHRRL	A8B202
78	STQMHRALL	A8B203
79	TQMHRALLL	A8B205
80	VQKKFSRNL	A8B204
81	ISYDPDTCL	A8B206
82	SMPSAKVSL	A8B207
83	LGVCMYGML	A8B208
84	LAQKIHQNL	A8B209
85	LYLSSRSLL	A8B210
86	CSYLPELPL	A8B211
87	QVFKVIGNL	A9B200
88	ASLLPSMPL	A9B201
89	WNCPFSQRL	A9B202
90	QLYLLCCQL	A9B203
91	VQLASRSLL	A9B205
92	MSYFLQGTL	A9B204
93	SSPYSLHYL	A9B206
94	STSFNFNSL	A9B207
95	QVVKYHRVL	A9B208
96	VVKYHRVLL	A9B209
97	GSWAYCRAL	A9B210
98	KLYTRYAFL	A9B211
99	ASIIVFNLL	A1B214
100	IIVFNLLEL	A1B215
101	GKILTFDRL	A1B216
102	GGKILTFDRL	A1B217
103	No peptide control	A1B219
104	SIINFEKL	A1B218

8

Summary and future perspectives

Adaptive immunity in a nutshell

The two branches of the immune system work closely together to detect and eliminate threats. Our immune system has evolved to protect us from infection by viruses and other pathogens, but concomitantly also offers protection from cancer through elimination of cells that express mutated proteins. The first line of defense is provided by the innate immune system via detection of pathogenic or tumor cell fragments[1]. Pattern recognition receptors on innate immune cells recognize pathogen- or danger-associated molecular patterns, such as cell-free DNA, dsRNA or bacterial cell wall constituents[2]. Adaptive immune cells recognize and respond to pathogens or malignant cells more specifically by scanning peptides, small protein fragments. These peptides can be presented at the surface of all nucleated cells by major histocompatibility complex class I (MHCI) molecules, for surveillance by cytotoxic $CD8^+$ T cells[3]. These specialized T cells can scan the presented peptides and distinguish self- from non-self with their highly specific T cell receptors (TCRs) and directly eliminate cells that display signs of infection or mutation. Likewise, the extracellular space is monitored by $CD4^+$ T cells, or T helper (Th) cells, via TCR scanning of internalized extracellular peptides presented on MHC class II (MHCII)[4]. Upon recognition of foreign peptides, $CD4^+$ T cells produce cytokines that induce clonal expansion and activation of B cells so that these can release antibodies.

TCR activation is the first of the three signals necessary for mounting an effective adaptive immune response[5]. The second signal required for sustained activation and proliferation is provided by costimulation[6]. Costimulatory cell surface receptors are expressed on T cells and exert their function upon engagement by their ligands on activated antigen-presenting cells (APCs), such as dendritic cells (DCs). The best-characterized costimulatory pathway involves CD28, constitutively expressed on naïve T cells, and its ligands B7-1 (CD80) and B7-2 (CD86) found on activated DCs[7]. Help provided by $CD4^+$ T cells is crucial for the maturation of DCs and correspondingly increased expression of B7-1 and B7-2[5]. Professional APCs express a variety of additional costimulatory receptors, each with their own cognate ligands[8]. Although activated T cells may undergo several rounds of proliferation when costimulated, clonal expansion, survival and establishment of memory requires a third signal, delivered by cytokines[9]. Absence of this third signal eventually leads to tolerance10. The cytokines needed by $CD8^+$ T cells are interleukin (IL) 12 or type I interferons (IFNs), produced by $CD4^+$ Th cells[11].

A closer look at MHCI antigen presentation and TCR activation

MHCI is loaded with intracellularly-derived peptides, typically of 8-10 amino acids in size, in the endoplasmic reticulum. Two alpha-helices of the MHCI form a groove that contains several binding pockets, into which the side chains of the peptide's amino acids can fit[12]. The peptide-MHCI binding affinity is determined by the interactions of the MHCI heavy chain with the peptide backbone and amino acid side chains[13]. The TCR binds the amino acid side chains of the peptide that protrude out of the binding groove, as well as the exposed residues that make up the MHCI's alpha helices. The extreme selectivity of the TCR ensures that only one particular peptide-MHCI combination leads to activation, warranting the high specificity needed to maintain self-tolerance and prevent auto-immunity.

MHCI genes are divided in three groups, in humans referred to as human leukocyte antigen (HLA) A, B and C. These genes are highly polymorphic, i.e., they contain many variants due to mutation, recombination and conversion. The resulting allotypes can differ in one or multiple amino acids, mainly in the peptide-binding groove, that affect the preferred binding motifs[14]. Each individual inherits one HLA-A, one HLA-B and one HLA-C gene from each of their parents, resulting in 3-6 different HLAs expressed per individual. Through expression of multiple subtypes more fragments of a protein are presented, thus achieving broad immune protection.

Immunotherapy

Improving peptide vaccines through chemical modification

Our immune system is incredibly advanced in detecting and eliminating infected or transformed cells. This ability is gratefully embraced by clinicians: immune therapies that induce or promote anti-tumor or anti-viral responses have proven efficacious against infection as well as cancer. With increasing knowledge therapies are advancing to become increasingly specific and personalized. Activating $CD8^+$ T cells has been considered the most straightforward approach, for a cytotoxic response directed specifically at infected or transformed cells will result in elimination of just those cells expressing the antigen, even at distant sites. Various therapeutic strategies can be employed, such as vaccination with antigenic peptides, antigen-coding RNA, peptide-loaded DCs or even antigen-activated $CD8^+$ T cells[15]. In particular, the design of peptide vaccines has been of high interest for decades and their efficacy, stability and pharmacokinetics have been studied extensively. Moreover, their synthesis is easy, cheap and flexible[16]. Peptides by themselves are poorly immunogenic and efforts to increase antigenicity

of known epitopes may increase clinical benefit. The longstanding paradigm was that a high peptide-MHC affinity correlates with a high immunogenicity[17]. In line with this assumption, many studies have attempted to increase the immunogenicity of known epitopes by enhancing their affinity[18]. By modifying the anchoring amino acids the affinity for MHCI can be increased, without interfering with T cell recognition, which is mostly dependent on the central amino acids[19]. In **Chapters 2 and 3** we describe the design and use of chemically altered peptide ligands (CPLs), epitopes that are not only modified with naturally occurring (proteogenic) amino acids, but also with chemically modified amino acids. Using such synthetic amino acids can offer several advantages in addition to increased affinity, including improved protease resistance and enhanced bioavailability[20,21].

The study described in **Chapter 2** set out to increase the affinity of epitopes known to bind HLA-A*02:01, the most abundant HLA allele in the Caucasian population, by introducing non-proteogenic amino acids[22]. We made several amino acids substitutions at or around the anchoring positions of a high-affinity influenza epitope and an intermediate-affinity cytomegalovirus epitope. The binding affinities were determined using fluorescence polarization-based assays to learn which substitutions frequently resulted in enhanced binding[23-25.] This information was then used to optimize binding of a number of melanoma-associated epitopes. The enhanced interactions were demonstrated via crystal structures of HLA-A*02:01 in complex with a wild-type antigen or a CPL. These were next loaded on peptide-MHCI (pMHCI) multimers and used to stain peripheral blood mononuclear cells from a melanoma patient. The detected frequencies of antigen-specific $CD8^+$ T cells were similar between pMHCs loaded with the wild-type antigen or with CPLs, indicating maintained interactions with the TCRs. Functional assays demonstrated prolonged activation of clonal wild-type specific $CD8^+$ T cells coincubated with synthetic antigen-pulsed APCs in vitro, and enhanced T cell responses of HLA-A*02:01 transgenic mice in vivo. Finally, the use of CPLs was validated in a clinical setting. CPLs based on a minor histocompatibility antigen (UTA2-1), showed an increased capacity to induce antigen-specific T cell responses that maintained cytolytic function[26].

In **Chapter 3** we moved from a therapeutic to a preventive setting and from cancer to virus[27]. Preventive vaccines differ from therapeutic ones, as they aim at inducing a pool of memory T cells to prevent infection rather than to cure it. The initial immune response is generally slow, but once memory is established the response is fast and infection may even be asymptomatic. Presence of pre-existing T cells has been shown to confer cross-protection against influenza A virus, which is precisely the purpose of vaccination with epitopes from conserved regions[28,29]. Multi-peptide vaccines are generally more successful than single-peptide vaccines, for the obvious reason that such a vaccine activates multiple T cells and hence prepares a more diverse pool of memory T cells to ward off

even newly emerging subtypes of the same virus[30]. Furthermore, a vaccine that contains peptides that bind different MHC alleles will activate a larger set of T cells and confer broader protection. Therefore the study in **Chapter 3** describes the optimization of binding affinity of a second common allele in the Caucasian population, HLA-A*03:01, in addition to HLA-A*02:01. For both alleles three conserved influenza A virus epitopes of varying immunodominance were selected and modified with a selection of non-proteogenic amino acids derived from the binding studies described in **Chapter 2**. Binding affinities were enhanced to similar levels, regardless of the immunodominance of the wild-type epitope. However, substitutions that increased binding of one epitope did not always translate to another, demonstrating the complexity of predicting binding affinity.

For a selection of the HLA-A*02:01-binding CPLs the capacity of inducing relevant T cell responses was determined using in vitro and ex vivo screening assays. CPL-loaded APCs were cocultured for 24 hours with clonal T cells specific for the corresponding (immunodominant) wild-type antigen. After incubation T cell activation was quantified by measuring IFN-γ secretion, which increased for some, but not all CPLs. In a second in vitro assay reactivity to CPLs was tested in a DC coculture model where CPL-pulsed DCs were cultured with autologous T cells from HLA-A*02:01$^+$ donors, after which IFN-γ production was measured again. This assay showed high variation between CPLs and between donors. In a third assay, designed to decrease inter-donor variance, reactivity of splenocytes from HLA-A*02:01 transgenic mice to CPLs was followed. The responses differed considerably between the assays, which complicated selection of peptides for further investigation. Results obtained in the in vitro and ex vivo assays were then used to select peptides for in vivo testing. For each viral epitope four CPLs with varying binding scores and increased or similar reactivity were compared to their wild-type sequences. The transgenic mice were vaccinated with one of the three wild-type antigens or CPLs. Splenocytes were isolated two weeks post vaccination and restimulated ex vivo in homologous fashion with the same peptide or with the wild-type epitope. Measurements of IFN-γ secretion in response to restimulation revealed that T cell responses were indeed enhanced by vaccination with some of the CPLs, also when restimulated with wild-type antigen, indicating that the induced CD8$^+$ T cells do recognize and respond to the wild-type epitopes.

The in vitro and in vivo assays demonstrated that vaccination with CPLs could augment CD8$^+$ T cell responses compared to wild-type epitopes, but the most potent CPLs were not necessarily those with the highest affinities. There likely is an optimal window for affinity; a low affinity will result in incomplete activation, whereas vaccination with high-affinity peptides induces higher numbers of T cells, but of lower quality[31-34]. In addition, tumor cells have been shown to upregulate negative regulators of T cell activation in response to prolonged pMHCI-TCR

contact, thereby blocking full activation[35]. The intricate interplay of factors important for strong TCR activation cannot completely be accounted for in vitro, which is probably why we could not predict from our in vitro experiments which CPLs induced the most potent responses in vivo[36].

Cancer immunotherapy

In many cases cytotoxic responses directed at tumor cells do develop, but due to the low affinity of TCRs to self-antigens, or tumor-associated immune suppression, effective anti-tumor immunity is impaired[32,37-40]. Enhanced tumor-associated antigens to reach an affinity above the threshold for TCR activation can induce activation of effector functions and anti-tumor immunity[41,42]. Peptide vaccines often lack efficiency when provided as a monotherapy, but as an adjuvant to other treatment they may improve outcomes drastically. Formulations composed of long peptides and adjuvants co-activate DCs to induce costimulation and $CD4^+$ T cell help[43].

In combination with (neoadjuvant) checkpoint inhibition the perfect immune-stimulating environment for optimal anti-tumor immunity can be established. Since the Nobel Prize for Physiology and Medicine was awarded to this discovery, checkpoint inhibitors have gained exponential attention. Immune checkpoints are molecules expressed on immune cells that function as negative regulators of T cell activation, thereby maintaining the balance between activation and self-tolerance and thus preventing auto-immunity. Two of the most described and targeted checkpoints in treatment of cancer are programmed death 1 (PD-1), which binds the ligands PD-L1 and PD-L2 on tumor cells, and cytotoxic T lymphocyte-associated protein 4 (CTLA-4), which blocks costimulation by binding the CD28 ligands B7-1 and B7-2[44,45]. A total of six antibodies that block the interaction between PD-1 and CTLA-4 and their ligands have been approved for treatment of various types of cancer, and many clinical trials are still ongoing[46]. Repressing inhibitory immune signals reinstates pre-existing immune responses and therefore as a prerequisite for efficacious treatment cancerous cells have to be on the radar of the immune system. Patients suffering from cancers with a high mutational burden that express high levels of neoantigens therefore generally benefit most from cancer immunotherapy[47]. Vaccination with neoantigens or tumor-associated antigens may boost the first signal for T cell activation and help overcome the bottleneck of immune detection.

As a second prerequisite DC activation is crucial for delivering appropriate costimulatory signals and pro-inflammatory cytokines. Biological or chemical adjuvants that activate pattern recognition receptors on DCs greatly enhance the effect of immunotherapy. A third bottleneck in cancer immunotherapy is

tumor-associated immune suppression. In response to immune detection tumor cells have developed various mechanisms to evade and suppress detection, for example through recruitment of regulatory T (Treg) cells. Inhibiting the drivers of Treg cell recruitment or expansion may potentially relieve immune suppression and enhance clinical benefit. Vice versa agonists of factors involved in Treg suppression may bring about the same effect. Especially combinations of treatment modalities, including standard-of-care radiotherapy or chemotherapy will ultimately lead to maximal clinical benefit. The contribution of biochemistry is relatively unexplored in this field, and we believe it will support cancer immunotherapy as detailed in **Chapter 4**.

Visualizing immune responses using pMHCI multimers

Monitoring an individual's immune status and responses to treatment, as well as mapping of antigenic epitopes as therapeutic targets, can help diagnose disease and design treatment plans. The classical reagents used to visualize and monitor antigen-specific T cell responses consist of MHCI molecules loaded with antigenic peptides of interest[48]. The dissociation rate of pMHCI monomers is generally high and therefore multimerization is needed to achieve strong TCR binding required for further experimental analysis, such as flow cytometry[49]. The MHCI heavy chains are biotinylated and subsequently multimerized on streptavidin conjugated to a fluorophore for detection. Folding of heavy chain, light chain and peptide requires several time-consuming steps that must be performed for each studied peptide. A number of peptide exchange technologies have been developed to increase the throughput of pMHCI multimer generation a number of peptide exchange technologies have been developed[50-52]. Such technologies allow for folding of one large batch of conditional MHCI monomers with a peptide that, upon application of a defined trigger, vacates the binding groove. When performed in presence of a peptide of interest the complex will be loaded with this new peptide. One of the most commonly-used exchange technologies developed in our lab uses a photolabile peptide that is cleaved by UV radiation. However easy, some disadvantages of this technology include photodamage to the fluorophores, proteins or peptides, formation of reactive species and sample evaporation due to heat generation.

Chapter 5 describes a novel technology that circumvents these drawbacks. This method is based on a previous study on temperature-dependency of peptide affinities for MHCI[53]. At low temperatures the on-rates and off-rates are similar between peptides, but at physiological temperatures the off-rates differ considerably. Based on this finding we designed low-affinity template peptides for the most-studied human- and murine MHCI alleles, HLA-A*02:01 and H-2K^{b}, by

modifying the anchoring amino acids of known epitopes. By reducing the quality of the interactions between the peptide and the binding pockets one can form a pMHCI complex that is stable at low temperatures, but dissociates at increased temperatures. The conditional pMHCIs generated in this fashion can thermally be exchanged for any peptide of interest, provided that it has a higher affinity than the template peptide. As a major advantage, in contrast to UV-induced exchange that bleaches fluorophores, thermal exchange can also be performed on multimers, reducing pre-staining handling time significantly. Exchanged multimers stained similar percentages of clonal $CD8^+$ T cells as UV-exchanged multimers or conventional multimers folded with the peptide of interest. **Chapter 6** contains a step-by-step protocol on how to produce and thermally-exchange conditional pMHCI multimers.

The study described in **Chapter 5** successfully verified the applicability of thermally-exchanged pMHCI multimers in a clinically-relevant setting. The exchanged multimers were used for monitoring $CD8^+$ T cell kinetics in a human HLA-A*02:01$^+$ transplant recipient in response to viral reactivation. The frequencies of detected $CD8^+$ T cells were comparable between conventional multimers and those thermally exchanged ad hoc prior to staining, illustrating the efficiency and flexibility of the temperature-exchange technology. We have provided proof-of-principle for two alleles and the design of other exchangeable alleles is ongoing.

In clinical applications the amount of patient material is often limited and hence extensive analysis of T cell specificities may not be possible, since only a certain number of parameters can be measured simultaneously using flow cytometry, depending on the lasers equipped and the fluorophores used. To increase the number of measurable parameters combinatorial coding can be employed, but larger screens require a broader range[54,55]. **Chapter 7** describes a method that provides an essentially unlimited variety of pMHCI labeling, allowing a greatly enhanced screening range for T cells. By labeling each pMHCI with a DNA barcode and fluorescent label, multimer$^+$ $CD8^+$ T cells can be sorted and sequenced, so that many more specificities can be detected in parallel[56]. In this study, we used DNA-barcoded conditional pMHCI multimers to validate true neoantigens predicted from HLA-A*02:01$^+$ human colorectal cancer patients. This particular cancer type is associated with increased microsatellite instability, resulting in DNA mutations that potentially give rise to neoantigens. Neoantigens arise from somatic DNA mutations later in life and therefore no central tolerance has been raised towards them[57]. Combined with the fact that they are only expressed on tumor cells, this makes them extremely suitable immunotherapeutic targets[58]. Because they are patient-specific neoantigens have to be identified per individual, a procedure that with the advent of next-generation sequencing has become readily available. Potential neoantigens were identified by DNA sequencing of tumor and healthy tissue and identification of transcribed antigens

through RNA sequencing[59]. Putative neoantigen sequences were then be matched to the expressed MHCI allotypes using NetMHC.

Proof-of-principle was provided by using DNA-barcoded multimers exchanged for common viral antigens to stain peripheral blood mononuclear cells of healthy volunteers. Some of these specificities were detected in the same volunteers in earlier studies and similar frequencies of $CD8^+$ T cells were detected with exchanged multimers. In a next step multimers were exchanged for predicted neoantigens, derived from DNA sequencing of five colorectal cancer patients, with common viral antigens as control. Responses against some of these viral antigens were detected, but no barcode sequences corresponding to predicted neoantigens were retrieved. Because neoantigen frequencies are usually low it is not surprising that the number of $CD8^+$ T cell specific for neoantigens is lower than those specific for viral antigens. Nevertheless, a hit detected in a previous (coculture) assay was expected to turn up. This particular peptide is a weak binder and may inefficiently be loaded on HLA-A*02:01 multimers, although it has a higher affinity than the template peptide. Likewise, a screen using a murine colorectal cancer model did not provide any hits above the detection threshold. This most likely is due to low cell numbers obtained from the thawed cell suspensions. We expect that careful revision of the experimental set-up will uncover the potential of DNA-barcoded pMHCI screens for discovery of antigen-specific $CD8^+$ T cells responses.

References

1. Vivier, E. & Malissen, B. Innate and adaptive immunity: specificities and signaling hierarchies revisited. *Nat Immunol* **6**, 17-21 (2005).
2. Medzhitov, R. & Janeway, C. Innate immune recognition: mechanisms and pathways. *Immunol Rev* **173**, 89-97 (2000).
3. Rock, K.L., Reits, E. & Neefjes, J. Present Yourself! By MHC Class I and MHC Class II Molecules. *Trends Immunol* **37**, 724-737 (2016).
4. Neefjes, J., Jongsma, M.L., Paul, P. & Bakke, O. Towards a systems understanding of MHC class I and MHC class II antigen presentation. *Nat Rev Immunol* **11**, 823-836 (2011).
5. Mescher, M.F., *et al.* Signals required for programming effector and memory development by $CD8^+$ T cells. *Immunol Rev* **211**, 81-92 (2006).
6. Sharpe, A.H. & Abbas, A.K. T-cell costimulation--biology, therapeutic potential, and challenges. *N Engl J Med* **355**, 973-975 (2006).
7. Gross, J.A., Callas, E. & Allison, J.P. Identification and distribution of the costimulatory receptor CD28 in the mouse. *J Immunol* **149**, 380-388 (1992).
8. Croft, M. Costimulation of T cells by OX40, 4-1BB, and CD27. *Cytokine Growth Factor Rev* **14**, 265-273 (2003).
9. Curtsinger, J.M. & Mescher, M.F. Inflammatory cytokines as a third signal for T cell activation. *Curr Opin Immunol* **22**, 333-340 (2010).
10. Curtsinger, J.M., Lins, D.C. & Mescher, M.F. Signal 3 determines tolerance versus full activation of naive CD8 T cells: dissociating proliferation and development of effector function. *J Exp Med* **197**, 1141-1151 (2003).
11. Valenzuela, J., Schmidt, C. & Mescher, M. The roles of IL-12 in providing a third signal for clonal

expansion of naive CD8 T cells. *J Immunol* **169**, 6842-6849 (2002).
12. Madden, D.R. The three-dimensional structure of peptide-MHC complexes. *Annu Rev Immunol* **13**, 587-622 (1995).
13. Rammensee, H.G., Friede, T. & Stevanoviic, S. MHC ligands and peptide motifs: first listing. *Immunogenetics* **41**, 178-228 (1995).
14. Falk, K., Rotzschke, O., Stevanovic, S., Jung, G. & Rammensee, H.G. Allele-specific motifs revealed by sequencing of self-peptides eluted from MHC molecules. *Nature* **351**, 290-296 (1991).
15. Melief, C.J. & Kast, W.M. T-cell immunotherapy of tumors by adoptive transfer of cytotoxic T lymphocytes and by vaccination with minimal essential epitopes. *Immunol Rev* **145**, 167-177 (1995).
16. Purcell, A.W., McCluskey, J. & Rossjohn, J. More than one reason to rethink the use of peptides in vaccine design. *Nat Rev Drug Discov* **6**, 404-414 (2007).
17. Engels, B., *et al.* Relapse or eradication of cancer is predicted by peptide-major histocompatibility complex affinity. *Cancer Cell* **23**, 516-526 (2013).
18. Tangri, S., *et al.* Structural features of peptide analogs of human histocompatibility leukocyte antigen class I epitopes that are more potent and immunogenic than wild-type peptide. *J Exp Med* **194**, 833-846 (2001).
19. Valmori, D., *et al.* Enhanced generation of specific tumor-reactive CTL in vitro by selected Melan-A/MART-1 immunodominant peptide analogues. *J Immunol* **160**, 1750-1758 (1998).
20. Blanchet, J.S., *et al.* A new generation of Melan-A/MART-1 peptides that fulfill both increased immunogenicity and high resistance to biodegradation: implication for molecular anti-melanoma immunotherapy. *J Immunol* **167**, 5852-5861 (2001).
21. Marschutz, M.K., *et al.* Improvement of the enzymatic stability of a cytotoxic T-lymphocyte-epitope model peptide for its oral administration. *Peptides* **23**, 1727-1733 (2002).
22. Hoppes, R., *et al.* Altered peptide ligands revisited: vaccine design through chemically modified HLA-A2-restricted T cell epitopes. *J Immunol* **193**, 4803-4813 (2014).
23. Buchli, R., *et al.* Development and validation of a fluorescence polarization-based competitive peptide-binding assay for HLA-A*0201--a new tool for epitope discovery. *Biochemistry* **44**, 12491-12507 (2005).
24. Morrison, J., *et al.* Identification of the nonamer peptide from influenza A matrix protein and the role of pockets of HLA-A2 in its recognition by cytotoxic T lymphocytes. *Eur J Immunol* **22**, 903-907 (1992).
25. Diamond, D.J., York, J., Sun, J.Y., Wright, C.L. & Forman, S.J. Development of a candidate HLA A*0201 restricted peptide-based vaccine against human cytomegalovirus infection. *Blood* **90**, 1751-1767 (1997).
26. Oostvogels, R., *et al.* Towards effective and safe immunotherapy after allogeneic stem cell transplantation: identification of hematopoietic-specific minor histocompatibility antigen UTA2-1. *Leukemia* **27**, 642-649 (2013).
27. Rosendahl Huber, S.K., *et al.* Chemical Modification of Influenza $CD8^+$ T-Cell Epitopes Enhances Their Immunogenicity Regardless of Immunodominance. *PLoS One* **11**, e0156462 (2016).
28. McMichael, A.J., Gotch, F.M., Noble, G.R. & Beare, P.A. Cytotoxic T-cell immunity to influenza. *N Engl J Med* **309**, 13-17 (1983).
29. Epstein, S.L., *et al.* Protection against multiple influenza A subtypes by vaccination with highly conserved nucleoprotein. *Vaccine* **23**, 5404-5410 (2005).
30. Chianese-Bullock, K.A., *et al.* MAGE-A1-, MAGE-A10-, and gp100-derived peptides are immunogenic when combined with granulocyte-macrophage colony-stimulating factor and montanide ISA-51 adjuvant and administered as part of a multipeptide vaccine for melanoma. *J Immunol* **174**, 3080-3086 (2005).
31. McMahan, R.H., *et al.* Relating TCR-peptide-MHC affinity to immunogenicity for the design of tumor vaccines. *J Clin Invest* **116**, 2543-2551 (2006).
32. Zehn, D., Lee, S.Y. & Bevan, M.J. Complete but curtailed T-cell response to very low-affinity antigen. *Nature* **458**, 211-214 (2009).
33. Slansky, J.E. & Jordan, K.R. The Goldilocks model for TCR-too much attraction might not be best for vaccine design. *PLoS Biol* **8**(2010).
34. Kalergis, A.M., *et al.* Efficient T cell activation requires an optimal dwell-time of interaction between the TCR and the pMHC complex. *Nat Immunol* **2**, 229-234 (2001).

35. Zahm, C.D., Colluru, V.T. & McNeel, D.G. Vaccination with High-Affinity Epitopes Impairs Antitumor Efficacy by Increasing PD-1 Expression on CD8(+) T Cells. *Cancer Immunol Res* **5**, 630-641 (2017).
36. Corse, E., Gottschalk, R.A. & Allison, J.P. Strength of TCR-peptide/MHC interactions and in vivo T cell responses. *J Immunol* **186**, 5039-5045 (2011).
37. McWilliams, J.A., *et al.* Age-dependent tolerance to an endogenous tumor-associated antigen. *Vaccine* **26**, 1863-1873 (2008).
38. Colella, T.A., *et al.* Self-tolerance to the murine homologue of a tyrosinase-derived melanoma antigen: implications for tumor immunotherapy. *J Exp Med* **191**, 1221-1232 (2000).
39. Dunn, G.P., Bruce, A.T., Ikeda, H., Old, L.J. & Schreiber, R.D. Cancer immunoediting: from immunosurveillance to tumor escape. *Nat Immunol* **3**, 991-998 (2002).
40. Schreiber, R.D., Old, L.J. & Smyth, M.J. Cancer immunoediting: integrating immunity's roles in cancer suppression and promotion. *Science* **331**, 1565-1570 (2011).
41. Hemmer, B., Stefanova, I., Vergelli, M., Germain, R.N. & Martin, R. Relationships among TCR ligand potency, thresholds for effector function elicitation, and the quality of early signaling events in human T cells. *J Immunol* **160**, 5807-5814 (1998).
42. de Visser, K.E., *et al.* Low-avidity self-specific T cells display a pronounced expansion defect that can be overcome by altered peptide ligands. *J Immunol* **167**, 3818-3828 (2001).
43. Ahrends, T., *et al.* CD4(+) T Cell Help Confers a Cytotoxic T Cell Effector Program Including Coinhibitory Receptor Downregulation and Increased Tissue Invasiveness. *Immunity* **47**, 848-861 e845 (2017).
44. Leach, D.R., Krummel, M.F. & Allison, J.P. Enhancement of antitumor immunity by CTLA-4 blockade. *Science* **271**, 1734-1736 (1996).
45. Ribas, A. & Wolchok, J.D. Cancer immunotherapy using checkpoint blockade. *Science* **359**, 1350-1355 (2018).
46. Hargadon, K.M., Johnson, C.E. & Williams, C.J. Immune checkpoint blockade therapy for cancer: An overview of FDA-approved immune checkpoint inhibitors. *Int Immunopharmacol* **62**, 29-39 (2018).
47. Hellmann, M.D., *et al.* Tumor Mutational Burden and Efficacy of Nivolumab Monotherapy and in Combination with Ipilimumab in Small-Cell Lung Cancer. *Cancer Cell* **33**, 853-861 e854 (2018).
48. Altman, J.D., *et al.* Phenotypic analysis of antigen-specific T lymphocytes. *Science* **274**, 94-96 (1996).
49. Davis, M.M., Altman, J.D. & Newell, E.W. Interrogating the repertoire: broadening the scope of peptide-MHC multimer analysis. *Nat Rev Immunol* **11**, 551-558 (2011).
50. Saini, S.K., *et al.* Dipeptides catalyze rapid peptide exchange on MHC class I molecules. *Proc Natl Acad Sci U S A* **112**, 202-207 (2015).
51. Amore, A., *et al.* Development of a hypersensitive periodate-cleavable amino acid that is methionine- and disulfide-compatible and its application in MHC exchange reagents for T cell characterisation. *Chembiochem* **14**, 123-131 (2013).
52. Rodenko, B., *et al.* Class I major histocompatibility complexes loaded by a periodate trigger. *J Am Chem Soc* **131**, 12305-12313 (2009).
53. Garstka, M.A., *et al.* The first step of peptide selection in antigen presentation by MHC class I molecules. *P Natl Acad Sci USA* **112**, 1505-1510 (2015).
54. Hadrup, S.R., *et al.* Parallel detection of antigen-specific T-cell responses by multidimensional encoding of MHC multimers. *Nat Methods* **6**, 520-526 (2009).
55. Newell, E.W., *et al.* Combinatorial tetramer staining and mass cytometry analysis facilitate T-cell epitope mapping and characterization. *Nat Biotechnol* **31**, 623-629 (2013).
56. Bentzen, A.K., *et al.* Large-scale detection of antigen-specific T cells using peptide-MHC-I multimers labeled with DNA barcodes. *Nat Biotechnol* **34**, 1037-1045 (2016).
57. Corthay, A. Does the immune system naturally protect against cancer? *Front Immunol* **5**, 197 (2014).
58. Schumacher, T.N. & Schreiber, R.D. Neoantigens in cancer immunotherapy. *Science* **348**, 69-74 (2015).
59. Karasaki, T., *et al.* Prediction and prioritization of neoantigens: integration of RNA sequencing data with whole-exome sequencing. *Cancer Sci* **108**, 170-177 (2017).

A

A

Nederlandse samenvatting

Adaptieve immuniteit in een notendop

Ons immuunsysteem is geëvolueerd om ons te beschermen tegen infectie door virussen en andere pathogenen, maar biedt tegelijkertijd ook bescherming tegen kanker door cellen die gemuteerde eiwitten tot expressie brengen te elimineren. De twee takken van het immuunsysteem werken nauw samen om bedreigingen te detecteren en te elimineren. De eerstelijnsafweer wordt verzorgd door het aspecifieke aangeboren immuunsysteem, door middel van detectie van pathogene- of tumorcel-fragmenten[1]. Patroonherkenningsreceptoren op aangeboren immuuncellen kunnen pathogeen- of gevaar-geassocieerde moleculaire patronen herkennen, waaronder cel-vrij DNA, dubbelstrengs RNA of componenten van de bacteriële celwand[2]. Daarentegen kunnen cellen van het adaptieve (verworven) immuunsysteem pathogenen of maligne cellen specifieker herkennen en hierop reageren door het scannen van kleine fragmenten van eiwitten: peptiden. Deze peptiden kunnen door major histocompatibility complex klasse I (MHCI) moleculen worden gepresenteerd op het oppervlak van alle cellen die een kern hebben, voor surveillance door cytotoxische $CD8^+$ T cellen[3]. Deze gespecialiseerde T cellen kunnen het repertoire aan gepresenteerde peptiden scannen en het onderscheid maken tussen lichaamseigen- en niet-eigen peptiden, middels hun buitengewoon specifieke T cel receptoren (TCR's). Deze T cellen kunnen andere cellen die tekenen vertonen van infectie of mutatie direct elimineren. Op eenzelfde wijze wordt de extracellulaire ruimte gemonitord door helper T (Th), of $CD4^+$, cellen, die geïnternaliseerde extracellulaire peptiden scannen die worden gepresenteerd door MHC klasse II (MHCII)[4]. Bij herkenning van dergelijke uitheemse peptiden produceren $CD4^+$ T cellen cytokines die klonale expansie en activatie van B cellen induceren, die vervolgens antilichamen kunnen produceren.

TCR activatie is de eerste van de drie signalen die nodig is voor het opwekken van een effectieve adaptieve immuunrespons; voor aanhoudende activatie en proliferatie is een tweede signaal noodzakelijk, welke wordt verstrekt door costimulatie[5,6]. Costimulatoire receptoren op het celoppervlak van T cellen worden geactiveerd door het binden van hun liganden op geactiveerde antigeen-presenterende cellen, zoals dendritische cellen. Het costimulatoire pad dat het best gekarakteriseerd is omvat CD28, een receptor die constitutief tot expressie wordt gebracht op naïeve T cellen, en zijn liganden B7-1 (CD80) en B7-2 (CD86)[7]. $CD4^+$ T cellen verschaffen hulp die cruciaal is voor de maturatie van dendritische cellen en het verhogen van de expressie van B7-1 en B7-2[5]. Hoewel geactiveerde T cellen een aantal proliferatierondes kunnen doormaken wanneer costimulatie

plaatsvindt is een derde signaal, verstrekt door cytokines, nodig voor klonale expansie, overleving en het vormen van geheugen[9]. Afwezigheid van dit derde signaal zal uiteindelijk tot tolerantie leiden[10]. Voor volledig functionele $CD8^+$ T cellen zijn interleukine (IL) 12 of type I interferons (IFN's) nodig, die worden geproduceerd door $CD4^+$ Th cellen[11].

MHCI antigeen presentatie en TCR activatie

MHCI wordt in het endoplasmatisch reticulum geladen met intracellulair geproduceerde peptiden, bij voorkeur met een lengte van 8-10 aminozuren. Twee alfa-helices vormen een groef met enkele inkepingen waarin de zijketens van de aminozuren van het peptide kunnen binden[12]. De peptide-MHCI bindingsaffiniteit wordt bepaald door de interacties van de zware keten van MHCI met de ruggengraat en zijketens van het peptide[13]. De TCR bindt zowel de uitstekende zijketens van het peptide als de blootliggende residuen van de alfa-helices van het MHCI. De extreme selectiviteit van de TCR zorgt ervoor dat slechts één specifieke peptide-MHCI combinatie tot activatie leidt, om zo de hoge specificiteit te waarborgen die nodig is om zelftolerantie in stand te houden en auto-immuniteit te voorkomen.

De genen die coderen voor MHCI zijn verdeeld over drie groepen; in mensen humaan leukocytenantigeen (HLA) A, B en C. Deze genen zijn zeer polymorf, wat inhoudt dat er veel variaties zijn ontstaan door DNA mutatie, recombinatie en conversie. De verkregen allotypes kunnen verschillen in één of meerdere aminozuren, voornamelijk in de peptide-bindende groef, die van invloed zijn op de geprefereerde peptide motieven[14]. Ieder individu erft een HLA-A, een HLA-B en een HLA-C gen van iedere ouder, met als gevolg expressie van 3 tot 6 verschillende HLA allotypes per individu. Door expressie van meerdere subtypes kunnen meerdere fragmenten van een eiwit worden gepresenteerd, om zo brede immuun bescherming te bereiken.

Immuuntherapie

Verbeterde peptide vaccins door chemische modificatie

Ons immuunsysteem is ontzettend geavanceerd als het aankomt op het detecteren en elimineren van geïnfecteerde of getransformeerde cellen. Dit vermogen wordt dankbaar omarmd door clinici: immuuntherapieën die antivirale of antitumor responsen kunnen opwekken hebben hun effectiviteit bewezen tegen zowel infectie als kanker. Het activeren van $CD8^+$ T cellen wordt beschouwd al de meest rechtlijnige aanpak, omdat een cytotoxische respons specifiek gericht op geïnfecteerde of getransformeerde cellen zal leiden tot eliminatie van alléén die cellen die het antigeen tot expressie brengen, zelfs als

deze zich op afstand van de tumor bevinden. Diverse therapeutische strategieën kunnen worden toegepast, zoals vaccinatie met antigene peptiden, antigeen-coderend RNA, dendritische cellen geladen met antigeen of zelfs met antigeen-geactiveerde cellen[15]. Het ontwerpen van peptide vaccins heeft de afgelopen decennia bijzonder veel interesse gewekt en hun werkzaamheid, stabiliteit en farmacokinetiek zijn uitgebreid bestudeerd. Daarnaast is peptidesynthese gemakkelijk, goedkoop en flexibel[16]. Peptiden op zichzelf zijn maar matig immunogeen en pogingen om de antigeniciteit van bekende epitopen te verhogen zouden klinisch voordeel kunnen bieden. Lange tijd werd een hoge peptide-MHCI affiniteit gecorreleerd aan hoge immunogeniciteit en in die lijn hebben vele studies geprobeerd de immunogeniciteit van bekende epitopen te verhogen door hun affiniteit te verhogen[17,18]. Door de aminozuren die het peptide in de MHCI verankeren te modificeren kan de affiniteit van het peptide voor zijn MHCI verhoogd worden, zonder te interfereren met T cel herkenning, wat grotendeels afhangt van de centrale aminozuren[19]. In **Hoofdstuk 2 en 3** beschrijven wij het ontwerp en gebruik van chemisch aangepaste peptide liganden (CPL's): epitopen die niet alleen gemodificeerd zijn met natuurlijk-voorkomende aminozuren, maar ook met chemisch gemodificeerde aminozuren. Het gebruik van dergelijke synthetische aminozuren biedt een aantal voordelen bovenop de verhoogde affiniteit, zoals verhoogde resistentie tegen proteasen en verbeterde biologische beschikbaarheid[20,21].

Het werk beschreven in **Hoofdstuk 2** had als doel om met chemisch-gemodificeerde aminozuren de affiniteit te verbeteren van epitopen specifiek voor HLA-A*02:01, het meest voorkomende allotype in Kaukasische populaties[22]. De zo gecreëerde CPL's werden ingezet als therapeutisch vaccin in de context van kanker. In **Hoofdstuk 3** is een preventieve insteek onderzocht in de context van virale infectie[23]. In dat hoofdstuk zijn naast HLA-A*02:01 epitopen ook CPL's ontworpen voor een tweede veelvoorkomend allel in de Kaukasische bevolking, HLA-A*03:01, met als doel een breed beschermend influenza vaccin te creëren.

Kankerimmunotherapie

Sinds in 2018 de Nobelprijs voor Fysiologie of Geneeskunde is uitgereikt aan de nieuwe ontwikkelingen in kankerimmunotherapie heeft immuuntherapie veel aandacht verworven. In veel gevallen treden cytotoxische responsen tegen kanker wel op, maar door de lage affiniteit van zelfantigenen, of door tumor-geassocieerde immuun suppressie, wordt effectieve anti-tumor immuniteit verzwakt[32,37-40]. Immuuntherapie richt zich op het wegnemen van de rem op anti-tumor responsen. Huidige immuuntherapieën zijn voornamelijk biologisch, maar ook chemische stoffen, zogenaamde small molecules, kunnen een waardevolle bijdrage leveren, zoals beschreven in **Hoofdstuk 4**.

Het visualiseren van immuunresponsen met pMHCI multimeren

Het monitoren van de immuun status en respons op behandeling, samen met het in kaart brengen van antigene epitopen als therapeutische doelwitten, kan helpen bij diagnose en het ontwerpen van behandelplannen. De klassieke reagentia om antigeen-specifieke T cel responsen te visualiseren en monitoren bestaan uit MHCI moleculen geladen met relevante peptiden[24]. Omdat de dissociatiesnelheid van pMHCI monomeren hoog is kunnen deze moleculen worden gemultimeriseerd om sterke TCR binding te waarborgen voor verdere experimentele analyse, zoals flow cytometrie[25]. Het vouwen van pMHCI complexen is tijdrovend en moet voor ieder te analyseren peptide apart uitgevoerd worden. Om de doorvoer op te schalen is er een aantal peptide-uitwisselingstechnologieën ontwikkeld[26-28]. Door gebruik te maken van zulke technologieën kan één grote hoeveelheid conditionele pMHCI monomeren worden gegenereerd met een peptide dat onder aanbrenging van de juiste trigger zal dissociëren. Wanneer uitgevoerd in aanwezigheid van ander peptide zal deze in het complex worden geladen. Een van de meest gebruikte uitwisselingsmethodes maakt gebruik van een fotolabiel peptide dat wordt geknipt onder invloed van UV straling[29,30]. Deze methode heeft een aantal nadelen, zoals fotoschade aan fluoroforen, eiwitten of peptiden, de vorming van reactieve groepen en verdamping van het monster door hitteontwikkeling.

Hoofdstuk 5 beschrijft een nieuwe uitwisselingstechnologie, gebaseerd op peptide-dissociatie onder invloed van temperatuur. Door het modificeren van ankerresiduen hebben wij peptiden ontworpen voor HLA-A*02:01 en voor H-2K^{b}, het meest bestudeerde MHCI allel in muizen, welke kunnen worden uitgewisseld door het verhogen van de temperatuur. Een groot voordeel is dat deze methode ook toegepast kan worden op multimeren, in tegenstelling tot UV-geïnduceerde uitwisseling waarbij fluoroforen gebleekt worden. Dit verkleint de verwerkingstijd voor kleuring aanzienlijk. In **Hoofdstuk 6** wordt in een protocol stap voor stap beschreven hoe deze conditionele multimeren kunnen worden geproduceerd en gebruikt.

Vervolgens is de technologie voor het in **Hoofdstuk 7** beschreven onderzoek uitgebreid met een DNA labelingssysteem. Hiermee wordt het aantal parameters dat te meten is in één analyse aanzienlijk vermeerderd ten opzichte van fluorescente labels. Deze technologie werd als proof-of-principle screen ingezet voor het identificeren van neoantigenen als potentiele doelwitten voor kankerimmunotherapie.

Referenties

1. Vivier, E. & Malissen, B. Innate and adaptive immunity: specificities and signaling hierarchies revisited. *Nat Immunol* **6**, 17-21 (2005).
2. Medzhitov, R. & Janeway, C. Innate immune recognition: mechanisms and pathways. *Immunol Rev* **173**, 89-97 (2000).
3. Rock, K.L., Reits, E. & Neefjes, J. Present Yourself! By MHC Class I and MHC Class II Molecules. *Trends Immunol* **37**, 724-737 (2016).
4. Neefjes, J., Jongsma, M.L., Paul, P. & Bakke, O. Towards a systems understanding of MHC class I and MHC class II antigen presentation. *Nat Rev Immunol* **11**, 823-836 (2011).
5. Mescher, M.F., *et al.* Signals required for programming effector and memory development by CD8+ T cells. *Immunol Rev* **211**, 81-92 (2006).
6. Sharpe, A.H. & Abbas, A.K. T-cell costimulation--biology, therapeutic potential, and challenges. *N Engl J Med* **355**, 973-975 (2006).
7. Gross, J.A., Callas, E. & Allison, J.P. Identification and distribution of the costimulatory receptor CD28 in the mouse. *J Immunol* **149**, 380-388 (1992).
8. Croft, M. Costimulation of T cells by OX40, 4-1BB, and CD27. *Cytokine Growth Factor Rev* **14**, 265-273 (2003).
9. Curtsinger, J.M. & Mescher, M.F. Inflammatory cytokines as a third signal for T cell activation. *Curr Opin Immunol* **22**, 333-340 (2010).
10. Curtsinger, J.M., Lins, D.C. & Mescher, M.F. Signal 3 determines tolerance versus full activation of naive CD8 T cells: dissociating proliferation and development of effector function. *J Exp Med* **197**, 1141-1151 (2003).
11. Valenzuela, J., Schmidt, C. & Mescher, M. The roles of IL-12 in providing a third signal for clonal expansion of naive CD8 T cells. *J Immunol* **169**, 6842-6849 (2002).
12. Madden, D.R. The three-dimensional structure of peptide-MHC complexes. *Annu Rev Immunol* **13**, 587-622 (1995).
13. Rammensee, H.G., Friede, T. & Stevanoviic, S. MHC ligands and peptide motifs: first listing. *Immunogenetics* **41**, 178-228 (1995).
14. Falk, K., Rotzschke, O., Stevanovic, S., Jung, G. & Rammensee, H.G. Allele-specific motifs revealed by sequencing of self-peptides eluted from MHC molecules. *Nature* **351**, 290-296 (1991).
15. Melief, C.J. & Kast, W.M. T-cell immunotherapy of tumors by adoptive transfer of cytotoxic T lymphocytes and by vaccination with minimal essential epitopes. *Immunol Rev* **145**, 167-177 (1995).
16. Purcell, A.W., McCluskey, J. & Rossjohn, J. More than one reason to rethink the use of peptides in vaccine design. *Nat Rev Drug Discov* **6**, 404-414 (2007).
17. Engels, B., *et al.* Relapse or eradication of cancer is predicted by peptide-major histocompatibility complex affinity. *Cancer Cell* **23**, 516-526 (2013).
18. Tangri, S., *et al.* Structural features of peptide analogs of human histocompatibility leukocyte antigen class I epitopes that are more potent and immunogenic than wild-type peptide. *J Exp Med* **194**, 833-846 (2001).
19. Valmori, D., *et al.* Enhanced generation of specific tumor-reactive CTL in vitro by selected Melan-A/MART-1 immunodominant peptide analogues. *J Immunol* **160**, 1750-1758 (1998).
20. Blanchet, J.S., *et al.* A new generation of Melan-A/MART-1 peptides that fulfill both increased immunogenicity and high resistance to biodegradation: implication for molecular anti-melanoma immunotherapy. *J Immunol* **167**, 5852-5861 (2001).
21. Marschutz, M.K., *et al.* Improvement of the enzymatic stability of a cytotoxic T-lymphocyte-epitope model peptide for its oral administration. *Peptides* **23**, 1727-1733 (2002).
22. Hoppes, R., *et al.* Altered peptide ligands revisited: vaccine design through chemically modified HLA-A2-restricted T cell epitopes. *J Immunol* **193**, 4803-4813 (2014).
23. Rosendahl Huber, S.K., *et al.* Chemical Modification of Influenza CD8+ T-Cell Epitopes Enhances Their Immunogenicity Regardless of Immunodominance. *PLoS One* **11**, e0156462 (2016).
24. Altman, J.D., *et al.* Phenotypic analysis of antigen-specific T lymphocytes. *Science* **274**, 94-96 (1996).
25. Davis, M.M., Altman, J.D. & Newell, E.W. Interrogating the repertoire: broadening the scope of peptide-MHC multimer analysis. *Nat Rev Immunol* **11**, 551-558 (2011).

26. Saini, S.K., *et al.* Dipeptides catalyze rapid peptide exchange on MHC class I molecules. *Proc Natl Acad Sci U S A* **112**, 202-207 (2015).
27. Amore, A., *et al.* Development of a hypersensitive periodate-cleavable amino acid that is methionine- and disulfide-compatible and its application in MHC exchange reagents for T cell characterisation. *Chembiochem* **14**, 123-131 (2013).
28. Rodenko, B., *et al.* Class I major histocompatibility complexes loaded by a periodate trigger. *J Am Chem Soc* **131**, 12305-12313 (2009).
29. Rodenko, B., *et al.* Generation of peptide-MHC class I complexes through UV-mediated ligand exchange. *Nat Protoc* **1**, 1120-1132 (2006).
30. Toebes, M., *et al.* Design and use of conditional MHC class I ligands. *Nat Med* **12**, 246-251 (2006).

A

List of publications

Luimstra, J.J.; Neefjes, J.; Borst, J.G.; Ovaa, H. The future of cancer immunotherapy: opportunities for small molecules.
Manuscript under revision

Luimstra, J.J.; Franken, C.L.M.C.; Garstka, M.A.; Drijfhout, J.W.; Neefjes, J.; Ovaa, H. Production and thermal exchange of conditional peptide-MHC I multimers.
Current Protocols in Immunology 126, e85 (2019)

Luimstra, J.J.*; Garstka, M.A.*; Roex, M.C.J.; Redeker, A.; Janssen, G.M.C.; Van Veelen, P.A.; Arens, R.; Falkenburg, J.H.F.; Neefjes, J.; Ovaa, H. A flexible MHC class I multimer loading system for large-scale detection of antigen-specific T cells.
Journal of Experimental Medicine 215, 1493-1504 (2018)

Rosendahl Huber, S.K.*; **Luimstra, J.J.***; Van Beek, J.; Hoppes, R.; Jacobi, R.H.; Hendriks, M.; Kapteijn, K.; Ouwerkerk, C.; Rodenko, B.; Ovaa, H.; De Jonge, J. Chemical modification of influenza $CD8^+$ T-cell epitopes enhances their immunogenicity regardless of immunodominance.
PLoS One 11, e0156462 (2016)

Hoppes, R.*; Oostvogels, R.*; **Luimstra, J.J.**; Wals, K.; Toebes, M.; Bies, L.; Ekkebus, R.; Rijal, P.; Celie, P.H.; Huang, J.H.; Emmelot, M.E.; Spaapen, R.M.; Lokhorst, H.; Schumacher, T.N.; Mutis, T.; Rodenko, B.; Ovaa, H. Altered peptide ligands revisited: vaccine design through chemically modified HLA-A2-restricted T cell epitopes.
Journal of Immunology 193, 4803-4813 (2014)

*These authors contributed equally.

Patent application

Neefjes, J.J.; Ovaa, H.; Garstka, M.A.; **Luimstra, J.J.** Stichting Het Nederlands Kanker Instituut-Antoni van Leeuwenhoek Ziekenhuis, Leids Universitair Medisch Centrum. Methods for producing a MHC multimer.
International patent WO 2019/083370 A1 (2019).

A

A

Curriculum vitae

Jolien Luimstra was born on September 18th, 1987, in Amsterdam. She finished her VWO in 2005, at the Oostvaarders College in Almere. Already then, driven by a broad interest in medicine and chemistry, she obtained a double profile in 'Nature & Health' and 'Nature & Technology'. Directly after graduation, she began her Bachelor studies in Chemistry at the University of Amsterdam, which she completed in 2008. During the gap year that followed, she worked at the QC laboratory of Sanquin (the Dutch blood service), sparking her curiosity for immunology. Jolien then went on to continue her studies with the Biomolecular Sciences track in the Chemistry Master's program at the University of Amsterdam. Her first encounter with MHCI (major histocompatibility complex class I) antigen presentation occurred during a three-month research project on MHC class I epitope optimization, supervised by prof. dr. Huib Ovaa in the Division of Cell Biology at the Netherlands Cancer Institute. Jolien's bolstered interest in immunology led her to the Australian Red Cross Blood Service in Brisbane, Australia, where she spent nine months on her main research project, investigating immune cell maintenance and function in MBL-sufficient versus MBL-deficient individuals.

After obtaining her Master's degree in 2012, Jolien returned to the Netherlands Cancer Institute as a PhD candidate. There, she began her work at the interface of chemistry and immunology, on using the MHCI antigen presentation pathway to activate and monitor cytotoxic T cell immunity. In 2016, the Division of Cell Biology moved to the Leiden University Medical Center, to first become the Department of Chemical Immunology, and eventually the Department of Cell and Chemical Biology. In June 2018 Jolien joined the management team of the Institute for Chemical Immunology, led by prof. dr. Jacques Neefjes. In the course of her PhD, she learned about the field of Clinical Chemistry and thus found her next calling. In September 2019 Jolien began her ongoing Clinical Chemistry Training at Meander Medical Centre in Amersfoort, under the supervision of dr. Ayşe Demir.

A

Acknowledgements

I am grateful to everyone who contributed to the work in this dissertation. I owe most of my thanks to my doctoral advisors, Huib Ovaa and Jacques Neefjes, for the opportunity to work in such an inspiring and innovative field. This dissertation would not be what it is without the great collaborations and support from my colleagues.